1-20-2006

Synthesis of Molecular Baskets and Introduction of Inward Facing Functionality

Zachary Laughery
University of New Orleans

SYNTHESIS OF MOLECULAR BASKETS AND INTRODUCTION OF INWARD FACING FUNCTIONALITY

A Dissertation

Submitted to the Graduate Faculty of the
University of New Orleans
in partial fulfillment of the
requirement for the degree of

Doctor of Philosophy
in
Chemistry

by

Zachary R. Laughrey

A.D., Louisiana Tech University
B.A., University of New Orleans

December 2005

ACKNOWLEDGEMENTS

I would like to express my undying gratitude to my advisor, Professor Bruce C. Gibb for his patience, encouragement and open discussions during the winding course of my research. My gratitude is also expressed to the members of my research committee, Dr. Mark Trudell, Dr. Branko Jursic, Dr. Guijun Wang, and Dr. Steven Rick for their assistance and guidance.

I would also like to thank all the past and present members of the Gibb research group especially Corinne Gibb for her assistance, knowledge and guidance. I would also like to thank Dr. John Wiley for his assistance and Dr. Richard Cole for mass spectroscopy analysis.

Finally, I would like to thank my family. My greatest gratitude goes out to my daughters, Maggie, Cassie and Audrey for their support and love, and to my ever-patient wife, Stacey, who always waited for me and knows everything.

TABLE OF CONTENTS

List of Tables v

List of Figures vii

List of Schemes xii

Abbreviations xiv

Abstract xv

I. Introduction 1

1.1 Host-Guest interactions 1

1.2 Enzymes and enzyme mimics 5

1.3 Molecular hosts 6

1.3.1 Cyclodextrins 7

1.3.2 Calixarenes 10

1.3.3 Cavitands 22

1.3.4 Cyclotriveratrylene 28

1.3.5 Cucurbituril 33

1.3.6 Inward facing functionality 37

II. Synthesis and Characterization of *m*-baskets 44

2.1 Synthesis and conformation of molecular hosts 44

2.2 NMR binding studies of molecular hosts 48

2.3 Synthesis and hosting properties of a deuterated molecular host 59

III. Functionalization of molecular concavity 66

3.1 Possible products and nomenclature 68

3.2 Base strength and product yield....77

3.3 Synthesis of carboxylic acids *m*-baskets....81

3.4 Carboxylic acid *m*-baskets as acid catalysts....86

3.5 Binding properties of carboxylic acid *m*-baskets....87

IV. Synthesis of a Carbonic anhydrase mimic....101

4.1 Synthesis of the enzyme mimic....106

4.2 Zinc binding and physical studies of the enzyme mimic....117

V. Conclusion....120

VI. Experimental Section....121

6.1 General....121

6.2 Synthesized Compounds....121

6.3 Binding Studies of 5-Methyl-*m*-basket, 2-Methyl-*m*-basket, and d_4-*m*-basket....147

6.4 1D- and 2D-NMRs of aldehyde *m*-baskets....160

6.5 NMR and UV-Vis titrations of **157**....163

6.6 Crystal structure of **145**....164

6.7 Crystal structure of **149**....191

VII. References....204

Vita....214

LIST OF TABLES

Table 1.1 Dimensions of cyclodextrins....8

Table 1.2 Binding Constants of Host **12** 13

Table 1.3 Binding Constants of Calix[4]arene with Increasing Alkyl Groups 14

Table 1.4 Dimensions of Cucurbit[n]uril 35

Table 2.1 Physical Properties of Guests....51

Table 2.2 Association Constants of Hosts **36** and **70**....52

Table 2.3 Thermodynamic Characteristics of Host **70**....54

Table 2.4 Association Constants of Host **71** 56

Table 2.5 Thermodynamic Characteristics of Host **71**....56

Table 2.6 Association Constants of Hosts **36** and **99** with Bromide Guests 63

Table 2.7 Association Constants of Hosts **36** and **99** with Iodide Guests....64

Table 3.1 Product distribution and yields of lithiation/formylation reaction 78

Table 3.2 Product Yield in the Presence of Guest 80

Table 3.3 Yield of methyl ester *m*-basket utilizing three different bases....84

Table 4.1 Yields of Partially/Fully Weaved 2-Me *m*-baskets Products 108

Table 4.2 Yields of Partially/Fully Weaved *m*-baskets Products 111

Table 4.3 Yields of **153** 114

Table 6.1 Crystal data and structure refinement for **145**....165

Table 6.2 Atomic coordinates (x104) and equivalent isotropic displacement parameters ($Å^2$ x10^3) for **145** 166

Table 6.3 Bond lengths [Å] and angles [deg] for **145**....170

Table 6.4 Anisotropic displacement parameters ($Å^2$ x10^3) for **145**....179

Table 6.5 Hydrogen coordinates (x10^4) and isotropic displacement parameters ($Å^2$ x10^3) for **145** 183

Table 6.6 Torsion angles [deg] for **145** 185

Table 6.7 Crystal data and structure refinement for **149** 192

Table 6.8 Atomic coordinates (x10^4) and equivalent isotropic displacement parameters ($Å^2$ x10^3) for **149** 193

Table 6.9 Bond lengths [Å] and angles [deg] for **149** 195

Table 6.10 Anisotropic displacement parameters ($Å^2$ x10^3) for **149** 198

Table 6.11 Hydrogen coordinates (x10^4) and isotropic displacement parameter ($Å^2$ x10^3) for **149** 200

Table 6.12 Torsion angles [deg] for **149** 201

LIST OF FIGURES

Figure 1.1 Potassium cation bound by benzo[18]crown-6.....1

Figure 1.2 The two possible orientations of dipole-dipole interactions of carbonyl groups 2

Figure 1.3 Watson-Crick base pairing 2

Figure 1.4 Quadrapole moments of aromatic rings 3

Figure 1.5 Orientations of aromatic rings 3

Figure 1.6 Peptidocalixarenes used to bind amino acids in $CDCl_3$ and D_2O 5

Figure 1.7 Cyclodextrin 7

Figure 1.8 Space filling model of β-cyclodextrin.....7

Figure 1.9 Modified cyclodextrin and rocuronium bromide.....9

Figure 1.10 Conformations of calix[4]arene 11

Figure 1.11 Conformations of calix[6]arene found in the solid state 16

Figure 1.12 Bridged calixarene regioisomers.....18

Figure 1.13 Ribose in solution.....23

Figure 1.14 Crystal structure of **36** and iodoadamantane 28

Figure 1.15 Requirements of functionalized benzyl alcohols 29

Figure 1.16 Space filling model of CB[6].....34

Figure 1.17 Stabilization of tetrahedral intermediate by pyridone.....42

Figure 2.1 Open and closed conformations of **70**.....46

Figure 2.2 Optimized geometry of **70** with restrained dihedral angles 46

Figure 2.3 Proton designation for hosts **36**, **70** and **71** 47

Figure 2.4 Potential density maps of **36**, **70** and **71**.....47

Figure 2.5 Free and bound host peaks of **70** and **77** in $CDCl_3$ 48

Figure 2.6 Binding isotherm of host **70** and **73** 49

Figure 2.7 Guests used in binding studies 50

Figure 2.8 von Hoft plot of host **70** and **77** in $CDCl_3$ 54

Figure 2.9 Upfield portion of EXSY NMR of **70** and **77** 57

Figure 2.10 Upfield portion of EXSY NMR of **71** and **86** 58

Figure 2.11 Model of **86** binding to **71** 59

Figure 2.12 Hydrogen bond preference of protium and deuterium 60

Figure 2.13 Percent change of association constants as a function of cycle size 64

Figure 3.1 *endo-* and *exo-* position and nomenclature 68

Figure 3.2 Possible substitution patterns from per-lithiation 70

Figure 3.3 ChemDraw and cartoon structures of aldehydes produced under reaction conditions 71

Figure 3.4 ^{1}H-NMR of **101** 72

Figure 3.5 ^{1}H-NMR of **100** 73

Figure 3.6 Indicator protons used to identify aldehyde *m*-baskets 73

Figure 3.7 d1 array of **101** 76

Figure 3.8 Product distribution using a) 5.5 equivalent or b) 10 equivalent of base 78

Figure 3.9 Substitution patterns seldom or never seen in the lithiation/formylation of **36** 79

Figure 3.10 Methyl esters formed from lithio-*m*-basket and methyl chloroformate 83

Figure 3.11 Products formed from the saponification of the methyl esters *m*-baskets 85

Figure 3.12 Cyclic and bicyclic acetals 87

Figure 3.13 a) Protons H_e, H_f, and H_c of **124** in DMSO-d_6 b) Protons H_e, H_f, and H_c of **124** in DMSO-d_6 with 100 equivalents of (*s*)-nicotine 88

Figure 3.14 Binding Isotherm of **124** binding **137** 89

Figure 3.15 Conformations of guest inside hosts 90

Figure 3.16 Upfield NMR region of **123/137** showing bound **137** 91

Figure 3.17 Upfield NMR region of **124/137** showing bound **137** 92

Figure 3.18 Upfield 2D-EXSY showing bound **137** by **124** 92

Figure 3.19 Model of **124** bound to **137** 93

Figure 3.20 Upfield NMR region of **129/137** showing bound **137** 94

Figure 3.21 Upfield NMR region of **131/137** showing bound **137** 95

Figure 3.22 2D-EXSY of **124/137** 95

Figure 3.23 Model of **131** bound to **137** 96

Figure 3.24 Two possible orientations of a guest within a host with both *endo*- and *exo*-carboxylic acids 96

Figure 3.25 Upfield NMR region of **128/137** showing bound **137** 97

Figure 3.26 Two binding orientations of **137** within **128** 97

Figure 3.27 Upfield NMR region of **130/137** showing bound **137** 98

Figure 3.28 2D-EXSY of **130/137** 99

Figure 4.1 Common tripodal ligands used to mimic carbonic anhydrase.....102

Figure 4.2 Tris(pyridyl) ligands with amino acid blocking groups 104

Figure 4.3 Funnel complex using imidizole as the nitrogen donor with zinc 105

Figure 4.4 Products formed attempting to make 2-Me-tris-*m*-basket.....107

Figure 4.5 Space filling model of mimic synthesized from 2-Me tris-*m*-basket.....109

Figure 4.6 Products formed attempting to make tris-*m*-basket 109

Figure 4.7 Crystal structure of **145** 110

Figure 4.8 Space filling model of the optimized structure of **156** 117

Figure 4.9 NMR zinc titration of **156** a) in the absence of zinc b) with one equivalent of zinc.....118

Figure 4.10 Binding isotherm of **156** titration with zinc 119

Figure 6.1 Binding isotherm of host **70** and adamantane in toluene-d_8.....147

Figure 6.2 Binding isotherm of host **70** and cyanoadamantane in toluene-d_8.....148

Figure 6.3 Binding isotherm of host **70** and bromocyclohexane in DMSO-d_6 148

Figure 6.4 Binding isotherm of host **70** and iodocyclohexane in DMSO-d_6 149

Figure 6.5 Binding isotherm of host **70** and bromocyclopentane in DMSO-d_6 149

Figure 6.6 Binding isotherm of host **70** and iodocyclopentane in DMSO-d_6 150

Figure 6.7 Binding isotherm of host **70** and iodopentane in DMSO-d_6.....150

Figure 6.8 Binding isotherm of host **70** and bromobenzene in DMSO-d_6.....151

Figure 6.9 Binding isotherm of host **70** and iodobenzene in DMSO-d_6.....151

Figure 6.10 Binding isotherm of host **71** and bromocycloheptane in DMSO-d_6 152

Figure 6.11 Binding isotherm of host **71** and cyclohexane in DMSO-d_6 152

Figure 6.12 Binding isotherm of host **71** and bromocyclohexane in DMSO-d_6 153

Figure 6.13 Binding isotherm of host **71** and iodocyclohexane in DMSO-d_6 153

Figure 6.14 Binding isotherm of host **71** and bromocyclobutane in DMSO-d_6.....154

Figure 6.15 Binding isotherm of host **71** and iodopentane in DMSO-d_6.....154

Figure 6.16 Binding isotherm of host **99** and bromocyclooctane in DMSO-d_6 155

Figure 6.17 Binding isotherm of host **99** and iodocyclooctane in DMSO-d_6 155

Figure 6.18 Binding isotherm of host **99** and bromocycloheptane in DMSO-d_6 156

Figure 6.19 Binding isotherm of host **99** and iodocycloheptane in DMSO-d_6 156

Figure 6.20 Binding isotherm of host **99** and bromocyclohexane in DMSO-d_6 157

Figure 6.21 Binding isotherm of host **99** and iodocyclohexane in DMSO-d_6 157

Figure 6.22 Binding isotherm of host **99** and bromocyclopentane in DMSO-d_6 158

Figure 6.23 Binding isotherm of host **99** and iodocyclopentane in DMSO-d_6 158

Figure 6.24 Binding isotherm of host **99** and *exo*-2-bromonorborane in DMSO-d_6 159

Figure 6.25 ^{1}H-NMR of (+/-)-**105** in $CDCl_3$ 160

Figure 6.26 2D-ROESY of (+/-)-**105** in DMSO-d_6 160

Figure 6.27 ^{1}H-NMR of **107** in $CDCl_3$.....161

Figure 6.28 2D-NOESY of **107** in DMSO-d_6 161

Figure 6.29 ^{1}H-NMR of (+/-)-**109** in CD_2Cl_2 162

Figure 6.30 2D-ROESY of (+/-)-**109** in DMSO-d_6 162

Figure 6.31 Crystal structure of **145** 164

Figure 6.32 Crystal structure of **149** 191

LIST OF SCHEMES

Scheme 1.1 Synthesis of calixarenes....11

Scheme 1.2 Synthesis of resorcinarenes....21

Scheme 1.3 Synthesis of ditopic host **29**....24

Scheme 1.4 Synthesis of **30**....25

Scheme 1.5 Synthesis of deep cavity cavitands....27

Scheme 1.6 Synthesis of *m*-basket....27

Scheme 1.7 Synthesis of cyclotriveratrylene (**37**)....29

Scheme 1.8 Mock's pseudorotaxane switch....34

Scheme 1.9 Cyclization of cyclopropanes....40

Scheme 2.1 Synthesis of 5-Me *m*-basket (**70**)....45

Scheme 2.2 Synthesis of 2-Me *m*-basket (**71**)....45

Scheme 2.3 Synthesis d_4-*m*-basket (**99**)....61

Scheme 2.4 Synthesis of **82**....62

Scheme 2.5 Synthesis of **80**....62

Scheme 3.1 Reaction mechanism of Directed *Ortho* Metallation....67

Scheme 3.2 Synthesis of benzyl alcohol *m*-baskets....75

Scheme 3.3 General synthesis of ester *m*-baskets....82

Scheme 3.4 General synthesis of carboxylic acid *m*-baskets....84

Scheme 3.5 Synthesis of acetals....86

Scheme 4.1 Mechanism of reversible hydrolysis of carbon dioxide by Carbonic Anhydrase....102

Scheme 4.2 Formation of inactive sandwich compounds....103

Scheme 4.3 Hydrolysis of carbon dioxide by *tert*-butyl tris(pyrazolyl)borate....104

Scheme 4.4 Proposed scheme for the synthesis of *m*-basket CA mimic.....106

Scheme 4.5 Synthesis of 2-Me-*m*-*tris*-basket.....106

Scheme 4.6 Synthesis of *tris*-*m*-basket.....110

Scheme 4.7 Synthesis of tripodal ligand 112

Scheme 4.8 Model reaction to test the Pd source 113

Scheme 4.9 Model Suzuki reaction using **35**.....113

Scheme 4.10 Model Suzuki reaction using **149**.....114

Scheme 4.11 Synthesis of *tris*-*m*-basket diol.....115

Scheme 4.12 Synthesis of **156** using Ullmann ether synthesis.....116

ABBREVIATIONS

^{t}BuOH	*tert*-butanol
n-BuLi	*n*-butyllithium
sec-BuLi	*sec*-butyllithium
tert-BuLi	*tert*-butyllithium
CB	Cuccurbituril
CD	Cyclodextrin
$CDCl_3$	Chloroform-*d*
COSY	Correlated spectroscopy
CTC	Cyclotricatechylene
CTV	Cyclotriveratrylenes
DMA	*N*,*N*-dimethylacetamide
DME	Ethylene glycol dimethyl ether
DMF	*N*,*N*-dimethylforamide
DMSO	Dimethyl sulfoxide
Eq	Equivalents
EXSY	Exchange spectroscopy
ITC	Isothermal titration calorimetry
^{i}PrOH	Isopropyl alcohol
K_a	Association constant
NOESY	Nuclear Overhauser Effect spectroscopy
PNPCC	*para*-nitrophenyl choline carbonate
THF	Tetrahydrofuran

ABSTRACT

As a first step to producing a shape selective catalysts or enzyme mimic, two preorganized host molecules were synthesized. Binding studies of the two hosts with a variety of guests in three solvents demonstrated that an important driving force in the association was the formation of C-H···X-R hydrogen bonds (X = halogen). A deuterated host was utilized to further examine the formation of the C-H···X-R hydrogen bonds.

In an effort to place functionality in the hydrophobic pocket of these hosts, two methods were developed. The first utilized directed *ortho* metallation to place electrophiles above and/or directed into the cavity. Perlithiation of the host could lead to sixty-nine products but reaction conditions and host rigidity limited product formation. This reaction technique led to the placement of carboxylic acid groups onto the host and the isolation of twelve products. Two different positions of the carboxylic acids (*endo*- and *exo*-) direct the orientation of the guest. 1D- and 2D-NMR were utilized to examine how the was orientated inside the host.

The second method employed to place functionality on the host, sited a tripodal zinc binding ligand on the side of the hydrophobic pocket of the host. The synthesized host was able to bind zinc strongly and in a 1:1 manner.

I. INTRODUCTION

1.1 Host-Guest Interactions

Host-Guest chemistry has evolved from cation binding crown ethers and macrocyclic Schiff bases, to larger molecules that have the ability to encapsulate biologically relevant and complex molecules. Hosts have been designed to bind cations, anions, both (ditopic), or neutral molecules.[1] Hosts can utilize many different, subtle interactions to increase selectivity and affinity for a particular guest. These noncovalent interactions are:

1) Ion-ion interactions are particularly strong intermolecular interactions with energies ranging from 100-350 kJ/mol.[1] An example of an ion-ion interaction is a salt bridge found in proteins (-COO^- $^+NH_3$-).[1]

2) Ion-dipole interactions have been extremely important in supramolecular chemistry. These interactions are often used to build extended molecular architectures.[2, 3] These interactions range in energy from 50-200 kJ/mol and are the driving force in the association between cations and crown ethers (Figure 1.1).[1]

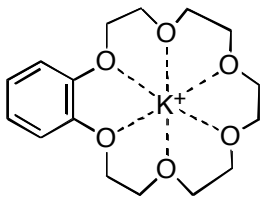

Figure 1.1 Potassium cation bound by benzo[18]crown-6

3) Dipole-dipole interactions arise from the alignment of two different dipoles. One example is the interaction between two carbonyl groups (Figure 1.2)[1] of which there are two possible alignments. The orthogonal alignment (a) allows for one point of interaction with the partially negative oxygen of one carbonyl pointing at the partially positive carbon of another.

The anti-parallel alignment (b) has the dipoles arranged so that there are two points of interaction.

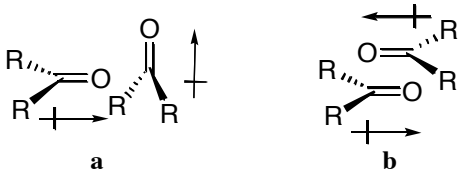

Figure 1.2 The two possible orientations of dipole-dipole interactions of carbonyl groups

4) Hydrogen bonding can be considered a type of dipole-dipole interaction.[1] There are however additional components to hydrogen bonds, such as electrostatic, charge transfer, dispersion, and polarization forces.[4, 5] Strong hydrogen bonds, such as F-H···F$^-$ and N-H···O, are primarily electrostatic in nature. In contrast, weaker hydrogen bonds, such as C-H···O, are more dispersive in nature.[6, 7] Hydrogen bonding, along with π-π stacking and hydrophobic forces (see later), are among the most important in biological systems. They participate in DNA double helix in addition to protein secondary and higher order structure formation, along with countless other recognition events. An example of biologically important hydrogen bonds is the Watson-Crick base-pairing model (Figure 1.3).[8]

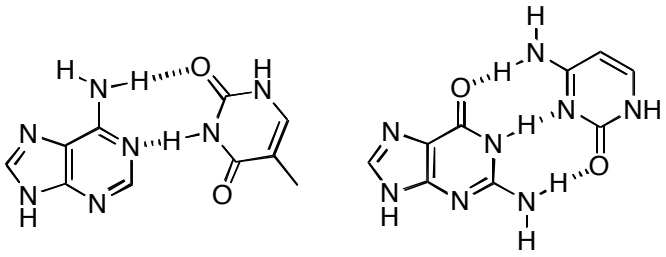

Figure 1.3 Watson-Crick Base Pairing

5) Cation-π interactions have been widely utilized in calixarene and cavitand chemistry as recognition elements.[9-13] Their energy can range from 5-80 kJ/mol.[1] Researchers have also found that cation-π interaction is critical in protein secondary structure stabilization.[14, 15]

6) π-π interactions, as mentioned above, play a key role in biological systems as a driving force for DNA and protein assembly.[16] The interaction is governed by the quadrapole moments of the aromatic rings (Figure 1.4).[1]

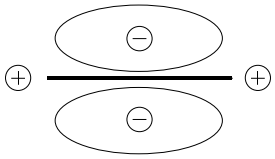

Figure 1.4 Quadrapole moments of aromatic rings

There are two orientations that can be adopted by interacting aromatic systems (Figure 1.5). The edge to face orientation (a) can be considered a C-H···π interaction[17] and is primarily electrostatic. The offset stacked interaction (b) is the orientation found in DNA duplex. This orientation allows for greater van der Waals interaction and thereby reduces the surface area exposed to solvent.[18, 19]

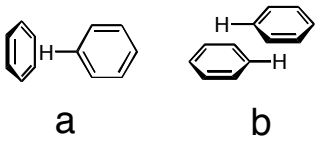

Figure 1.5 Orientations of aromatic rings

7) The weakest of all intermolecular forces are van der Waals interactions.[1] When the nucleus of one atom approaches a second atom, the electron cloud polarizes and gives rise to these attractive forces. The individual interaction energy is minimal, and the molecules must be in very close proximity for this interaction to have any effect. However, many of these, interacting in concert, can give rise to relatively large association constants. Several of the previously mentioned forces partially involve van der Waal interactions.

The "hydrophobic effect" can promote association, although it is not a force of interaction.[20] This effect is also apparent in other polar solvents albeit in a reduced amount (solvophobic effect).[1] The hydrophobic effect can give rise to favorable changes in enthalpy and

entropy. There are two means by which an increase in the enthalpic gain can be achieved. Solvent molecules present in the host are higher in energy than bulk solvent due to the reduced interaction between the host and solvent as compared with solvent-solvent interactions. When these solvent molecules are released through guest binding, an enthalpic gain is seen. Additionally, the solvent molecules around the guests are higher in energy than in bulk solvent. When these are released through association, there is a decrease in enthalpy. Entropy is increased by the release of these high-energy solvent molecules. For example, there are twelve water molecules that solvate the interior of β-cyclodextrin. When a guest is bound, there is an increase in entropy. However, the ordering of the host and guest often "hides" this increase in entropy.

A host-guest complex arises from many of these forces and it is often difficult to determine which force is dominant. Additionally, the interaction that dominates depends on external conditions such as solvent and temperature. One example is the complexation studies of hosts **1** and **2** (Figure 1.6).[21] When **1** binds amino acids in $CDCl_3$ the major driving force is the formation of hydrogen bonds between the ammonium and the host's amide carbonyl. Alternately, when using **2** as a host in water, the main driving force is the hydrophobic effect. The R-groups of **1** and **2** are not involved in molecular recognition.

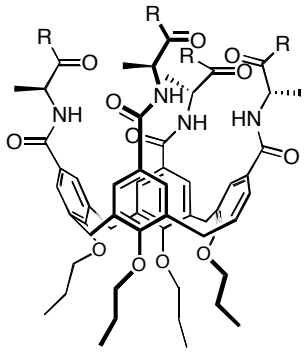

1 R = -OMe
2 R = -OH

Figure 1.6 Peptidocalixarene used to bind amino acids in $CDCl_3$ and D_2O

1.2 Enzymes and Enzyme Mimics

Enzymes are extremely active and selective catalysts and serve as an inspiration to host-guest chemists.[1] They derive their catalytic power from several phenomena.[22, 23] They increase the effective molarity of substrate and reactive groups by binding the substrate in an active-site.[24] Additionally, enzymes can stabilize a transition state and/or destabilize a ground state. The selectivity of an enzyme arises from the active site. The active site is generally a concave part of the enzyme that contains all the functionality required to affect a transformation. The amino acid residues in the active site are arranged in such a way that only the desired substrate will be catalyzed, while the residues in or around the active site can direct the substrate into the active site. For example, the opening into the active site of acetylcholine esterase has a negative charge that attracts the positively charged acetylcholine.[25]

While enzymes are exceptional catalysts, studying them can prove challenging. Proteins are very large, conformationally complex molecules and are usually available in very small quantities. They are, therefore, difficult to study using traditional spectroscopic techniques. Accordingly, it is advantageous to use small molecule mimics of the active site to determine what interactions are important in catalysis and selectivity.

Nature has not required that all possible reactions and substrates of interest to synthetic organic chemistry be catalyzed. As a result, the majority of reactions and substrates of interest to organic chemistry are not catalyzed by enzymes. Additionally, life has evolved in relatively narrow limits. Enzymes are only active at certain temperatures, salt concentrations, solvents, and pH. When not within these windows, enzymes lose much of their catalytic power. Another consideration is that not all organic molecules are soluble in water. It would therefore be beneficial to develop enzyme mimics that would catalyze reactions and substrates not essential to natural selection.

1.3 Molecular Hosts

There have been hundreds of hosts described in the literature. To limit the number of hosts described here, several requirements were put into place, with the primary restriction being that the host molecule must be concave. The host must also be organic in nature. This requirement removes zeolites and other inorganic host molecules from consideration. Thirdly, the host must be monomeric, which eliminates "molecular capsules" and other self-assembling systems.[26] The host must be large enough to encapsulate greater than 50% of the guest. Many rotaxanes and catenanes are ineligible for consideration due to this restraint.[27] Finally, the host must have a permanent entrance/exit, thereby excluding carceplexes and hemicarceplexes.[28] The host molecules that fulfill all these requirements are: cyclodextrins (CD); calixarenes; cavitands; cyclotriveratrylenes (CTV) and cucurbiturils (CB).

1.3.1 Cyclodextrins

Cyclodextrins (CD) are a group of macrocyclic host molecules synthesized from α-(+)-glycopyranose units (Figure 1.7). They have been exceedingly important in the development of

host-guest chemistry as well as enzyme mimicry. Industrially, CDs are made from the degradation of starch by cyclodextrin glucosyl transferase.[29] Depending on the desired CD size (see later) several templates may be added to form complexes with the selected cyclodextrin that remove it from solution. All CDs are cone-shaped molecules with a hydrophobic interior made structurally rigid from a ring of hydrogen bonds. There are two portals to the hydrophobic interior. The largest portal is the "secondary face", so called because it is ringed by secondary alcohols. The smaller portal is the primary face. The secondary alcohols hydrogen bond to each other in an interglucose fashion, which gives the host rigidity. The hydrophobic interior is lined with C-H groups and glycosidic oxygens. This interior is less hydrophobic as compared with calixarenes or cavitands, but it does allow for favorable van der Waals interactions and shields the hydrophobic guest from bulk water (Figure 1.8).

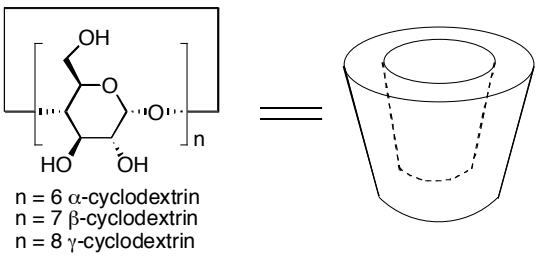

Figure 1.7 Cyclodextrin

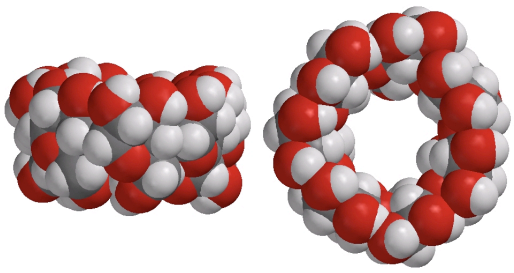

Figure 1.8 Space filling model of β-cyclodextrin

CDs come in primarily three sizes: α, β, γ (Table 1.1). All of the CDs are 7.9 Å in height. α-CD contains six α-(+)-glycopyranose units. Its cavity diameter is 5.2 Å and its

volume is 174 Å^3.[29-31] β-CD has seven α-(+)-glycopyranose units, a cavity diameter of 6.6 Å and a cavity volume of 262 Å^3. Finally the largest cyclodextrin, γ-CD, is made from eight α-(+)-glycopyranose units. Its cavity diameter and volume are 8.4 Å and 427 Å^3 respectively.

Table 1.1 Dimensions of cyclodextrins

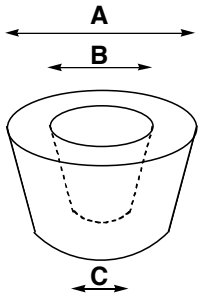

CD	A (Å)	B (Å)	C (Å)
α	13.7	5.2	4.7
β	15.3	6.6	6.0
γ	16.9	9.5	7.5

Due to the relative ease of their synthesis, CDs have been widely studied. They have been found to form stabile complexes with a wide range of guests including aliphatic and aromatic hydrocarbons, aliphatic and aromatic alcohols, amino acids, sugars and a variety of drug molecules.[30, 31] CDs prefer binding to guests that will interact simultaneously with the hydrophobic interior as well as the alcohols at the rim of the hosts. Therefore, α-CD prefers to bind amino acids, β-CD prefers to bind adamantane carboxylic acid, and γ-CD prefers to bind larger guests such as anionic methyl orange (**3**).[31]

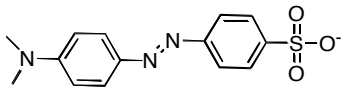

3

Several noncovalent forces drive these complexations. The most important being the hydrophobic effect in which the organic guest as well as the CD is desolvated (β-CD has been found in the crystal state to have up to twelve water molecules residing inside the cavity). This

provides a large increase in entropy upon guest binding. Other forces include the formation of hydrogen bonds and beneficial van der Waals interactions between host and guest.[31]

One recent example of using a modified CD is the binding of rocuronium bromide, **4** (Figure 1.9).[32] Rocuronium bromide is a neuromuscular blocker used in anesthesia to relax muscle tissue and facilitate access to internal cavities and organs. The physiological action of rocuronium bromide involves stopping the action of acetylcholine and nicotine acetylcholine. To reverse this action, drugs are given that inhibit the action of acetylcholine esterase, thereby increasing the concentration of acetylcholine. These "recovery" drugs can have deleterious side effects such as nausea, vomiting and hypotension. If however, the neuromuscular blockers could be encapsulated and removed from the body, the reversal drugs would not be necessary. Initially, α, β, and γ-CD were tested but the only γ-CD demonstrated any binding ability.

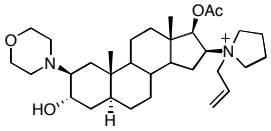

4

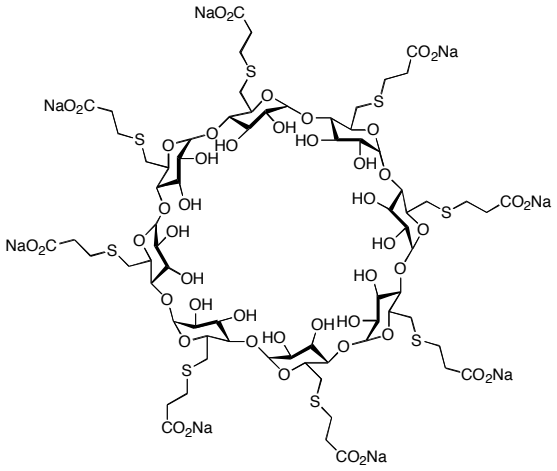

5

Figure 1.9 Modified cyclodextrin and rocuronium bromide

To increase the association of **4**, a γ-cyclodextrin was modified to produce **5**. The modifications increase the lipophilicity of CD, and the anionic groups near the cavity increase the association by ion-ion interactions with the ammonium ion of **4**. The association constant for **5** with **4** was found to be greater than 10^7 M^{-1} by isothermal titration calorimetry (ITC). The association is

both enthalpically and entropically favored. Researchers have found, using Rhesus monkeys, that when administered 0.5 μmol/kg of **5**, the action of **4** is reduced to 90% within three minutes and there were no changes in vital signs even when **5** was used up to 10 μmol/kg. This is an improvement of half the recovery time without any of the adverse side effects.

While CDs are excellent host molecules, they still possess several drawbacks. There is no position to place functionality so that it would continually face into the hydrophobic pocket. Additionally, there are three different types of hydroxyl groups on the two faces of cyclodextrin (Figure 1.7). D'Souza has developed methods to place functionality where it is desired on cyclodextrins.[33] The 6-position is the most nucleophilic and the most basic. The 2-position is the most acidic and the 3-position is most inaccessible. Using this knowledge it is possible to promote one product over another. However, it is not possible to eliminate the formation of the unwanted regioisomers.

The secondary alcohols rigidify the structure of CD through a ring of hydrogen bonds. If substitution takes place on these alcohols, then the rigidity is subsequently reduced. Researchers must therefore be aware of the increased flexibility of the host CD. This becomes important when attempting to functionalize CD to allow for solubility in solvents other than water and polar protic solvents.

1.3.2 Calixarenes

Calixarenes are macrocyclic compounds made from the condensation of *p*-alkyl phenols with formaldehyde (Scheme 1.1).[34] There are several different sizes of calixarenes.

Scheme 1.1 Synthesis of calixarenes

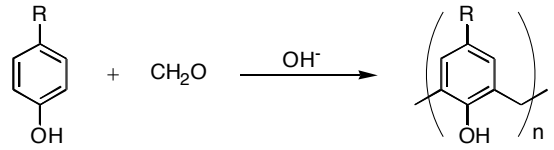

n = 4-8

The products formed are determined by reaction conditions (amount of base, temperature, etc). The largest yields are with n = 4, 6, and 8 (50, 85 and 63%) and are therefore the most studied. Calix[4]arenes (**6**) and calix[6]arenes (**7**) have four and six aromatic units respectively.[35]

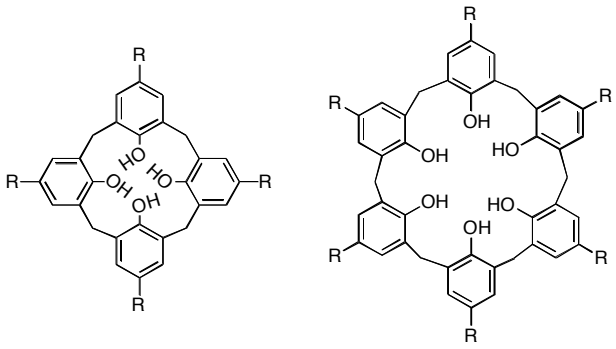

6 **7**

Calix[4]arene have a cup shaped structure. Four different conformations arise from the rotation about the σ-bonds of the Ar-CH_2-Ar: the cone; partial cone; 1,3 alternate; and the 1,2-alternate conformation (Figure 1.10). The unmodified calix[4]arene is in equilibrium between these four conformations. The cone conformation is stabilized by the formation of intramolecular hydrogen bonds between the phenols.

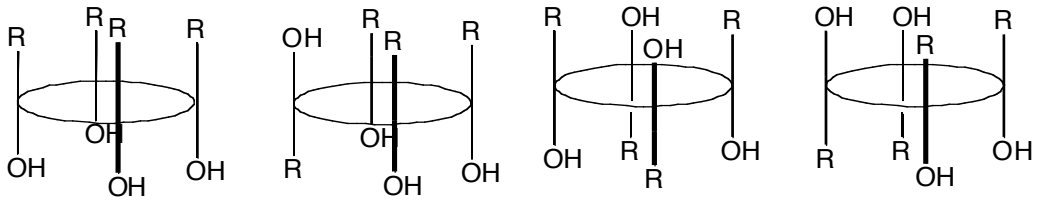

Figure 1.10 Conformations of calix[4]arene

In the cone conformation there are two sides to the calixarene. Traditionally the rim with the alkyl groups is known as the upper rim and the side with the phenols is known as the lower rim.

Solid-state structures have shown that calix[4]arenes can bind neutral organic molecules. They do not however, act as host in solution due to rapid conformational changes.

Rigidification of the cone conformation is required to allow the calix[4]arene to act as a host in solution. There are two places to rigidify the cone conformation: the upper and lower rim. One method is to position bulky groups on the phenolitic oxygens of the lower rim. This mechanically prevents the rotation around the Ar-CH_2-Ar bonds. An example is **8**.[36] While the bulky amide is able to maintain the calixarene in the cone conformation, there is still residual movement around the Ar-CH_2-Ar bonds. The calixarene adopts two conformations, a C_{4v} conformation (cone) and a C_{2v} conformation ("pinched cone"). If sodium is added to a solution of **8**, the carbonyl oxygens bind the sodium (**9**) that in turn increases the rigidity of the calixarene. This rigidity allows it to act as a host for nitromethane in $CDCl_3$ (K_a = 34 M^{-1}).

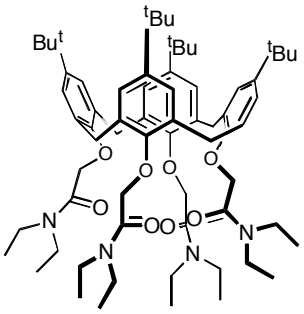

8

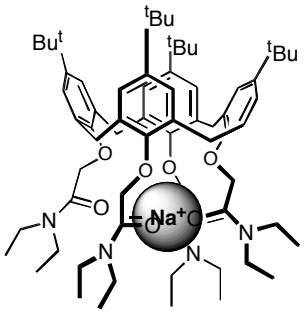

9

The oxygens of the calixarene may also be linked covalently. Various spacers have been used.[36] The calixarene **10** and **11** both bind nitromethane in CCl_4 with association constants of

230 and 50 M^{-1} respectively. The higher association constants of **10** with nitromethane demonstrate the importance of preorganization and rigidity of hosts.

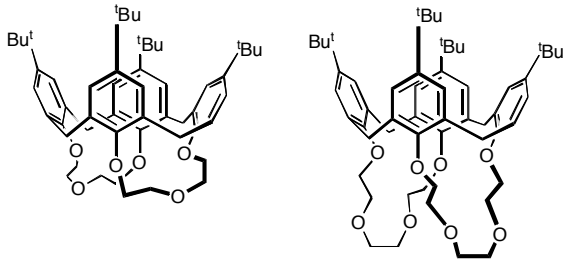

10 **11**

The upper rim may also be covalently joined to reduce the residual motions. Ungaro *et al*. used a variety of aromatic spacers to bridge the upper rim (**12**).[37] This technique also allowed for the introduction of a pyridine nitrogen to act as an additional recognition point. These hosts were able to bind solvent sized molecules with acidic protons (Table 1.2).

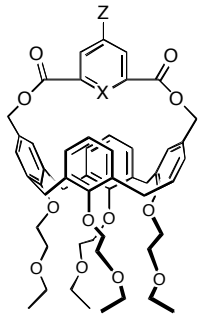

12

Table 1.2 Binding Constants of host **12**[a]

Guest (Solvent)	X = CH Z = H	X = N Z = H	X = N Z = OMe	X = N Z = $N(Me)_2$
CH_3CN (CCl_4)	-	36	13	-
CH_3NO_2 (CCl_4)	-	57	124	-
$CH_2(CN)_2$ ($CDCl_3$)	-	79	50	37

Key: [a]The symbol "-" indicates that binding was not noted

Overall, modified calix[4]arenes can act as hosts for small, neutral, solvent-sized molecules. The driving force for complexation is the formation of favorable van der Walls interactions and C-H-π interactions. To further develop the chemistry of these molecules, researchers have used electrophilic substitution at the upper rim to both enlarge the cavity and add recognition points to increase selectivity and binding strength.

Additional depth has been used to increase a molecule's ability to act as a host. In the case of calixarenes, this has been achieved by increasing the cavity walls.[38] A range of calixarenes (**6**) was synthesized and their K_as were determined (Table 1.3). It does appear that deepening the cavity will increase the affinity of the guest.

Table 1.3 Binding Constants of calix[4]arene with increasing alkyl groups[a]

R =	$K_a(M^{-1})$ $CDCl_3$
H	5
Tert-Bu	27
Cyclohexyl	36
Phenyl	-

Key: [a]The symbol "-" indicates that binding was not noted

An example of adding a recognition point is the calixarene **13**.[36] The researchers use two points of binding to allow the modified calixarene to act as a host. The carbonyl group of the amide guest forms hydrogen bonds with the urea group of the calixarene. Additionally, the NH group of the guest forms an NH-π interaction with the arenes of the host. The guest species exhibited no binding affinity with either benzylphenylurea (**14**) or calix[4]arene-*bis*-crown-3 (**15**) demonstrating the importance of these binding interactions acting in concert.

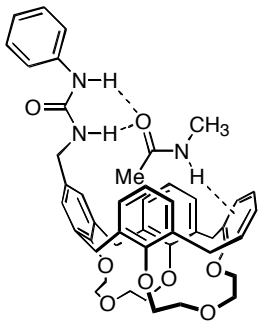

13

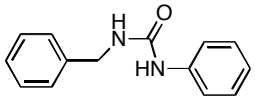

14

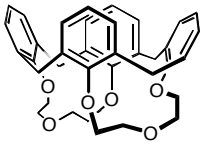

15

To further enhance the binding ability of calixarenes, the Ungaro group has placed peptides at the upper rim. This substitution has the advantage of stabilizing the cone conformation by formation of intramolecular hydrogen bonds.[21, 39]

The calixarenes **16** and **17** both bind carboxylic acids and ammonium cations in $CDCl_3$. However, **16** had larger association constants. The greater flexibility of **16** allows it to form more effective hydrogen bonds.[21] It is worthwhile to note that the researchers do not believe that the hydrophobic pocket is involved in the reception of these guests. The calixarene acts as a scaffold for the hydrogen bond donors/acceptors to be arranged.

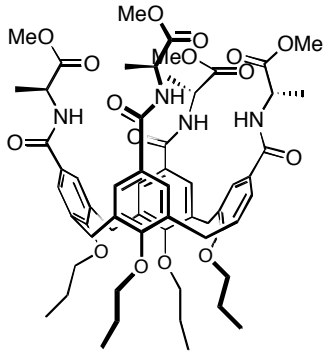

16

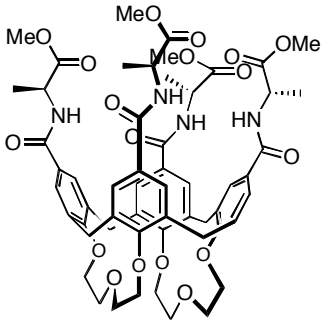

17

Hydrolysis of the ester makes the calixarenes (**18** and **19**) water-soluble. When these new hosts are exposed to esters of amino acids, the calixarene **19** becomes the better host. The

driving force of association has changed from the formation of hydrogen bonds to hydrophobic effects and the esters bind into the cavity of the calixarene.

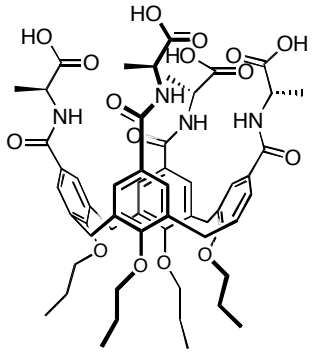

18

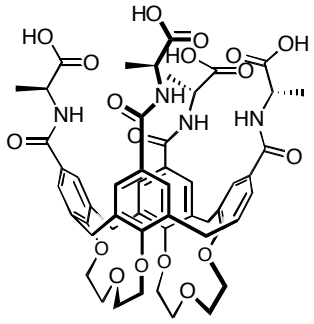

19

Calix[6]arenes (**7**) are significantly more flexible. While calix[4]arene has always been found in the cone conformation in the solid state, two conformations of calix[6]arene have been described. One conformation has all of its –OH groups on the same side of the molecule (cone conformation, Figure 1.11a). The second conformation has two sets of three neighboring phenol –OH groups on opposite sides of the molecule (1,2,3 alternate conformation, Figure 1.11b).

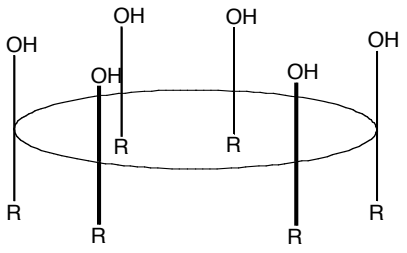

a

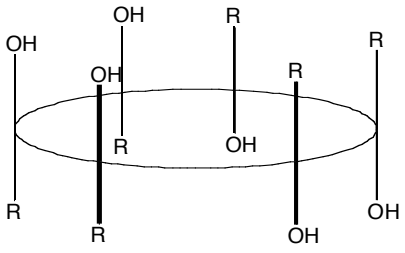

b

Figure 1.11 Conformations of calix[6]arene found in the solid state

One might consider rigidifying the calix[6]arene by alkylating each phenol individually. This proves to be unsatisfactory for two reasons. Large alkyl groups are required to slow the rotation around the Ar-CH_2-Ar bonds. For example, the calixarene **20** has a great amount of flexibility and is found primarily in the 1,2,3 alternate conformation. If however, **20** is bound to

Cs^+, it can then act as a host for C_{60}.[40] Secondly, incomplete alkylation gives rise to a large number of regioisomeric products.[41] These reasons have led researchers to bridge the phenols with a variety of aromatic spacers.[42]

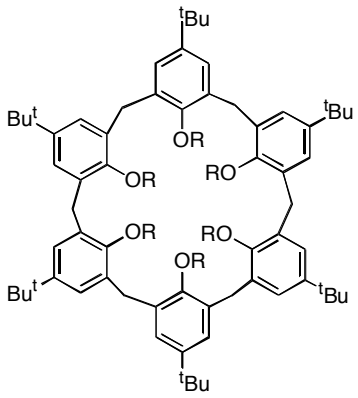

R = -CH_2COOEt

20

Gutsche's group reported A/D linkage by reacting *tert*-butyl calix[6]arene with α,α'-dibromo-p-xylene. When the remaining phenols are methylated a "self-anchored rotaxane" **21** was formed, a clear indication that the cone conformation was not rigid.[43]

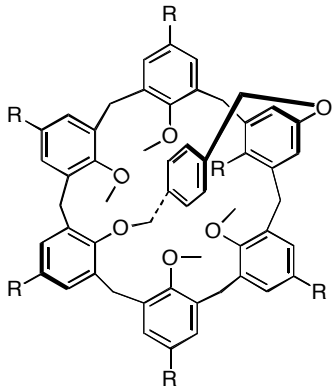

R = tBu

21

Several other groups have bridged the calix[6]arene A/D positions.[44, 45] The Shinkai group has carried out an in-depth variable temperature and 2D NMR study of calix[6]arene

regioisomers arising from bridging with aromatic spacers at different positions (A/B v. A/C v. A/D). They found that all bridges stabilized the calixarene in the cone conformation relative to the unmodified calixarene. Under these circumstances, the most stable was the A/C bridged calix[6]arene (Figure 1.12).

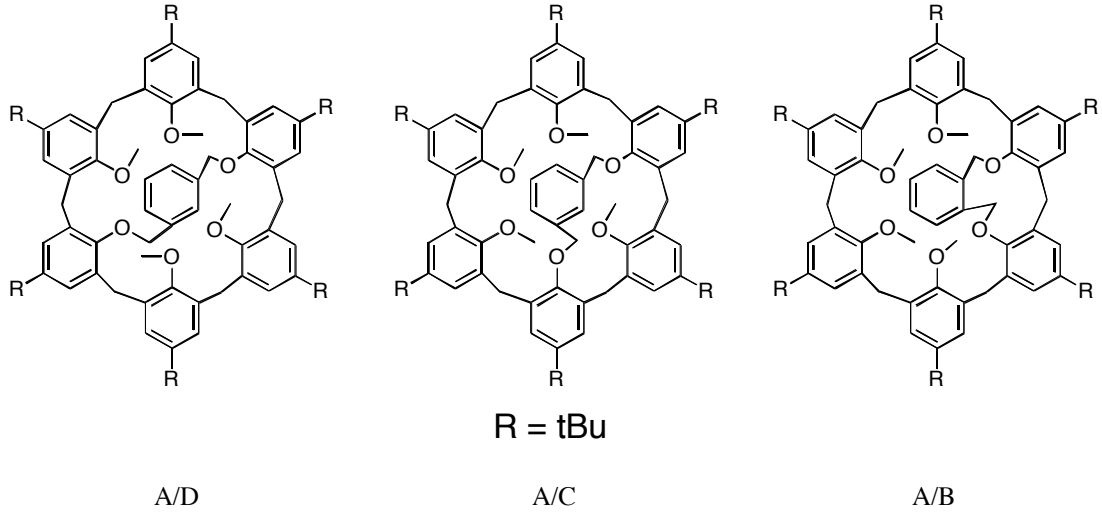

Figure 1.12 Bridged Calixarene regioisomers

Another way to rigidify the calix[6]arene is to bridge three phenol positions, the A/C/E positions. These compounds are also known as "capped" calixarenes. The capping can be accomplished in several ways.

Shinkai group used covalent bonds to link the phenolitic oxygens on the lower rim.[44] They bridged 1,3,5-tri-O-methylated *tert*-butyl calixarene with 1,3,5-tris(bromomethyl)benzene and obtained a 91% yield of **22**. The cone conformation of this compound was found to be remarkably stable.

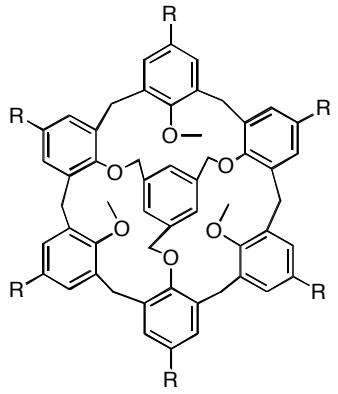

22

An unfortunate result of this method is the effective sealing of the calix[6]arene. The aromatic cap seals the lower rim while alternating tert-butyl groups effectively seals the upper rim. The capped calix[6]arenes do act as hosts toward primary ammonium cations, but are selective for Cs^+.[46]

Quadruple bridging of calix[6]arene has been accomplished at the A/B/D/E positions of the lower rim using 1,2,4,5-tetrakis(bromomethyl)benzene with a surprisingly high yield (65-80%)(**23**). NMR studies have demonstrated that these capped calixarenes are also stable in the cone conformation.[47] These molecules have been used to encapsulate Cs^+.[48, 49]

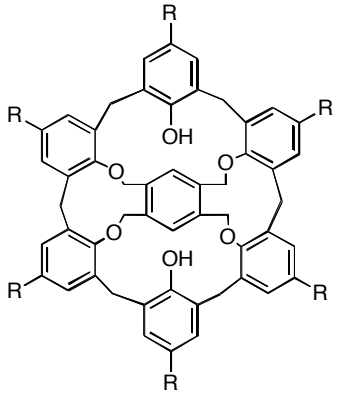

23

Reinaud *et al.* have synthesized a variety of functionalized capped calix[6]arenes.[50-52] One example is **24** which has a triphenylphosphine cap on the lower rim of calix[6]arene.[52] This stabilizes the cone conformation on the NMR time scale and allows the calixarene to act as a host for several primary amines. The primary driving force appears to be the formation of hydrogen bonds with the amines of the cap and the guest.

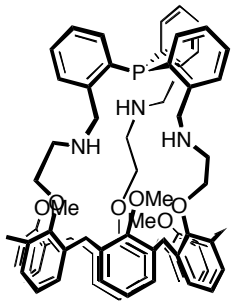

24

Another way to stabilize the calix[6]arene is to bridge sequential aromatic rings. One example is **25**. Shinkai bridged a benzyl chloride calixarene with *N*,*N*-dihexyl-1,3 *m*-aminobenzene.[53] Shinkai have called these hosts "stapled calixarenes". Such hosts can bind C_{60} in toluene due to charge transfer interactions between the m-phenyl diamine bridges and C_{60}.[40]

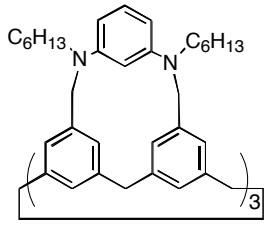

25

The upper rim of calix[6]arenes can also be capped.[54] 1,3,5-tris(mercaptomethyl)benzene reacted with tetrachloromethyl calixarene to give the capped product **26** in 28% yield. The association constant of **26** with $PhNMe_3I$ is >5 times greater than with *t*-Butyl calix[6]arene.

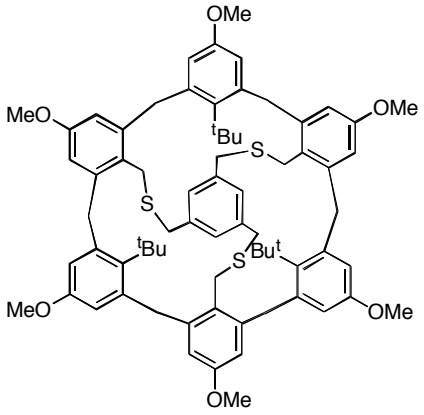

26

Calixarenes act as molecular hosts. However, they suffer from several drawbacks. All calixarenes are conformationally flexible and care must be taken to ensure that the conformation is sufficiently rigid. Calix[4]arenes' hydrophobic pocket is only large enough to encapsulate solvent size molecules. Extension of the cavity is required to encapsulate larger guests. Finally, the lack of any inward facing functional groups usually requires that functionality be added above or below the cavity, which might react with substrates not bound by the cavity.

1.3.3 Cavitands

Cavitands have been defined by Cram as "synthetic organic compounds that contain enforced cavities of dimensions at least equal to those of the smaller ions, atoms or molecules".[55] This broad definition has been narrowed by other authors to include only molecules that arise from functionalization of resorcinarenes.

Resorcinarenes are synthesized by the acid catalyzed[56] condensation of resorcinol with aldehydes (Scheme 1.2).

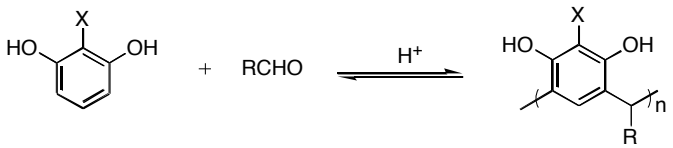

Scheme 1.2 Synthesis of resorcinarenes

The yield of this reaction is very high when n = 4. The macrocycle precipitates out of solution and therefore is a thermodynamic sink. There have been recent attempts to synthesize resorcinarenes with n > 4.[57-59] So far, they have only been obtained in low yield (n = 5, 4%; n = 6, 14%; and n = 8, 1%). A large range of resorcinarenes can be produced and the properties changed by altering the aldehyde.

Resorcinarenes have a bowl shaped structure that is held in place by four hydrogen bonds at the rim. These bowls are slightly flexible but not nearly as flexible as the corresponding calixarenes.

Resorcinarenes themselves have been used as hosts for polar organic molecules. Aoyama *et al*. have bound sugars, diols, and amino acids with resorcinarenes.[60-65] One example is the binding of ribose with **27**. There are five different constitutional isomers of ribose in solution (Figure 1.13).

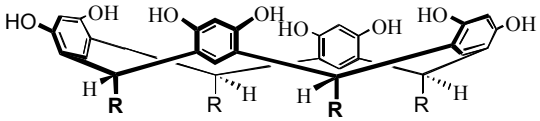

R = $-(CH_2)_{10}CH_3$

27

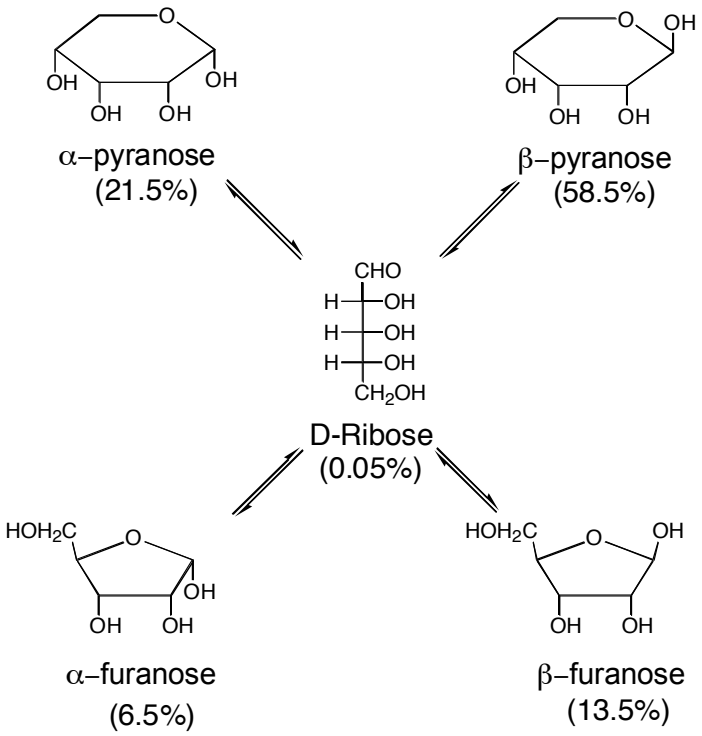

Figure 1.13 Ribose in Solution

The major isomer is β-pyranose in solution. However, when ribose is extracted into CCl_4 with **27**, pyranose is the only isomer found and the α- is preferred to the β- in a 10:1 ratio. The selectivity can be accounted for by the fact that the α-pyranose can form two hydrogen bonds with the resorcinarene host and the β-pyranose can form only one.

Resorcinarenes have some residual flexibility. To further rigidify the structures and enlarge the cavities, Cram *et al*. used different groups to link neighboring phenolitic oxygens (**28**) to synthesize the first cavitands.[55, 66]

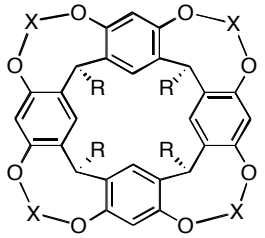

28

Initially, Cram used simple alkyl groups to link the oxygens.[55, 66] When X = CH_2, the cavity is rigid enough to bind small molecules in the solution and the solid state.[56, 67, 68] The host-guest systems were, unfortunately, fast on the NMR time scale and further elaboration of the cavity was required.

The Cram group also used silyl bridges (X = R_2Si). The inward facing alkyl groups reduced the volume of the cavity and only linear guests could bind (carbon disulfide, acetylene and molecular oxygen).[67-69] Thermodynamic evaluation demonstrates that the binding is enthalpically driven with an entropic penalty.

To entrap larger molecules and to increase the association constant, larger cavitands were synthesized. One way is to build up over the resorcinol rings.[70, 71] An example is the cavitand **29**.[72] Atwood *et al.* used the Mannich reaction to form several of these examples.[72] These cavitands were used as ditopic receptors for tetrabutylammonium chloride.

Scheme 1.3 Synthesis of ditopic hosts **29**

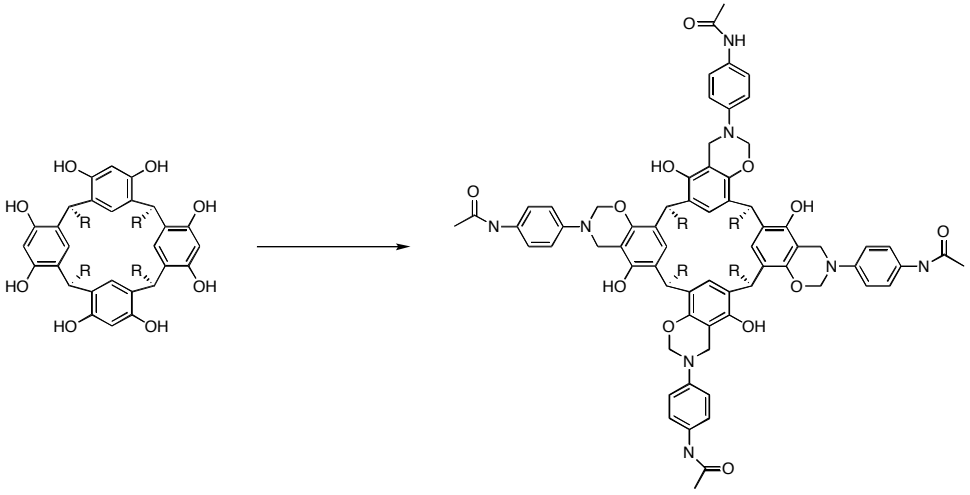

29

Cram continued to link neighboring phenolitic oxygens to make larger cavitands. He synthesized **30** in 34% yield by reacting resorcinarene and 2,3-dichloro-1,4-diazanapthalene.[66]

Scheme 1.4 Synthesis of **30**

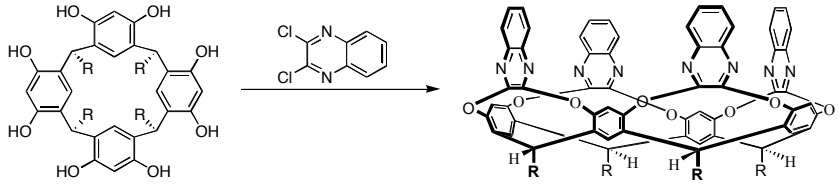

30

The host-guest chemistry of cavitand **30** was studied by Dalcanale *et al*.[73, 74] They found that **30** acted as a good host for substituted aromatic rings.

Cavitands such as **30** have high conformational freedom. The two extreme conformations are known as the "vase" and the "kite": the "vase" conformation with the aromatic walls of the cavity up and the "kite" conformation with the aromatic walls extended. The extent to which conformation is dominant depends on several factors including substitution, electrostatic factors, temperature and solvent.[66, 75, 76] The extended cavitands form dimmers in solution and are known as "velcrands". The considerable conformational freedom enjoyed by these cavitands reduces their ability to act as hosts.

In order to stabilize the vase conformation of these hosts, Rebek synthesized a group of cavitands known as "self-folding cavitands".[77, 78] They began with resorcinarenes that were bridged with 1,2-diflouro-4,5-dinitobenzene to give the octa nitro compound **31**. This was reduced to the octa amine compound **32**. **32** was in turn acylated with various acid chlorides to give the octa amides **33**.

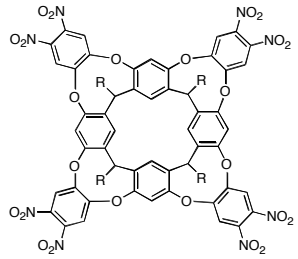

31

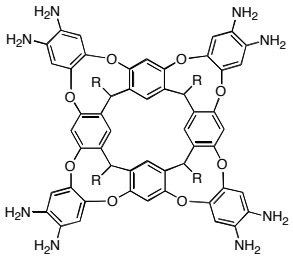

32

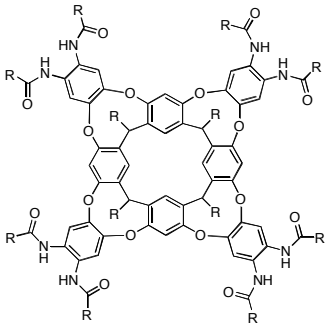

33

The upper rim of **33** allows for the formation of a seam of hydrogen bonds that stabilize the cavitand in a vase formation to the point where guest exchange is slow on the NMR timescale. This cavitand has also been used as a chiroselective receptor by placing strereocenters on the R groups of the amide.[79]

The intermediate octa amine **32** is also a host for choline and other tetramethyl ammonium salts.[9] It has been used by the Rebek group to make a range of deep-cavity cavitands. Other groups can be condensed with the amines to build even deeper cavitands. **34** was synthesized from the condensation of acenaphthenequinone and **32**.[80] The cavity of **34** is ~14Å deep and can act as a host for C_{60} with a K_a of 900 M^{-1}.

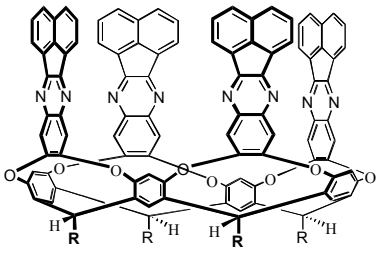

34

Deep cavity cavitands have also been synthesized using substituted benzal bromides as bridging groups (Scheme 1.5). This reaction was largely tolerant of functionality (X = -H, -Br, -I, -Me, -Phenyl, $-CO_2Et$, $-OCH_2OEt$, $-NO_2$, -CN). Unfortunately, these concave molecules were unable to act as hosts due to the rotation around the acetal carbon-aryl bond.[81-83]

Scheme 1.5 Synthesis of Deep cavity cavitands

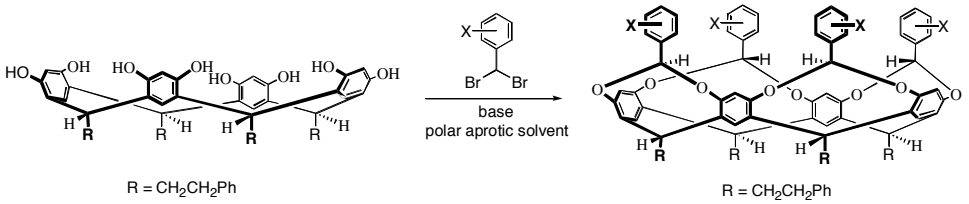

In an attempt to eliminate this rotation, a new host (**36**) was synthesized from the deep cavity cavitand **35** and resorcinol utilizing the Ullmann ether synthesis (Scheme 1.6).[84, 85] This new host (**36**) was called the *meta*-basket (*m*-basket) because of the relationship between the phenols on resorcinol.

Scheme 1.6 Synthesis of *m*-basket

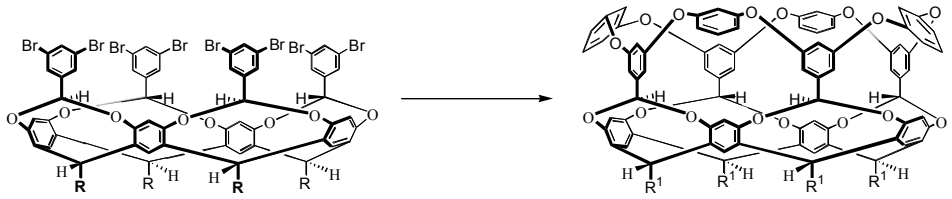

35 **36**

The host **36** was found to selectively bind halogenated guests, especially halogenated substituted adamantanes. A crystal structure of **36** binding iodoadamantane was obtained. Interestingly, the adamatane guest does not completely fill the concave host but instead hovers over its base. The reason for this inefficient packing is the van der Waal overlap of the iodine of the guest, and the ring of four interior acetal hydrogens of the host (Figure 1.14).[84] The x-ray crystal structure as well as 1D- and 2D-NMR indicated the formation of C-H···X-R hydrogen bonds.

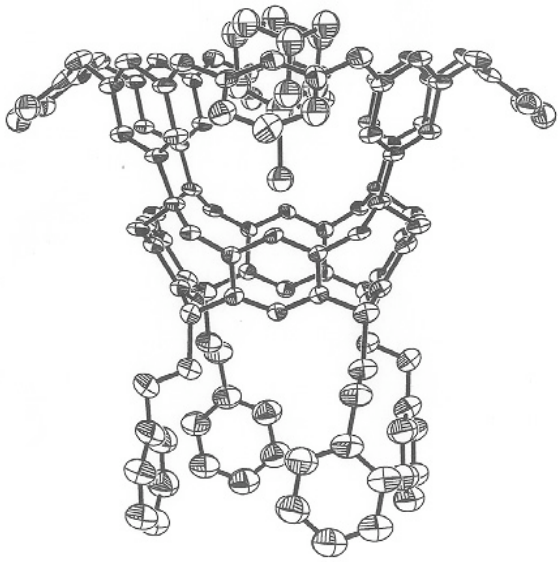

Figure 1.14 Crystal Structure of **36** and Iodoadamantane

C-H···X-R interactions had previously been noted in several other systems. This was however, exclusively in the solid state, and it was unknown if these interactions were attractive.[86-88] Other researchers have since noted C-H···X-R hydrogen bonds in inter- and intramolecular interactions in solution.[89, 90]

Cavitand and resorcinarene hosts have been a fruitful area of research and many new hosts have been developed from the original Cram models. This evolution has allowed the accommodation of larger guests as well as placement of possible reaction centers along the rim. The thermodynamic driving force for complexation is enthalpic gain while there is usually an accompanying entropic loss. The enthalpic gain arises primarily from C-H-π interactions, as well as van der Waals contacts.

1.3.4 Cyclotriveratrylene

Cyclotriveratrylene (CTV, **37**) is a shallow bowl shaped molecule obtained by the condensation of veratryl alcohols under strong acidic conditions (Scheme 1.7).[91-93] Unlike

resorcinarenes and calixarenes, it is unclear whether CTV is a thermodynamic or kinetic product.[92]

Scheme 1.7 Synthesis of cyclotriveratrylene (**37**)

37

Many CTV analogs have been prepared. The requirements of the 3, 4-substituted benzyl alcohols to react are very few (Figure 1.15). The 3-position must be electron donating, which will activate the 6-position toward electrophilic attack. The 4-position's only role is to block this position from undergoing reaction leading to unwanted polymer products.

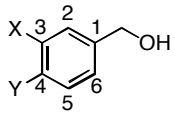

Figure 1.15 Requirements of functionalized benzyl alcohols

If the benzyl alcohol is suitably substituted (X ≠ Y) the resulting CTV will be chiral. An example is **38**.[92] The rasemization rate of this compound was obtained and from that the crown-crown interconversion barrier was found to be 26.5 kcal mol^{-1}. Examination of other substituted CTVs demonstrates similar energy barriers. However the rates of interconversion can be very different.

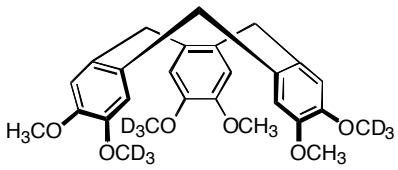

38

Cyclotricatechylene (CTC) **39** is the hexaphenol derivative of CTV. Both of these compounds have been shown to form host/guest complexes in the solid-state,[91-98] although

neither has been shown to act as a host in solution. This inability is due to the shallowness of the cavity and the lack of functionality. To expand the range of host-guest chemistry of this class of molecule, researchers have attempted to deepen the cavity and place recognition points onto the cavity.

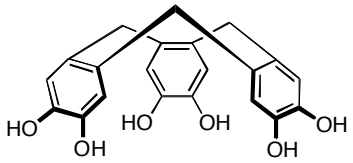

39

Some of the first attempts to increase the binding ability of CTV were made by Hyatt with "octopus" molecules **40**.[92] These long chain polyethers (n = 1-4) are able to non-selectively complex monocations but not dications in aprotic solvent.

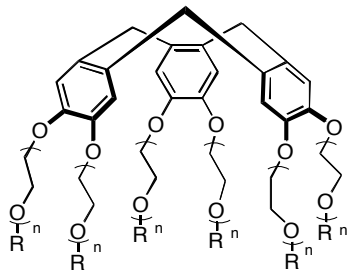

40

Menger *et al*. placed six long chain carboxylic acids on CTV which makes the molecule soluble in basic (pH = 8.6) water.[99] These molecules form micelles (nine molecules) at low concentrations. These micelles will complex a variety of organic, aromatic molecules. For example, *p*-Nitrophenyl butylate is bound and protected from base catalyzed hydrolysis.

In order to expand the concavity and stop the crown-to-crown conversion at higher temperature, Cram bridged neighboring phenols on different aromatic rings with a variety of aromatic molecules **41**.[100] The bridging did rigidify the CTV but the molecule has not been used as a host in solution.

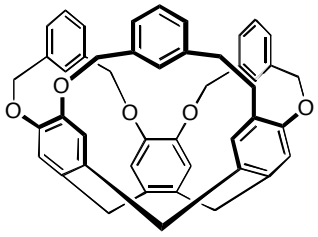

41

To arrange metal coordination sites, as well as to extend the hydrophobic pocket of CTVs, Weiss has bridged the phenolitic oxygens with a variety of pyridine groups (for example, **42**).[101, 102] This locks the CTV in one crown conformation. They are currently exploring the ligand possibilities and host-guest chemistry of this type of CTV.

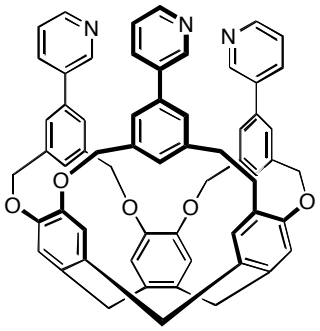

42

Another way to increase the size of the cavity is to build up directly above the aromatic walls of the CTV. The Bohle group has employed metal coordination to increase the size of the cavity.[103, 104] The group has used Schiff base chemistry to place a coordinated nickel on the upper rim (**43**). This rigidifies the structure and offers an additional recognition point for guests.

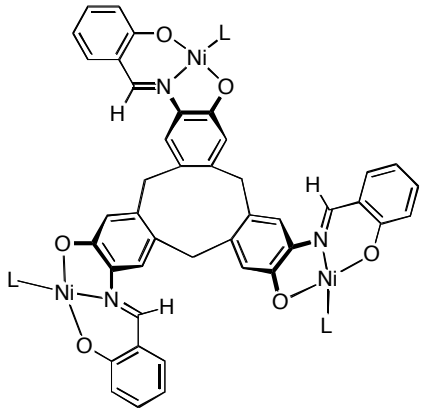

43

Aromatic nucleophilic substitution has been used to increase the volume of the CTV cavity by Pochin.[105] Various substituted aryl fluorides have been utilized to increase the size of the walls of the hydrophobic pocket. The CTV **44** has been shown to bind tetramethyl ammonium tosylate in $CDCl_3$.

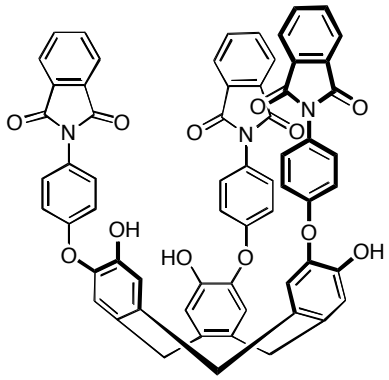

44

CTVs can also act as molecular scaffolds[106, 107] to allow the folding of collagen peptides into triple helixes. This ability to form a helix model using native collagen peptides sequence will allow researchers to evaluate how collagen interacts with peptides and small molecules.

Modified CTVs have also been used as scaffolds in both solution and solid phase combinatorial chemistry.[108-110] Solution studies show that the triple amino acids derivatives (**45**) selectively bind dipeptides. The researchers went on to build a solid phase library consisting of

2197 molecules to identify small peptide trios that were selective for D-Ala-D-Ala or D-Ala-D-Lac dipeptides, which are important in the study of vancomycin resistant bacteria.

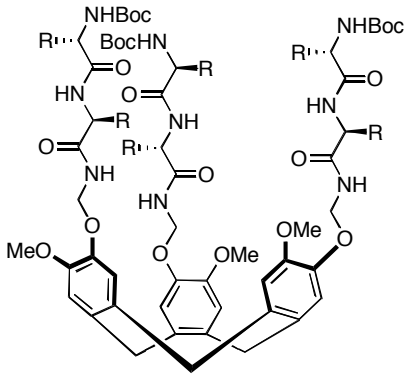

45

CTVs and modified CTVs are beginning to become viable host molecules. Much research has been done to rigidify and increase the size of the cavity while adding recognition points to the cavity. These molecules are unique in that they are chiral when appropriately substituted which may be of use in future research.

1.3.5 Cucurbituril

Cucurbiturils (CB) (**46**) are barrel-shaped molecules which are the product of acid condensation between glycouril and formaldehyde.[111-114] This method gives primarily the cyclic hexamer (n = 6) (Figure 1.15) in 40-70% yield.[115]

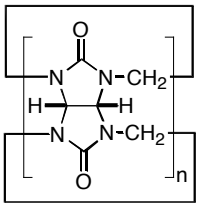

46

Like cyclodextrin, CB has two portals. However, unlike cyclodextrin, which has two dissimilar portals, CB has two indistinguishable portals rimmed by carbonyl oxygens. This

portal has a ~4Å diameter. It opens into a hydrophobic interior which is ~5.5Å in diameter. The combination of the carbonyl oxygens and the hydrophobic interior allow CB to act as hosts.

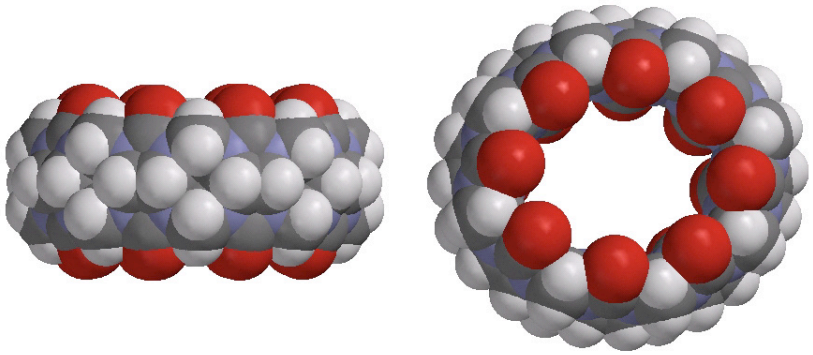

Figure 1.16 Space filling model of CB[6]

The best guests for **46** are linear alkyl chains with multiple amine groups to interact with both the portals' carbonyls simultaneously through ion-dipole and hydrogen bond interactions.[111, 116] These interactions are pH dependent. Therefore, pH has been used to control the motions of molecular machines synthesized with CB.[117, 118] For example, Mock synthesized a pseudorotaxane using CB[6] as a "bead" and a triamine "string" (Scheme 1.8).[119] At acidic pH, CB[6] resides at the doubly protonated diaminohexane "station" because CB[6] forms a more stable complex with diaminohexane. However, when the pH is raised (pH > 6.7), deprotonation of the aniline nitrogen causes the CB[6] to migrate to the fully protonated diaminobutane station to allow the carbonyl oxygens to interact with the protonated amines.

Scheme 1.8 Mock's pseudorotaxane switch

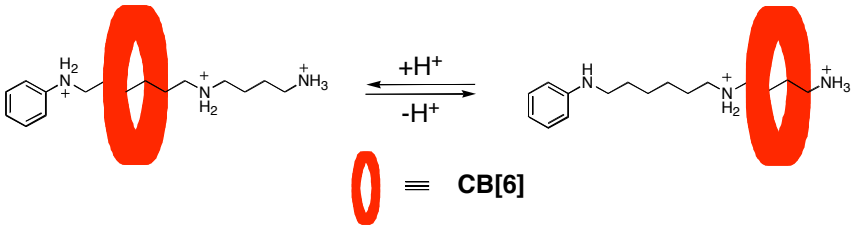

There have been three limitations to using CB as molecular hosts, several of which have been overcome by tireless researchers. Firstly, there was no variety in the size of the

macrocyclic rings of the CB. Secondly, there was no general way to functionalize the exterior of the CB to make it soluble in common solvents. CB[6] is only soluble in formic acid/water solutions. Lastly, there was no general way to functionalize the interior of the hydrophobic pocket to allow for enzyme mimicry or supramolecular catalysis.

In an effort to increase the host-guest chemistry of CB, the Kim group carried out a group of experiments to change the number of glycourils incorporated into the macrocycle.[112, 113, 120] They found that by reducing the temperature of the reaction, CB[5], CB[6], CB[7], and CB[8] could be produced in 15%, 50%, 20% and 15% respectively. The different sizes of the cavities are shown in Table 1.4

Table 1.4 Dimensions of Cucurbit[n]uril

	CB[5]	CB[6]	CB[7]	CB[8]
Outer diameter (Å)	13.1	14.4	16.0	17.5
Portal Diameter (Å)	2.4	3.9	5.4	6.9
Cavity Diameter (Å)	4.4	5.8	7.3	8.8

The change in the size of the host also modifies which guests will be preferred. CB[5] binds Pb^{2+} and ammonium cation. CB[7] prefers to bind 4,4'-dimethyl bipyridinium and adamantaneamine.[121]

CB[8] is large enough to encapsulate several guests in its interior.[122] It is also able to encapsulate cyclen (**47**) or cyclam (**48**). The encapsulated macrocycle can then be metallated with copper(II). The redox chemistry of the copper is significantly different when encapsulated in CB[8] than when it is only ligated by either **47** or **48**.

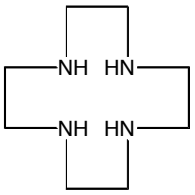

47

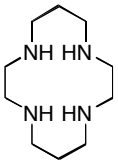

48

Larger CBs have also been observed by MS.[112] CB[10] has been characterized by NMR, MS, and x-ray crystallography with CB[5] as a guest. The two CBs rotate independently of each other and are called "gyroscane".[123] CB[10] is never found without encapsulated CB[5] and therefore it has been postulated that the relative high yield of CB[10] compared to CB[9] and CB[11] is due to temptation by CB[5].

Having increased the number of possible cucurbiturils available for study, researchers then turned to the problem of external functionalization to increase solubility in common solvents. Initially, groups attempted to use different glycourils. The first successful attempt was reported by several groups using dimethylglycouril (**49**).[116, 124] This gives the decamethylcucurbit[5]uril (**50**) in 36% yield with the portals capped by ammonium chloride coordinated to the portal oxygens. When these caps are removed **50** can be used as a molecular sieve in the solid state. However, these homologues are still insoluble in common solvents.

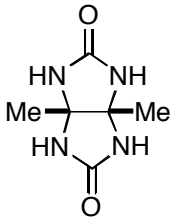

49

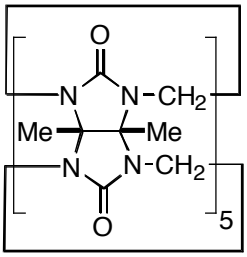

50

Kim's research group used cyclohexanoglycouril and formed **51** with n = 5, 6 in 16% and 2% respectively.[112, 125] Both of these modified CB are soluble in water, DMF, DMSO and methanol.

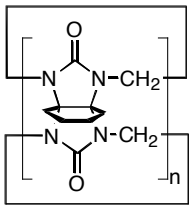

51

Modifying the glycouril does introduce groups on the outside of the CBs. They are however, limited to the few glycourils that will undergo reaction and the sizes of the CBs that are produced. Kim's group developed a more direct synthetic method. Reacting CB[5-8] with $K_2S_2O_8$ in water results in perhydroxylation around the equator of the CB (**52**).[126] These alcohols can be further modified for solvation in a particular solvent or whatever purposes the researcher may have.

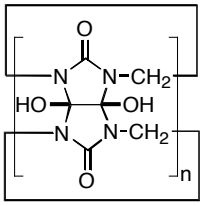

52

These recent advances in cucurbituril chemistry have helped to solve many of the problems presented by the original cucurbituril as a host. Further work is required to functionalize the interior and allow development of an enzyme mimic or catalyst.

1.3.6 Inward Facing Functionality

As demonstrated by the previous examples, there are relatively few concave molecules that have inward facing functionality. Cyclodextrins, the most studied hosts, have few examples of functionality pointed into the cavity, although they have been used successfully as enzyme mimics.[127, 128] Most of these mimics use "caps" to place their functionality near, but not in, the

hydrophobic pocket. Reactive sites placed outside of the hydrophobic pocket can react with substrates not bound by the host. One example is the hydrolysis of *m*- and *p*-nitrophenyl acetate by β-CD. Tee *et al*. used a variety of molecules as inhibitors for the reaction between *p*-nitrophenyl acetate and β-CD.[129, 130] When an inhibitor was used to bind the interior of β-CD, the hydrolysis of *m*-nitrophenol acetate stopped. When the researchers attempted to halt the hydrolysis of *p*-nitrophenol acetate with the same inhibitors they found that instead of slowing or stopping the hydrolysis, several of the inhibitors increased the rate. They found that the hydrolysis was still between the CD and activated ester but that it was occurring outside the hydrophobic pocket.[129, 130]

Breslow has mimicked the co-enzyme pyridoxamine phosphate (**53**) by attaching pyridoxamine to a β-cyclodextrin (**54**).[127, 131] **54** selectively transforms phenyl pyruvic acid to phenylalanine ~100 times faster than pyruvic acid.

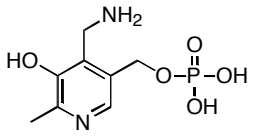

53

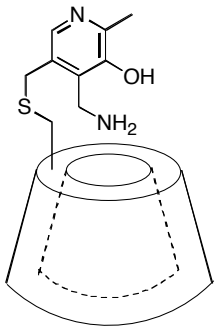

54

More recent examples of CDs having inward facing functionality come from the Bols' group. They have produced several CDs (**55**) that can hydrolyze 4-nitrophenol-β-D-glycoside (**56**). When R = COOH, the rate in water at pH 7.4 is 35 times the background rate.[132] If the R group is changed to –CH(OH)CN, the rate is increased to 1047 times background reaction.[133]

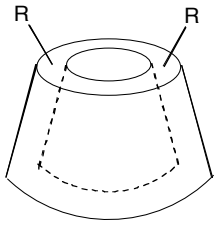

55

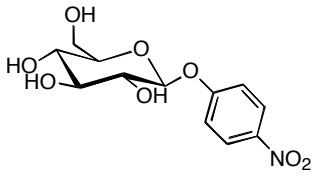

56

Calix[4]arene's relatively small cavity limits the ability to place inward facing functionality.[134] The Chang group used one (**57**)[135] or two (**58**)[136] Kemps triacid moieties to dangle a carboxylic acid(s) into the cavity. The monoacid prefers to bind Cs^{2+} while the di-acid is selective for Hg^{2+}.

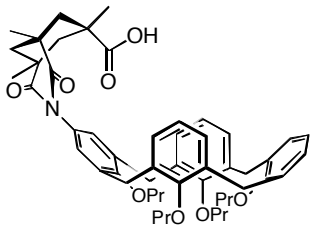

57

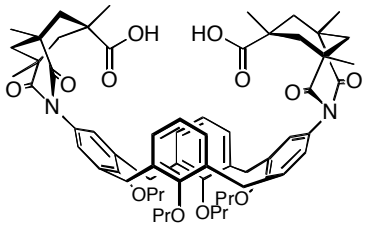

58

The Reinhoudt group has successfully synthesized enzyme mimics by placing metal coordination sites on the rim of the calix[4]arene **59**.[137-144] This does act as a catalyst for phosphate diester transesterification. However, the calixarene is used merely as a scaffold to arrange reactive sites in space. There is no binding of the substrate in the hydrophobic interior.

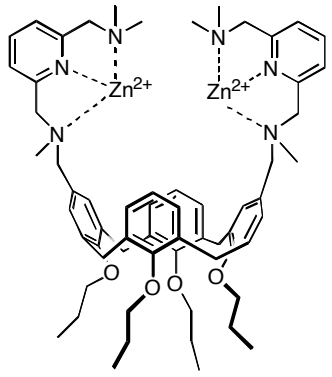

59

Inward facing functionality has also been placed on calix[6]arenes. Unlike calix[4]arenes, the calix[6]arenes have a larger volume and can more easily accommodate inward facing functionality.

The de Mendoza group has used a modified calix[6]arene, **60**, to mimic the action of acetylcholine esterase.[11, 12] They used *para*-nitrophenyl choline carbonate (PNPCC) (**61**) as a mimic of acetylcholine. There are two recognition points. The calixarene cavity will bind the trimethylamine portion of **61** via C-H···π interactions, while the bicyclic guanidinium will bind and stabilize the tetrahedral transition state. When **60** was used, the rate of hydrolysis was increased 1000 fold.[11, 12]

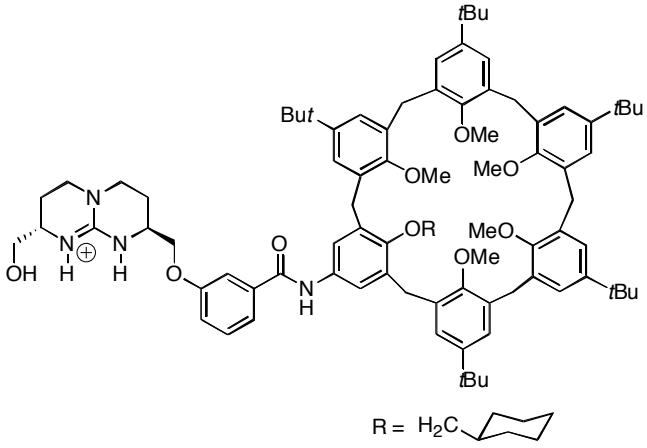

60

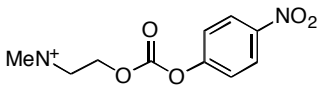

61

A 1, 10,-phenanthroline bridged calixarene has been used to direct the cyclization of cyclopropanes (Scheme 1.9).[12, 145] When no ligand was used, there was a ratio of 66:34 (*exo:endo*). When **62** was used as a ligand, the ratio changed to 99:1, further favoring *exo*. Conversely when **63** was used, the ratio changes to 14:86 in favor of *endo*.[146]

Scheme 1.9 Cyclization of cyclopropanes

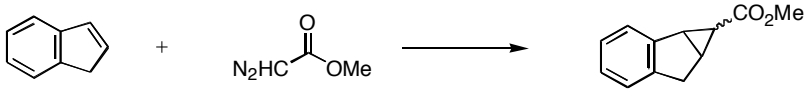

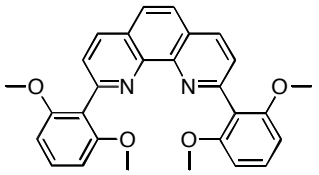

62

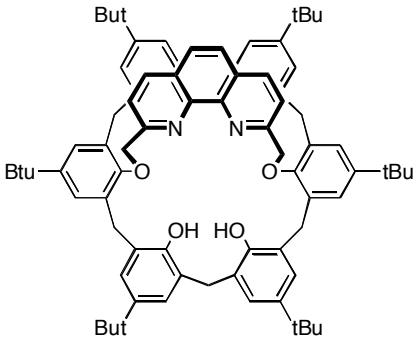

63

The Reinaud group has synthesized a series of "funnel complexes" by placing a nitrogen donor on every other phenol on the lower rim of the calixarene (for example **64**).[147-149] These calixarenes have been stabilized by coordination of a transition metal to the nitrogen donors (Zinc[150-153], Copper (I) and (II)[154-157], Cobalt (II) and Nickel[158]). The metals are tetrahedronally coordinated, three by the nitrogenous ligands and the last coordination site directed into the hydrophobic interior of the calixarene. Therefore access to the metal center is controlled by the size and shape of the cavity.

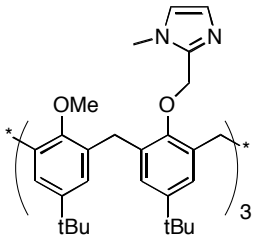

64

The Rebek group has introduced inward facing functionality onto their self-folding cavitands using Kemp's tri-acid. This dangles a carboxylic acid into the deep-cavity cavitand, **65**. The association of **65** and amines is much greater than with self folding cavitand **33**.[159, 160] The methyl ester of **65** has been used to accelerate the methylation of amine guests. For

example, the methylation rate of quinuclidine is 20,000 times greater using the modified DCC then using the model compound **66**.[161]

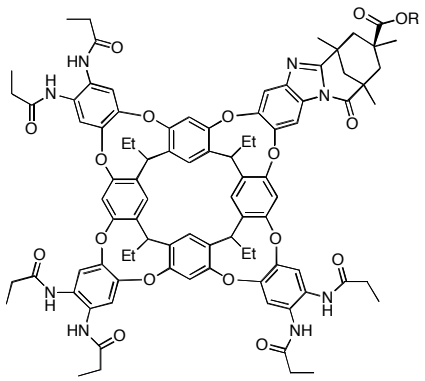

65

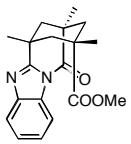

66

Pyridone is a known catalyst for the aminolysis of esters by stabilizing the tetrahedral intermediate (Figure 1.18). With this in mind, Rebek *et al*. have placed a pyridone moiety on the rim of a cavitand (**67**).[10] Consequently, this host can catalyze the aminolysis of only those substrates that are also good guests. The cavity also has an effect because **67** catalyzes the aminolysis of PNPCC (**61**) at a rate twice that of pyridone alone.[10]

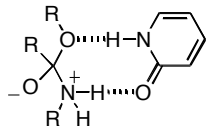

Figure 1.17 Stabilization of tetrahedral intermediate by pyridone

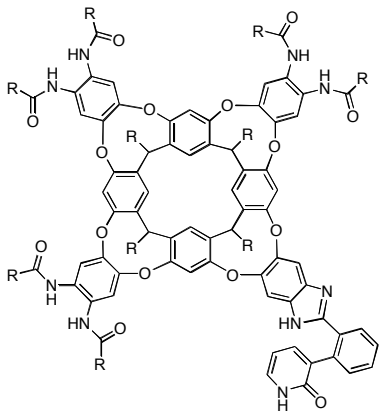

67

The Rebek group has also placed metal centers on their deep-cavity cavitands,[162, 163] with one example being the Schiff base cavitand **68**. This cavitand will catalyze the hydrolysis of **61** with a rate six times that of the uncatalyzed reaction (10 mole %) and when the catalysis is carried out using the ligand **69** (20 mole %).

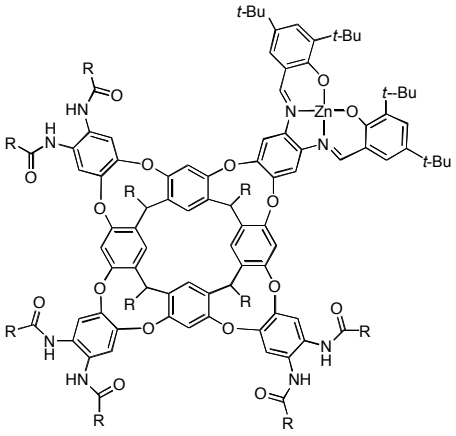

68

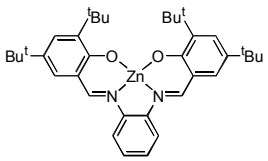

69

While there are many examples of enzyme mimics among these different classes of molecules, very few of them have inward facing functionality similar to an enzyme. This reduces their effectiveness as well as their selectivity. An active site too distant from the binding site will react with loose specificity. When the functionality is placed inside the binding site, there is an increase in both specificity and activity.

II. SYNTHESIS AND CHARACTERIZATION OF *m*-BASKETS

One of the reasons for the catalytic power of enzymes lies in their ability to encase their substrates in an active site. This is usually a concave, hydrophobic area of the enzyme that shields the substrate from the bulk solvent. In this shielded environment usually weak forces can predominate.

Few concave molecules contain a rigid, hydrophobic cavity. Cyclodextrins[30, 127, 128], cucubiturils[111-113, 116], calixarenes[164] and cavitands[55, 165, 166] have been the most studied and the most influential in developing host-guest chemistry. These molecules have demonstrated exceptional hosting ability with a wide range of guests.

The synthesis and binding ability of *m*-basket (**36**) had been completed previously in the group.[84, 85] This host demonstrated selectivity for halogenated adamantanes. NMR spectroscopy and x-ray crystallography demonstrated the formation of C-H···X-R hydrogen bonds between the halogen of the guest and the acetal protons of the host. These hydrogen bonds proved to be a driving force in the host-guest complexation. Previous to this report C-H···X-R hydrogen bonds were seen exclusively in the solid state, and it was unclear if they were attractive.[86-88] Since the initial report, several other groups have demonstrated inter- and intramolecular C-H···X-R hydrogen bonds.[89, 90]

2.1 Syntheses and Conformation of Molecular Hosts

In an effort to better understand the binding of molecular host **36**, two new hosts were constructed. The first host, 5-methyl-*m*-basket, **70** (Scheme 2.1) was designed to hinder the egress of the guest from the host (see below). The second host, 2-methyl-*m*-basket, **71** (Scheme 2.2) was synthesized to reduce the portal radii and the interior volume of the host thereby

changing the guest selectivity. Additionally, the parent host, **36**, was seemingly unreactive and it was hoped that these two new hosts would be jumping off points for further functionality.

The synthesis of 5-methyl *m*-basket (**70**) was similar to **36** using deep cavity cavitand **35** and 5-methyl resorcinol under Ullmann ether synthesis conditions.[167] and was obtained in an 88% yield.

Scheme 2.1 Synthesis of 5-Me *m*-basket (**70**)

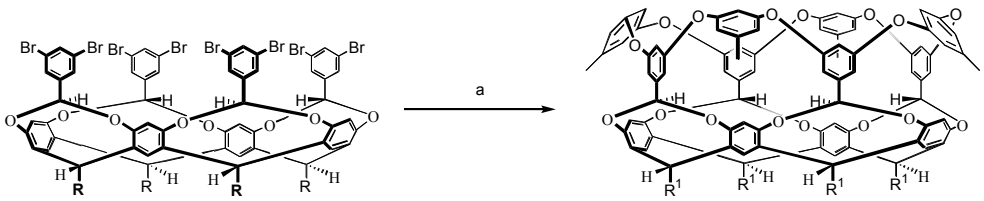

35 **70**

Key: a) 5-methyl resorcinol, K_2CO_3, pyridine, CuO, Δ.

The synthesis of **71** was nearly identical to the other two hosts. The differences included not only the use of 2-methyl resorcinol, but also the reaction time was doubled. This increased reaction time no doubt arises from the steric interactions between the methyl groups of the forming hosts.

Scheme 2.2 Synthesis of 2-Me *m*-basket (**71**)

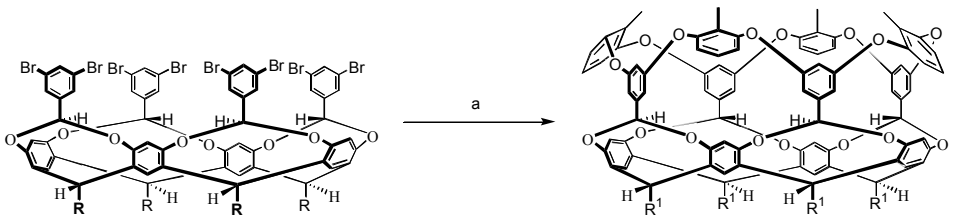

35 **71**

Key: a) 2-methyl resorcinol, K_2CO_3, pyridine, Δ.

Host **70** has a portal and cavity similar in size to that of **36**. As previously mentioned, **70** was designed to reduce the egress of the guests. Two extreme configurations can be envisioned for **36**, **70** and **71**. In one conformation all of the upper row of aromatic rings are out ("open", Fig 2.1a). The alternative conformation has all the aromatic rings in ("closed", Fig 2.1b).

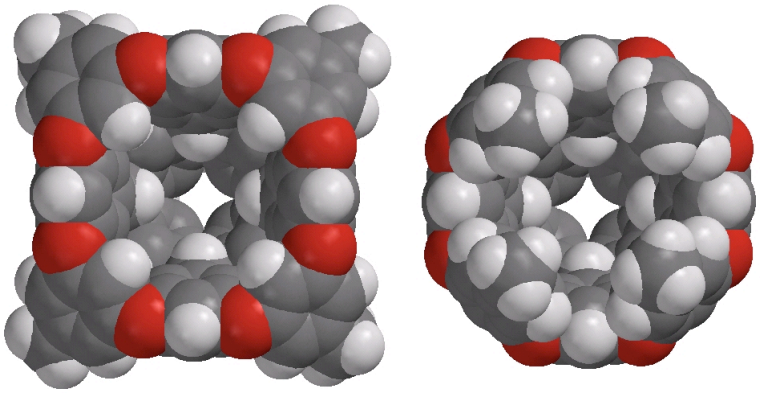

a **b**

Figure 2.1 a. "open" conformation b. "closed" conformation of **70**

The closed portal of **70** would be smaller than the closed portal of **36** due to the intruding methyl groups, and it was believed that in this closed conformation guest egression from **70** would be slowed relative to **36**. Subsequently, however, computational modeling (MNDO) suggests that the open conformation for **36**, **70** and **71** are 9-17 kcal mol^{-1} more stable than the closed conformation.[85, 167, 168] The energy required to flip one of the aromatic rings (Figure 2.2) is relatively low (< 6.5 kcal mol^{-1}). This latter computational work was accomplished by building the respective host and then varying the dihedral angle between the two upper rows of aromatic rings (Figure 2.2). The molecular geometry was then optimized conditional to the dihedral restraints. The phenethyl feet were abbreviated to methyl feet to speed computation.

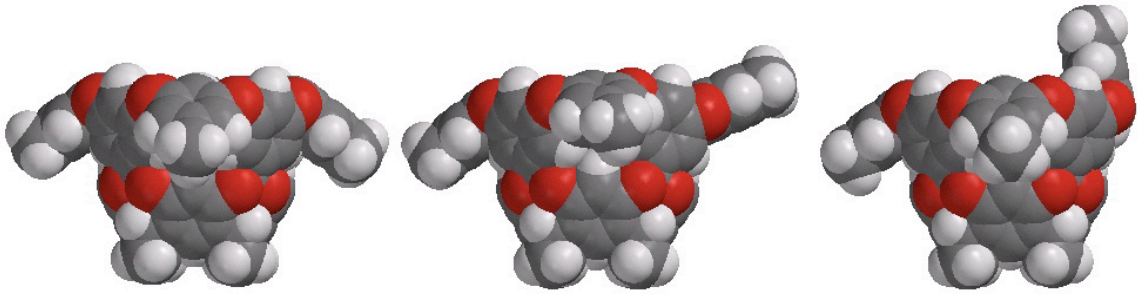

A **B** **C**

Figure 2.2 Optimized geometry of **70** with restrained dihedral angles A - 95° B - 175° C - 285°

1D-NOESY for **70** and 2D-NOESY NMR for **36** and **71** also indicated that the three hosts are primarily in an open conformation (Figure 2.3). If the open position were favored, an NOE interaction would be expected between protons H_f and H_g. However, if the closed position was preferred, then an interaction between protons H_f and H_d would be present. In fact, only the H_f/H_g interaction was observed and there were no cross peaks to indicate a H_f/H_d interaction. This suggests that these three hosts are predominantly in the open conformation with perhaps only an occasional flip of one of the upper row aromatic rings.[167]

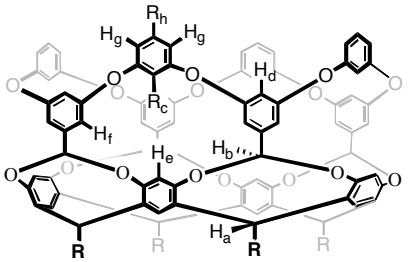

Figure 2.3 Proton designation for hosts **36** (R_c and R_h = H), **70** (R_c = H, R_h = Me) and **71** (R_c = Me, R_h = H)

PC Spartan Pro was utilized to produce potential density maps of the three hosts (Figure 2.4). Note that the most electron deficient portion of each of the hosts is the ring of four acetal hydrogens near the base of the cavity.

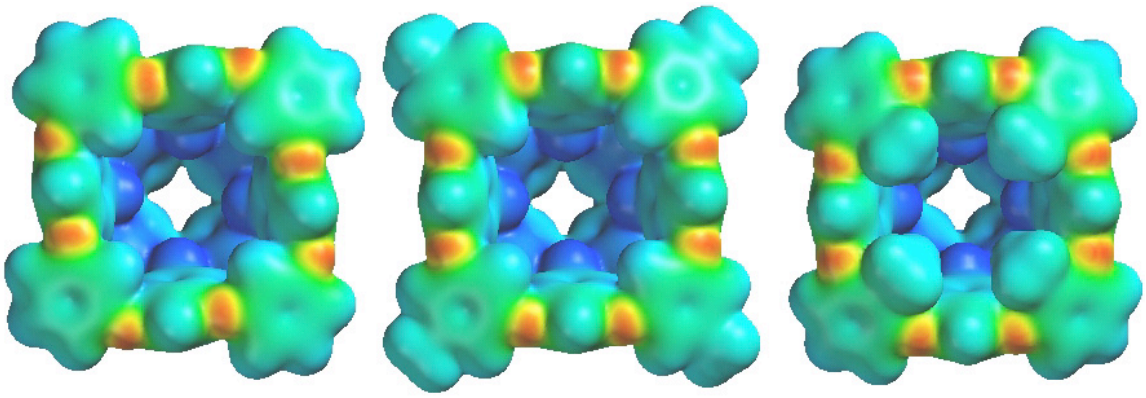

36 **70** **71**

Figure 2.4 Potential Density Maps of Host **36**, **70**, and **71**

2.2 NMR Binding Studies of Molecular Hosts

Binding events can be either fast or slow on the NMR time scale. When guest exchange is slow in the NMR, both peaks for the free and bound species are observed. This is the case with host **70** binding guest **77** in $CDCl_3$ (Figure 2.5).

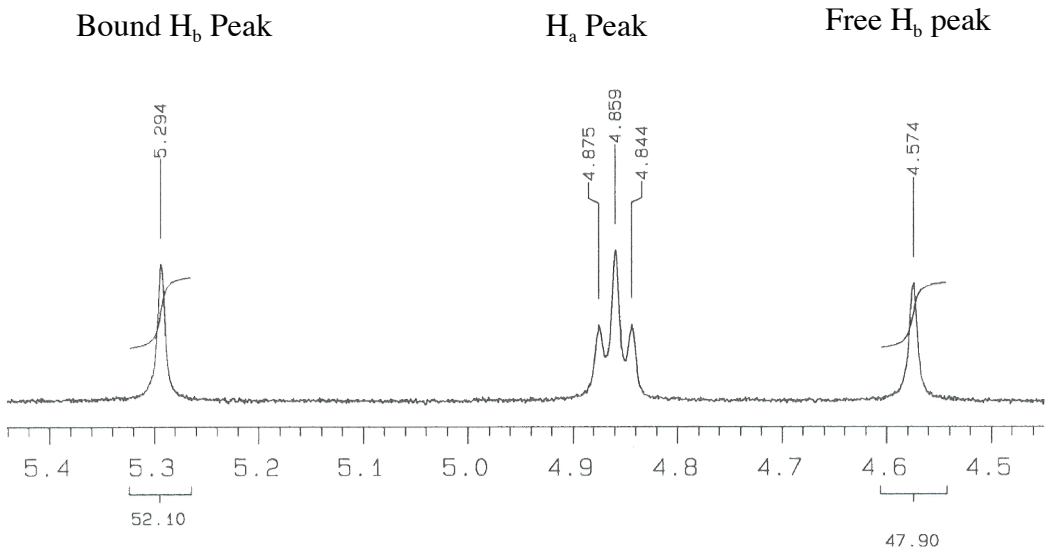

Figure 2.5 Free and Bound Host peaks of **70** binding **77** in $CDCl_3$. See Figure 2.3 for peak assignment.

The free and bound host peaks were integrated to get a ratio of free: bound from which an association constant (K_a) can be obtained with equation 1:

$$K_a = \frac{[HG]}{[H][G]} \quad (1)$$

[HG], [H], and [G] are the concentrations of the host-guest complex, the amount of free host and the amount of free guest respectively.[169]

Alternatively, the exchange of guest from the free to bound states can be fast on the NMR time scale. In this case an average signal of free and bound host peaks are observed. By plotting its shift as a function of concentration of guest, a binding isotherm is obtained. For example, the binding of 1-cyanoadamantane (**73**, Figure 2.7) to **70** in toluene-d_8 was fast on the NMR time

scale (Figure 2.6). Proton H_b was used for this example. In these cases, the association constant can be obtained using equation 2.

$$\Delta = \frac{\Delta_{11} K_a [G]}{1 + K_a [G]} \tag{2}$$

In equation 2, Δ is the shift of the proton of interest, Δ_{11} is the maximum theoretical shift of the proton if it was in the fully bound state, K_a is the association constant, and [G] is the total guest concentration.

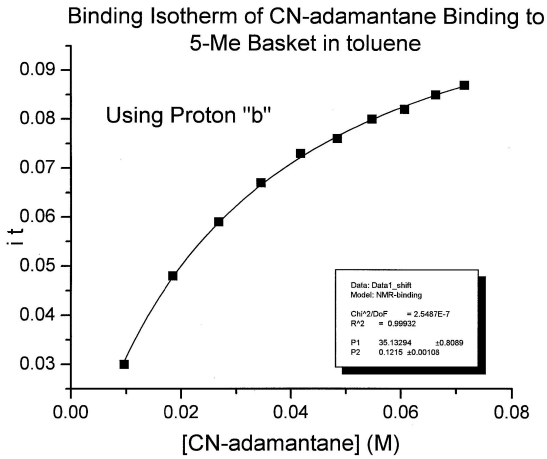

Figure 2.6 Binding Isotherm of Host **70** with **73**

It should be noted that this equation is only appropriate when $[G]_{free} \cong [G]_{total}$.[169] When the association is very strong and this assumption cannot be made, an alternative equation is required (Equation 3).[170]

$$\Delta = \frac{\frac{\Delta_{11}}{2}}{\frac{K[G] - 1 - K[H] + \sqrt{(1 + K[H] - K[G])^2 + 4K[G]}}{2} + 1} \tag{3}$$

This equation adds an additional parameter [H], which is the initial concentration of the host. Both equation 2 and 3 are solved using the nonlinear curve fitting software in Origin.[171]

In order to compare hosts **70** and **71** to their parent host, the data from host **36** is included.[84] (This author did not complete any of the initial binding studies with this host and its inclusion is only for comparison). The hosting properties of hosts **36** and **70** were examined in three solvents: $CDCl_3$, toluene-d_8, and DMSO-d_6. **71** was studied exclusively in DMSO-d_6. Chloroform and toluene are nonpolar solvents with dielectric constants of 4.81 and 2.38 respectively.[172] DMSO is a relatively polar solvent with a dielectric constant of 47.24.[172] All three hosts were readily soluble in $CDCl_3$ and toluene-d_8. However, the hosts were not as soluble in DMSO-d_6 (**70** max solubility is 0.5 mM). The open cavity and rigid nature of the hosts required that their interior be solvated prior to complexation with a guest. Therefore the strength of interaction between the host and solvent played a role in the strength of association between host and guest.

The interior volume of host **70** was similar to **36**, ~280 Å. The smaller internal volume of **71** is 200 Å. The size of the portal and internal volume of these hosts played a role in determining which guest is selected for inclusion. Therefore, a broad range of guests were examined, including linear, cyclic and bicyclic alkanes, and aromatic molecules (Figure 2.7 and Table 2.1).

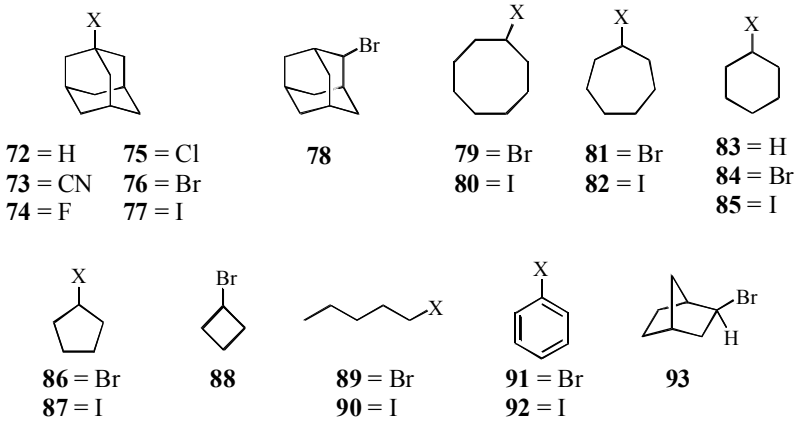

Figure 2.7 Guests used in binding studies

Table 2.1 Physical Properties of Guests[a]

Guest	Dipole (D)	Volume (Å^3)	Symmetry Group
72	0	176	T_d
73	3.04	205	C_{3v}
74	2.12	187	C_{3v}
75	2.25	198	C_{3v}
76	2.24	204	C_{3v}
77	2.20	212	C_{3v}
78	2.12	204	C_1
79	2.20	191	C_s
80	2.17	200	C_s
81	2.18	171	C_s
81	2.14	180	C_s
84	2.14	151	C_s
85	2.10	160	C_s
86	2.01	132	C_s
87	1.96	141	C_s
88	1.95	113	C_s
89	2.05	167	C_s
90	2.00	176	C_s
91	1.76	131	C_{2v}
92	1.76	140	C_{2v}
93	2.08	160	C_1

[a] Dipole and Volume values obtained from PC Spartan Pro using the semi-empirical MNDO model[168]

The adamantane guests were conformationally rigid and therefore the substituted adamantanes have a "permanent directionality" associated with their functional group. The adamantanes were also the largest guests used. Their volume varied from 176 Å^3 to 212 Å^3. All the substituted adamantane guests, excluding **78**, had C_{3v} symmetry. **78** had C_1 symmetry and the highly symmetrical guest, **72** had T_d symmetry. The cyclic guests (**79**-**88**) ranged in size from 113 Å^3 to 200 Å^3. The larger cyclic guests were similar in volume to the adamantane guests. The cyclic molecules (excluding **83**) all had C_s symmetry. The most conformationally flexible of all the guests were the linear halogenated hexanes. The volume of **90** and **89** were 176 Å^3 and 167 Å^3 respectively. The aromatic guests **92** and **91** had the smallest dipoles of any

of the substituted guests (both 1.76 D). Their volume was similar to that of the aliphatic cycles (140 and 131 $Å^3$ respectively).

As expected, host **70** had similar hosting properties to **36**. (Table 2.2). The size and shape complementary of the guest to the host were of paramount importance.[173] For example, **85** was smaller than **90** (160 $Å^3$ v. 176 $Å^3$) but the shape of the **85** was more complementary to host **70** then **90** and therefore had a larger association constant (1100 M^{-1} and 10 M^{-1} respectively). The adamantane guests were the most shape complementary to hosts **36** and **70** and were correspondingly bound more strongly than their smaller counterparts. **77** in DMSO-d_6, for example, had the largest association constant (220,000 M^{-1}) of all the guests tested. When compared to the other iodinated guests in DMSO-d_6: **85** (1100 M^{-1}); **87** (380 M^{-1}); **90** (10 M^{-1}); and **92** (19 M^{-1}) it is apparent what an important consideration size-shape complementary was between host and guest.

Table 2.2 Association Constants of host **36** and **70** at 298K[a]

Guest	$CDCl_3$ (M^{-1})		Toluene-d_8 (M^{-1})		DMSO-d_6 (M^{-1})	
	36[c]	**70**	**36**[c]	**70**	**36**[c]	**70**
72	-	-	15	11	790	1100
73	-	-	36	36	160	200
74	-	-	-	-	400	600
75	53	56	310	520	3600	6000
76	290	240	1600	2300	33000[b]	45000[b]
77	670	740	4400	7000	140000[b]	220000[b]
78	78	77	380	440	9800	17000
84	-	-	13	-	180	270
85	7	-	35	-	580	1100
86	-	-	7	-	76	85
87	-	-	17	-	200	380
89	-	-	-	-	-	-
90	-	-	-	-	9	10
91	-	-	-	-	7	8
92	-	-	-	-	15	19

[a] K_a values are the average of three titrations with an error within 10%. The symbol, "-", indicates that binding was not observed. [b] Calculated by a competition experiment with adamantane. [c] Values from Ref. 84.

Another consideration was the rigidity and preorganization of the guest, as was illustrated by the relatively conformationally free linear hexanes, which are considerably weaker binders than the cyclic hexanes. The cyclic molecules had more conformational degrees of freedom than the rigid adamatanes and were correspondingly more weakly bound.

An additional trend was the increase in association constant with the size and polarizibility of the halogen substituent. As the volume of the halogenated guest decreased from **77** (212 Å) to **74** (187 Å) there was also a dramatic change in the association constant. However, this was not a guest size issue, nor was it a preorganization issue. To illustrate, **73** (volume of 205 $Å^3$) had a similar volume to **76** (204 $Å^3$) while the difference between their association constants was greater than two orders of magnitude. It was indeed apparent that all halogenated guests, save **74**, bind more strongly than non-halogenated guests. The dipole of the guests was also not the reason for an increased association constant. The guest with the largest association with host **70** was **77** (K_a 220,000 M^{-1}). **77** had a dipole of 2.20 D while the guest with largest dipole (**73** – 3.04 D) had an association constant of 200 M^{-1}. These association trends demonstrate that host **70**, like **36**, utilized C-H···X-R hydrogen bonds to drive complexation.

The solvation of the internal cavity affected the strength of association.[167] The weakest association constants were found in chloroform-*d* and the strongest were found in DMSO-d_6. In other words, chloroform-*d* was a more effective competitor for the hydrophobic interior than either DMSO-d_6 or toluene-d_8.

It is interesting to note that in many cases the difference in association constants between **36** and **70** with the same guest is statistically significant. The difference was only present in toluene-d_8 and DMSO-d_6. It is most pronounced with guests that had large association constants. This was an example of a structural alteration, distant from the binding site, having an impact on

the magnitude of the association. It was not clear why this difference was observed but it may be because the methyl groups "push" the upper row of aromatic rings up slightly when compared to parent host **36**, reducing the portal size. This slight reduction of portal diameter could have possibly increased guest residency time, and thus, the association constant. Alternatively, the methyl groups could alter the electronic density of the walls of the cavity, which alters the interaction with the guest.

Thermodynamic characterization of **70** binding was carried out with selected guests in each of the three solvents. For each guest, and in every solvent, the association was enthalpically favored and entropically penalized (Figure 2.8 and Table 2.3).

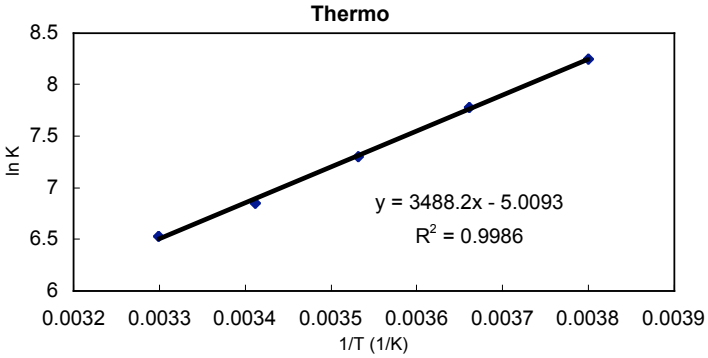

Figure 2.8 von Hoff Plot of Host **70** and **77** in $CDCl_3$

Table 2.3 Thermodynamic Characteristics of host **70**[a]

Guest	$CDCl_3$ (kcal mol^{-1})			Toluene-d_6 (kcal mol^{-1})			DMSO-d_6 (kcal mol^{-1})		
	ΔG	ΔH	TΔS	ΔG	ΔH	TΔS	ΔG	ΔH	TΔS
72	-	-	-	-1.6	-3.2	-1.6	-4.2	-10.1	-6.0
74	-	-	-	-	-	-	-3.8	-8.9	-5.1
75	-2.5	-3.7	-1.2	-3.6	-6.3	-2.8	-5.1	-13.0	-7.9
76	-3.4	-5.8	-2.4	-4.6	-8.2	-3.6	-	-	-
77	-3.9	-7.0	-3.1	-5.2	-9.8	-4.6	-	-	-
78	-2.5	-5.8	-3.3	-3.5	-7.8	-4.2	-5.6	-13.1	-7.5
87	-	-	-	-	-	-	-3.3	-10.4	-7.0

[a]Errors are within ±15% for and average of at least two titrations. The thermodynamic values were determined using the same NMR signals as those used for the determination of the association constants. The symbol "-" denotes that the binding was either too weak or too strong to be determined.

Examination of the thermodynamic trends of **75** with host **70** proved valuable to understanding solvent affects. The free energy and enthalpy of complexation increased from $CDCl_3$ to toluene-d_8 to DMSO-d_6. Additionally, the entropy of complexation decreased in this same sense. These values demonstrated that the complex had become more rigid in DMSO-d_6 and toluene-d_8 compared to $CDCl_3$. In each case however, the enthalpic gain was greater than the entropic penalty, giving rise to an increasing free energy of complexation.

The thermodynamic values obtained in toluene-d_8 can be used to examine substituent effects on complexation. As the volume and polarizablity of the halogen on the adamantane was increased, an enthalpic gain along with an entropic penalty was observed. This was indicative of the complexation becoming increasingly tighter. These values can also give an indication of the strength of C-H···X-R hydrogen bonds. If adamantane can be said to have the same type and strength of interactions as iodoadamantane (except for C-H···X-R hydrogen bonds) then the difference between their free energies must be due to the formation of these four hydrogen bonds. The difference between them is –3.6 kcal mol^{-1} and therefore each C-H···X-R hydrogen bond is worth about –0.9 kcal mol^{-1} in toluene-d_8. However, there may be some synergy and the individual hydrogen bonds are worth less then 0.9 kcal mol^{-1}.

In contrast to hosts **36** and **70**, host **71** did not bind adamantanes due to the methyls that point into the cavity and reduce its size. The largest guest that was observed to bind, albeit weakly, was **81** (Table 2.3). The halogenated cyclohexanes also bound weakly. Surprisingly, both **86** and **87** had relatively large association constants and bound slowly on the NMR time scale.

Table 2.4 Binding Constants of Host **71**[a]

Guest	DMSO-d_6 (M^{-1})
81	12
83	10
84	9
85	22
86	500
87	740
88	32
89	-
90	7
91	-
92	-

[a] K_a values are the average of three titrations with an error within 10%. The symbol "-" indicates that the binding was too weak to be determined.

However, guests smaller than cyclopentane had smaller association constants. To further investigate this preference, van Hoft analysis was performed on several guests (Table 2.4).

Table 2.5 Thermodynamic Characterization of Host **71**[a]

Guest	DMSO-d_6		
	ΔG (kcal mol^{-1})	ΔH (kcal mol^{-1})	TΔS (kcal mol^{-1})
81	-1.4	-8.5	-7.2
86	-3.6	-17.6	-14.0
87	-3.9	-18.6	-14.7

[a]Errors are within ±15% for and average of at least two titrations. The thermodynamic values were determined using the same NMR signals as those used for the determination of the association constants.

The binding of **71**, as with hosts **36** and **70**, was enthalpically favored and entropically penalized. However, the cyclopentyl guests produced both the largest enthalpic gain and entropic penalty of any of the other host/guest systems examined. To further investigate the binding of **71** to **87**, 2D-NMR techniques were employed.

When a guest is bound slowly on the NMR time scale, the bound guest signals are shifted upfield relative to the free signals. This was originally noted in permanently entrapped guests in carceplexes and has also been noted in other open similar host-guest systems.[28, 77, 78, 117]

Additionally, the greater the shift of signal, the deeper the guest's proton is in the host. The 2D-NMR technique, exchange spectroscopy (EXSY), produces cross peaks between two signals that correspond to the same proton in two different environments, such as free and bound. Thus, by examining the cross peaks, the orientation of the guest inside the host can be determined. As an example, **77** was bound slowly on the NMR timescale in $CDCl_3$ (Figure 2.9). The peaks below 1.5 ppm correspond to bound guest peaks. The peaks corresponding to free **77** are at 1.80 ppm, 1.95 ppm and 2.65 ppm. Figure 2.9 shows the cross peaks between the bound and free guest peaks.

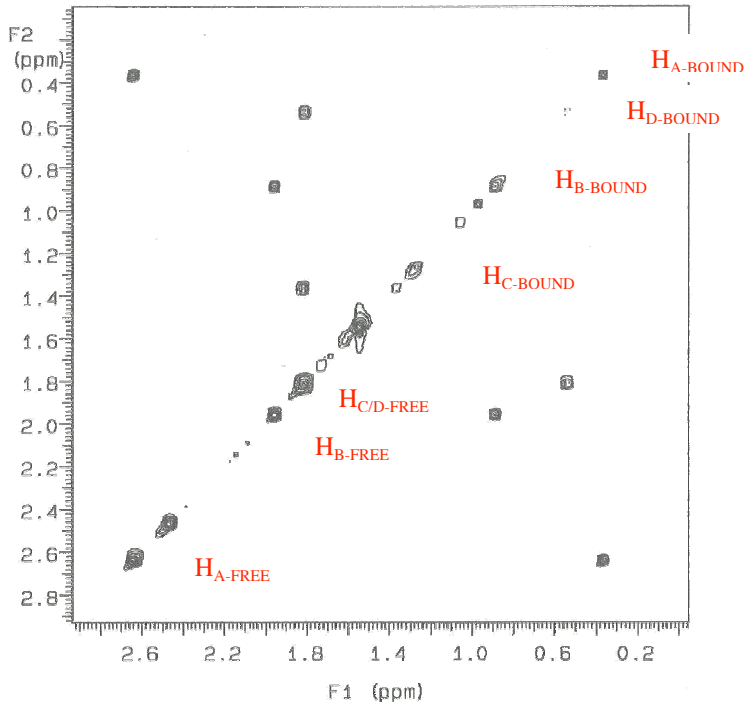

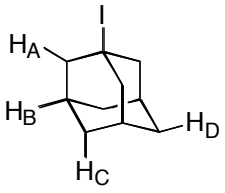

77

Figure 2.9 Up field portion of EXSY NMR of **70** and **77**

The largest change was the protons H_A. This indicated that the iodine was located at the bottom of the cavity. Using this method it was determined that all the halogenated guests (except **74** with its relatively small fluorine atom) bound halogen 'down' in host **36** and **70**. Additionally,

this technique was able to discern why the cyclopentyl guests bound so strongly in host **71** and why the enthalpy and entropy were different than the other guests (Figure 2.10). Once again the protons nearest to the halogen shifted the most. For example, H_A shifted –2.85 ppm. Protons H_B, H_C and H_E are shifted –2.20, -2.32 and –2.26 ppm respectively. The least shifting was observed with peak H_D that 'only' shifted –1.48 ppm.

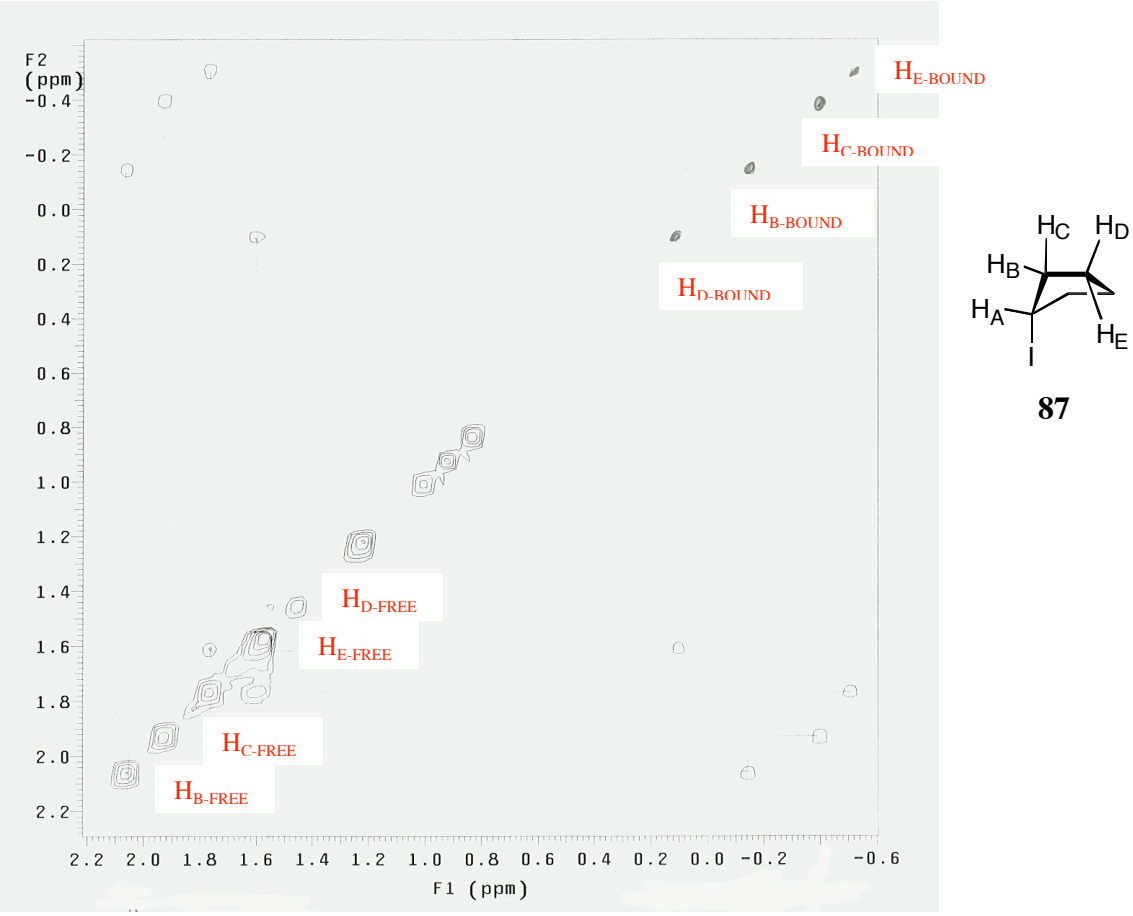

Figure 2.10 2D-EXSY of **71** binding **87** in DMSO-d_6

These shifts indicated that the orientation has H_A deepest in the cavity and H_D nearest to the portal. Unlike cyclohexanes, the conformational preference of cyclopentanes is ambivalent to the axial/equatorial orientation of the halogen substituent.[174, 175] Hence, the cyclopentyl guest was able to fit underneath the methyl groups of **71** with the iodine atom able to form the C-H···X-R hydrogen bonds with the actal hydrogens of the host (Figure 2.11). This restricted

conformation accounted for the large entropic penalty. The ring was not able to flip within the cavity and maintain the C-H···X-R hydrogen bonds.

1D-NMR also indicated the formation of C-H···X-R. When the guest had a -Br, -Cl, or -I, the acetal proton H_b is shifted downfield. When the guest did not have these functional groups, the acetal proton shifted upfield.

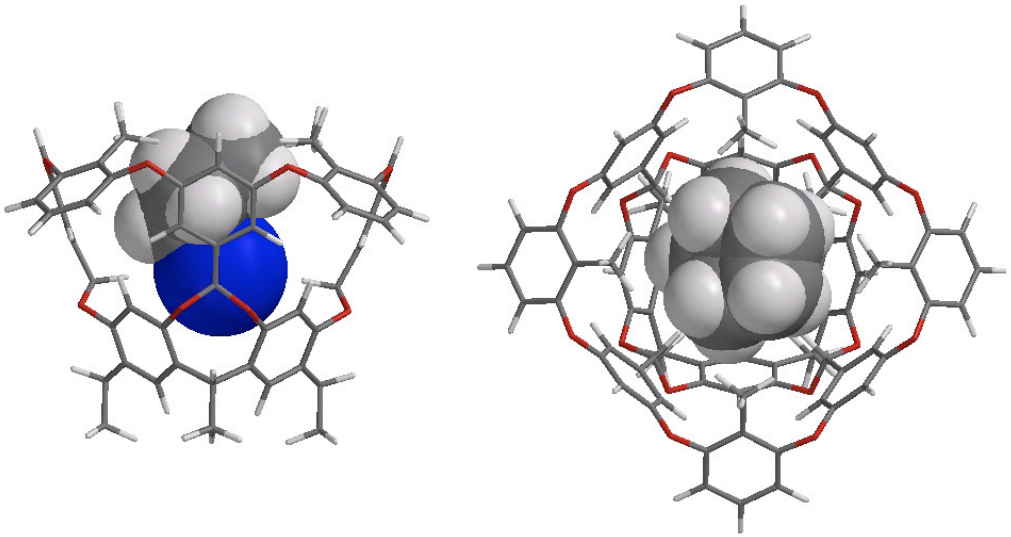

Figure 2.11 Model of **86** binding to **71**

The 1D- and 2D-NMR evidence of hosts **36**, **70**, and **71**, the x-ray crystal structure of **77** binding **36** (Figure 1.14), and the potential density maps of the hosts indicated the formation of C-H···X-R hydrogen bonds were an important force driving the complexation and controlling the orientation of these host/guest systems.

2.3 Synthesis and Hosting Properties of a Deuterated Molecular Host

Researchers have examined the importance of the hydrogen/deuterium substitution in hydrogen bonding and host-guest chemistry.[176-181] Theoretical studies have been carried out to determine the isotope effect in hydrogen bonds. It has been found computationally by Scheiner *et al*. that deuterium is preferred in the bridging position (Figure 2.12) when the hydrogen

acceptor is neutral. Alternatively, when the hydrogen acceptor is anionic, the bridging atom is preferentially a protium.[179]

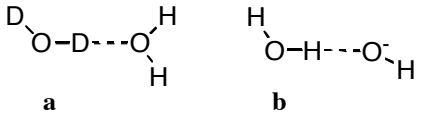

Figure 2.12 Hydrogen bond preference of protium and deuterium

Other experiments are more difficult to interpret. In all cases the guest is deuterated and interacts with an unaltered host. However, in most cases the specific interaction between the guest and the host was unknown and therefore the effect of the deuteration is mostly conjecture.[176, 178] To illustrate, several research groups have attempted to measure the effect of deuteration of caffeine on the association constant with human serum albumin using equilibrium dialysis. The association was decreased depending where on the caffeine the isotope substitution takes place. However, there is no change in the association constant when caffeine was compared to the most deuterated isotopamer. Because the interaction between human serum albumin and caffeine is unclear, the change in association is unknown.

In an effort to examine the effect of deuteration on host-guest dynamics, Rebek and his group have built a host that forms a capsule using two cavitands (**94**) around guest(s) in solution. Because the host molecule was well structured and understood, the researchers could examine how deuteration of the guest affects its interaction with the capsule, other encapsulated guests, and how deuteration effects ability to compete with its protio counterpart for the interior of the cavity.[177, 181] The researchers found that *p*-xylene-d_{10} is preferred as a guest over the protio variant. When only one of the methyls of *p*-xylene was deuterated and used as a guest, the $-CD_3$ group of the *p*-xylene points into the base of the cavity to form C-D···π interactions. These results indicated that C-D···π interactions were slightly preferred over C-H···π interactions.

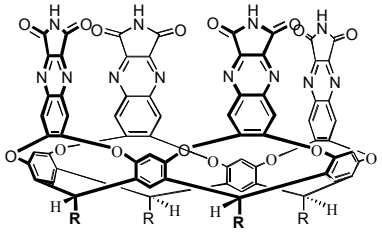

94

Scheme 2.3 Synthesis of d_4-*m*-basket (**99**)

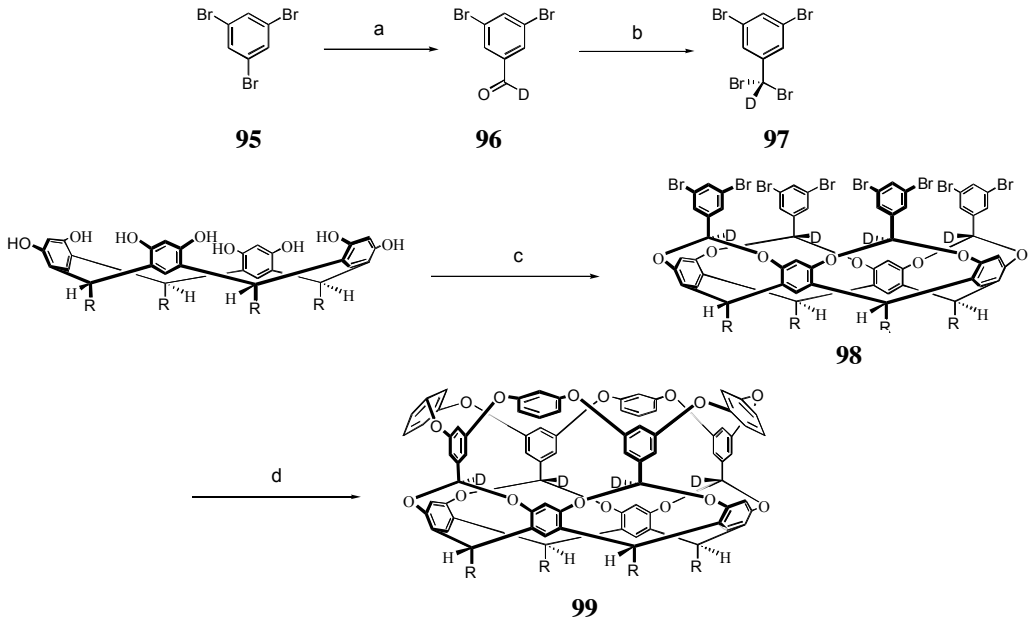

Key: a. *n*-BuLi, diethyl ether, DMF-d_7, H_3O^+ b. BBr_3, CH_2Cl_2 c. **97**, DMA, DBU d. resorcinol, K_2CO_3, CuO pyridine. Thomas Upton completed this synthesis.

To confirm that the C-H···X-R hydrogen bonds are important for guests binding, host **99** was synthesized by Thomas Upton and contained > 90% deuterium acetals by integration. The isotopic substitution of the H_b protons with deuteriums would affect the K_a if the formation of these bonds were essential for complexation.

Several difficulties were encountered in the physical studies of host **99**. The primary difficulty was that the proton used to obtain association constants in host **36** was now a deuterium and therefore not seen by ^{1}H-NMR. ^{2}H-NMR could not be used for two reasons. The

ease with which a particular atom is observed is related to its gyromagnetic ratio.[182] The gyromagnetic ratio of ^{2}H is $4.11x10^{7}$ rad T^{-1} s^{-1}. This is smaller than both ^{1}H ($26.75x10^{7}$ rad T^{-1} s^{-1}) and ^{13}C ($6.73x10^{7}$ rad T^{-1} s^{-1}). Additionally, isotope effects from solvents have been observed when determining association constants with isothermal titration calorimetry (ITC) in H_2O versus D_2O.[180] If ^{2}H NMR was to be utilized, protium solvent would be used and the solvent isotope effect could disguise the isotope effect of forming C-H···X-R hydrogen bonds. Therefore, guests were chosen that would allow the observation of complexation using NMR in both **36** and **99**. Cyclic systems were believed to be ideal because of their relatively high association constant, while binding fast on the NMR time scale allowed the use of several proton signals. To complete the series of cyclic guests, two new guests, **82** and **80**, were synthesized (Scheme 2.4 and 2.5) using modified Finkelstein reaction conditions.[183-186] Additionally, **78** and **93** were chosen to test the effects of guest rigidity.

Scheme 2.4 Synthesis of **82**

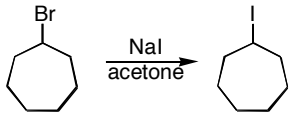

Scheme 2.5 Synthesis of **80**

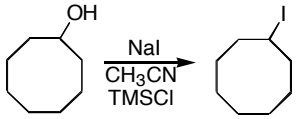

Two guests were used as "blanks", **72** and **73**. Guest **72** has no substituents and therefore the deuteration should have no effect on the association. **73** has a –CN group that points towards the floor of the cavity. If there is a change in association between host and host **99** with **73** then any isotope effects observed arise from different interactions than the formation of C-H···X-R hydrogen bonds.

As expected, the deuteration had no effect on the association constants of the two "blank" guests **72** and **73**. The deuteration also had no effect on the association constants of the cyclic bromines, **79**, **81**, **84**, **86** (Table 2.6). In contrast, the more rigid bromide guests **78** and **93** had significantly different association constants with **99** when compared to host **36**

Table 2.6 Association Constants of bromide guests with Hosts **36** and **99**[a,b]

Guest	Host **36**	Host **99**
72	791	763
73	160	151
78	11330	18104
79	1326	1227
81	419	448
84	208	198
86	85	86
93	610	837

[a]K_a values are the average of three titrations with an error within 10%. [b]Host **99** was > 90% deuterium.

Alternatively, most of the cyclic iodides (**82**, **83**, and **85**) had significant increases in their association constants (Table 2.6). The one exception to the increased association constant is **87**. Models indicate that cyclic guests fill the cavity more efficiently when the halogen is in the equatorial position. While cyclohexanes prefer to have the halogen in the equatorial position, the cyclopentanes have no preference. This elucidates the change of association constant with the cyclohexyl **85** but not the cyclopentyl **87**. The larger volume of iodine allows it to interact with all four acetal protons/deuteriums at once. The increased interaction between the iodine and the deuteriums increases the isotope effect. When the bromide is on a preorganized guest, there is no conformational ambiguity and the bromide has an increased residency time interacting with the acetal protons/deuteriums and an increase in the association constant is observed. Figure 2.13 is a bar graph analyzing the percent change of association constant as the methylenes of the cyclic guest is increased by one (for example, the percent change in association constant when comparing cyclopentyl and cyclohexyl halogen rings). This graph clearly demonstrates that the

largest change in increasing cycles arose from the iodocyclopentane to iodocyclohexane. This further reiterates the importance of guest rigidity to increase the interaction between the halogen and the acetal protons.

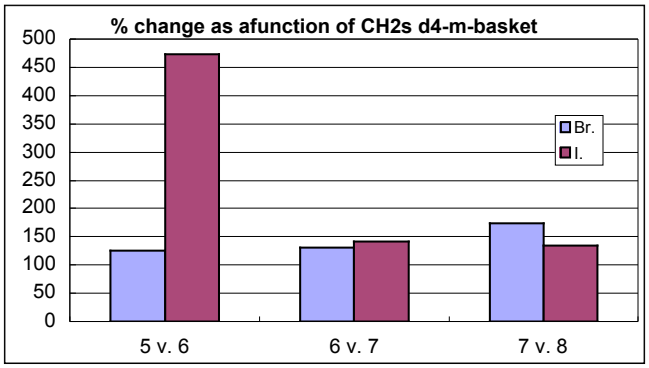

Figure 2.13 Percent change of association constants as a function of cycle size

Table 2.7 Association Constants between Hosts **36**, **99** and Iodide guests[a]

Guest	Host 36	Host 99
80	5958	7923
82	2228	3372
85	923	1391
87	226	243

[a] K_a values are the average of three titrations with an error within 10%. [b] Host **99** was > 90% deuterium.

To further define the isotope effect, a thermodynamic characterization of **99** using **78** as a guest was undertaken. The ΔG°, ΔH°, and TΔS° for **99** were determined to be -5.8, -10.9 and –5.1 kcal mol^{-1}. Alternatively, the ΔG°, ΔH°, and TΔS° for protium host **36** were determined to be –5.5, -8.6, -3.1 kcal mol^{-1}. The same trend of enthalpic gain and entropic penalty was apparent. There was an additional enthalpic gain due to isotopic substitution. This was not unexpected because when C-H···X-R hydrogen bonds are present the free energy change must arise from the alteration of the zero point energy of the CH/CD bond. The zero-point energy is an enthalpic term and therefore changes in the free energy of association must arise from a change in ΔH°.[176] There was a corresponding change in entropy due to the tighter association between **99** and **78**.

To summarize, two new molecular hosts were synthesized from a deep cavity cavitand. The hosting ability of these new molecules was tested. A ring of electron deficient acetal protons near the bottom of these hosts allowed the formation of unusual hydrogen bonds (C-H···X-R) that were selective for halogenated guests. To further elucidate the importance of these hydrogen bonds, a deuterated host was tested. When the C-D···X-R hydrogen bonds were the driving force behind association, an isotopic effect was noted.

III. FUNCTIONALIZATION OF MOLECULAR CONCAVITY

The evolution of host-guest chemistry into enzyme mimetic chemistry necessitates the achievement of certain basic characteristics.[1] These include a rigid hydrophobic pocket; recognition sites; catalytic groups and water solubility at relevant pH.

The placement of *endo*-facing functionality onto a hydrophobic pocket has been explored using several different host molecules including: cyclodextrins[127, 128]; calixarenes[11, 12, 151-158, 164, 187] and cavitands.[10, 159-162] However, due to the difficulty involved, the functional groups are usually "above" the hydrophobic pocket and there are few examples of functionality directed into the cavity. Often the host is merely used as a scaffold to position the reaction centers in space.[137-143] Furthermore, when adding functionality to a host such as cyclodextrin, there are a number of regioisomers that can result.[33]

Some recent successes in developing hosts with *endo*-facing functionality have been reported. A recent example from the Rebek group utilizes Kemp's triacid to suspend a carboxylic acid into a deep-cavity cavitand **65**.[159-161] This has been used to increase the host's affinity for amine guests.

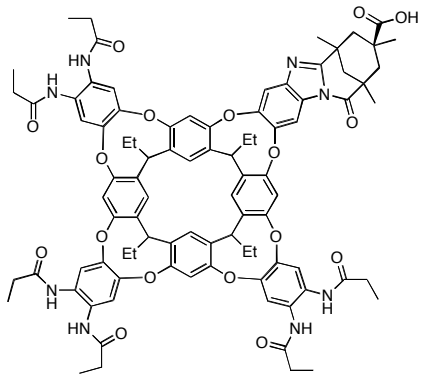

65

In order to further develop host-guest chemistry, tactics must be developed to place functionality onto concave molecules. These tactics should include methods to integrate

functionality at chemically/environmentally distinct positions as well as avoiding the nonselective difficulties encountered with cyclodextrins.

With these points in mind, possible reaction sites on host **36**, **70** and **71** were sought for. The host molecules, **36** and **70** have twelve protons that could be active toward directed *ortho* metallation while **71** has eight. These protons are activated due to the presence of two ether oxygens *ortho* to them. However, the four protons on the original resorcinarene macrocycle (H_e in Figure 2.3) are inaccessible. The remaining eight protons are located on the upper rim of the cavity. One of these protons point into the cavity (called "*endo*" proton, see below) and the other set of protons points along the cavity wall away from the cavity (called "*exo*"-proton, see below). In order to investigate the formation of a host with inward facing functionality directed ortho metallation was investigated using host **36**.

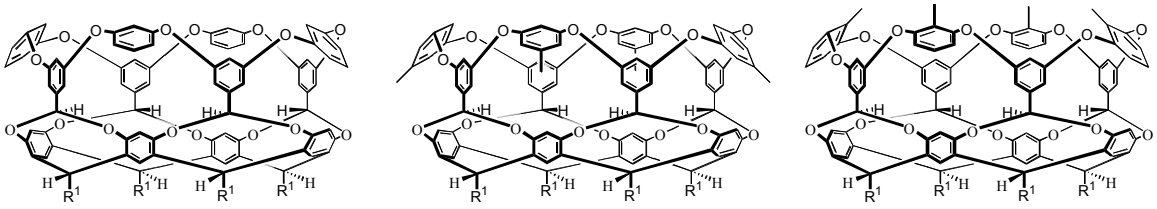

36 **70** **71**

Directed *Ortho* Metallation is a reaction technique that was originally discovered by Gilman and Wittig.[188] The principal of the reaction is that directing groups on an aromatic ring will direct metal-bases to remove protons *ortho* to themselves.[189, 190] A general, simplistic scheme is shown (Scheme 3.1). This scheme ignores any aggregation of the lithiate before and during reaction.

Scheme 3.1 Reaction Mechanism of Directed *Ortho* Metallation

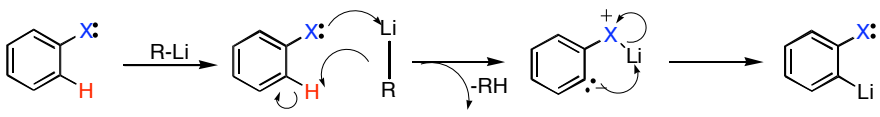

The X-substituent is known as the directing group. The only requirement for directed *ortho* metallation is that the directing group, X, has at least one pair of unshared electrons to coordinate the lithium. Many groups can direct this reaction, however not all directing groups have the same ability. Strong directing groups include carbamates and phenyl ethers. Moderate directors include triflouromethyl and methyl ethers. The weakest directors are deprotonated alcohols and thiols.[189]

3.1 Possible Products and Nomenclature

The ether oxygens along the rim of **36** act as directing groups. There are two sets of four "activated" protons, *endo* and *exo* (Figure 3.1a and b). The *endo* proton is directed into the hydrophobic interior while the *exo* proton is directed up and away from the interior.

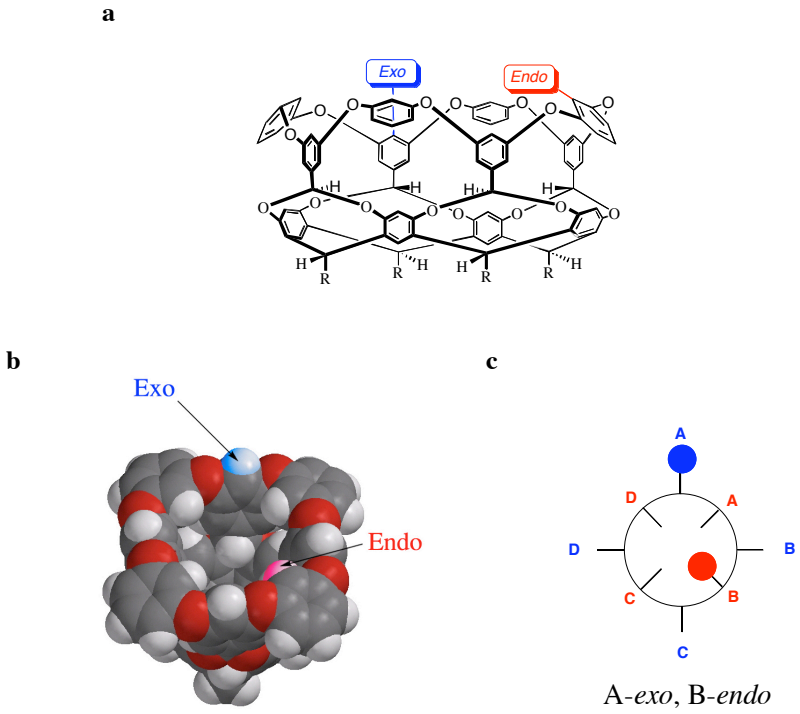

Figure 3.1 *endo*- and *exo*- position and nomenclature

For convenience, the following nomenclature has been developed (Fig 3.1c). Looking down into the pocket, the *exo*-positions are given priority and are labeled A-D in a clockwise

manner. Similarly, the *endo* positions are labeled A-D starting with the *endo* position immediately clockwise to the A-*exo* position. The substituents are given the lowest possible alphabetical designation. Therefore the substitution pattern shown in Figure 3.1b and c is A-*exo*-B-*endo*. Per-lithiation could give rise to sixty-nine products (seventy if the starting material is included) ranging from mono-substitution through octa-substitution (Figure 3.2). There is symmetry to the range of possible product formation. There is only one regioisomer that can arise from either zero or eight substitutions. There are two regioisomers that can arise from either mono or hepta-substitution. There are eight regioisomers that can arise from either tri- or hex-substitutions. Fourteen regioisomer can arise from either tri- or pentasubstitution products. Finally, there are twenty regioisomers that can arise from tetrasubstituted products.

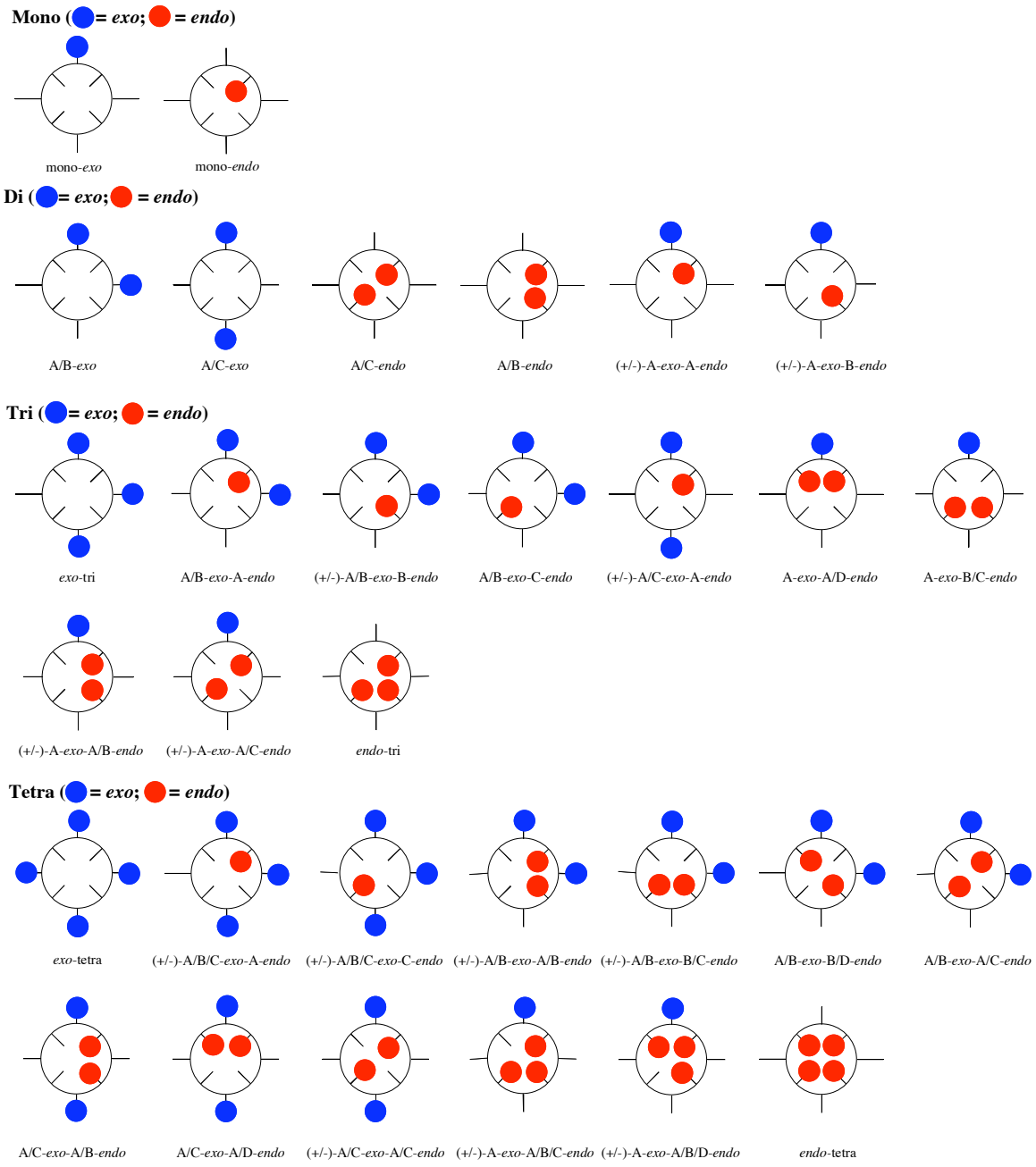

Figure 3.2 Possible Substitution Patterns from per-lithiation

The electrophile initially chosen to quench the reaction was *N*,*N*-dimethylforamide (DMF) which after acidic work up produces the respective aldehyde. DMF was selected as the electrophile for several reasons. The aldehyde ^{1}H-NMR signal is distinct and distant from other proton signals of the host. Additionally, the carbonyl functional group allows a great number of

subsequent transformations. When DMF was used as the electrophile, twelve products were obtained under three different reaction conditions (Figure 3.3).

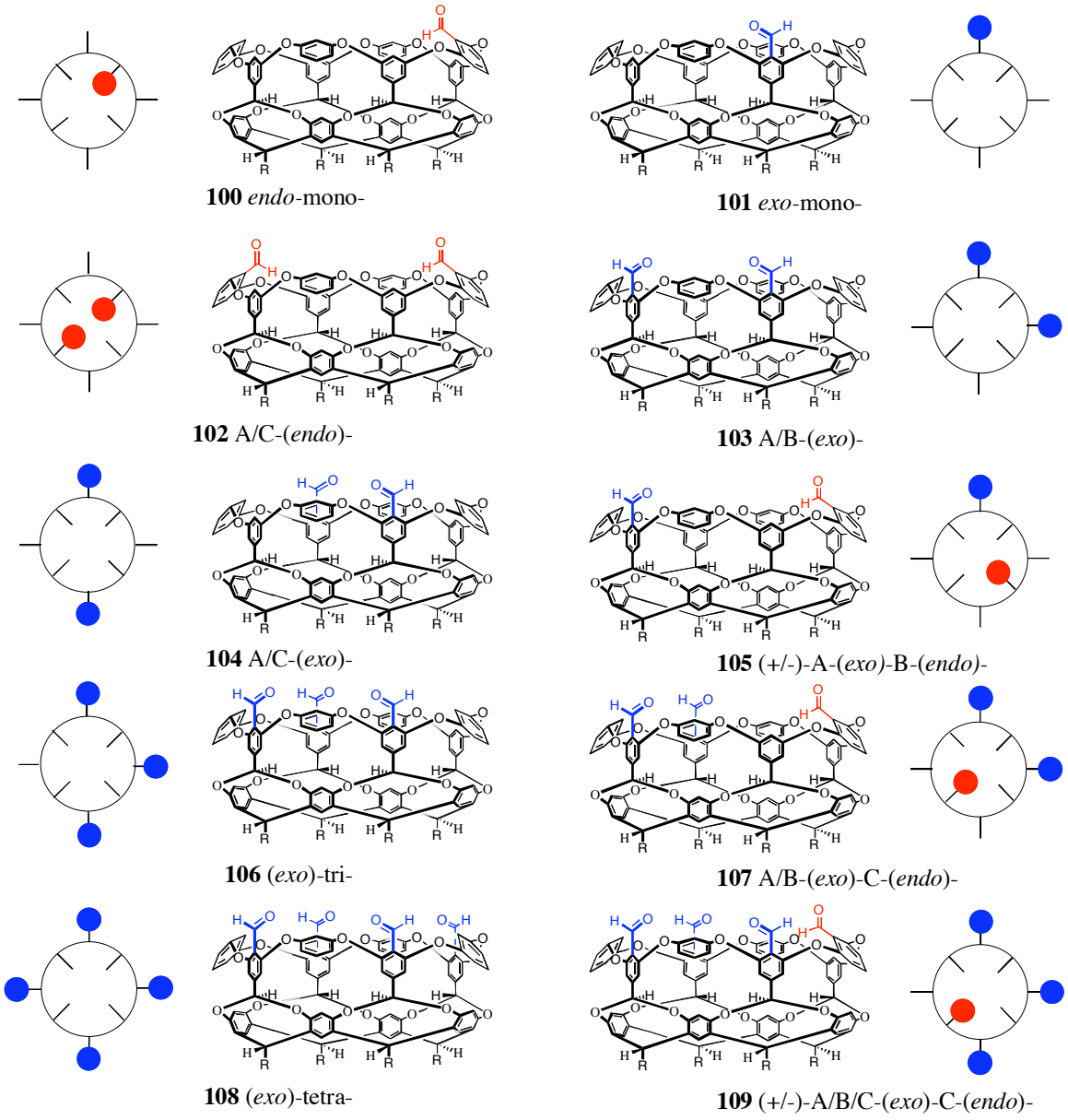

Figure 3.3 Chemdraw and cartoon structures of aldehydes produced under the reaction conditions used.

Product determination was accomplished using 1D- and 2D-NMR spectroscopy, MALDI-MS, and symmetry considerations. For example, both of the mono-substituted aldehydes (**100** and **101**) have C_s-symmetry, the same molecular weight, and the same elemental analysis. However their NMRs can be expected to be very different (Figures 3.4, 3.5 and 3.6).

- Benzal protons: Exo-substitution gave rise to two singlets in a 1:3 ratio. Endo-substitution gave two singlets in a 2:2 ratio.
- E – protons: Exo-substitution produced two singlets in a 2:2 ratio and endo-substitution gave three singlets in a 1:2:1 ratio.
- H - protons: Exo-substitution had very little effect on the shift of this proton. However, endo-substitution, on the same aromatic ring as H, shifted this triplet downfield to 7.8ppm.
- Aldehyde protons: There was a difference of 0.7ppm between the aldehyde protons of the two singly substituted products. The shielding afforded to the endo facing aldehyde shifts the signal for this proton upfield while the exo-aldehyde proton is seemingly unaffected.

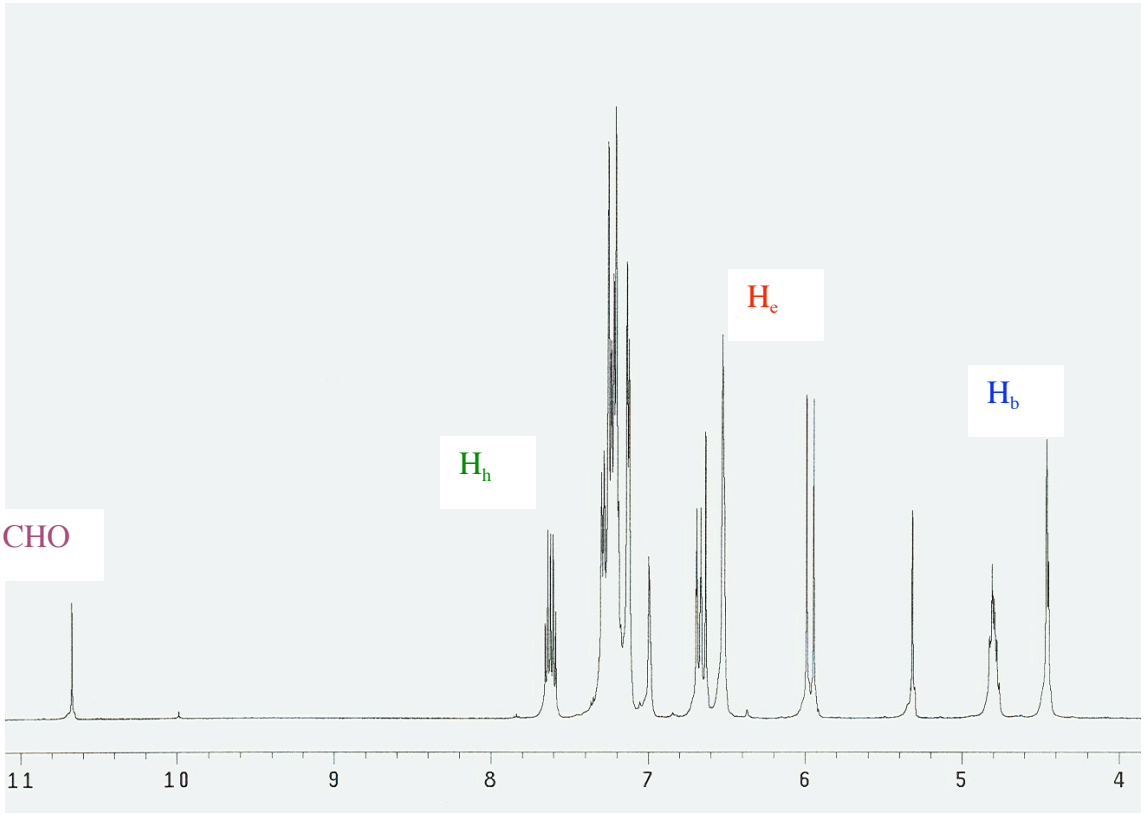

Figure 3.4 ^{1}H-NMR of **101**

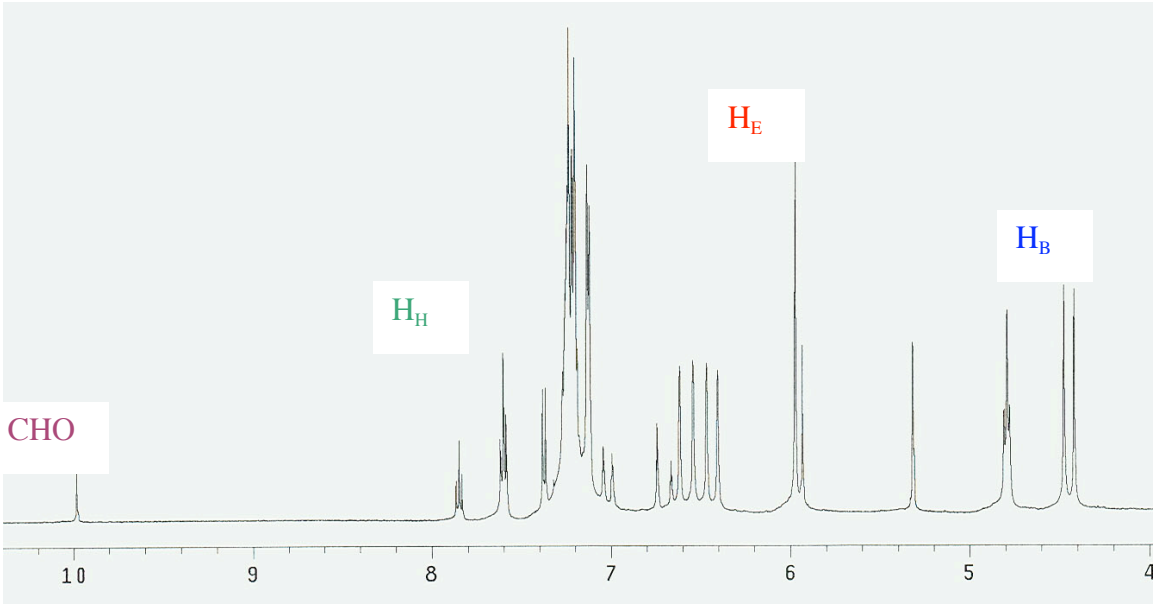

Figure 3.5 ^{1}H-NMR of **100**

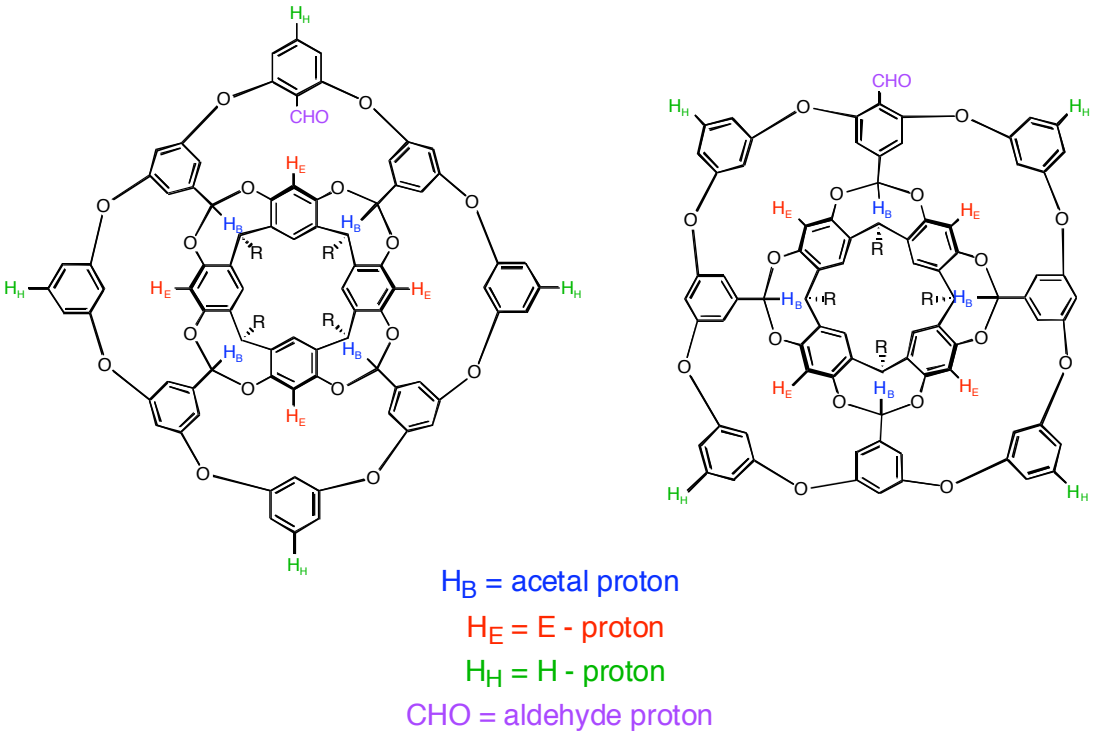

Figure 3.6 Chemdraw pictures of substituted *m*-baskets indicating reporter protons (Plan view).

One difficulty encountered during product identification was that the aldehyde proton signal always integrated for less than expected. However, signals from multiple aldehyde groups were always in the appropriate ratio. For example, the aldehyde peaks for A/B-exo-C-endo

(**107**) integrated in a 2:1 fashion when compared to each other, while they collectively integrated for <3 when compared to the rest of the molecule. Two routes were chosen to ensure that product determination was correct. The first was to reduce four of the aldehyde substituted hosts to their corresponding benzyl alcohols. The aldehydes selected were **100, 101**, **107**, and **108**. The second was to determine the T1 and d1 times of the respective aldehyde proton signals. If the relaxation time of the pulse sequence is too short for a proton to relax, the peak of the proton will not integrate for the correct number of protons when compared to the rest of the molecule.[182]

The reduction of the aldehydes was accomplished using $LiAlH_4$ for the mono-aldehydes (yields: 80% **100** and 99% **101**) and $NaBH_4$ for **107**, and **108** (94% yield for both) (Scheme 3.2).

Scheme 3.2 Synthesis of benzyl alcohols *m*-baskets

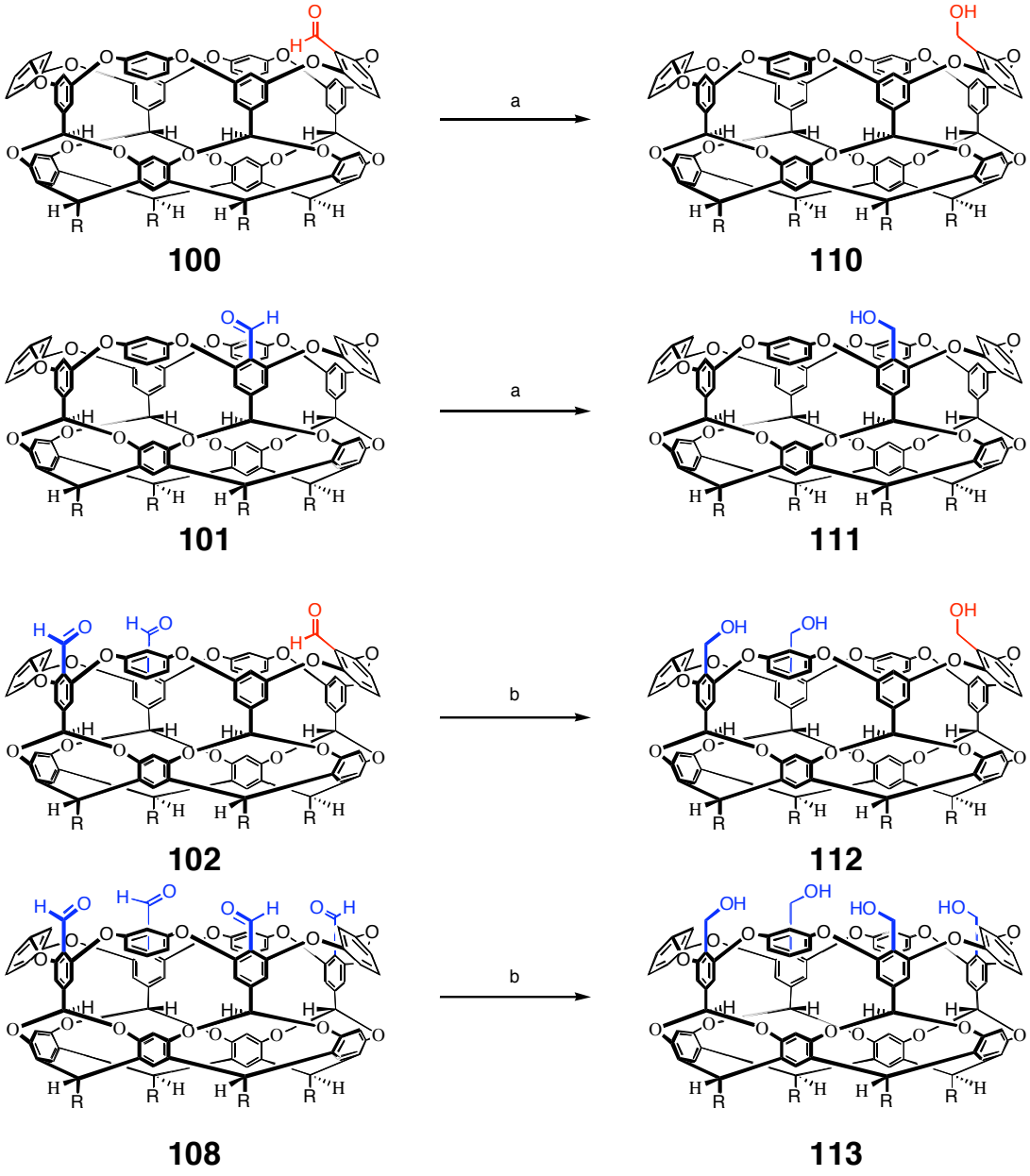

Key: a. $LiAlH_4$, THF b. $NaBH_4$, THF

The benzyl alcohols gave the same integration pattern as their corresponding aldehydes. In addition, there was a new singlet in the NMRs of **110** and **111** that integrates for 2Hs. In **111** the new peak appeared at 5.56 ppm and at 4.38 ppm in **110**. **112** gave two new singlets: one at 5.04ppm, which integrated for 4H, and one at 4.38 ppm that integrated for 2H. Once again, the aromatic rings of the cavity shield the *endo* protons and shift their signal upfield. The reduction

of **108** gave rise to a new doublet at 4.71ppm in DMSO-d_6, which integrated for 8Hs. Unlike the proton signals of the aldehydes, the integration of the protons of the benzyl proton was correct when compared to the rest of the spectrum. Therefore it seemed that the change in d1 and T1 times were unique to the aldehydes.

The d1 and T1 relaxation times were determined by arraying d1 and d2 of the NMR pulse sequence. The d1 time is the delay time between magnetic pulses. A too short delay time makes it impossible for the protons to relax back to their resting state. The d1 time was arrayed and the integration of the aldehyde peak and the proton H (Figures 2.3 and 3.6) were examined to determine the d1 time of the formyl proton. The formyl proton of **101** should integrate in a 1:4 (aldehyde proton: H_H-proton) fashion while the formyl proton of **100** should integrate in a 1:1 fashion (Aldehyde proton: H-proton *para* to aldehyde substitution). The lowest d1 time that gave the proper integration is the d1 time of proton. The d1 time of the formyl peak of **101** was determined to be 40 s and the d1 time of the formyl peak of **100** was 25 s (Figure 3.7).

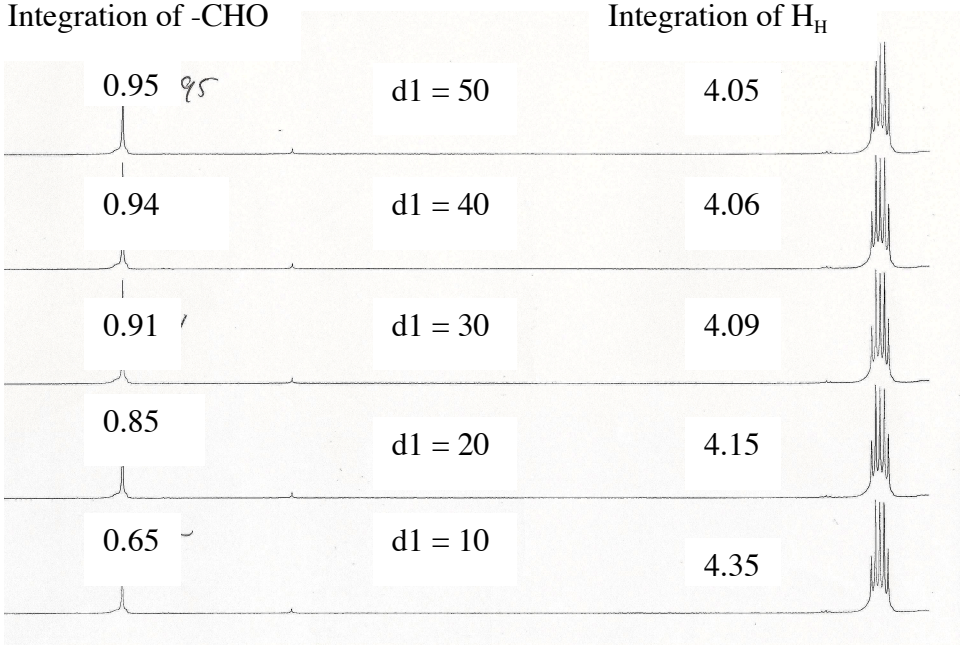

Figure 3.7 d1 array of **101**

T1, also known as the spin-lattice relaxation time, is the time it takes for a population of protons to relax back into a resting state after a magnetic pulse. The T1 time of a proton signal is determined by arraying the d2 time, which was then related to the intensity of the peak of interest. The inverse of T1 (1/T1) is the rate-constant of relaxation. It is determined by equation 4:

$$\ln(I_0 - I_Z) = (-1/T1)t + \ln 2(I_o) \quad (4)$$

In this equation I_0 is the maximum intensity possible; I_z is the intensity at d2; and t is the time (d2). When $\ln(I_0 - I_Z)$ is plotted as a function of t, a linear plot is formed whose slope is equal to –1/T1. This was accomplished using built-in VNMR Varian programs. The T1 of the formyl proton of **101** was 8.33 s and the T1 of the formyl proton of **100** was 5.53 s. In order to verify that these values were applicable to multiple substituted baskets, A-*exo*-B-*endo* di-aldehyde (**105**) was tested. The T1 of the *exo* proton was found to be 8.20 s and the *endo* was 6.02 s. The faster relaxation time of the *endo* proton could arise from interactions with bound solvent or intramolecular interactions unavailable to the *exo* proton such as interaction with the aryl rings across the cavity from the aldehyde proton.[182]

3.2 Base strength and Product Yield

MeLi and PhLi did not remove any of the activated protons. The more powerful *n-, sec-* and *tert*-BuLi, however, were able to deprotonate **36** (Table 3.1).

Table 3.1 Product distribution of lithiation/formylation reaction[a]

Base	Equivalents	**36**	**100**	**101**	**102**	**103/104**	**105**	**106**	**107**	**108**	**109**
n-BuLi	1.1	100	-	-	-	-	-	-	-	-	-
n-BuLi	2.2	68	11	12	-	-	-	-	-	-	-
n-BuLi	5.5	-	7	8	13	31	24	-	-	-	-
n-BuLi	10	-	4	6	10	43	22	-	-	-	-
sec-BuLi	1.1	100	-	-	-	-	-	-	-	-	-
sec-BuLi	2.2	100	-	-	-	-	-	-	-	-	-
sec-BuLi	5.5	-	-	-	-	-	-	20	20	30	3
sec-BuLi	10	-	-	-	-	-	-	14	8	60	-
tert-BuLi	1.1	100	-	-	-	-	-	-	-	-	-
tert-BuLi	2.2	100	-	-	-	-	-	-	-	-	-
tert-BuLi	5.5	-	9	10	-	19	10	12	11	-	-
tert-BuLi	10	-	-	-	-	-	-	18	23	19	13

Key: [a] All yields are the average of at least two reactions. The symbol "-" indicates that the product was not formed under the reaction conditions. [b] Combined yield of two products that were inseparable.

As the results show, the product distribution is a function of the amount and choice of base (Figure 3.8a and b). Mono- and di- substitutions were obtained from *n*-BuLi, while tri- and tetra- substitutions were obtained from *sec*-BuLi. *Tert*-BuLi gave the widest range of products from mono- to tetra-substitution. It appears that there is a balance between strength and the bulkiness of the base. For example, *sec*-BuLi is a weaker base than *tert*-BuLi but produces a greater amount of substituted **36**. *n*-BuLi gives product at 2.2 equivalents, while the stronger, bulkier bases give no product until 5.5 equivalents.

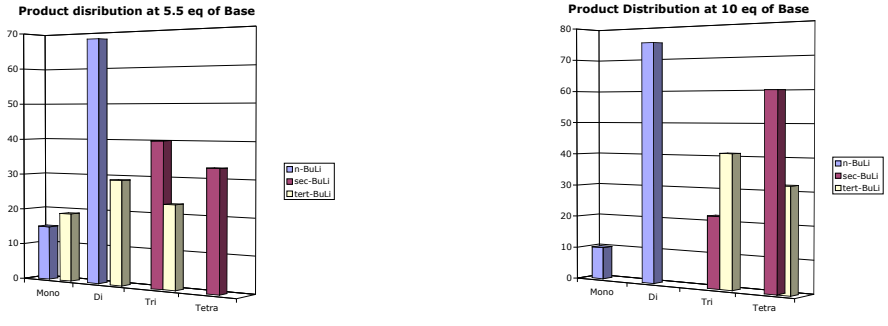

Figure 3.8 Product distribution using a) 5.5 or b) 10 equivalents of base

There are limits to the lithiation power of each base. *n*-BuLi cannot produce any greater substitution than di-substitution. Similarly, tetra-substitution is the limit of both *sec*- and *tert*-BuLi, even up to twenty equivalents. It is evident that there is a limit to the number of anionic centers that can be stabilized by the host or created by the base.

A more detailed examination of the product distribution demonstrates several other features. The *exo* position is nearly always preferred in multiple substitutions. There are six products that are multiply substituted at *exo* positions (**103**, **104**, **106**, **107**, **108**, **109**), while only one product, **102** has more than one *endo* substitution. Several factors may be responsible for this preference. The *endo*-lithiate may be more difficult to solvate than the *exo*. Alternatively, the precoordination of the alkyl lithium to the ether oxygens may predispose the alkyl anion to extract the *exo* proton.[191]

An examination of products not obtained was also informative. For example, the pattern (A/B)-*endo* was never seen (Figure 3.9) and the A-*exo*-A-*endo* pattern was only seen in the chiral tetra-substituted aldehyde **109**.

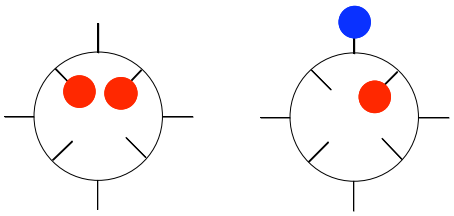

Figure 3.9 Substitution patterns seldom or never seen in the lithiation/formylation of **36**

Both of these patterns can only be obtained through a (presumably) high-energy intermediate in which the carbanionic centers are in close proximity. When all products with these two substitution patterns are removed from the sixty-nine possible formylated hosts, only products **100**-**108** remain. Therefore, another controlling feature in the range of possible substitution patterns was the rigidity and preorganization of **36**. This feature of **36** also prevents substitution

greater than tetra because any more substitution necessarily requires either (A/B)-*endo* or A-*exo*-A-*endo* substitution patterns.

In an attempt to increase the yield of *endo*-substitution, several guests were used to influence the regioselectivity of lithiation. The guests all had functionality that could coordinate to the lithium and, in theory, stabilize the host lithiate. Alternatively, the guest may sterically hinder the base's ability to access the *endo* proton and thus would favor *exo* substitution. Adamantane was used as a reference (Table 3.2).

Table 3.2 Product yield in the presence of guest

Guest	36	100	101
None	68	11	12
Adamantane	39	12	33
DABCO	35	19	19
1-Adamantyl methyl ether	14	11	34
1-$MeOCH_2$adamantane	63	7	24
1-MOMOadamantane	52	15	16

Key: [a]Reactions run using 2.2 eq of *n*-BuLi as base.

The total yields of these reactions were different than those without any guest. In three of the five cases, the addition of a guest increased the yield of the *exo* product. In the remaining cases the *exo*/*endo* ratio was the same (~50:50). The guest hinders the base from entering the cavity and removing an *endo* proton.

In summary, there are two distinct sites of **36** that could undergo reaction when metallated; the *endo* and *exo*. These positions are activated due to the ether oxygens that are *ortho* to them. Perlithiation of host **36** could lead to sixty-nine products. Only twelve products were obtained. The product distribution was a function of type and amount of base. In order to obtain a greater number of substituted products, the lithiated host would need to adopt high-energy intermediate carbanions. Therefore, the reduction in the number of products from sixty-

nine to twelve is due to the preorganization of host **36** as well as the strength and bulkiness of the base.

3.3 Synthesis of Carboxylic acid *m*-baskets

Acid catalysis plays an important role in organic and biochemistry. Additionally, acids can act as recognition points in the active site of enzymes by forming hydrogen bonds or salt bridges with substrates and therefore, it would be a good starting point for adding functionality found in biologically relevant systems.

There have been several examples of carboxylic acids being used to impart water solubility,[192] as recognition points,[159] and as proton donors in host-guest chemistry.[132, 133] However, most of these systems have the acid pointing out of the cavity, unlike enzyme active sites, which have all functional groups directed inside.

The first attempt to place carboxylic acids on *m*-basket using the aldehydes as an intermediate proved unsatisfactory. *Exo*-mono aldehyde and *endo*-mono aldehyde were oxidized using $KMnO_4$ in DMA/*t*-BuOH at 90°C. Three days were required to obtain mono-*exo* carboxylic acid in 70% yield. It took seven days to obtain mono-*endo* carboxylic acid in 60% yield. This was example of how *endo*- and *exo*-positioning affected the reactivity of a functional group. $KMnO_4$ is a polar salt that is not designed to go into the cavity. When multi-aldehyde *m*-baskets were placed under similar reaction conditions, poor yields and incomplete reactions resulted. Other oxidants that were used included CrO_4 and H_2O_2. As these oxidants proved inefficient and in order to test the general applicability of the directed *ortho* lithiation reaction with *m*-basket, alkyl chloroformates were used as electrophiles (Scheme 3.3). The resulting esters could then be hydrolyzed to the corresponding carboxylic acids.

Scheme 3.3 General synthesis of ester *m*-baskets

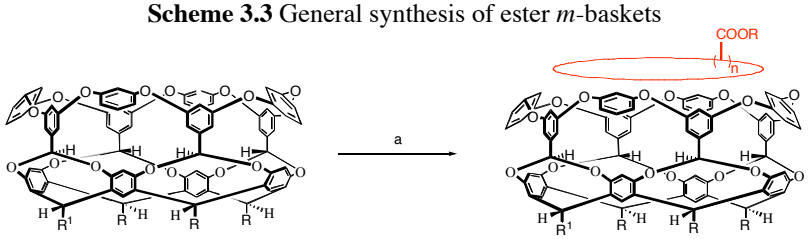

Key. a. x-BuLi, ROCOCl, THF, -78 °C.

Several alkyl choloroformates were used, including methyl, ethyl, *iso*-propyl, and *tert*-butyl cloroformate. After reacting these four chloroformates with the lithiated *m*-basket, methyl chloroformate was chosen for systematic study for two reasons. When any alkyl group was larger than methyl, there was no *endo*-A/C formed. This was a desirable product as it was the only product with more than one *endo* ester. Secondly, when the alkyl group was larger than ethyl, the products could not be separated. This later observation is most likely due to the increasing lipophilicity of increasing the alkyl chain. The chiral tetrasubstituted product A/B/C-*exo*-B-*endo* was not formed with any of the alkyl chloroformates. This is the one product that disobeyed the patterning rule (A-*exo*-*B*-*endo* pattern). Excluding this exception, the substitution and yield trends were the same as when DMF was used as the electrophile. The formed products and the yields of the different methyl esters *m*-baskets with the three bases are shown in Figure 3.9 and Table 3.3.

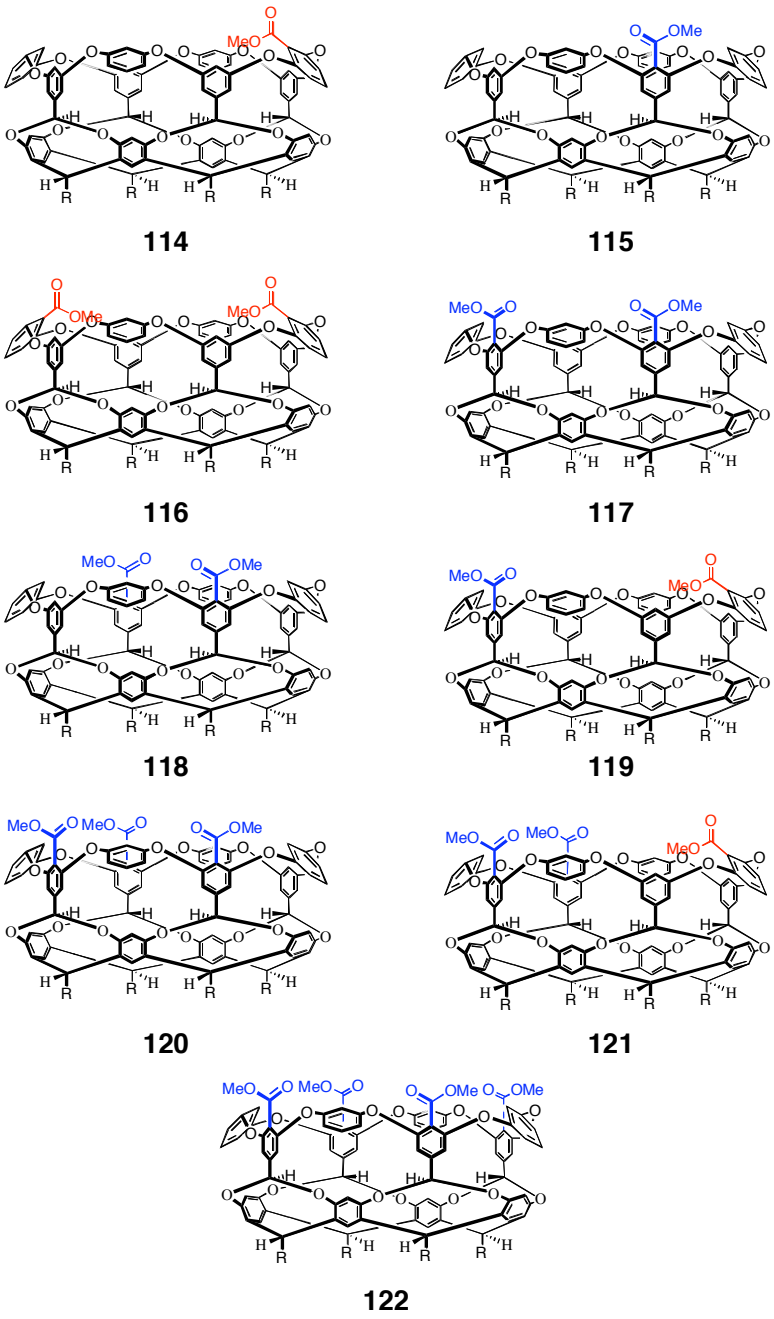

Figure 3.10 Methyl esters formed from lithio-*m*-basket and methyl chloroformate

Table 3.3 Percent Yield of Methyl ester *m*-basket utilizing three different bases[a]

Base	Eq	**37**	**114**	**115**	**116**	**117/118**[b]	**119**	**120**	**121**	**122**
n-BuLi	5.5	12	12	22	8	23	14	-	-	-
n-BuLi	10	2	4	10	10	22	28	-	-	-
sec-BuLi	5.5	-	-	-	-	-	-	27	30	37
sec-BuLi	10	-	-	-	-	-	-	12	12	70
tert-BuLi	5.5	-	-	-	10	15	18	22	14	11
tert-BuLi	10	-	-	-	-	-	-	13	20	62

Key: [a]Reaction yields are the average of at least two different reactions. The symbol "-" indicates that the product is not formed under these conditions. [b] Combined yield of two products that proved inseparable.

After the separation of the methyl esters by column chromatography, the acids were obtained by saponification using aqueous lithium hydroxide in refluxing pyridine (Scheme 3.4 and Figure 3.10). The yields were all quantitative.

Scheme 3.4 Synthesis of the carboxylic *m*-baskets

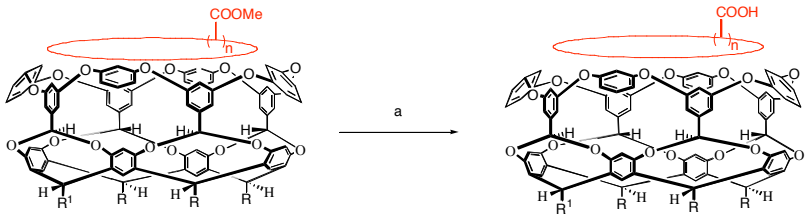

Key. a. 1M LiOH(aq), pyridine, Δ.

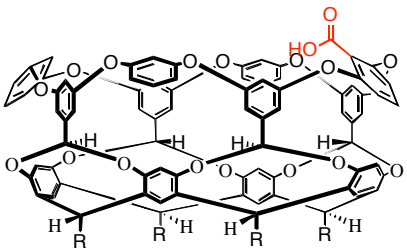

123

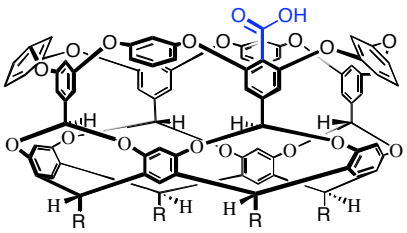

124

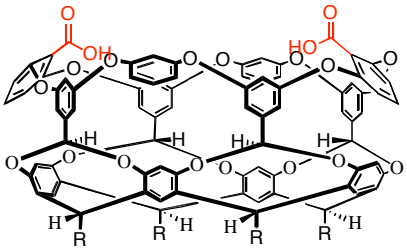

125

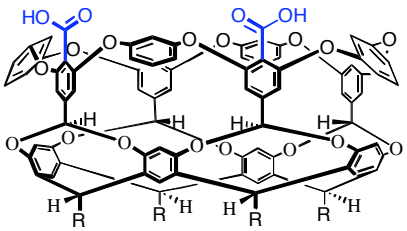

126

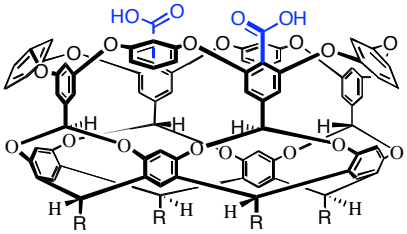

127

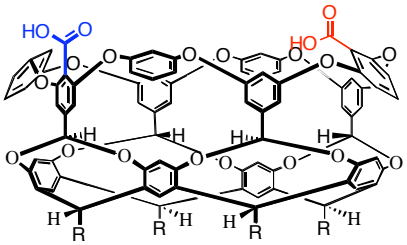

128

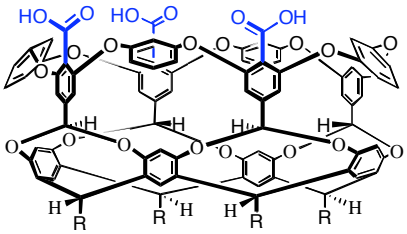

129

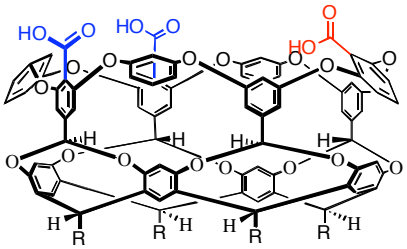

130

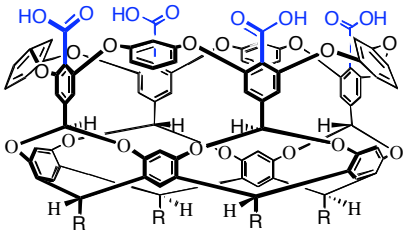

131

Figure 3.11 Products formed from the saponification of the Methyl ester *m*-baskets

3.4 Carboxylic Acid *m*-baskets as Catalysts

Cyclic acetal cleavage was the first target for using the carboxylic acid *m*-baskets as catalysts. Cyclic acetals are a widely used protecting group for carbonyl compounds (Scheme 3.5).[193]

Scheme 3.5 Synthesis of acetals

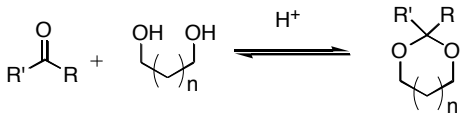

Cleavage of acetals has been reported with acetic acid.[193] The pH of acetic acid is 4.76 while the pH of benzoic acid is 4.20 hence it seemed reasonable that the hosts would be capable of cleaving acetals.[172] One barrier to using acetals as protecting groups is that the cleavage method can be unspecific. The carboxylic acids present on these hosts would make this process selective by cleaving only the acetals that also act as "good" guests. Therefore, if a molecule had two different acetals, it could be possible to cleave only the one that fit into the cavity of the host. An additional benefit is that by and large cyclic compounds (the substrates) has been shown to be much better guests than noncyclic compounds (the products).[167] Hence product inhibition would be avoided.

Several cyclic and bicyclic acetals (Figure 3.12) were prepared using the parent diols, *p*-Toluenesulfonic acid in catalytic amount, and hexanal as the aldehyde. Benzene was used as solvent and refluxed with a Dean-Stark trap to azatropically remove water. Acetals **132** and **133** had been previously reported.[194, 195] The products **134** and **135** are produced as diasteromers but were not separated but used as a mixture.

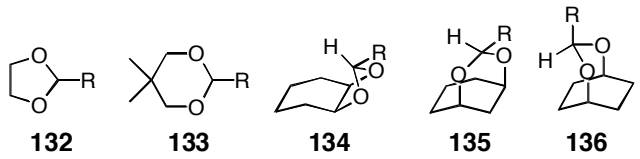

Figure 3.12 Cyclic and bicyclic acetals (R = *n*-pentyl)

The ten carboxylic acid baskets were all tested varying the amount of acetal, basket, solvent and water. A variety of solvents were used including: methanol; ethanol; isopropanol; acetone; tetrahydrofuran; chloroform; dichloromethane; dimethyl sulfoxde; acetonitrile; toluene; benzene; and anisole. At room temperature all attempts to cleave these acetals failed. In order to test the validity of the literature procedure the acetals were dissolved in 4 ml acetic acid/1 ml of water at room temperature the acetals also failed to react. It seems that the acids of the host as well as acetic acid are not sufficiently strong to cleave the acetal. In order to determine the reason behind the non-activity of these hosts toward the acetals, a binding study was instigated in several solvents. THF-d_8 was initially used as the solvent. None of the synthesized cyclic or bicyclic acetals demonstrated any binding in the acid hosts. When the solvent was changed to the stronger DMSO-d_6, there was still no binding noted with any of the acetals.

3.5 Binding Properties of the Carboxylic acid *m*-baskets

In order to determine the binding preferences of these new hosts, a binding study was undertaken. Initially, several guests and solvents were examined. However, the host's ability to bind primary amine guests was too strong to be measured by NMR. An additional obstacle was the overlapping of free/bound peaks. For example, due to the reduced symmetry of the hosts, when a guest would bind slowly on the NMR time scale, the free and bound host peaks would overlap making integration impossible. Many guests caused this to happen including 1-adamantol, 2-adamantol, 1-adamantanemethanol and 1-adamantaneethanol. One example of a guest whose exchange was fast on the NMR timescale was (*S*)-nicotine. While the binding

constant was small (12 M^{-1}) with host **124**, the guest caused interesting splitting of the H_C, H_E, and H_F protons (Figure 3.13a and b). These splittings occurred because these protons are enantiotopic.[196] Therefore, when placed in a chiral environment, these protons are no longer equivalent by NMR (they become diastereotopic).

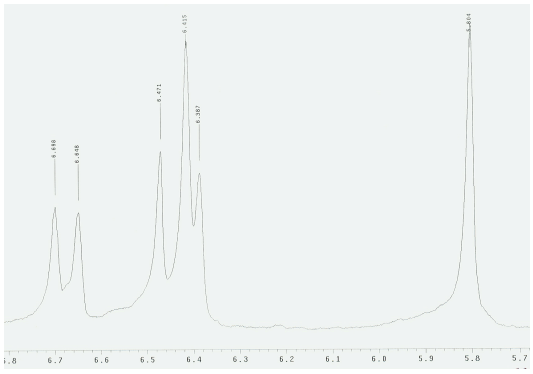

a

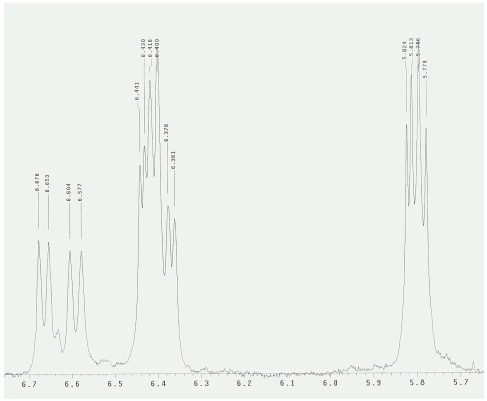

b

Figure 3.13 a) Protons H_e, H_f, and H_c of **124** in DMSO b) Protons H_e, H_f, and H_c of **124** in DMSO with 100 equivalents of (*S*)-nicotine

In an effort to determine how the spatial orientation of the carboxylic acid groups affect the guests orientation only one guest was used, 1-adamantamine (**137**).

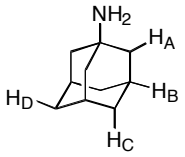

137

Additionally, due to solubility issues with the more substituted carboxylic acid *m*-baskets, the solvent used was exclusively DMSO-d_6. Also, in solvents such as $CDCl_3$ sigmoid binding curves were encountered which indicated a cooperative binding event.[169] Such a case is shown in Figure 3.14, which is the binding isotherm of **124** hosting **137** in $CDCl_3$. It is unclear why such behavior was observed in these systems.

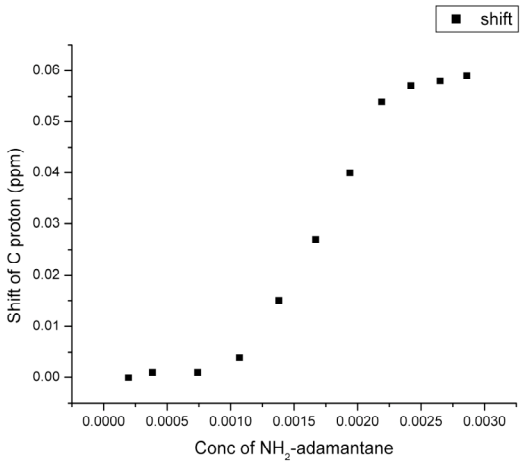

Figure 3.14 Binding Isotherm of **124** binding **137**

Even this reduced binding study (one guest, one solvent) was complex. First, in several cases, the guest, **137** bound too strongly to obtain a K_a value from NMR. In that case all of the host peaks were bound host peaks and there were no free peaks to integrate. Additionally, even when the guest did not bind 100% to the host, the host bound peaks were beneath the host free peaks and were therefore unable to be integrated. Although these facts limited the amount of information gleaned from these systems, both 1D- and 2D-NMR studies provided essential information.

In the unsubstituted *m*-basket, there are two conformations that a guest can adopt. The functional group can be either "up" (pointing toward the portal of the cavity) or "down" (toward the bottom of the cavity) (Figure 3.15A and B). However, when the *m*-basket is substituted there are two different "up" conformations. The C_3 axis of the guest can be aligned with the pseudo-

C_4 axis of the host (Figure 3.15c). Alternatively, the C_3 axis of the guest could be tilted relative to the C_4 axis of the host (Figure 3.15D). The determination of the guest's orientation was evident by the number of NMR peaks corresponding to the bound guest. It was expected that when the C_3 axis of the guest was out of alignment with the pseudo-C_4 axis of the host, the NMR spectra would present a greater number of bound guest peaks.

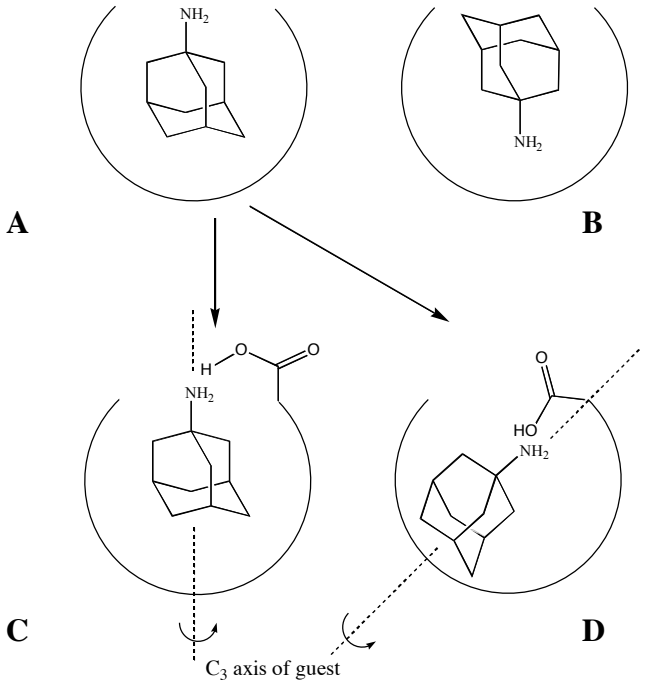

Figure 3.15 Possible orientations of a guest in *m*-baskets and substituted *m*-baskets

The simplest interactions found between **137** and the hosts allow only one orientation of the guest. These include **123**-**127** and **131**.

Host **123** bound **137** slowly on the NMR time scale. It was impossible to obtain a K_a due to the overlapping signals of the host. It bound less strongly then any of the other hosts presumably because the *endo*-carboxylic acid reduced the size of the portal and volume of the interior. The bound guest peaks were less intense and more complicated than when bound by the other hosts (Figure 3.16). 2D-EXSY experiments demonstrated that, in contrast to the other

hosts, each of the free guest's protons exchanged with two bound guest's signals, indicating that the guest's protons were in two different bound positions. This would be expected with a guest whose C_3 axis was not aligned with the pseudo-C_4 axis of the host. The most shifted proton is the H_C proton ($\Delta\delta$ = 2.70 ppm). This shift was larger than the other hosts because in order for the amine to interact with the carboxylic acid the guest must be buried deeper in the host.

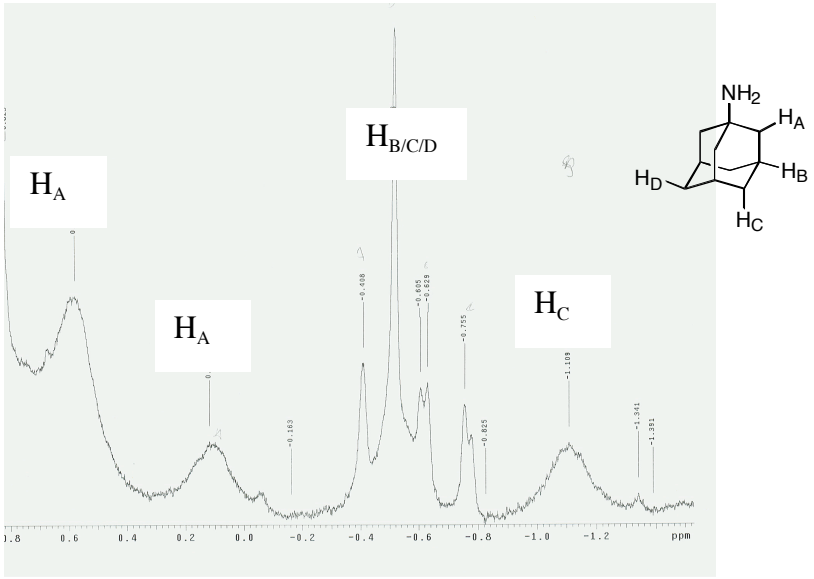

Figure 3.16 Upfield NMR region of **123**/**137** showing bound **137**.

Host **124** also bound **137** slowly on the NMR timescale. Binding was too strong to determine an exact association constant. In the bound guest region of the NMR there were three peaks that correspond to the guest bound in the host with the C_3 axis of the guest aligned with the pseudo-C_4 of the host (Figure 3.17 and Figure 3.18). The most shifted protons are H_C ($\Delta\delta$ = 2.31 ppm) and the least shifted protons are H_A ($\Delta\delta$ = 1.15 ppm) which indicated that the guest is situated inside the host with its amine hydrogen directed toward the entrance. This orientation allowed the amine to interact with the host's carboxylic acid (Figure 3.19).

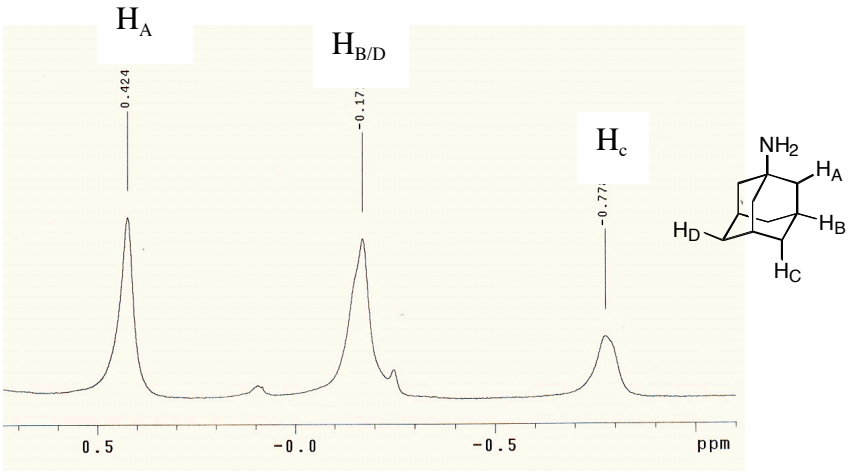

Figure 3.17 Upfield NMR region of **124/137** showing bound **137**.

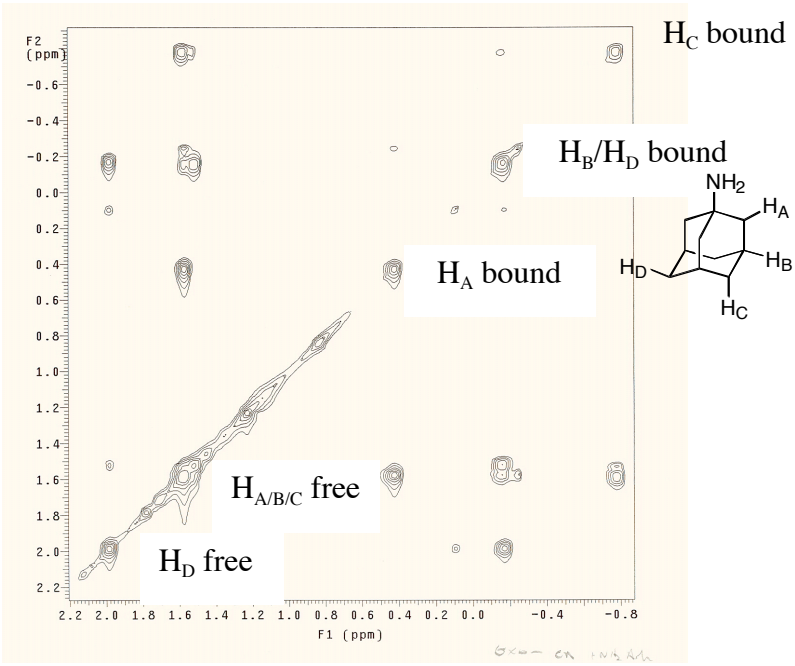

Figure 3.18 Upfield portion of 2D-NOESY showing bound **137** by **124**.

Comparison of the bound **137** peaks in **123** and **124** reveal the orientation of the guest. The large number of peaks in the *endo*-carboxylic acid *m*-basket demonstrates that **137** was orientated with its C_3 axis not aligned with the pseudo-C_4 axis of the host. While the simplicity of the bound region of the complex **124/137** demonstrates that the C_3 axis is aligned with the pseudo-C_4 axis of the host. Additionally, the largest peaks shift of **137** was greater than the

largest peak shift when **124** bound **137** indicating that the proton is bound deeper within the cavity then the corresponding proton in the *exo*-carboxylic acid *m*-basket.

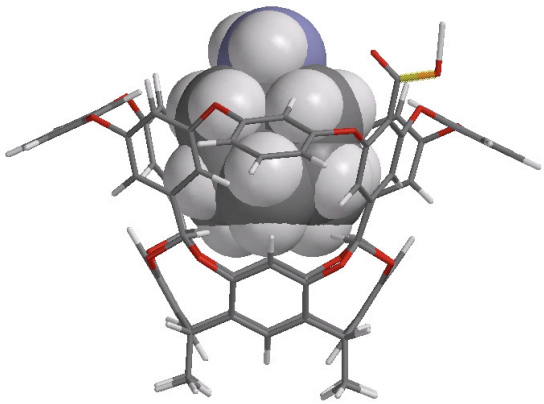

Figure 3.19 Model of **124** bound to **137**

The diacid **125** also bound **137** strongly. However, there were no bound guest peaks found upfield indicating that the adamantane portion of the guest was not inside the hydrophobic pocket of the host. The only changes on the NMR were found on the upper rim of the host primarily, protons H_C and H_F. These protons disappear when two equivalents of **137** are added to a solution of **124**. After four equivalents of the guest are added these peaks reappear and no further changes are noted. These results indicate that binding is on the NMR timescale and that the guest's amine is bridging between the hosts carboxylic acid but the adamantane is not entering the cavity. Presumably, the intruding carboxylic acid groups made the cavity volume insufficient to accommodate the adamantane.

The tricarboxylic acid **129**, like **124**, orientated 1-adamantamine so that the amine group is positioned towards the opening of the cavity and the H_C protons were the deepest inside the host. However, unlike **124**, the tricarboxylic host allows differentiation between protons H_B and H_D of the guest (Figure 3.20). The reason behind the differentiation between these two protons is unclear. The shift could arise from the shielding/deshielding effects from the carboxylic acids not involved in the salt bridge and the guest. Alternatively, the guest could be bound deeper in

the cavity when compared to the mono-*exo*-carboxylic acid. The simplistic NMR bound region indicates that the C_3 axis of the guest is aligned with the pseudo-C_4 of the host.

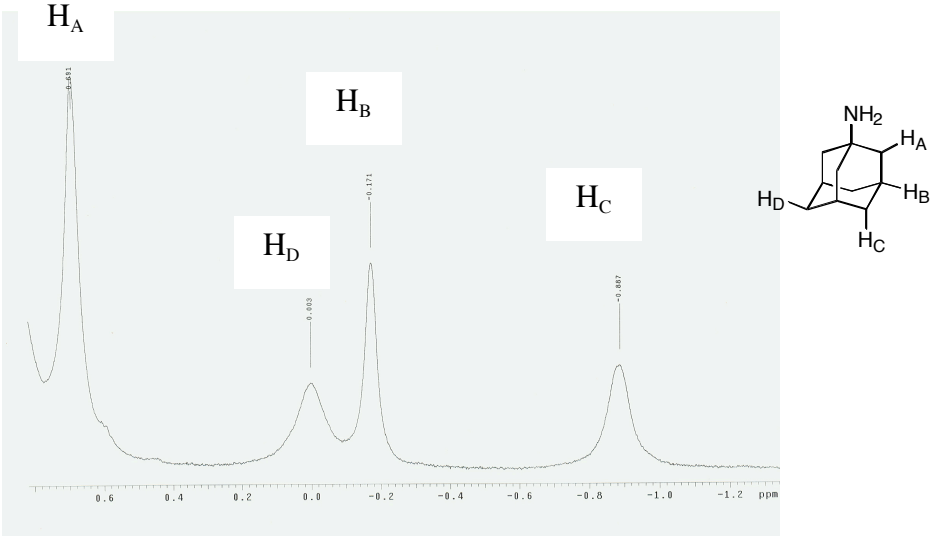

Figure 3.20 Upfield NMR region of **129/137** showing bound **137**.

The guest **137** also bound strongly to host **131**. The orientation of the guest was similar to the orientation it adopted when bound to **124** and **129**. Once again the largest shift of a proton signal arose with proton H_C ($\Delta\delta$ = 2.22 ppm) and the smallest shift arose with proton signal H_A ($\Delta\delta$ = 1.16 ppm) (Figures 3.21 and 3.22). Therefore, like **124** the guest adopted an orientation that placed its amine near the entrance of the cavity and the carboxylic acids and the H_C buried at the bottom of the cavity (Figure 3.23). The NMR signals of the bound guest have even more differentiation between H_D and H_B then with host **129**.

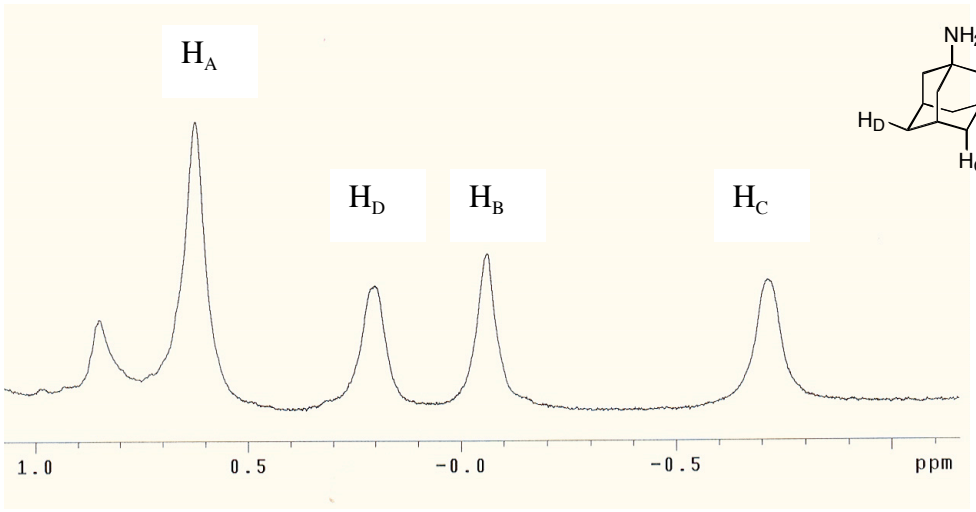

Figure 3.21 Upfield NMR region of **131/137** (bound **137**).

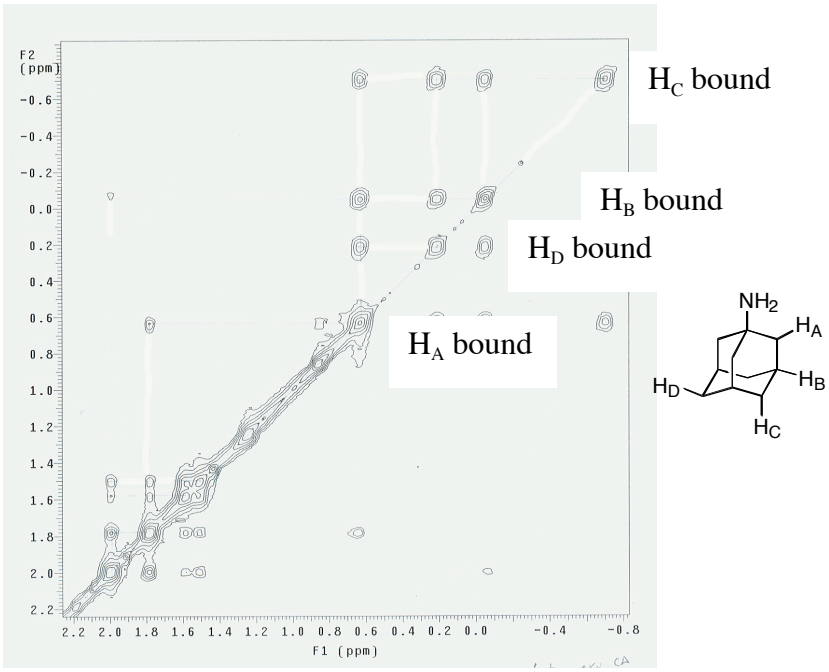

Figure 3.22 2-D EXSY of **131/137**

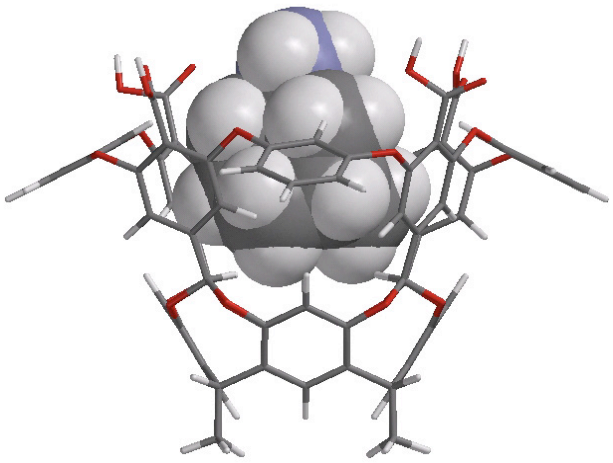

Figure 3.23 Model of **131** bound by **137**

If the hosts had all the carboxylic acids in one position (*exo* or *endo*) than the guest can only adopt one orientation. The *exo*- orientation was more conducive to binding aminoadamantane than *endo*- due to the intruding carboxylic acid of *endo*-carboxylic acid *m*-basket.

The remaining two carboxylic acid *m*-baskets had more complicated guest orientations. These two hosts, **128** and **130**, had two nonequivalent carboxylic acid groups that resulted in the guest adopting different orientations within the host (Figure 3.24).

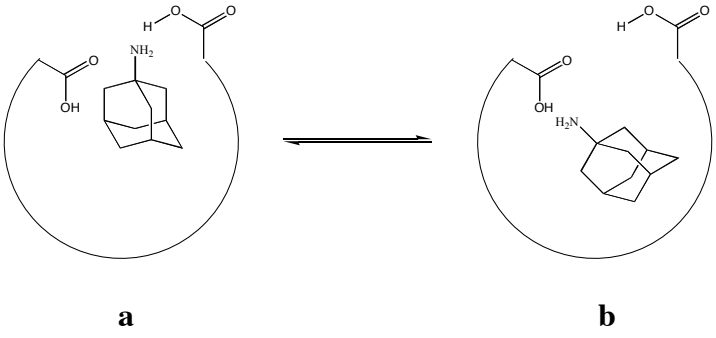

a **b**

Figure 3.24 Two possible orientation of the guest within a host with both a. *exo* functionality or b. *endo*-functionality.

For example, the chiral host **128** had both an *endo*- and an *exo*-facing carboxylic acids. Therefore, the guest had two different orientations when bound. 1D and 2D-NMR revealed two

sets of bound guest peaks that interchange with the free guest and, more weakly, with each other (Figures 3.25 and 3.26). This indicated two different binding orientations that are in slow exchange on the NMR timescale (Figure 3.25). The integration of one of these sets is much larger then the other which indicated that one orientation is preferred but that the energy difference is not prohibitive. Integration indicated that *exo*-orientation is preferred by a 1:4 ratio. The preferred orientation of **137** aligns its C_3 axis with the pseudo-C_4 axis of the host. However, the larger shift of the guest's H_C proton indicated that it was more deeply bound in the cavity than when bound by a host, which had all carboxylic acids in the *exo*-orientation.

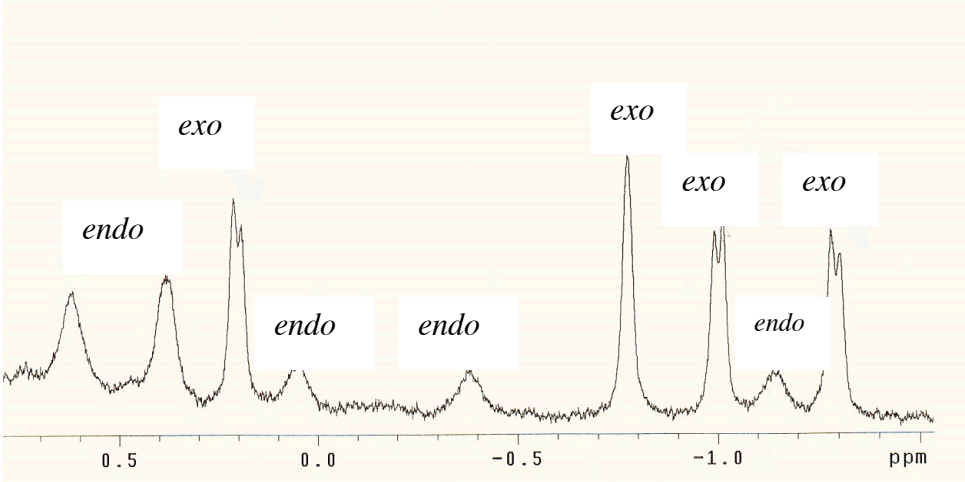

Figure 3.25 Upfield NMR region of **128/137** (bound **137**)

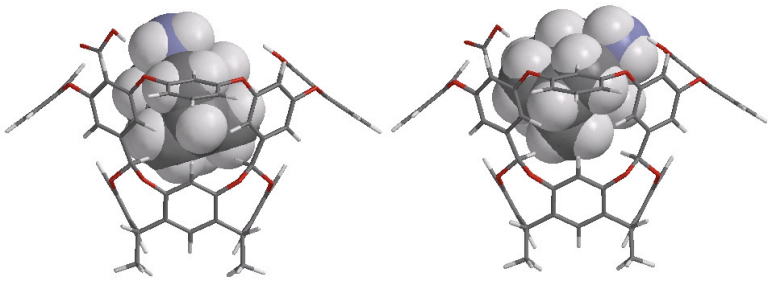

Figure 3.26 Two binding orientation of **137** within **128**

Finally, the triacid **130** presented two *exo*- and one *endo*-carboxylic acid recognition points for the guest **137**. The orientation of the guest in **130** had a similar orientation to that of **128**. There were two sets of guest peaks that interchanged slowly on the NMR timescale (Figures 3.27 and 3.28). As with **128**, one guest orientation is preferred. In this case, as with **128**, the preferred orientation had the C_3 axis of the guest aligned with the pseudo-C_4 axis off the host. Integration demonstrated that the preference was a 1:9 ratio. The preference for the *exo*-position was greater then **128**. This probably arose from the greater number of *exo*-positions for it seems unlikely that the *exo*-carboxylic acids could be acting cooperatively given the distance between them.

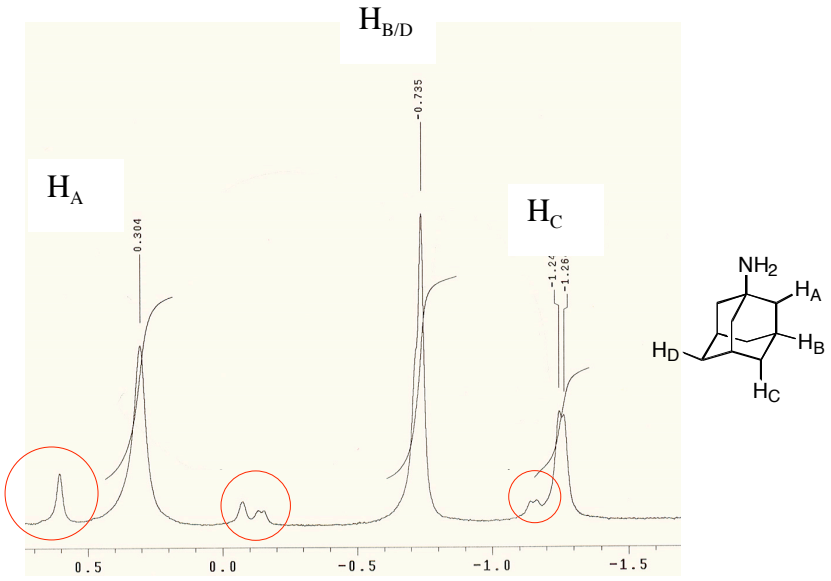

Figure 3.27 Upfield NMR region of **130/137** (bound **137**). Circles indicate *endo*-interaction

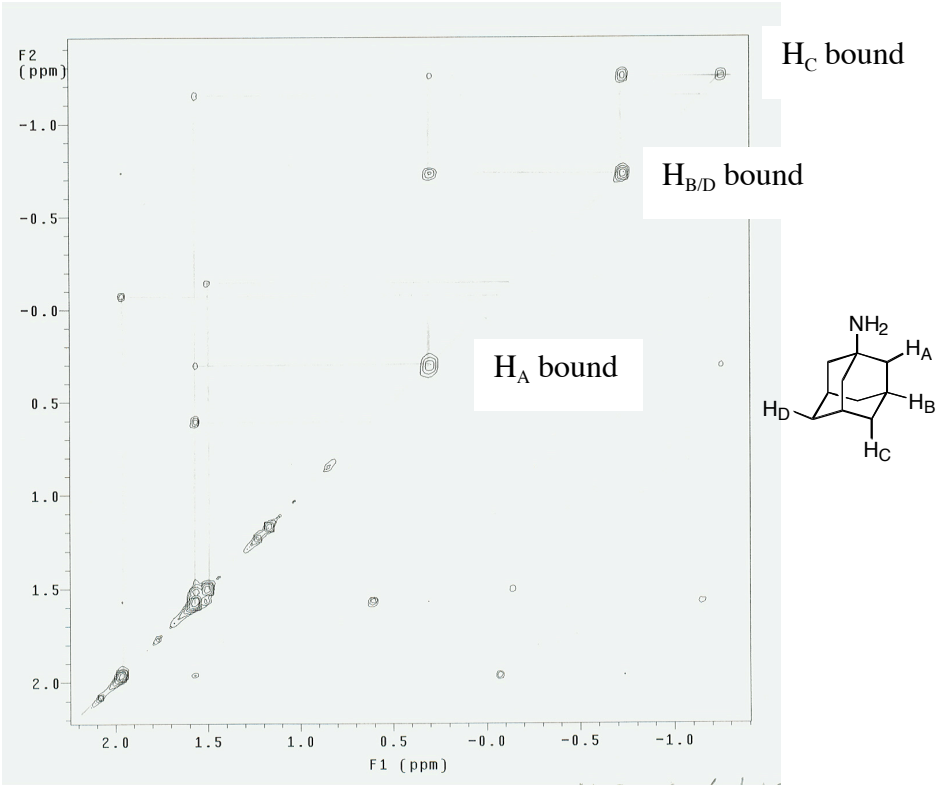

Figure 3.28 2-D EXSY of **130/137**

The carboxylic acid *m*-baskets are able to bind aminoadamantane in three different orientations. Two of the guest's orientations are within the host with the amine directed toward the portal. One of these orientations aligns the C_3 axis of the guest with the pseudo-C_4 axis of the host. The second of these two orientations have the C_3 axis of the guest diagonal to the C_4 axis of the host. The third orientation was adopted by only one of the host/guest systems, A/C-*endo*-dicarboxylic acid *m*-basket (**125**). The guest did not enter the cavity but instead, the amine of the guest bounds to the carboxylic acids of the hosts and the adamantane portion was directed away from the cavity. Presumably, the adamantane was unable to enter the cavity due to the intruding carboxylic acids. When there are two possible orientations that a guest may adopt, such as with **126** and **130**, the guest prefers to align its C_3 axis with the pseudo-C_4 axis of the host and interact with the *exo*-carboxylic acids.

The use of alkyl chloroformates as electrophiles expanded the use of directed ortho metallation of **37**. The esters were readily hydrolyzed to the respective acids. Attempts to use these acids as catalysts to cleave cyclic and bicyclic acetals proved unsuccessful due to the inability of the acetals to act as guests. Binding studies with 1-adamantamine as guest and the carboxylic acid *m*-baskets as hosts demonstrated that the orientation of the guest was dependant on the *endo*- or *exo*- orientation of the carboxylic acid. When both *exo*- and *endo*-carboxylic acids were present on the host, the amine preferred to interact with the carboxylic acid in the *exo*-position.

IV. SYNTHESIS OF A CARBONIC ANHYDRASE MIMIC

Zinc is ubiquitous in biochemistry and is of great utility in protein chemistry. Many enzymes' active sites contain a tetrahedrally coordinated zinc. Zinc is different than most of the other metals used as catalytic centers. There are several properties that are responsible for its common use as enzyme metal centers.[197, 198] Namely, triple coordination to various groups increases the Lewis acidity of the zinc and hence the Brønstead acidity of a coordinated water molecule that is part of the tetrahedral geometry. Secondly, zinc is a borderline case in the hard/soft acid theory. It therefore will interact with all of the prevalent Lewis bases in biological systems (nitrogen, oxygen, and sulfur). Possible the most important property of zinc is its inertness toward redox chemistry unlike iron, copper, and manganese. Finally, anions bound to zinc retain their nucleophilic character. This characteristic allows them to react with substrates.

Carbonic anhydrase is an enzyme responsible for maintaining the correct pH in the blood by the reversible hydrolysis of carbon dioxide and is used to transport carbon dioxide around the body (Scheme 4.1).[199] Carbonic anhydrase has also been shown to hydrolyze some esters. Carbonic anhydrase's active site is in part composed of three histadine residues that are coordinated to a zinc atom. The fourth coordination site of the zinc is occupied by water. This water molecule is acidic, and under physiological conditions it is deprotonated (pK_a = 7.3).[200] The resulting hydroxide is a very potent nucleophile. This enzyme rate of reaction approaches the diffusion limit.

Scheme 4.1 Mechanism of reversible hydrolysis of carbon dioxide by Carbonic anhydrase

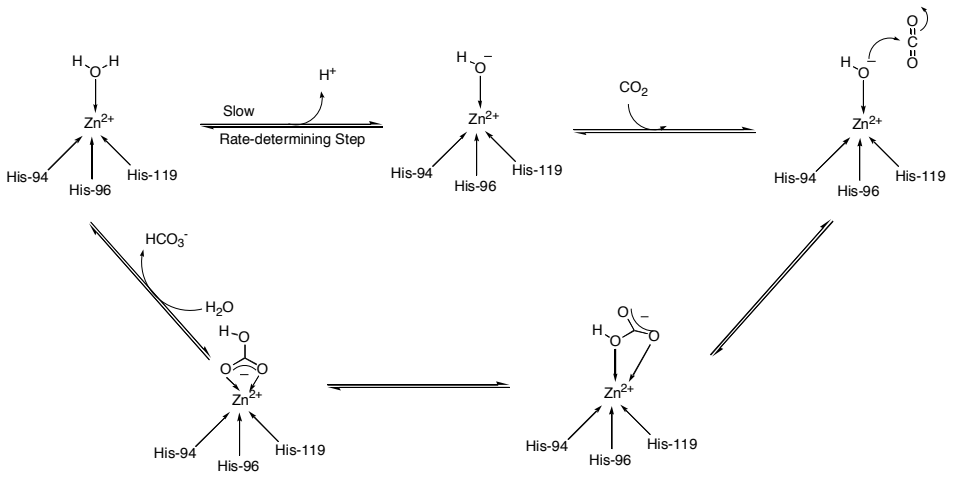

The mechanism of carbonic anhydrase is shown in Scheme 4.1.[199] The first step is the loss of the proton from the coordinated water molecule. This is the rate-determining step. Once the water molecule is deprotonated, the hydroxide nucleophile attacks the carbon dioxide, which produces a carbonate intermediate. The carbonate rearranges so that the oxygens coordinated to the zinc are the most electron rich. A water molecule then displaces the hydrogen carbonate from the zinc regenerating the catalyst.

The importance of this enzyme, as well as its speed and efficiency, has led many researchers to attempt to make a small molecule mimic of carbonic anhydrase. The tetrahedral coordination of the zinc has made tripodal ligands the scaffold of choice (Figure 4.1).

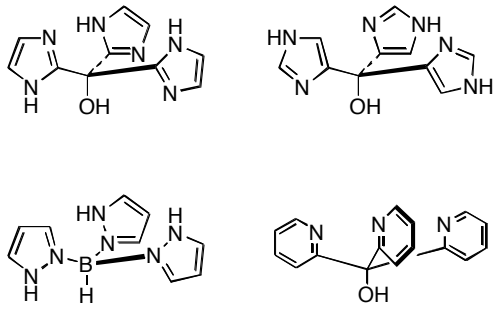

Figure 4.1 Common tripodal ligands used to mimic carbonic anhydrase

Tripodal ligands are preferable to other ("T-shaped", macrocyclic) ligands for several reasons.[197, 198] The tripodal ligand forces a facial orientation and therefore there is only one approach to the zinc. Additionally, tripodal ligands have only one binding geometry. In contrast, the "T-shaped" ligands and macrocyclic ligands are much more flexible. The rigidity of the tripodal ligands is of additional benefit when attaching substituents that influence binding. The substituents are not as stable in the other ligands. Finally, the "t-shaped" and macrocyclic ligands have no biological relevance. However, all the tripodal ligands shown in Figure 4.1 suffer from the same shortcoming. They tend to form sandwich compounds (2:1, ligand:zinc) with zinc rather then a catalytically active 1:1 compounds (Scheme 4.2).

Scheme 4.2 Formation of inactive sandwich compounds

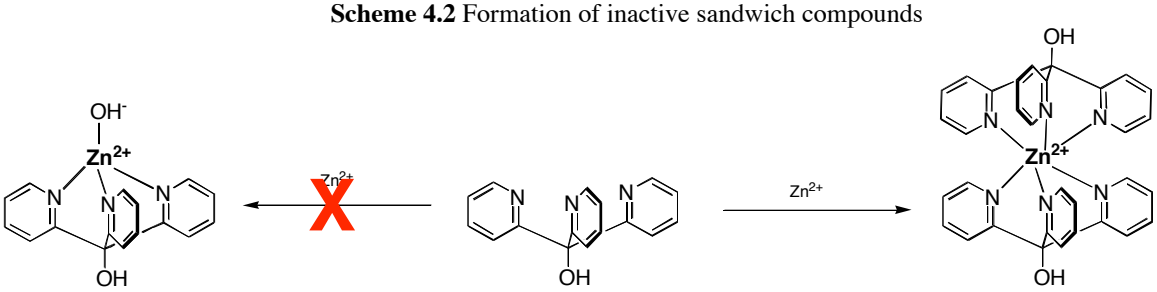

In an effort to produce the catalytically active, monomeric species, several research groups have placed "blocking" groups on the tripodal ligand. One example uses the tris(pyrazolyl)borate ligand (Scheme 4.3).[201] When *tert*-butyl groups are placed on the pyrazole rings the zinc then prefers tetrahedral coordination (Scheme 4.3). Counter ion exchange using KOH produces the hydroxide ligated to the zinc. When exposed to CO_2 the hydroxide does attack the electrophilic carbon. However, the reaction stops at this stage and the ligand cannot act as a catalyst.

Scheme 4.3 Hydrolysis of carbon dioxide by *tert*-butyl tris(pyrazolyl)borate

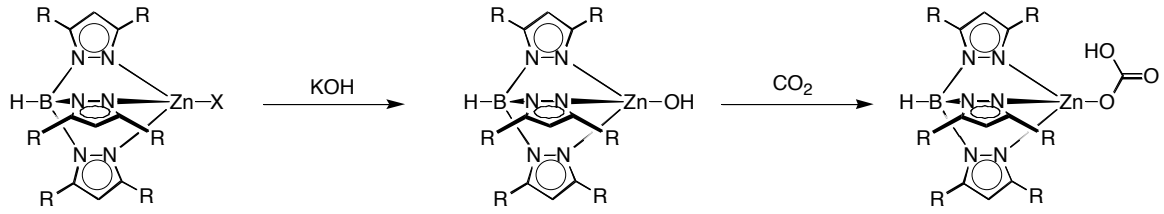

Previous work in the Gibb group has focused on blocking the formation of sandwich complexes from *tris*-pyridyl methanols. The initial trispyridyl ligands were simple carboxylic acid derivatives (**138**).[202]

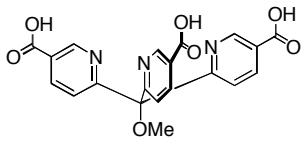

138

These compounds were not suitable to stop the formation of the sandwich complexes. Additionally, the zinc binding to these ligands was found to be relatively weak. In an effort to develop these tripodal ligands amino acids were placed on the 5-positions of the pyridines (Figure 4.2).[203] The amino acids might not only hinder the formation of the sandwich complexes but also allow for stereospecific reactions.

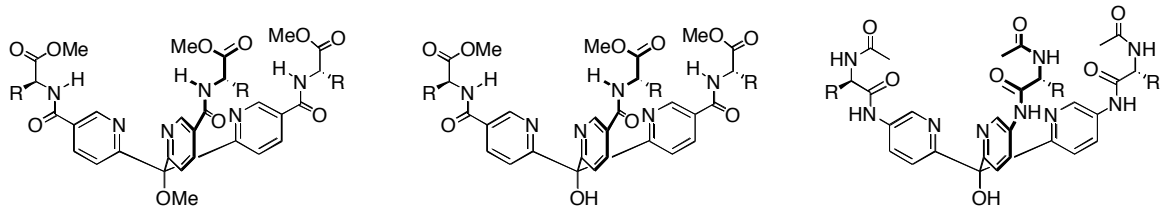

139 **140** **141**

Figure 4.2 Tris(pyridyl) tripodal ligands with amino acid blocking groups

It was found that removing the methyl protecting group of the alcohol of **139** to make **140** dramatically increased the binding of zinc to the ligand in D_2O.[203] When the nitrogen of the amine was directly attached to the pyridine rings the association with zinc increased. This study

implies that there are many subtle steric and electronic features of these mimics that control how zinc interacts with the ligands.[203] Like the previous examples however, even the monomeric **141**+Zn did not act as a catalyst for the hydrolysis of *p*-nitrophenyl acetate. It seems that the blocking groups on these tripodal ligands block both the formation of the sandwich complex formation as well as the approach of the substrate.

In the literature, there are several examples of host molecules acting as ligands for zinc to mimic carbonic anhydrase. Reinaud's funnel complexes use the lower rim of calix[6]arenes to bind a zinc with different nitrogenous donors (Figure 4.3).[150-153, 157] The zinc is in a tetrahedral coordination with its last coordination site pointed into the cavity of the calixarene. NMR and x-ray crystallography have shown that there is a coordinated water molecule directed into the cavity of this complex and that this ligand is exchangeable with alcohols.

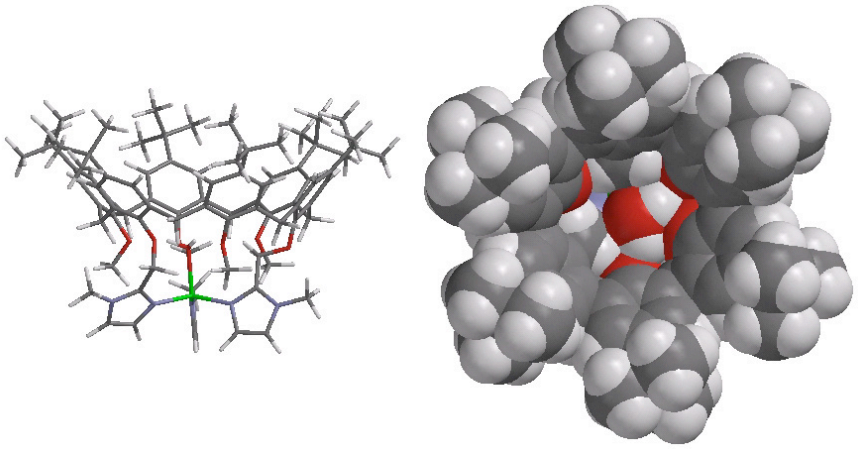

Figure 4.3 Funnel complex using imidizole as the nitrogen donor with zinc

In an effort to halt the formation of the sandwich complexes while allowing enough room for the substrate to approach, it was envisioned that the *m*-basket could be used as the blocking group. Not only would the *m*-basket stop the formation of the sandwich complexes, the substrates that were reacted with the zinc bound hydroxide would be selected by the cavity of the

host. Only those substrates that were good guests would be reacted. The mimic would be shape selective.

4.1 Synthesis of the enzyme mimic

The initial mimic design was based on the partially weaved host molecules **36** and **71** and the tris(pyridyl)methanol ligands (Scheme 4.4).

Scheme 4.4 Proposed scheme for the synthesis of *m*-basket CA mimic

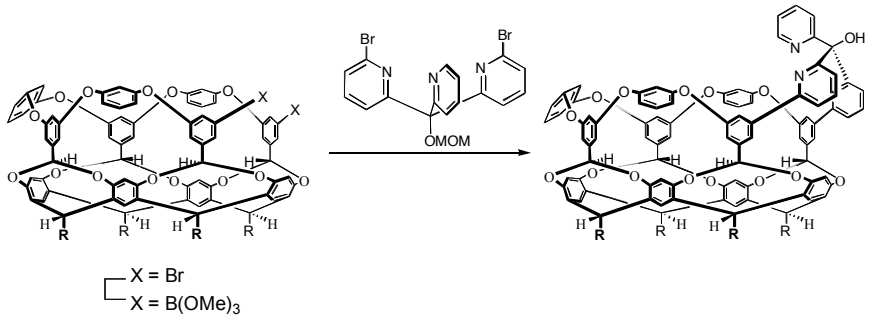

The mimic could be made from the partially weaved 2-Me-*m*-basket. The parent compound (**71**) was exceptionally selective for cyclopentyl guests. Additionally, the synthesis time for **71** (fourteen days) might also be in favor of making the partially weaved basket as compared to **36** which only has a synthesis time of seven days.[167] Therefore initial attempts were made to synthesize and increase the yield of the partially weaved 2-Me-*m-tris*-basket (Scheme 4.5 and Table 4.1). However, the synthesis of the desired partially weaved product always produced other partially weaved products (Figure 4.4).

Scheme 4.5 Synthesis of 2-Me-*m-tris*-basket

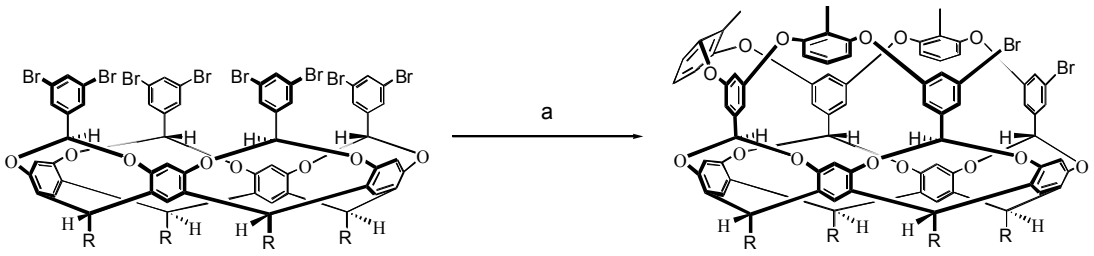

Key: a) 2-methyl resorcinol, base, solvent, copper(I or II)

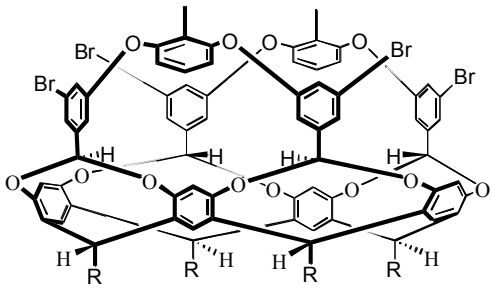

2-Me-*bis*-*m*-basket **142**

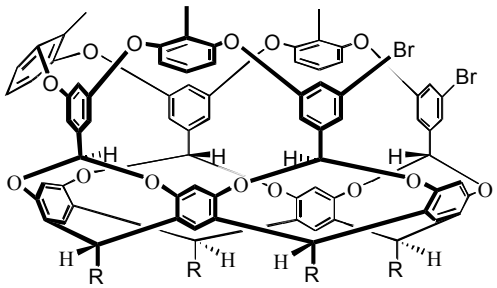

2-Me-*tris*-*m*-basket **143**

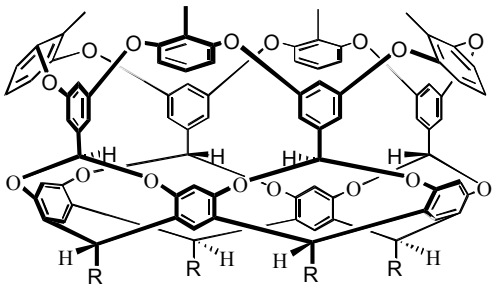

2-Me-*m*-basket **71**

Figure 4.4 Products formed attempting to make 2-Me-*tris*-*m*-basket (**143**)

Table 4.1 Yields of Partially/Fully Weaved 2-Me basket products[a]

Solvent	Time (hr)	Eq of 2-Me resorcinol	Eq of K_2CO_3	Eq of CuO	% **142**	% **143**	% **71**
Pyridine	62	7.5	7.5	15	2	17	20
″	74	″	″	″	1	17	27
″	86	″	″	″	-	9	44
″	50	″	″	″	4	19	12
″	62	5	″	″	1	15	25
″	50	5	″	″	14	15	5
″	50	7.5	7	″	5	19	44
″	50	″	6.5	″	3	11	28
″	50	″	6	″	7	19	30
″	65	″	7	12	-	13	30
″	65	″	″	9	-	9	23
″	65	″	″	6	-	10	16
″	50	″	″	12	7	25	16
″	″	″	″	9	9	17	15
″	″	″	″	6	3	12	28
″	″	″	″	18	7	16	36
″	″	″	″	21	7	16	21
″	″	″	″	12	2	14	35
″	″	″	″	6	3	15	30
″	24	″	″	12	14	5	-
3-picoline	24	″	″	12	-	-	47
″	8	″	″	12	1	13	29
″	4	″	″	22	5	24	30
″	6	″	″	22	7	21	-
″	2	″	″	12	-	-	-
″	4	″	″	12	-	-	-

Key: [a] "-" indicates that this product was not formed under these reaction conditions.

The changes in different variables alter the ratio of partially weaved products but did not significantly increase the yield of the desired product, **143**. The largest yield of **143** (25%) is with pyridine, 12 eq of CuO, 7eq of K_2CO_3, and 7.5eq of 2-Me resorcinol for fifty hours. However, there are many yields that are close to this and therefore it seems that the statistical yield is the best outcome for this reaction.

Models and computational techniques indicate that the portal of the mimic made from 2-Me-*tris*-basket would be small, 6.96 Å in diameter (Figure 4.5). In order to create a mimic that

has a reasonable portal size and to attempt to increase the yield of the intermediate, *m*-tris-basket was chosen to be the intermediate. According to semi-empirical (AM1) conformational analysis the portal would then be 7.57 Å at its smallest point. As with the synthesis of **143**, the other products were unavoidable (Figure 4.6, Scheme 4.6 and Table 4.2).

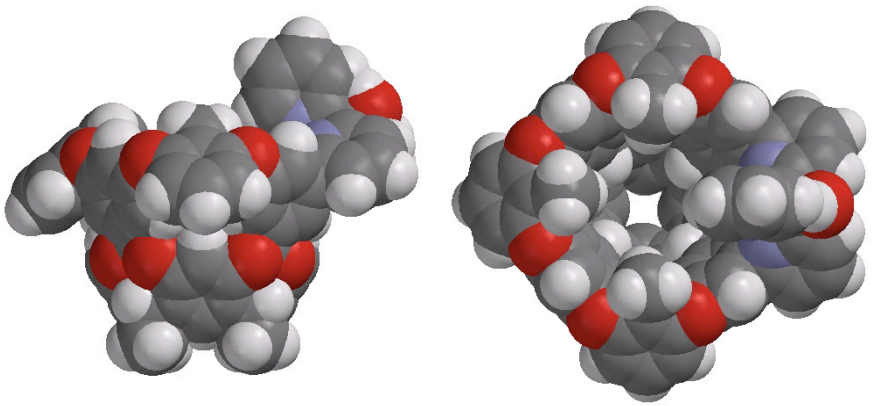

Figure 4.5 Space-Filling Model of mimic synthesized from 2-Me-*tris*-*m*-basket (Spartan Pro semi-empirical AM1 method)

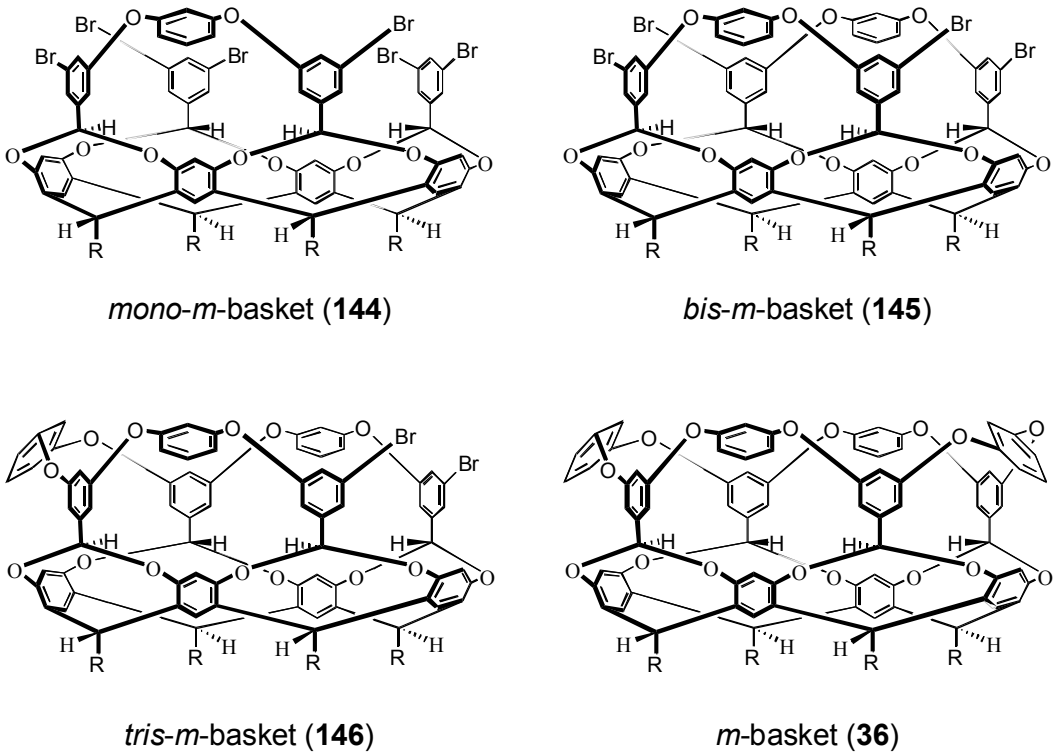

Figure 4.6 Products formed from attempting to make *m*-tris basket (**146**)

Scheme 4.6 Synthesis of *tris-m*-basket (**146**)

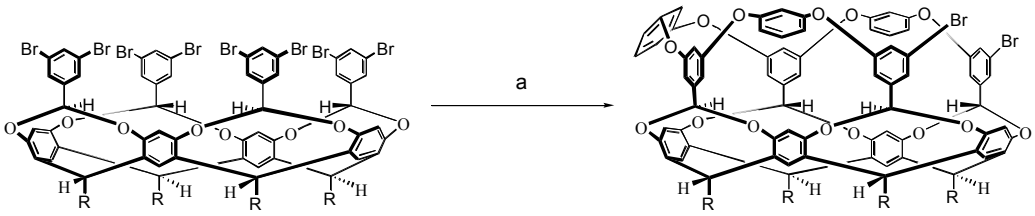

Key: a) resorcinol, base, solvent, copper

A crystal of **145** was grown from $CHCl_3$/hexane and its structure was solved by Dr. Edwin Stevens (Figure 4.7). Surprisingly, the upper row of aromatic rings are "closed" which was not a conformation observed in the fully weaved compound **36**. Presumably, this conformation is available due to the increased freedom to rotate about the Ar-O-Ar bonds. The presence of a disorganized chloroform guest conceivably imparts some stability to the "closed" conformation.

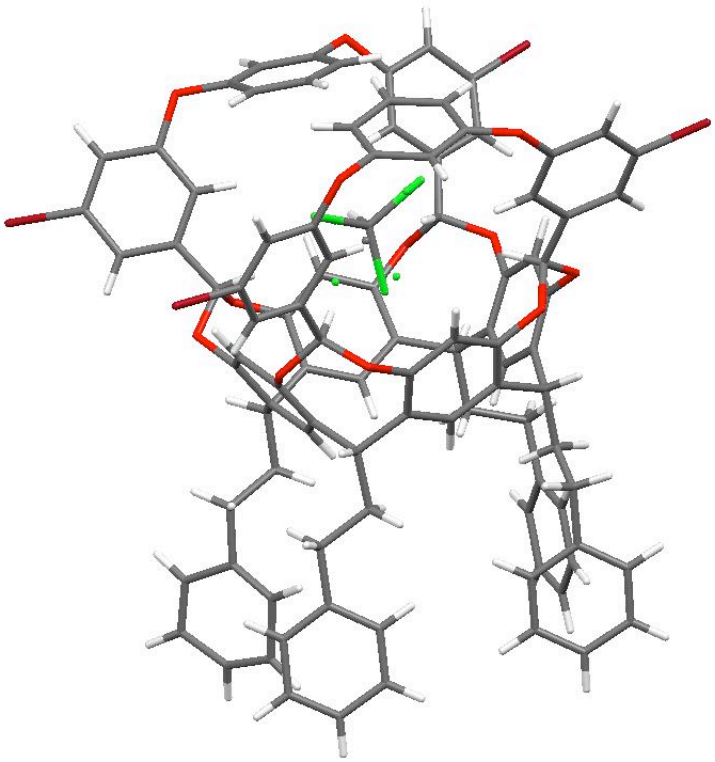

Figure 4.7 Crystal structure of **145** solved by Zakhia Moore and Dr. Edwin Stevens. Organized $CHCl_3$ molecules outside the cavity have been removed for clarity. Image generated by Mercury.[204]

Table 4.2 Product yields of **145**, **146**, and **36** under different conditions

Solvent	Time (hr)	Eq of resorcinol	Base	Eq of Base	Copper source	Eq of Cu	% **145**	% **146**	% **36**
3-picoline	96	6	K_2CO_3	12	CuO	12	2	12	37
3-picoline	16	6	″	″	″	″	8	20	24
Pyridine	72	6	″	″	″	″	11	16	29
3-picoline	16	6	″	″	″	″	-	-	32
″	18	6	″	″	″	″	2	15	44
″	20	6	″	″	″	″	-	10	35
Pyridine	72	6	″	″	″	″	1	13	20
Pyridine	80	6	″	″	″	″	1	26	14
NMP	168	6	″	″	″	″	-	-	-
Pyridine	24	5.6	″	14.4	$CuBrMe_2S$	5.44	-	14	19
″	48	5.6	Cs_2CO_3	″	″	8	-	14	30
″	22	5.6	K_2CO_3	″	″	5.44	10	34	11
″	48	4.2	Cs_2CO_3	″	″	8	11	26	15
″	48	4.2	K_2CO_3	″	″	″	41	25	1
″	72	4.2	″	″	″	″	6	15	51
″	60	4.2	″	″	″	″	-	17	25
″	48	5.6	Cs_2CO_3	″	″	5.44	-	35	26
″	48	5.6	″	″	″	4	21	19	11
″	48	5.6	″	″	″	2.4	34	15	11
″	72	4.2	K_2CO_3	″	CuO (n)	8	5	22	34
″	72	4.2	″	″	″	5.2	18	27	17
″	72	4.2	″	″	″	12	-	10	60
″	48	6	″	12	″	12	-	8	27
″	48	6	″	″	″	10	-	7	29
″	48	6	″	″	″	6	1	20	39
″	48	6	″	″	″	5	3	22	28
″	48	6	″	″	″	4	10	27	20
″	48	7.5	″	″	″	4	-	9	30
″	48	6	″	″	″	3	-	9	44
″	48	6	″	″	″	2	5	21	15
″	48	6	″	″	″	1	4	7	13
″	48	6	″	″	″	0.5	15	18	11
″	48	4.5	″	″	″	4	7	20	28
″	48	3.5	″	″	″	″	20	18	10
″	48	3	″	″	″	″	28	18	8
″	48	6	″	9	″	″	5	13	25
″	48	6	″	6	″	″	4	17	30
″	63	6	″	12	″	″	-	4	50
″	48	6	″	12	″	″	-	11	24
″	48	6	″	12	″	3	-	5	40
″	48	6	″	9	″	4	-	12	25

Key: [a] The symbol "-" indicates that the product was not formed under the reaction conditions [b] The symbol (n) indicates "nanopowder"

The best yields occurred when $CuBrMe_2S$ was used as the catalyst (5.44 eq). When K_2CO_3 was used as the base only 22 hours was required to achieve a 34% yield. When Cs_2CO_3 was the base the reaction gave similar yield but in double the reaction time. However, many of the yields were close to the best yield, which indicated that near statistical yield would be the best. When using other carbonate bases (Na_2CO_3, $NaHCO_3$) only starting material was recovered. Nitrogenous bases (NEt_3, N^iPr_3) were also unsuccessful. In contrast to $CuBrMe_2S$, other Cu(I) catalysts (such as Cu_2O and CuI) were unsuccessful.

The synthesis of the tripodal ligand is shown in Scheme 4.7. Mono-lithiation of 2,6 dibromopyridine and quenching with diethyl carbonate gave the dipyridyl ketone **147**.[202]. This ketone was reacted with 2-lithiopyridine to give the alcohol **148**. The alcohol was protected with a methoxymethyl (MOM) group to give **149**.

Scheme 4.7 Synthesis of tripodal ligand

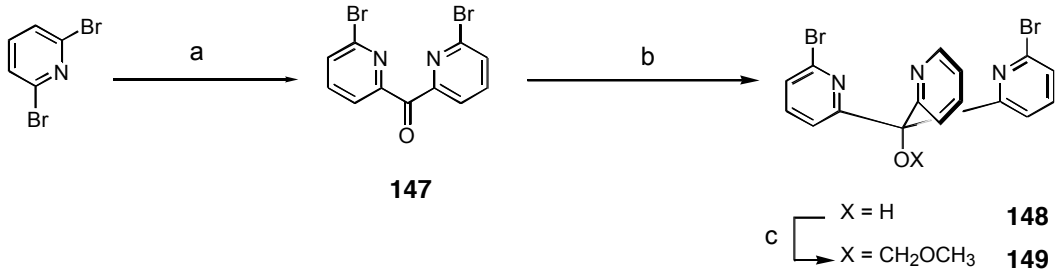

Key: a) i. *n*-BuLi ii. $(EtO)_2CO$ iii. H_3O^+ b) i. 2-lithiopyridine ii. H_3O^+ c) NaH, BrMOM

Initially, Suzuki chemistry was thought to be a viable method of brining the tripodal ligand and the **146** together.[205, 206] However, boronic esters in the 2-positions of pyridines are not stable. Therefore, the synthesis of boronic acid **150** was undertaken. The product of this reaction was insoluble in common organic solvents and the product mixture was placed in Suzuki conditions using $Pd(PPh_3)_6$ as the palladium catalyst with the tripodal dibromide ligand **149**. No desired product was formed and the only reaction product was the diprotio *tris-m*-basket (**151**).[207]

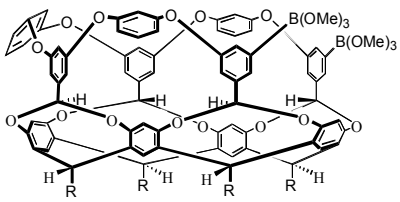

150

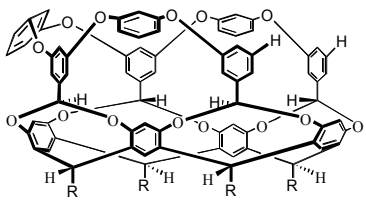

151

Several model reactions were conducted to determine what caused the reaction to fail. The first was to test the palladium by coupling 2-bromopyridine and phenyl boronic acid (Scheme 4.8). This reaction proceeded without difficulty in 84% yield. When the boronic acid was placed on the pyridine and the bromine on the benzene, the yield fell to 14% under the same conditions.

Scheme 4.8 Model Reaction to test the Pd source

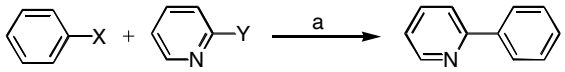

X = Br, Y = $B(OMe)_2$
X = $B(OMe)_2$ Y = Br

Key a. Cs_2CO_3, DMA, $Pd(PPh_3)_4$

The second model reaction that was undertaken was to place octa-bromine deep cavity cavitand **35** under Suzuki conditions with phenyl boronic acid. **35** is more congested then bromobenzene but less congested then **146**. This created the octa-phenyl deep cavity cavitand **152** (Scheme 4.9).

Scheme 4.9 Model Suzuki Reaction using Octa-Bromide DCC (**35**)

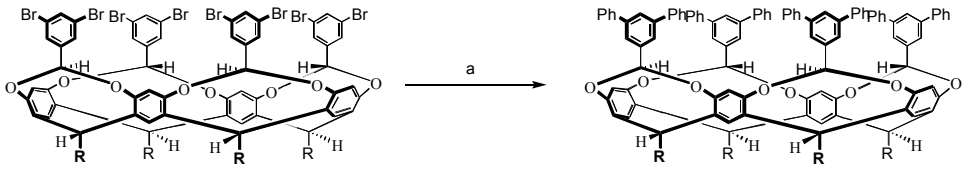

152

Key; a. Cs_2CO_3, DMA, phenyl boronic acid

This reaction was successful in several solvents (DME, DMA, benzene, toluene) but the best yield came with the conditions listed above (75%).

The ligating nature of **149** could cause it to complex and tie up the palladium. Therefore, the last model reaction was between **149** and phenyl boronic acid or the boronic ester of **149** and bromobenzene to give the biphenyl product **153** (Scheme 4.10 and Table 4.3).

Scheme 4.10 Model Reactions to test the ability of **149** to undergo Suzuki Coupling

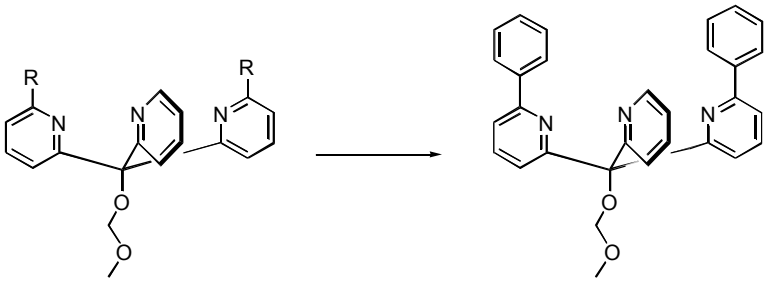

R = -Br
R = -B(OMe)$_2$

153

Key: phenyl boronic acid, $Pd(PPh_3)_4$, DME, K_2CO_3

Table 4.3. Yields of **153**[a]

Solvent	R group	% Yield of 154[b]
Benzene	-Br	36
Toluene	-Br	51
Xylenes	-Br	67
Dioxane	-Br	9
DME	-Br	88
THF	-Br	19
DMF	-Br	38
DMA	-Br	-
^{i}PrOH	-Br	56
Toluene	-B(OMe)$_3$	6
Xylenes	-B(OMe)$_3$	3
Dioxane	-B(OMe)$_3$	-
DME	-B(OMe)$_3$	4
^{i}PrOH	-B(OMe)$_3$	13

[a] K_2CO_3 as base and $Pd(PPh_3)_4$ as catalyst. [b] The symbol "-" indicates that the product was not formed under these conditions.

This model reaction was most successful when bromide was the R group. DME was found to be the best solvent for this reaction. When the R group was –B(OMe)$_2$ the reaction yields were greatly reduced.

These model reactions demonstrated that the problem was not the palladium, nor was it the size of the substrate, nor the entrapment of the palladium by the tripodal ligand. The difficulty was two-fold. The first difficulty was placing the boronic acid on either of the reactants. The lithiation and boronation of **146** caused separation problems and therefore it was unclear even if the boronic acid was being formed. Additionally, the boronic acid was unstable on the pyridine. The second problem was the crowded reaction sites. The tris-*m*-basket was sterically crowded when compared to the octa bromide deep cavity cavitand (**35**). Moreover, the tripodal ligand **149** was also crowded in the conformation it was required to adopt to form the desired products. Hence, a new synthetic strategy was devised.

If the reaction site could be extended away from the bulk of **146** a reaction between the cavitand and the tripodal ligand might be possible. To this end the bromides were exchanged for phenols producing the diol **154** (Scheme 4.11).

Scheme 4.11 Synthesis of tris-*m*-basket diol (**154**)

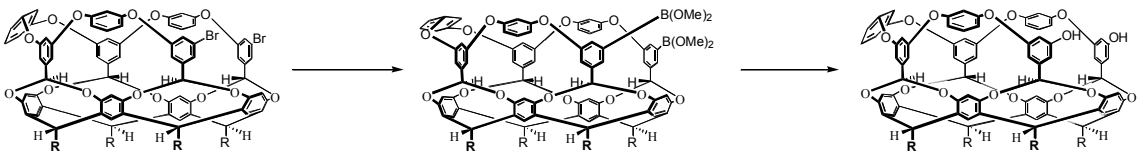

154

Key: a. 1. *n*-BuLi, $B(OMe)_3$ 2. H_3O^+ b. 3N $NaOH/H_2O_2$ (1:1)

The reaction yield was strongly dependent on the base. If 2.2eq of *n*-BuLi was used the reaction produced a large number of products and the desired diol **154** was formed in very low yield (10-30%) after a difficult separation.[208] If, however, *tert*-BuLi was employed only three products were produced, the diprotio tris-*m*-basket (**151**), the chiral tris-*m*-basket mono-ol (**155**) and the desired tris-*m*-basket diol (**154**). The yield of the desired **154** was 62%. These results can be understood from examination of the lithiation/formylation of the previous chapter. For unknown reasons *tert*-BuLi does not easily remove a proton *ortho* to the ether oxygens and so

the only reaction is metal-halogen exchange. On the other hand, *n*-BuLi has been shown to remove *ortho* protons at 2.2 equivalents of base, which gave rise to numerous products.

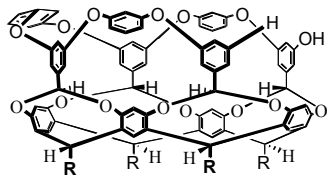

155

The diol **154** underwent the Ullmann ether synthesis with the dibromide tripodal ligand **149**. The 2-position of pyridine is particularly activated to S_NAr mechanism.[183] Therefore, **154** and **149** were reacted with CuO in refluxing pyridine (Scheme 4.12) to give a mixture of diasteromers in 65% yield. The desired diasteromer (**155**) was the major isomer, making up 65% of the overall yield. The diastereromers are separated by column chromatography.

Scheme 4.12 Synthesis of the enzyme mimic using the Ullmann ether Synthesis

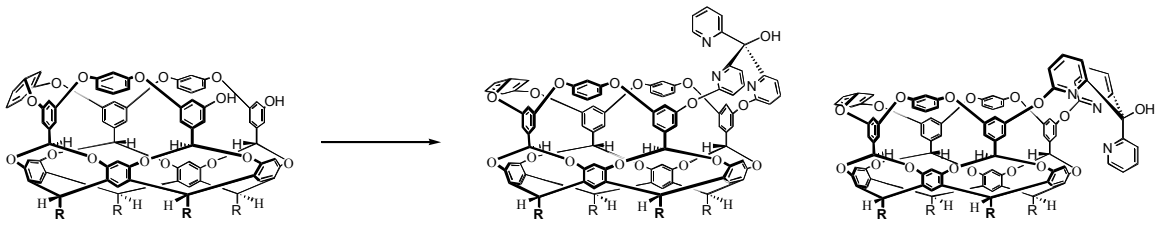

154 **156** **157**

Key: a. **149**, CuO, K_2CO_3, pyridine, Δ b. H_3O^+

The structures of **156** and **157** were deduced from the NMR shifts of protons. For example the position of the H_b proton signal (the acetal proton) is dependant on how shielded it is. The shift of this proton in the deep cavity cavitands **35** and **152** is 5.38 and 5.68 ppm respectively. When compared to the shift of this proton in **36** (4.58 ppm) it was evident how dependant position of the signal was on shielding. There were two signals for this proton in each of the diasteromers. The most downfielded shift in **156** is 4.80 ppm. Alternatively, the most downfield shifted H_b proton in **157** is at 4.93 ppm. In addition to the H_b proton, another telling

proton was in the 2-position of the pyridine. It would be expected that the most downfield shifted proton between the two diasteromers would be **156** as it would not be buried into the side of the basket. Therefore the products were labeled as shown.

The new host **156** had a much larger portal then the two planned hosts. The portal diameter was 13.02 Å at its smallest point according to Spartan Pro semi-empirical AM1 model (Figure 4.8). This effectively moved the tripodal ligand away from the portal allowing a relatively unobstructed entrance. As has been observed in previous chapters, any obstruction of the portal quickly reduces the binding ability of the host (i.e. **71**, and **125**). An additional benefit of **156** over the originally planned product was the increased flexibility of the host. The increased flexibility would allow **156** to optimize the orientation of the zinc bound hydroxide for maximum effectiveness.

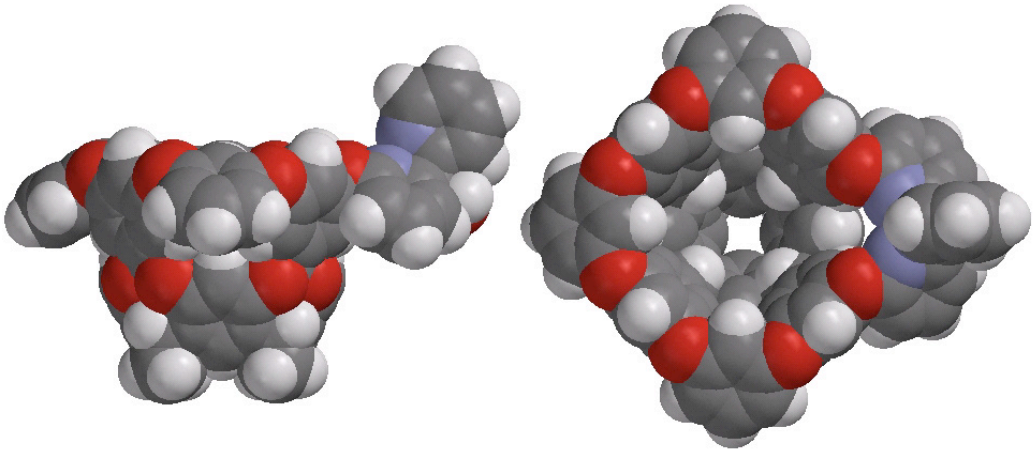

Figure 4.8 Space filling model of the optimized structure of **156**.

4.2 Zinc Binding and Physical Studies of the enzyme mimic

NMR and UV-Vis titration studies of **156** with zinc were carried out. NMR studies involved titrating a zinc perchlorate solution in acetonitrile-d_3 into a solution of **156** in CD_2Cl_2. The spectroscopic proton signal that was followed was the proton in the 2-position of the tripodal ligand. When the zinc was added this proton disappeared at moved downfield with one

equivalent of zinc (Figure 4.9a and b). There was no further change after one equivalent and no change in the NMR after 24 hours.

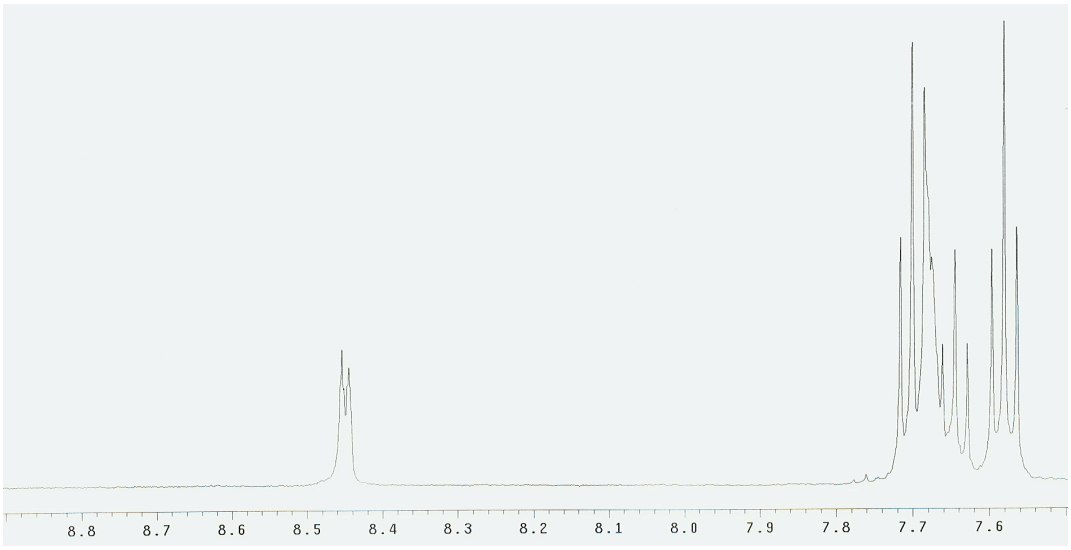

a

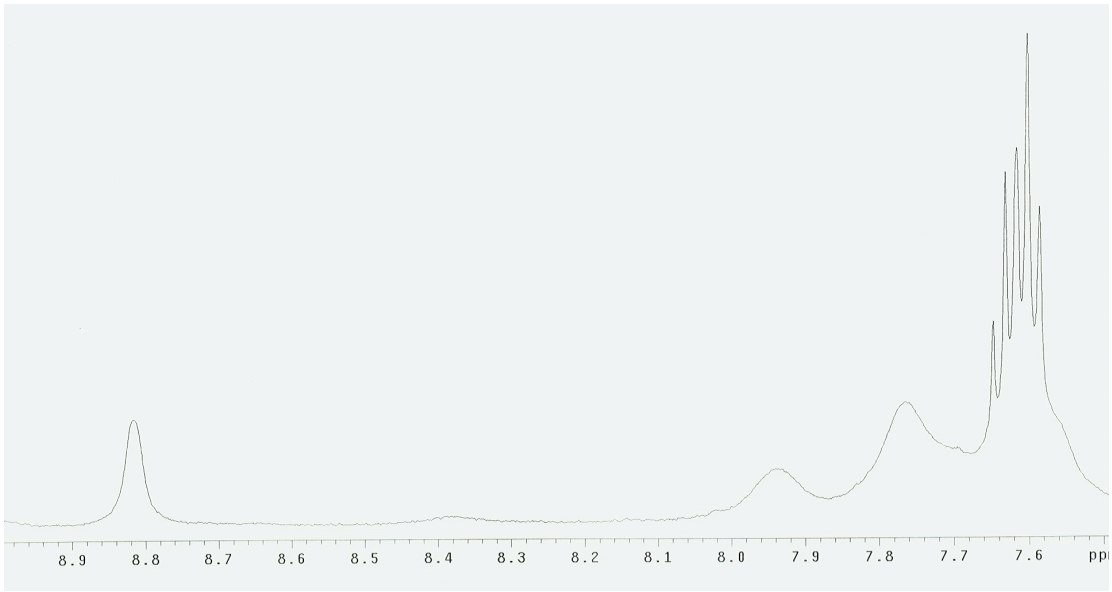

b

Figure 4.9 NMR zinc titration of **156** a) in the absence of zinc b) with one equivalent of zinc

The UV-Vis titration was carried out using the same technique as with the NMR. The appearance of a new peak at λ = 293 cm was followed while titrating **156** with zinc. A binding isotherm was obtained by plotting the change in absorbance as a function of the concentration of zinc (Figure 4.10).

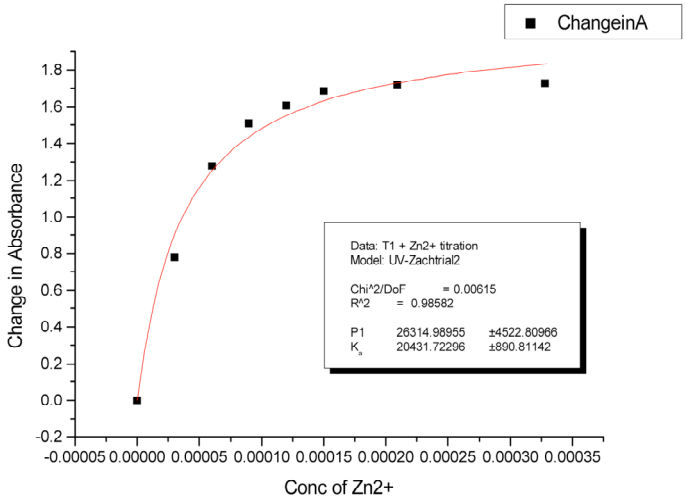

Figure 4.10 Binding isotherm of **156** titrated with zinc using wavelength 293 cm

Both of these experiments indicated that the zinc binding was strong and that the ratio of zinc:ligand was 1:1. The 1:1 binding is proof that the basket is able to block the formation of the sandwich compounds. Additionally, the binding of the zinc to the tripodal ligand was strong and therefore unique for a *tris*(pyridyl)methanol.

V. CONCLUSIONS

In an effort to synthesize an enzyme mimic or shape selective catalysts, two new, rigid, hydrophobic hosts were synthesized. A variety of guests were examined in three different solvents. One of the important driving forces of association was the formation of C-H···X-R hydrogen bonds between halogens on the guest and a ring of electron deficient acetal hydrogens buried within the host. A deuterated host was tested to further examine the formation of the C-H···X-R hydrogen bonds. It was learned that if the guest was rigid and forced a conformation that "pushed" the halogen to interact with the acetal protons, then there was a significant isotope effect on the association constant.

Two methods were employed to place inward facing functionality onto the hosts. The first method was to utilize directed *ortho* metallation, which would place electrophiles along the rim of the hydrophobic pocket. Perlithialtion of the host could have led to sixty-nine product. However, reaction conditions and host rigidity reduced the number of formed product to twelve when the electrophile was dimethylforamide. The resulting aldehydes were resistant to oxidation and the electrophile was changed to methyl chloroformate. The resulting esters were readily hydrolyzed to the acids. The extent to which *endo-* or *exo-* carboxylic acids affect the conformation of the guest was examined. It was determined that both *endo-* and *exo-* will direct the orientation; when they are on the same host, *exo-* is the dominant director.

The second method to place inward facing functionality onto the basket architecture was to use a zinc-binding tripodal ligand to direct a zinc-bound hydroxide into the cavity. The resulting host has demonstrated its ability to bind zinc strongly and without forming inactive 2:1 (ligand:zinc) sandwich complexes.

VI. EXPERIMENTAL SECTION

6.1 General

All reagents were purchased from either Aldrich Chemical Company or VWR Chemical Company. Deuterated solvents were purchased from Cambridge Isotope Laboratories. Dimethylforamide (DMF) and dimethylacetamide (DMA) were stored over molecular sieves and degassed prior to use. Diethyl ether and tetrahydrofuran (THF) was dried by distillation from sodium benzyl ketal. n-BuLi, *sec*-BuLi, and *tert*-BuLi were freshly titrated using biphenyl acetic acid. Other reagents were used as received. All reactions were run under a nitrogen atmosphere.

Chromatography (silica gel 60Å. 200-400 mesh; National International) was used for product purification. ^{1}H NMR spectra were recorded on Varian Inova instruments (400 MHz or 500 MHz). MS analysis was preformed with a PerSeptive Biosystems Voyager Elite MALDI-TOF instrument and a Micromass Quattro-II when using electrospray technique. UV-Vis spectra were recorded using an HP 8453 UV-Vis spectrometer. Elemental Analyses were preformed by Atlantic Microlab Inc. Melting points are uncorrected.

6.2 Synthesized Compounds

5-Methyl *m*-basket (70)

To an oven dried round bottom flask containing 24 mL pyridine was added 100 mg (5.30 x 10^{-5} mol) of deep cavity cavitand **36**. To this stirring solution was added 146.4 mg (1.06 mmol) of K_2CO_3 and 65.8 mg (0.53 mmol) of 5-methyl resorcinol. Nitrogen was bubbled through the mixture for 5 minutes before 84.3 mg of CuO (1.06 mmol) was added, and the solution was heated to a vigorous reflux (sand bath) and stirred for seven days. After cooling the solvent was removed under reduced pressure to give a crude solid mixture that was suspended in $CHCl_3$ and loaded onto a short silica plug. Flushing with $CHCl_3$ and removal of the solvent of

the resulting colorless solution gave the crude product. Chromatography (1:1 $CHCl_3$/hexanes) and then re-crystallization with $CHCl_3$/hexanes gave pure **70** as a colorless solid in 88% yield: mp > 250 °C. ^{1}H NMR (500 MHz, $CDCl_3$) δ 2.43 (s, 12H), 2.55 (m, 16H), 4.56 (s, 4H), 4.84 (t, 4H, *J* = 8 Hz), 6.05 (s, 4H), 6.39 (t, 4H, *J* = 2 Hz), 6.52 (d, 8H, *J* = 2 Hz), 6.93 (t, 4H, *J* = 2 Hz), 7.00 (d, 8H, *J* = 2 Hz), 7.10 (m, 8H), 7.19 (m, 16H); MS *m/z* $(M + Ag^+)^+$ Calculated: 1845, Found: 1845.38. Anal. Calculated for $C_{116}H_{88}O_{16}$: C, 80.17 H, 5.10. Found: C, 80.05; H, 5.17.

2-Methyl *m*-basket (71)

To an oven dried round bottom flask containing 24 mL pyridine was added 100 mg (5.30 x 10^{-5} mol) of deep cavity cavitand **36**. To this stirring solution was added 146.4 mg (1.06 mmol) of K_2CO_3 and 65.8 mg (0.53 mmol) of 2-methyl resorcinol. Nitrogen was bubbled through the mixture for 5 minutes before 84.3 mg of CuO (1.06 mmol) was added, and the solution was heated to a vigorous reflux (sand bath) and stirred for fourteen days. After cooling the solvent was removed under reduced pressure to give a crude solid mixture that was suspended in $CHCl_3$ and loaded onto a short silica plug. Flushing with $CHCl_3$ and removal of the solvent of the resulting colorless solution gave the crude product. Chromatography (1:1 $CHCl_3$/hexanes) and then re-crystallization with $CHCl_3$/hexanes gave pure **71** as a colorless solid in 80% yield: mp > 250 °C. ^{1}H NMR (500 MHz, $CDCl_3$) δ 1.64 (s, 12H), 2.53 (m, 16H), 4.50 (s, 4H), 4.81 (t, 4H, *J* = 8 Hz), 5.93 (s, 4H), 6.48 (d, 8H, *J* = 1 Hz), 7.04 (s, 4H), 7.09 (m, 8H), 7.14 (s, 4H), 7.20 (m, 20H), 7.40 (t, 4H, *J* = 8 Hz); MS *m/z* $(M + Ag^+)^+$ Calculated: 1845, Found: 1845.97. Anal. Calculated for $C_{116}H_{88}O_{16}.CHCl_3$: C, 75.66 H, 4.93. Found: C, 75.66 H, 5.13.

General procedure for the formation of aldehydes (100-109)

To a dried flask was added 0.3g (0.18 mmol) of **37** and 20 mL of distilled THF. This solution was brought to –78 °C with a dry ice/acetone bath. The alkyl lithiate was then slowly injected and the solution was allowed to stir for 20 minutes. DMF was then injected slowly and the solution was allowed to stir at –78 °C for two hours. The solution was then brought to ~-20 °C and acidified with 10% HCl. The mixture was then partitioned between $CHCl_3$ and water. The organic layer was collected and the water layer was washed twice with $CHCl_3$. The organic layers were combined and dried with anhydrous Na_2SO_4 then filtered. The solution was concentrated under reduced pressure. The resulting white solid was placed on an Abderhalden apparatus at 210 °C overnight to remove unreacted DMF.

n-BuLi as base

2.2eq - 0.16 mL (0.4 mmol) n-BuLi and 0.0745 mL (1.08mmol) DMF. Resuspened mixture in CH_2Cl_2 and added ~10 mL dry silica. Solvent was removed by reduced pressure. Placed dry silica onto column prepared with 70% CH_2Cl_2/Hexane. Ran column with 70% CH_2Cl_2/Hexane for one volume then changed mobile phase to 90% CH_2Cl_2/Hexane until product stops eluting. Products are white solid.

***Endo*-aldehyde *m*-basket (100)**

Yield 11%: m.p. > 250°C. ^{1}H NMR (500MHz, $CDCl_3$) δ 2.56 (m, 16H), 4.54 (s, 2H), 4.55 (s, 2H), 4.84 (m, 4H), 5.95 (s, 1H), 6.01 (m, 3H), 6.40 (s, 2H), 6.48 (s, 2H), 6.48 (s, 2H), 6.54 (s, 2H), 6.60 (t, 1H, J = 2 Hz), 6.62 (s, 2H), 6.73 (t, 2H, J = 2), 6.99 (t, 2H, J = 2), 7.06 (t, 2H, J = 2), 7.12 (m, 8H), 7.17-7.30 (m, 22H), 7.35 (d, 2H, J = 8.5), 7.58 (m, 3H), 7.82 (t, 1H, J =

8.5 Hz), 10.0 (s, 1H); MS *m/z* $(M + Ag^+)^+$ Calculated: 1816, Found: 1816.97. Anal. Calculated for $C_{113}H_{80}O_{17}$.1/2 CH_2Cl_2: C, 77.80 H, 4.66. Found C, 77.77 H, 4.82.

***Exo*-aldehyde *m*-basket (101)**

Yield 12%: m.p. > 250°C. ^{1}H NMR (500MHz, CD_2Cl_2) δ 2.59 (m, 16H), 4.45 (m, 4H), 4.80 (m, 4H), 5.95 (s, 2H), 5.99 (s, 2H), 6.52 (m, 6H), 6.63 (s, 2H), 6.66 (t, 2H, *J* = 2Hz), 6.69 (t, 2H, *J* = 2Hz), 6.99 (m, 2H), 7.13 (m, 8H), 7.18-7.30 (m, 25H), 7.62 (m, 4H), 10.67 (s, 1H); MS *m/z* $(M + Ag^+)^+$ Calculated: 1816, Found: 1817.45. Anal. Calculated for $C_{113}H_{80}O_{17}.H_2O$: C, 78.55 H, 4.78. Found C, 78.85 H, 4.69.

<u>*5.5eq*</u> – 0.4 mL (0.99 mmol) n-BuLi and 0.21 mL (2.7 mmol) DMF. Redissolved product mixture in a small amount of 90% CH_2Cl_2/Hexane. Placed solution onto column prepared with 90% CH_2Cl_2/Hexane. Ran column with 90% CH_2Cl_2/Hexane for one volume then changed mobile phase to CH_2Cl_2 until product stops eluting. Products are white solid. **100** 7%; **101** 8%.

A/C-*endo*-dialdehyde *m*-basket (102)

Yield 13% m.p. > 250°C. ^{1}H NMR (400 MHz, $CDCl_3$) δ 2.57 (m, 16H), 4.54 (s, 4H), 4.84 (t, 4H, *J* = 8 Hz), 5.95 (s, 2H), 5.99 (s, 2H), 6.39 (s, 4H), 6.60(s, 4H), 6.82 (bs, 2H), 7.07 (bs, 4H), 7.12 (m, 8H), 7.24 (m, 20H), 7.35 (d, 4H *J* = 8.4 Hz), 7.58 (t, 2H, *J* = 8.4 Hz), 7.82 (t, 2H, *J* = 8.4 Hz), 9.99 (s, 2H); MS *m/z* $(M + Ag^+)^+$ Calculated: 1844, Found: 1845.47. Anal. Calculated for $C_{114}H_{80}O_{18}$.1/2CH_2Cl_2: C, 77.19 H, 4.77. Found C, 76.84 H, 4.73.

***Exo*-bis dialdehyde *m*-basket (both 103/104)**

Yield 31%, m.p. > 250°C. ^{1}H NMR; MS *m/z* $(M + Ag^+)^+$ Calculated: 1844, Found: 1845.43. Anal. Calculated for $C_{114}H_{80}O_{18}.H_2O$: C, 77.98 H, 4.71. Found C, 77.97 H, 4.84.

A-*exo*-B-*endo*-dialdehyde *m*-basket (105)

Yield 24% m.p. > 250°C. ^{1}H NMR (500MHz, CD_2Cl_2) δ 2.56 (m, 16H), 4.42 (m, 2H), 4.47 (m, 2H), 4.80 (m, 4H), 5.94 (m, 3H), 5.98 (s, 1H), 6.40 (m, 2H), 6.47 (s, 1H), 6.54 (s, 1H), 6.58 (s, 1H), 6.63 (s, 2H), 6.65 (s, 1H), 6.69 (t, 1H, *J* = 2Hz), 6.74 (t, 1H, *J* = 2Hz), 6.78 (t, 1H, *J* = 2Hz), 7.01 (bs, 1H), 7.05 (m, 2H), 7.13 (m, 8H), 7.15-7.34 (m, 22H), 7.38 (d, 2H, *J* = 8.5 Hz), 7.63 (m, 3H), 7.85 (t, 1H, *J* = 8Hz), 9.98 (s, 1H), 10.68 (s, 1H); MS *m/z* $(M + Ag^+)^+$ Calculated: 1844, Found: 1844.78. Anal. Calculated for $C_{114}H_{80}O_{18}.1/2CH_2Cl_2$: C, 77.25 H, 4.59. Found C, 77.55 H, 4.76.

<u>*10eq*</u> – 0.72 mL (1.8 mmol) n-BuLi and 0.42 mL (5.4 mmol) DMF. Redissolved product mixture in a small amount of 90% CH_2Cl_2/Hexane. Placed solution onto column prepared with 90% CH_2Cl_2/Hexane. Ran column with 90% CH_2Cl_2/Hexane for one volume then changed mobile phase to CH_2Cl_2 until product stops eluting. Products are white solid. **100** 4%; **101** 6%; **102** 10%; **103/104** 22%; **105** 43%.

<u>*Sec*-BuLi as base</u>

<u>*5.5eq*</u> – 0.71 mL (0.99 mmol) *sec*-BuLi and 0.21 mL (2.7 mmol) DMF. Redissolved product mixture in a small amount of CH_2Cl_2. Placed solution onto column prepared with 100% CH_2Cl_2. Ran column with CH_2Cl_2 for one volume then changed mobile phase to 5% ethyl acetate/CH_2Cl_2

for one volume then 10% ethyl acetate/CH_2Cl_2 until product stops eluting. Products are white solid.

exo-trialdehyde _m_-basket (106)

Yield 20% m.p. >250°C; ^{1}H NMR (400MHz, $CDCl_3$) δ 2.57 (m, 16H), 4.54 (m, 4H), 4.84 (m, 4H), 5.91 (s, 2H), 5.97 (s, 2H), 6.50 (bs, 2H), 6.63 (s, 6H), 6.68 (bs, 2H), 6.72 (bs, 2H), 7.01 (bs, 1H), 7.12 (m, 8H), 7.20-7.35 (m, 24H), 7.65 (m, 4H), 10.7 (m, 3H); MS *m*/*z* $(M + Ag^+)^+$ Calculated: 1872, Found: 1873.58. Anal. Calculated for $C_{115}H_{80}O_{19}.H_2O$: C, 77.43 H, 4.63. Found C, 77.43 H, 4.56.

A/B-_exo_-C-_endo_-trialdehyde _m_-basket (107)

Yield 20% m.p. >250°C; ^{1}H NMR (500MHz, $CDCl_3$) δ 2.57 (m, 16H), 4.52 (m, 4H), 4.83 (m, 4H), 5.92 (s, 1H), 5.96 (m, 3H), 6.38 (bs, 2H), 6.59 (s, 2H), 6.62 (s, 2H), 6.65 (m, 3H), 6.77 (bs, 2H), 7.06 (bs, 2H), 7.12 (m, 8H), 7.19-7.36 (m, 27H), 7.64 (m, 3H), 7.83 (t, 1H, *J* = 8.5), 10.0 (s, 1H), 10.71 (s, 2H); MS *m*/*z* $(M + Ag^+)^+$ Calculated: 1872, Found: 1873.58. Anal. Calculated for $C_{115}H_{80}O_{19}.3H_2O$: C, 75.90 H, 4.76. Found C, 75.96 H, 4.55.

exo-tetra-aldehyde _m_-basket (108)

Yield 30% m.p. > 250°C; ^{1}H NMR (400MHz, $CDCl_3$) δ 2.57 (m, 16H), 4.51 (s, 4H), 4.83 (t, 4H, *J* = 8 Hz), 5.91 (s, 4H), 6.62 (bs, 8H), 6.72 (bs, 4H), 7.12 (m, 8H), 7.22 (m, 16H), 7.34 (dd, 8H *J* = 8.2 Hz), 7.67 (t, 4H, *J* = 8.2 Hz), 10.70 (s, 4H); MS *m*/*z* $(M + Ag^+)^+$ Calculated: 1900, Found: 1901.44. Anal. Calculated for $C_{116}H_{80}O_{20}.2H_2O$: C, 76.14 H, 4.63. Found C, 75.77 H, 4.54.

A/B/C-*exo*-C-*endo*-tetra-aldehyde *m*-basket (109)

Yield 3% m.p. > 250°C; ^{1}H NMR (400MHz, $CDCl_3$) δ 2.61 (m, 16H), 4.44 (m, 4H), 4.78 (m, 4H), 5.90 (s, 3H), 5.93 (s, 1H), 6.40 (s, 1H), 6.51 (s, 1H), 6.57 (s, 1H), 6.59 (s, 1H0, 6.64 (m, 3H), 6.72 (m, 2H), 6.76 (t, 1H, *J* = 2Hz), 6.82 (t, 1H, *J* = 2Hz), 7.08 (bs, 1H), 7.13 (m, 8H), 7.19-7.39 (m, 22H), 7.43 (d, 2H, *J* = 8.4Hz), 7.67 (m, 3H), 7.89 (t, 1H, *J* = 8.4Hz), 9.95 (s, 1H), 10.68 (m, 3H); MS *m/z* $(M + Ag^+)^+$ Calculated: 1900, Found: 1901.52. Anal. Calculated for $C_{116}H_{80}O_{20}.CH_2Cl_2$: C, 74.57 H, 4.40. Found C, 74.21 H, 4.42.

<u>*10eq*</u> – 1.29 mL (1.8 mmol) *sec*-BuLi and 0.4 mL (5.4 mmol) DMF. Redissolved in 10% ethyl acetate/CH_2Cl_2 and loaded onto a silica column made with 10% ethyl acetate/CH_2Cl_2. Used 10% ethyl acetate/CH_2Cl_2 as the mobile phase. **106** 14%; **107** 8%; **108** 60%

***tert*-BuLi**

<u>*5.5eq*</u> 0.58 mL (0.99 mmol) *tert*-BuLi and 0.21 mL (2.7 mmol) DMF. **100** 8%; **101** 10%; **103/104** 19%; **105** 10%; **106** 12%; **107** 11%.

<u>*10 eq*</u> 1.1 mL (1.8 mmol) *tert*-BuLi and 0.4 mL (5.4 mmol) DMF. **106** 18%; **107** 23%; **108** 19%; **109** 13%.

***Endo*-benzyl alcohol *m*-basket (110)**

Dissolved 50 mg (.03 mmol) **100** in 2 mL distilled THF. Slowly injected 0.033ml (0.033 mmol) of 1M $LiAlH_4$. Allowed to stir at room temperature overnight. Quench reaction with saturated NH_4Cl. The mixture was then partitioned between $CHCl_3$ and water. The organic layer

was collected and the water layer was washed twice with $CHCl_3$. The organic layers were combined and dried with anhydrous Na_2SO_4 then filtered. The solution was concentrated under reduced pressure to make a white solid. This was redissolved in CH_2Cl_2 and placed on column using CH_2Cl_2 as mobile phase. Yield 80%. m.p. > 250°C; ^{1}H NMR (500MHz, $CDCl_3$) δ 2.57 (m, 16H), 4.38 (s, 2H), 4.53 (s, 2H), 4.58 (s, 2H), 4.844 (m, 4H), 5.99 (s, 3H), 6.04 (s, 1H), 6.49 (s, 2H), 6.52 (m, 4H), 6.59 (bs, 1H), 6.61 (s, 2H), 6.66 (s, 2H), 6.97 (bs, 2H), 7.08 (bs, 2H), 7.12 (m, 8H), 7.16-7.30 (m, 24H), 7.58 (t, 4H, J = 8.5); MS m/z $(M + Ag^+)^+$ Calculated: 1819, Found: 1819.51 Anal. Calculated for $C_{113}H_{82}O_{17}.2H_2O$: C, 77.65 H, 4.96. Found C, 77.78 H, 5.10.

***Exo*-benzyl alcohol *m*-basket (111)**

Dissolved 115 mg (.067 mmol) **101** in 4 mL distilled THF. Slowly injected 0.074ml (0.074 mmol) of 1M $LiAlH_4$. Allowed to stir at room temperature overnight. Quench reaction with saturated NH_4Cl. The mixture was then partitioned between $CHCl_3$ and water. The organic layer was collected and the water layer was washed twice with $CHCl_3$. The organic layers were combined and dried with anhydrous Na_2SO_4 then filtered. The solution was concentrated under reduced pressure to make a white solid. This was redissolved in CH_2Cl_2 and placed on column using CH_2Cl_2 as mobile phase. Yield 99%. m.p. > 250°C; ^{1}H NMR (500MHz, $CDCl_3$) δ 2.52 (m, 16H), 4.54 (s, 3H), 4.57 (s, 1H), 4.84 (m, 4H), 5.05 (s, 2H), 6.00 (s, 2H), 6.01 (s, 2H), 6.52 (m, 6H), 6.58 (s, 2H), 6.63 (t, 2H, J = 2 Hz), 6.65 (t, 2H, J = 2 Hz), 6.99 (bs, 2H), 7.00 (bs, 1H), 7.12 (m, 8H), 7.18-7.28 (m, 20H), 7.59 (m, 4H); MS m/z $(M + Ag^+)^+$ Calculated: 1819, Found: 1820.45 Anal. Calculated for $C_{113}H_{82}O_{17}.H_2O$: C, 78.46 H, 4.89. Found C, 78.47 H, 5.01.

A/B-*exo*-C-*endo* tribenzyl alcohol *m*-basket (112)

Dissolved 100 mg (.057 mmol) **107** in 4 mL distilled THF. Added 13 mg (0.34 mmol) $NaBH_4$. Allowed to stir at room temperature overnight. Quench reaction with saturated NH_4Cl. The mixture was then partitioned between $CHCl_3$ and water. The organic layer was collected and the water layer was washed twice with $CHCl_3$. The organic layers were combined and dried with anhydrous Na_2SO_4 then filtered. The solution was concentrated under reduced pressure to make a white solid. This was redissolved in CH_2Cl_2 and placed on column using 10% ethyl acetate/CH_2Cl_2 as mobile phase. Yield 94%. m.p. > 250°C; ^{1}H NMR (400MHz, $CDCl_3$) δ 2.55 (m, 16H), 4.38 (s, 2H), 4.52 (s, 2H), 4.58 (s, 2H), 4.85 (t, 4H, J = 8 Hz), 5.04 (s, 4H), 5.97 (s, 2H), 5.98 (s, 1H), 6.02 (s, 1H), 6.51 (bs, 2H), 6.54 (bs, 2H), 6.59 (m, 4H), 6.68 (t, 2H, J = 2 Hz), 7.08 (bs, 2H), 7.13 (m, 8H), 7.18-7.31 (m, 20H), 7.60 (m, 4H); MS m/z $(M + Ag^+)^+$ Calculated: 1878, Found: 1879.30 Anal. Calculated for $C_{115}H_{86}O_{19}.2H_2O$: C, 76.40 H, 5.02. Found C, 76.67 H, 5.07.

***Exo*-tetrabenzyl alcohol *m*-basket (113)**

Dissolved 130 mg (.073 mmol) **108** in 5 mL distilled THF. Slowly added 22.1 mg (0.58 mmol) of $NaBH_4$. Allowed to stir at room temperature overnight. Quench reaction with MeOH. The mixture was then partitioned between $CHCl_3$ and water. The organic layer was collected and the water layer was washed twice with $CHCl_3$. The organic layers were combined and dried with anhydrous Na_2SO_4 then filtered. The solution was concentrated under reduced pressure to make a white solid. Product was recrystallized from THF Yield 94%. m.p. > 250°C; ^{1}H NMR (500MHz, DMSO-d_6) δ 2.57 (m, 16H), 4.42 (s, 4H), 4.60 (t, 4H, J = 7), 4.71 (d, 8H, J = 5), 4.95 (t, 4H, J = 5), 5.80 (s, 4H), 6.42 (s, 8H), 6.69 (bs, 4H), 7.1-7.26 (m, 20H), 7.30 (d, 8H, J = 8),

7.70 (m, 10H); MS *m/z* $(M + Ag^+)^+$ Calculated: 1908, Found: 1909.80 Anal. Calculated for $C_{116}H_{88}O_{20}.3H_2O$: C, 75.07 H, 5.10. Found C, 75.23 H, 5.14.

General procedure for the formation of methyl esters (114-122)

To a dried flask was added 0.3g (0.18 mmol) of **37** and 20 mL of distilled THF. This solution was brought to –78 °C with a dry ice/acetone bath. The alkyl lithiate was then slowly injected and the solution was allowed to stir for 20 minutes. Methyl chloroformate was then injected slowly and the solution was allowed to stir at –78 °C for two hours. The solution was then brought to ~-20 °C and acidified with 10% HCl. The mixture was then partitioned between $CHCl_3$ and water. The organic layer was collected and the water layer was washed twice with $CHCl_3$. The organic layers were combined and dried with anhydrous Na_2SO_4 then filtered. The solution was concentrated under reduced pressure. The resulting white solid was placed on an Abderhalden apparatus at 210 °C overnight to remove unreacted methyl chloroformate.

<u>*n*-BuLi as base</u>

<u>*5.5eq*</u> – 0.4 mL (0.99 mmol) n-BuLi and 0.21 mL (2.7 mmol) methyl chloroformate. Redissolved product mixture in a small amount of 100% CH_2Cl_2. Placed solution onto column prepared with 100% CH_2Cl_2. Ran column with 100% CH_2Cl_2 for one volume then changed mobile phase to 5 % ethyl acetate/CH_2Cl_2 until product stops eluting.

***Endo*-methyl ester *m*-basket (114)**

Yield 12% m.p. > 250°C; ^{1}H NMR (500MHz, $CDCl_3$) δ 2.58 (m, 16H), 3.44 (s, 3H), 4.59 (s, 2H), 4.65 (s, 2H), 4.85 (m, 4H), 6.00 (s, 2H), 6.09 (s, 1H), 6.13 (s, 1H), 6.52 (bs, 2H), 6.54

(m, 4H), 6.58 (bs, 2H), 6.61 (bs, 2H), 6.64 (t, 1H, *J* = 2 Hz), 6.96 (m, 4H), 7.13 (m, 8H), 7.19-7.26 (m, 24H), 7.58 (m, 3H), 7.64 (t, 1H, *J* = 8 Hz); MS *m*/*z* $(M + Ag^+)^+$ Calculated: 1846, Found: 1846.49. Anal. Calculated for $C_{114}H_{82}O_{18}.1/2CH_2Cl_2$: C, 77.24 H, 4.68. Found C, 77.28 H, 4.52.

***Exo*-methyl ester *m*-basket (115)**

Yield 22% m.p. > 250°C; ^{1}H NMR (500MHz, $CDCl_3$) δ 2.58 (m, 16H), 3.99 (s, 3H), 4.54 (m, 3H), 4.56 (s, 1H), 4.85 (m, 4H), 5.98 (s, 2H), 6.01 (s, 2H), 6.50 (bs, 2H), 6.53 (m, 4H), 6.60 (s, 2H), 6.65 (t, 2H, *J* = 2 Hz), 6.68 (t, 2H, *J* = 2 Hz), 6.99 (t, 2H, *J* = 2 Hz), 7.01 (t, 1H, *J* = 2 Hz), 7.12 (m, 8H), 7.19-7.26 (m, 24H), 7.59 (t, 4H, *J* = 8 Hz); MS *m*/*z* $(M + Ag^+)^+$ Calculated: 1846, Found: 1846.77. Anal. Calculated for $C_{114}H_{82}O_{18}.H_2O$: C, 77.89 H, 4.82. Found C, 77.77 H, 4.84.

A/C-*endo*-dimethyl ester *m*-basket (116)

Yield 8%; m.p. > 250 °C; ^{1}H NMR (400MHz, $CDCl_3$) δ 2.58 (m, 16H), 3.37 (s, 6H), 4.65 (s, 4H), 4.86 (t, 4H, *J* = 8 Hz), 6.00 (s, 2H), 6.10 (s, 2H), 6.51 (t, 2H, *J* = 2.4 Hz), 6.54 (bs, 4H), 6.59 (bs, 4H), 6.49 (bs, 4H), 7.13 (m, 8H), 7.18-7.32 (m, 24H), 7.58 (t, 2H, *J* = 8 Hz), 7.66 (t, 2H, *J* = 8 Hz); MS *m*/*z* $(M + Ag^+)^+$ Calculated: 1906, Found: 1906.06. Anal. Calculated for $C_{116}H_{84}O_{20}.1/2CH_2Cl_2$: C, 76.11 H, 4.64. Found C, 76.30 H, 4.84.

***Exo*-dimethyl ester *m*-basket (117/118)**

Yield 23%; m.p. > 250 °C; ^{1}H NMR (500MHz, $CDCl_3$) δ 2.58 (m, 16H), 3.95 (m, 6H), 4.54 (m, 4H), 4.84 (m, 4H,), 5.94 (s, 2H), 5.98 (s, 4H), 6.02 (s, 2H,), 6.49 (bs, 4H), 6.52 (bs, 2H),

6.56 (bs, 2H), 6.60 (bs, 4H), 6.66 (t, 1H, *J* = 2 Hz), 6.70 (t, 4H, *J* = 2 Hz), 6.72 (t, 1H, *J* = 2 Hz), 6.99 (t, 2H, *J* = 2 Hz), 7.01 (t, 2H, *J* = 2 Hz), 7.13 (m, 8H), 7.19-7.30 (m, 24H), 7.59 (t, 4H, *J* = 8 Hz); MS *m/z* $(M + Ag^+)^+$ Calculated: 1906, Found: 1906.02. Anal. Calculated for $C_{116}H_{84}O_{20}.1/2CHCl_3$: C, 75.49 H, 4.56. Found C, 75.36 H, 4.56.

A-*exo*-B-*endo*-dimethyl ester *m*-basket (119)

Yield 14%; m.p. > 250 °C; ^1H NMR (500MHz, $CDCl_3$) δ 2.58 (m, 16H), 3.47 (s, 3H), 3.98 (s, 3H), 4.58 (m, 2H,), 4.64 (s, 2H), 4.85 (m, 4H), 5.97 (s, 1H,), 6.00 (s, 1H), 6.06 (s, 1H), 6.13 (s, 1H), 6.52 (m, 2H), 6.55 (t, 1H, *J* = 2 Hz), 6.58 (m, 5H), 6.61 (m, 2H), 6.69 (t, 1H, *J* = 2 Hz), 6.97 (m, 3H), 7.13 (m, 8H), 7.19-7.30 (m, 24H), 7.58 (m, 3H), 7.64 (t, 1H, *J* = 8 Hz); MS *m/z* $(M + Ag^+)^+$ Calculated: 1906, Found: 1906.01. Anal. Calculated for $C_{116}H_{84}O_{20}$: C, 77.49 H, 4.71. Found C, 77.19 H, 4.76.

10 eq — 0.72 mL (1.8 mmol) n-BuLi and 0.42 mL (5.4 mmol) methyl chloroformate. Redissolved product mixture in a small amount of 100% CH_2Cl_2. Placed solution onto column prepared with 100% CH_2Cl_2. Ran column with 100% CH_2Cl_2 for one volume then changed mobile phase to 5 % ethyl acetate/CH_2Cl_2 until product stops eluting. **114** 4%; **115** 10%; **116** 10%; **117/118** 22%; **119** 28%.

***Sec*-BuLi as base**

5.5eq – 0.71 mL (0.99 mmol) *sec*-BuLi and 0.21 mL (2.7 mmol) methyl chloroformate. Redissolved product mixture in a small amount of CH_2Cl_2. Placed solution onto column prepared with 100% CH_2Cl_2. Ran column with CH_2Cl_2 for one volume then changed mobile

phase to 5% ethyl acetate/CH_2Cl_2 for one volume then 10% ethyl acetate/CH_2Cl_2 until product stops eluting. Products are white solid.

***Exo*-trimethyl ester *m*-basket (120)**

Yield 27%; m.p. > 250 °C; ^{1}H NMR (400MHz, $CDCl_3$) δ 2.62 (m, 16H), 4.07 (s, 9H), 4.60 (m, 4H), 4.92 (m, 4H,), 6.02 (s, 2H), 6.05 (s, 2H), 6.57 (bs, 2H,), 6.64 (bs, 4H), 6.68 (bs, 2H), 6.78 (m, 2H), 6.81 (m, 2H), 7.08 (bs, 1H), 7.20 (m, 8H), 7.27-7.35 (m, 24H), 7.67 (t, 4H, *J* = 8 Hz); MS *m*/*z* $(M + Ag^+)^+$ Calculated: 1962, Found: 1962.90. Anal. Calculated for $C_{116}H_{84}O_{20}.1/2CH_2Cl_2$: C, 74.97 H, 4.62. Found C, 75.14 H, 4.74.

A/B-*exo*-C-*endo*-trimethyl ester *m*-basket (121)

Yield 30%; m.p. > 250 °C; ^{1}H NMR (500MHz, $CDCl_3$) δ 2.57 (m, 16H), 3.48 (s, 3H), 3.98 (s, 6H), 4.58 (s, 2H,), 4.63 (s, 2H), 4.85 (t, 4H, *J* = 8 Hz), 5.97 (s, 2H,), 6.02 (s, 1H), 6.13 (s, 1H), 6.58 (m, 10H), 6.73 (m, 1H), 6.97 (m, 2H), 7.12 (m, 8H), 7.18-7.28 (m, 24H), 7.58 (m, 3H), 7.64 (t, 1H, *J* = 8 Hz); MS *m*/*z* $(M + Ag^+)^+$ Calculated: 1962, Found: 1962.93. Anal. Calculated for $C_{116}H_{84}O_{20}.CH_2Cl_2$: C, 73.64 H, 4.57. Found C, 73.46 H, 4.76.

***Exo*-tetramethyl ester (122)**

Yield 37%; m.p. > 250 °C; ^{1}H NMR (500MHz, $CDCl_3$) δ 2.57 (m, 16H), 4.01 (s, 12H), 4.53 (s, 4H), 4.85 (t, 4H, *J* = 8 Hz), 5.95 (s, 4H), 6.58 (s, 8H), 6.76 (t, 4H, *J* = 2 Hz), 7.13 (m, 8H), 7.21-7.30 (m, 24H), 7.61 (t, 4H, *J* = 8 Hz); MS *m*/*z* $(M + Ag^+)^+$ Calculated: 2020, Found: 2020.79. Anal. Calculated for $C_{120}H_{88}O_{24}$: C, H,. Found C, H,.

10eq – 1.29 mL (1.8 mmol) *sec*-BuLi and 0.4 mL (5.4 mmol) methyl chloroformate. Redissolved in 10% ethyl acetate/CH_2Cl_2 and loaded onto a silica column made with 10% ethyl acetate/CH_2Cl_2. Used 10% ethyl acetate/CH_2Cl_2 as the mobile phase. **120** 12%; **121** 12%; **122** 70%.

***tert*-BuLi as base**

5.5eq 0.58 mL (0.99 mmol) *tert*-BuLi and 0.21 mL (2.7 mmol) methyl chloroformate. **116** 10%; **117/118** 15%; **119** 18%; **120** 22%; **121** 14%; **122** 11%.

10 eq 1.1 mL (1.8 mmol) *tert*-BuLi and 0.4 mL (5.4 mmol) methyl chloroformate. **120** 13%; **121** 20%; **122** 62%.

General procedure for the formation of carboxylic acids (123-131)

Placed methyl ester in dried round bottom flask. Add pyridine. Add 1M LiOH(aq) drop by drop with gentle stirring until white precipitate forms. Add more pyridine until white precipice dissolves. Heat to reflux overnight. Cool to room temperature. Remove solvent by reduced pressure. Further dry on room temperature vacuum line. Redissolve in MeOH then add 10% HCl until white precipitate forms. Filter off precipice. Placed on vacuum line.

***Endo*-carboxylic acid *m*-basket (123)**

0.1g (0.06 mmol) in 10 mL pyridine. Yield quantitative. m.p. > 250 °C; ^{1}H NMR (400MHz, $CDCl_3$) δ 2.57 (m, 16H), 4.56 (s, 2H), 4.61 (s, 2H), 4.84 (m, 4H), 6.00 (s, 2H), 6.05 (s, 1H), 6.06 (s, 1H), 6.50 (bs, 4H), 6.55 (bs, 2H), 6.63 (m, 4H), 6.91 (bs, 2H), 7.00 (bs, 2H), 7.13

(m, 8H), 7.18-7.35 (m, 24H), 7.57 (m, 3H), 7.73 (t, 1H, J = 8H); MS m/z $(M + Ag^+)^+$ Calculated: 1832, Found: 1833.40. Anal. Calculated for $C_{120}H_{88}O_{24}$: C, H,. Found C, H,.

Exo-carboxylic acid _m_-basket (124)

0.25g (0.25 mmol) in 25 mL pyridine. Yield quantitative. m.p. > 250 °C; ^{1}H NMR (500MHz, DMSO-d_6) δ 2.57 (m, 16H), 4.41 (s, 1H), 4.44 (s, 2H), 4.50 (s, 1H), 4.60 (m, 4H), 5.80 (s, 4H), 6.39 (s, 2H), 6.41 (s, 4H), 6.49 (s, 2H), 6.67 (bs, 2H), 6.70 (bs, 2H), 7.11-7.22 (m, 24H), 7.36 (d, 6H, J = 8 Hz), 7.71 (m, 8H), 13.52 (bs, 1H); MS m/z $(M + Ag^+)^+$ Calculated: 1832, Found: 1833.40. Anal. Calculated for $C_{120}H_{88}O_{24}$: C, H,. Found C, H,.

A/C-_endo_-dicarboxylic acid _m_-basket (125)

0.12g (0.07 mmol) in 15 mL pyridine. Yield quantitative. m.p. > 250 °C; ^{1}H NMR (500MHz, DMSO-d_6) δ 2.57 (m, 16H), 4.57 (t, 2H, J = 8 Hz), 4.64 (s, 4H), 5.76 (s, 2H), 5.87 (s, 2H), 6.33 (s, 4H), 6.49 (s, 4H), 6.90 (bs, 2H), 7.09 (bs, 4H), 7.16-7.24 (m, 24H), 7.32 (d, 4H, J = 8 Hz), 7.61 (s, 4H), 7.67 (m, 6H); MS m/z $(M + Ag^+)^+$ Calculated: 1832, Found: 1833.40. Anal. Calculated for $C_{120}H_{88}O_{24}$: C, H,. Found C, H,.

A/B-_exo_-dicarboxylic acid _m_-basket (126)

m.p. > 250 °C; ^{1}H NMR (400MHz, $CDCl_3$) δ 2.57 (m, 16H), 4.52 (s, 2H), 4.54 (s, 2H), 4.85 (m, 4H), 5.93 (s, 1H), 5.98 (s, 2H), 6.01 (s, 1H), 6.49 (bs, 2H), 6.54 (bs, 2H), 6.60 (bs, 2H), 6.66 (m, 5H), 6.76 (bs, 1H), 7.02 (bs, 2H), 7.13 (m, 8H), 7.20-7.28 (m, 24H), 7.59 (t, 4H, J = 8 Hz); MS m/z $(M + Ag^+)^+$ Calculated: 1877, Found: 1878.20. Anal. Calculated for $C_{120}H_{88}O_{24}$: C, H,. Found C, H,.

A/C-*exo*-dicarboxylic acid *m*-basket (127)

m.p. > 250 °C; ^{1}H NMR (500MHz, $CDCl_3$) δ 2.57 (m, 16H), 4.51 (s, 2H), 4.58 (s, 2H), 4.86 (m, 4H), 6.00 (s, 4H), 6.56 (bs, 4H), 6.64 (bs, 4H), 6.72 (bs, 4H), 7.14 (m, 10H), 7.22 (m, 24H), 7.60 (t, 4H, J = 8 Hz); MS m/z $(M + Ag^+)^+$ Calculated: 1877, Found: 1878.20. Anal. Calculated for $C_{120}H_{88}O_{24}$: C, H,. Found C, H,.

A-*exo*-B-*endo*-dicarboxylic acid *m*-basket (128)

0.24g (0.14 mmol) in 20 mL pyridine. Yield quantitative. m.p. > 250 °C; ^{1}H NMR (500MHz, DMSO-d_6) δ 2.57 (m, 16H), 4.31 (s, 1H), 4.36 (s, 1H), 4.56 (s, 1H), 4.60 (m, 5H), 5.79 (m, 2H), 5.82 (m, 2H), 6.39 (bs, 2H), 6.41 (bs, 2H), 6.54 (bs, 2H), 6.52 (s, 2H), 6.58 (bs, 1H), 6.62 (bs, 1H), 6.69 (bs, 1H), 7.05 (m, 2H), 7.10 (bs, 1H), 7.17-7.25 (m, 22H), 7.37 (m, 6H), 7.46 (m, 2H), 7.66-7.78 (m, 8H), 12.78 (s, 1H), 13.54 (s, 1H); MS m/z $(M + Ag^+)^+$ Calculated: 1877, Found: 1877.34. Anal. Calculated for $C_{120}H_{88}O_{24}$: C, H,. Found C, H,.

***Exo*-tricarboxylic acid *m*-basket (129)**

0.26g (0.14 mmol) in 25 mL pyridine. Yield quantitative. m.p. > 250 °C; ^{1}H NMR (500MHz, DMSO-d_6) δ 2.57 (m, 16H), 4.39 (s, 1H), 4.46 (s, 2H), 4.50 (s, 1H), 4.63 (m, 4H), 5.81 (s, 4H), 6.41 (s, 2H), 6.48 (m, 6H), 6.69 (m, 4H), 7.18-7.23 (m, 22H), 7.38 (m, 6H), 7.74 (m, 8H), 13.55 (bs, 3H); MS m/z $(M + Ag^+)^+$ Calculated: 1921, Found: 1921.43. Anal. Calculated for $C_{120}H_{88}O_{24}$: C, H,. Found C, H,.

A/B-*exo*-C-*endo*-tricarboxylic acid (130)

0.11g (0.061 mmol) in 15 mL pyridine. Yield quantitative. m.p. > 250 °C; ^{1}H NMR (500MHz, DMSO-d_6) δ 2.57 (m, 16H), 4.38 (s, 2H), 4.62 (m, 6H), 5.78 (s, 2H), 5.86 (s, 1H), 5.93 (s, 1H), 6.35 (bs, 2H), 6.37 (bs, 2H), 6.40 (bs, 2H), 6.52 (bs, 2H), 6.59 (bs, 2H), 6.92 (bs, 1H), 7.08 (bs, 2H), 7.14-7.30 (m, 24H), 7.52 (m, 1H), 7.58-7.74 (m, 8H); MS *m/z* $(M + Ag^+)^+$ Calculated: 1921, Found: 1921.80. Anal. Calculated for $C_{120}H_{88}O_{24}$: C, H,. Found C, H,.

***Exo*-tetracarboxylic acid (131)**

0.3g (0.16 mmol) in 30 mL pyridine. Yield quantitative. m.p. > 250 °C; ^{1}H NMR (500MHz, DMSO-d_6) δ 2.57 (m, 16H), 4.49 (s, 4H), 4.63 (m, 4H), 5.81 (s, 4H), 6.48 (s, 8H), 6.72 (bs, 4H), 7.17-7.28 (m, 22H), 7.37 (d, 8H, J = 10 Hz), 7.73 (m, 8H), 13.58 (bs, 4H); MS *m/z* $(M + Ag^+)^+$ Calculated: 1965, Found: 1965.75. Anal. Calculated for $C_{120}H_{88}O_{24}$: C, H,. Found C, H,.

2-pentyl-hexahydrobenzo[*d*][1,3]dioxole (134)

Dissolved 0.25g *cis*-1,2-cyclohexanediol (2.2 mmol) in 20 mL benzene in round bottom flask. Added two small crystals of p-Toluenesulfonic acid monohydrate. Dean-Stark trap placed on round bottom flask and solution brought to reflux (oil bath) for 1 hour. Injected 0.17 mL hexanal (1.4 mmol) into solution and allowed to reflux overnight. Removed from heat and added a few drops of NEt_3. Diluted the solution with ether and washed organic solution with 10% K_2CO_3. Collect and dry organic layer with Na_2SO_4. Filtered off Na_2SO_4 and remove solvent under reduced pressure and further dried on room temperature vacuum line to give a transparent

oil (0.2 g). Yield 46%. ^{1}H NMR (400MHz, Acetone-d_6) δ 0.89 (bs, 3H), 1.31-1.50 (m, 8H), 1.60-1.74 (m, 5H), 3.94 (bs, 2H), 4.00 (bs, 2H), 4.86 (t, 1H, J = 4 Hz), 5.17 (t, 1H, J = 4 Hz).

3-pentyl-2,4-dioxa-bicyclo[3.3.1]nonane (134)

Dissolved 3.5 g (30 mmol) 1,3-cyclohexanediol in 40 mL benzene in round bottom flask. Added 10 small crystals of p-toluenesulfonic acid monohydrate. Dean-Stark trap placed on round bottom flask and solution brought to reflux (oil bath) for 1 hour. Injected 1.2 mL hexanal (9.98 mmol) into solution and allowed to reflux overnight. Removed from heat and added a few drops of NEt_3. Diluted the solution with ether and washed organic solution with 10% K_2CO_3. Collect and dry organic layer with Na_2SO_4. Filtered off Na_2SO_4 and remove solvent under reduced pressure and further dried on room temperature vacuum line to give a transparent oil (0.79 g). Yield 40%. ^{1}H NMR (400MHz, Acetone-d_6) δ 0.91 (bs, 3H), 1.20-1.50 (m, 9H), 1.74 (bs, 3H), 2.14 (m, 2H), 2.60 (bs, 2H), 4.25 (bs, 2H), 5.12 (s, 1H).

3-pentyl-2,4-dioxa-bicyclo[3.2.2]nonane (135)

Dissolved 3.5 g (30 mmol) 1,3-cyclohexanediol in 40 mL benzene in round bottom flask. Added 10 small crystals of p-toluenesulfonic acid monohydrate. Dean-Stark trap placed on round bottom flask and solution brought to reflux (oil bath) for 1 hour. Injected 1.2 mL hexanal (9.98 mmol) into solution and allowed to reflux overnight. Removed from heat and added a few drops of NEt_3. Diluted the solution with ether and washed organic solution with 10% K_2CO_3. Collect and dry organic layer with Na_2SO_4. Filtered off Na_2SO_4 and remove solvent under reduced pressure and further dried on room temperature vacuum line to give a transparent oil

(0.69 g). Yield 35%. ^{1}H NMR (400MHz, Acetone-d_6) δ 0.88 (bs, 3H), 1.20-1.40 (m, 6H), 1.42-1.80 (m, 6H), 1.93 (m, 3H), 3.62 (m, 3H), 4.62 (m, 1H).

General Method for the Synthesis of 2-methyl tris-*m*-basket

Deep cavity cavitand **35** (0.3g, 0.16 mmol), 2-methyl resorcinol, and K_2CO_3 placed in oven dried round bottom flask. Pyridine (20 mL) added to round bottom flask. Nitrogen bubbled though solution for 5 minutes. CuO added to solution and the round bottom flask was fitted with a water condenser. The solution was brought to reflux (sand bath).

2-methyl bis-*m*-basket (142)

Reaction time 24 hours; 2-methyl resorcinol (1.2 mmol, 0.15 g), K_2CO_3 (1.1 mmol, 0.15 g), and CuO (1.9 mmol, 0.15 g). Yield 14%. m.p. > 250 °C; ^{1}H NMR (400MHz, $CDCl_3$) δ 1.82 (s, 6H), 2.65 (m, 16H), 4.95 (t, 4H, J = 8 Hz), 5.08 (s, 4H), 6.12 (s, 2H), 6.50 (s, 2H), 6.59 (s, 2H), 6.70 (s, 2H), 7.10-7.31 (m, 24H), 7.45 (m, 4H), 7.70 (m, 6H); MS m/z $(M + Ag^+)^+$ Calculated:, Found:

2-methyl *m*-tris basket (143)

Reaction time 50 hours; 2-methyl resorcinol (1.2 mmol, 0.15 g), K_2CO_3 (1.1 mmol, 0.15 g), and CuO (1.9 mmol, 0.15 g). Yield 24%. m.p. > 250 °C; ^{1}H NMR (500MHz, $CDCl_3$) δ 1.79 (s, 3H), 1.80 (s, 6H), 2.57 (m, 16H), 4.81 (s, 2H), 4.85 (m, 6H), 4.90 (m, 4H), 6.00 (s, 2H), 6.12 (s, 1H), 6.41 (bs, 2H), 6.55 (bs, 2H), 6.58 (s, 1H), 6.66 (bs, 2H), 7.04 (d, 2H, J = 8 Hz), 7.11 (bs, 2H), 7.16 (m, 8H), 7.21 (s, 2H), 7.22-7.38 (m, 16H), 7.29 (s, 2H), 7.31(d, 2H, J = 8 Hz), 7.40 (t,

2H, J = 8 Hz), 7.45 (bs, 1H), 7.49 (t, 1H, J = 8 Hz), 7.70 (bs, 2H); MS m/z $(M + Ag^+)^+$ Calculated: 1883, Found: 1883.12.

General Method for the Synthesis tris-*m*-basket

Deep cavity cavitand **35** (0.3g, 0.16 mmol), resorcinol, and K_2CO_3 placed in oven dried round bottom flask. Pyridine (20 mL) added to round bottom flask. Nitrogen bubbled though solution for 5 minutes. CuO added to solution and the round bottom flask was fitted with a water condenser. The solution was brought to reflux (sand bath).

Mono-*m*-basket (144)

m.p. > 250 °C; ^{1}H NMR (400MHz, $CDCl_3$) δ 2.63 (m, 16H), 4.95 (m, 4H), 5.18 (s, 2H), 5.26 (s, 2H), 6.29 (s, 1H), 6.45 (bs, 2H), 6.60 (s, 1H), 6.84 (s, 2H), 6.92 (dd, 2H, J = 2 Hz), 7.06 (bs, 1H), 7.18 (m, 8H), 7.26 (m, 14H), 7.41 (t, 1H, J = 8 Hz), 7.46 (bs, 2H), 7.70 (bs, 4H), 7.73 (bs, 2H); MS m/z $(M + Ag^+)^+$ Calculated: 1943, Found: 1944.27.

Bis-*m*-basket (145)[207]

m.p. > 250 °C; ^{1}H NMR (400MHz, $CDCl_3$) δ 2.62 (m, 16H), 4.92 (t, 4H, J = 8 Hz), 5.05 (s, 4H), 6.21 (s, 2H), 6.40 (bs, 4H), 6.61 (s, 2H), 6.88 (dd, 4H, J = 8 Hz, 2 Hz), 7.03 (t, 2H, J = 2 Hz), 7.10-7.30 (m, 24H), 7.35 (t, 2H, J = 8 Hz), 7.45 (t, 4H, J = 2 Hz), 7.71 (s, 4H); MS m/z $(M + Ag^+)^+$ Calculated: 1894, Found: 1893.21.

Tris-*m*-basket (146)[85]

m.p. > 250 °C; ^{1}H NMR (500MHz, $CDCl_3$) δ 2.58 (m, 16H), 4.74 (s, 2H), 4.84 (s, 2H), 4.87 (m, 4H), 6.01 (s, 2H), 6.11 (s, 1H), 6.44 (bs, 2H), 6.52 (s, 1H), 6.54 (bs, 2H), 6.62 (bs, 2H), 6.68 (t, 1H, *J* = 2 Hz), 6.74 (t, 2H, *J* = 2 Hz), 7.03 (m, 3H), 7.13 (m, 8H), 7.19-7.28 (m, 23H), 7.40 (bs, 1H), 7.53 (t, 2H, *J* = 8 Hz), 7.60 (t, 1H, *J* = 8 Hz), 7.64 (bs, 2H).

2,2-dibromo-trispyridyl methanol (148)

2-bromopyridine (0.34 mL, 3.5 mmol) placed in oven dried round bottom flask. Added 50 mL diethyl ether and brought solution to –78 °C. *n*-BuLi (1.45 mL, 3.5 mmol) slowly injected into solution. This was allowed to react for 20 minutes. Then a solution of **148** (1.0 g, 2.9 mmol) in 20 mL diethyl ether was injected over 5 minutes. This solution was allowed to react at –78 °C for 2 hours. The solution was removed from dry ice/acetone bath and the temperature was allowed to come to 0 °C when it was acidified with 10% HCl. $CHCl_3/H_2O$ extraction done three times and the organic layer was collected and dried with Na_2SO_4. The solution was then filtered and the solvent removed under reduced pressure leaving a white solid (0.61 g, 50% yield). m.p. 113-115 °C; ^{1}H NMR (400MHz, Acetone-d_3) δ 6.93 (s, 1H), 7.36 (m, 1H), 7.52 (dd, 2H, *J* = 8 Hz), 7.73 (m, 4H), 7.84 (m, 2H), 8.52 (d, 1H, *J* = 6 Hz); MS *m*/*z* $(M + H^+)^+$ Calculated: 405.09, Found: 406. Anal. Calculated for $C_{16}H_{11}N_3O$: C, 45.64 H, 2.63. Found C, 45.91 H, 2.72.

MOM-protected 2,2-dibromo-trispyridyl methanol (149)

NaH (0.025 g, 0.78 mmol) was placed in a round bottom flask and washed with pentane twice and tetrahydrofuran. Added 15 mL tetrahydrofuran and then **148** (0.3 g, 0.71 mmol). This

solution was allowed to stir for 15 minutes. Then methoxy methyl bromide (64 uL, 0.78 mmol) was injected into solution. This was allowed to stir for 4 hours. The reaction was quenched with MeOH. The reaction was washed with H_2O three times and the organic layer was collected and dried with Na_2SO_4. The Na_2SO_4 was removed by filtration and the solvent was removed by reduced pressure leaving a white solid (0.36 g, 0.77 mmol). Yield 99%. m.p. 102-105 °C; ^{1}H NMR (400MHz, Acetone-d_3) δ 3.23 (s, 3H), 4.95 (s, 2H), 7.29 (dd, 1H, *J* = 8 Hz), 7.51 (d, 2H, *J* = 6 Hz), 7.62 (dt, 1H, *J* = 1 Hz), 7.66 (dd, 2H, 1 Hz), 7.72 (t, 2H, *J* = 8 Hz), 8.48 (td, 1H, *J* = 8 Hz); MS *m*/*z* $(M + H^+)^+$ Calculated: 465, Found: 466. Anal. Calculated for $C_{16}H_{11}N_3O$: C, 46.48 H, 3.25. Found C, 46.57 H, 3.25.

Octa phenyl (152)

0.1g **35** (0.053 mmol), $Pd(PPh_3)_4$ (0.0053 mmol) and Cs_2CO_3 (0.05 mmol) placed in a dried round bottom flask. Added 5 mL DMA. Air reflux placed on round bottom flask and the solution was brought to 60 °C for 72 hours. The solvent was then removed by reduced pressure leaving a yellow solid. The yellow solid was then redissolved in $CHCl_3$ and placed on a silica plug prepared with $CHCl_3$. $CHCl_3$ was used as the mobile phase. Two volumes were collected and solvent removed by reduced pressure leaving a white solid which was further dried on room temperature vacuum line (0.069 g, 0.038 mmol) Yield 71%. m.p. 205 °C; ^{1}H NMR (400MHz, $CDCl_3$) δ 2.67 (m, 16H), 5.16 (t, 4H, *J* = 8 Hz), 5.68 (s, 4H), 6.83 (s, 4H), 7.23-7.41 (m, 52H), 7.64 (d, 16H, *J* = 8 Hz), 7.83 (bs, 4H), 7.86 (bs, 8H); MS *m*/*z* $(M + Ag^+)^+$ Calculated: 1973, Found: 1972.47. Anal. Calculated for $C_{136}H_{104}O_8.1/2CHCl_3$: C, 85.12 H, 5.47. Found C, 85.21 H, 5.48.

MOM-2,2-diphenyl trispyridyl methanol (153)

Placed **149** (0.1 g, 0.21 mmol), K_2CO_3 (0.064 g, 0.46 mmol) and $Pd(PPh_3)_4$ (0.0025 g, 0.021 mmol) in a dried round bottom flask. 5 mL dimethoxy ethylene glycol was added to the round bottom flask and a condenser was placed on it. The solution was brought to 60 °C for eight hours. The solution was allowed to cool and the solvent was removed by reduced pressure. The off-white solid was redissolved in $CHCl_3$ and placed on a silica plug that was prepared using $CHCl_3$. $CHCl_3$ was used as the mobile phase. The solvent was removed by reduced pressure and the white solid was recrystalized from acetone (0.085 g). Yield 88%. m.p. 106-109 °C; ^{1}H NMR (400MHz, $CDCl_3$) δ 3.22 (s, 3H), 5.17 (s, 2H), 7.26 (q, 1H, *J* = 8), 7.34 (m, 6H), 7.62 (dd, 2H, *J* = 8 Hz), 7.78 (d, 4H, *J* = 8 Hz), 7.82-7.88 (m, 4H), 8.02 (d, 4H, *J* = 8 Hz), 8.52 (d, 1H, *J* = 8 Hz); MS *m*/*z* $(M + Na^+)^+$ Calculated: 482, Found: 482.4. Anal. Calculated for $C_{30}H_{25}O_2N_3.1/2H_2O$: C, 77.07 H, 5.39. Found C, 77.31 H, 5.43.

diol *m-tris* basket (154)

Placed 0.3 g (0.18 mmol) in oven dried round bottom flask. Added 20 mL freshly distilled THF. Placed in acetone/dry ice bath (-78 °C). Slowly inject 0.23 mL (0.39 mmol) *tert*-BuLi. This was allowed to stir at –78 °C for 20 minutes. 0.20 mL (1.79 mmol) $B(OMe)_3$ in 1 mL THF was injected into the solution. This was allowed to stir at –78 °C for 10 minutes. The solution was brought to room temperature for 2 hours. The solution was placed in an acetone/dry ice bath. A solution of 3N NaOH/30% H_2O_2 (1:1) was injected into the solution. This was allowed to stir at –78 °C for 20 minutes. The solution was then allowed to come to room temperature for 16 hours. $Na_2S_2O_4$ was added to the solution to quench excess peroxide. The solution was then dissolved in $CHCl_3$ and this was washed with water once and the water

was washed with $CHCl_3$ twice. The organic layers were collected and dried with Na_2SO_4, which was filtered off. The solvent was then removed by reduced pressure leaving a white solid. This was then dissolved in $CHCl_3$ and a small amount of silica was added to the solution. The solvent was removed by reduced pressure leaving a free flowing powder. This was placed on a silica column prepared with 100% CH_2Cl_2. The mobile phase was initially 100% CH_2Cl_2 for one volume to elute diprotio *m*-basket (**151**) then changed to 2% EA/CH_2Cl_2 for one volume to remove (**155**) then to 10% EA/CH_2Cl_2 to elute the product. The solvent was removed by reduced pressure leaving a white solid (0.xx g, xx mmol). Yield 64%. m.p. > 250 °C; ^{1}H NMR (500MHz, $CDCl_3$) δ 2.62 (m, 16H), 4.76 (s, 2H), 4.84 (s, 2H), 4.89 (m, 4H), 6.06 (s, 1H), 6.12 (s, 2H), 6.53 (s, 1H), 6.56 (bs, 2H), 6.63 (bs, 2H), 6.69 (m, 3H), 6.75 (t, 2H, *J* = 2 Hz), 6.98 (bs, 2H), 7.02 (bs, 2H), 7.06(d, 2H, *J* = 8 Hz), 7.14 (m, 8H), 7.20-7.28 (m, 24H), 7.53 (t, 2H, *J* = 8 Hz), 7.61 (t, 1H, *J* = 8 Hz); MS *m*/*z* $(M + Ag^+)^+$ Calculated: 1715, Found: 1715.22. Anal. Calculated for $C_{106}H_{78}O_{16}$.1/2$CHCl_3$: C, 76.71 H, 4.75. Found C, 76.94 H, 4.86.

mono-ol tris-*m*-basket (**155**)

Yield 14%. m.p. > 250 °C; ^{1}H NMR (500MHz, $CDCl_3$) δ 2.62 (m, 16H), 4.76 (m, 2H), 4.83 (s, 1H), 4.89 (m, 4H), 5.01 (s, 1H), 6.04 (s, 1H), 6.07 (s, 1H), 6.11 (s, 2H), 6.51 (s, 1H), 6.55 (bs, 3H), 6.58 (bs, 1H), 6.63 (bs, 3H), 6.69 (m, 2H), 6.74 (t, 1H, *J* = 2 Hz), 6.77 (t, 1H, *J* = 2 Hz), 7.05-7.28 (m, 28H), 7.44 (t, 1H, *J* = 8 Hz), 7.53 (t, 2H, *J* = 8 Hz), 7.61 (t, 1H, *J* = 8 Hz); MS *m*/*z* $(M + Ag^+)^+$ Calculated: 1698, Found: 1697.99.

Synthesis of tripodal ligand bearing cavitands (156 and 157)

Placed **154** (0.06 g, 0.034 mmol), K_2CO_3 (0.012 g, 0.085 mmol) and **149** (0.024 g, 0.051 mmol) in oven dried round bottom flask. 15 mL of pyridine added to round bottom flask and N_2 bubbled through solution. CuO (0.007 g, 0.085 mmol) added to solution. A water condenser was placed on the round bottom flask and the solution was brought to reflux for eight days. Removed from heat and pyridine removed by reduced pressure. The remaining solid was suspended in CH_2Cl_2 and placed on plug prepped with 10% EA/CH_2Cl_2 and ran with same. Fractions collected and those containing desired product were collected and solvent removed by reduced pressure leaving a white solid (0.023 g, 0.012 mmol) Yield **156** – 36%, (0.017 g, 0.009 mmol) **157** – 25%.

156

m.p. > 250 °C; ^{1}H NMR (500MHz, CD_2Cl_2) δ 2.62 (m, 16H), 4.69 (s, 2H), 4.83 (m, 6H), 6.04 (s, 2H), 6.09 (s, 1H), 6.20 (s, 1H), 6.38 (bs, 2H), 6.60 (bs, 2H), 6.63 (bs, 2H), 6.72 (t, 1H, *J* = 2 Hz), 6.88 (t, 2H, *J* = 2 Hz), 6.96 (t, 2H, *J* = 2 Hz), 7.02 (m, 6H), 7.08 (dd, 2H, *J* = 8 Hz), 7.12-7.30 (m, 40H), 7.57 (t, 2H, *J* = 8 Hz), 7.63 (m, 4H), 7.75 (t, 2H, *J* = 8 Hz), 8.47 (d, 1H, *J* = 5 Hz); MS *m*/*z* $(M + Ag^+)^+$ Calculated: 2018, Found: 2018.50. Anal. Calculated for $C_{106}H_{78}O_{16}$.1/2$CHCl_3$: C, 76.71 H, 4.75. Found C, 76.94 H, 4.86.

157

m.p. > 250 °C; ^{1}H NMR (500MHz, CD_2Cl_2) δ 2.62 (m, 16H), 4.73 (s, 2H), 4.82 (t, 4H, *J* = 7 Hz), 4.93 (s, 2H), 6.03 (s, 2H), 6.05 (s, 1H), 6.27 (s, 1H), 6.45 (bs, 2H), 6.59 (m, 4H), 6.70 (t, 1H, *J* = 2 Hz), 6.77 (d, 2H, *J* = 8 Hz), 6.81 (t, 2H, *J* = 2 Hz), 6.87 (bs, 2H), 7.00 (m, 6H), 7.14

(m, 8H), 7.10-7.30 (m, 40H), 7.40 (m, 6H), 7.60 (m, 5H), 8.40 (d, 1H, J = 4 Hz); MS m/z (M + $Ag^{+})^{+}$ Calculated: 2018, Found: 2022.44.

6.3 Binding Studies of 5-Methyl-*m*-basket, 2-Methyl-*m*-basket, and d_4-*m*-basket

All quoted association constants were the average of three titrations. In a typical binding study, a 1.0 mM host solution is prepared in the solvent of choice. The exception to this is host **70** in DMSO-d_6 (0.5 mM). Then 0.5 mL of the 1.0 mM host solution was measured into an NMR tube and its spectra recorded (500 MHz NMR, 298 K). Small aliquots of guest solutions prepared in the range 25 mM-250 mM were measured into the tube and the spectra recorded after each addition.

An iterative curve-fitting method using Origin 6.1 (Aston Scientific Ltd.) was used to generate the association constants. Typical binding isotherms are shown in Figure 6.1-6.24.

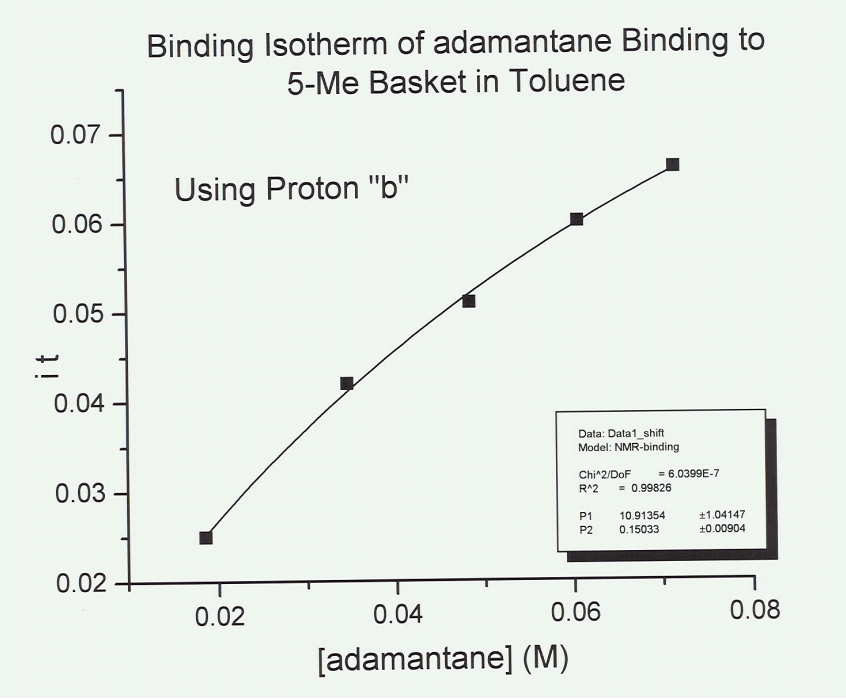

Figure 6.1 Binding isotherm for the complexation of host **70** and adamantane in toluene-d_8

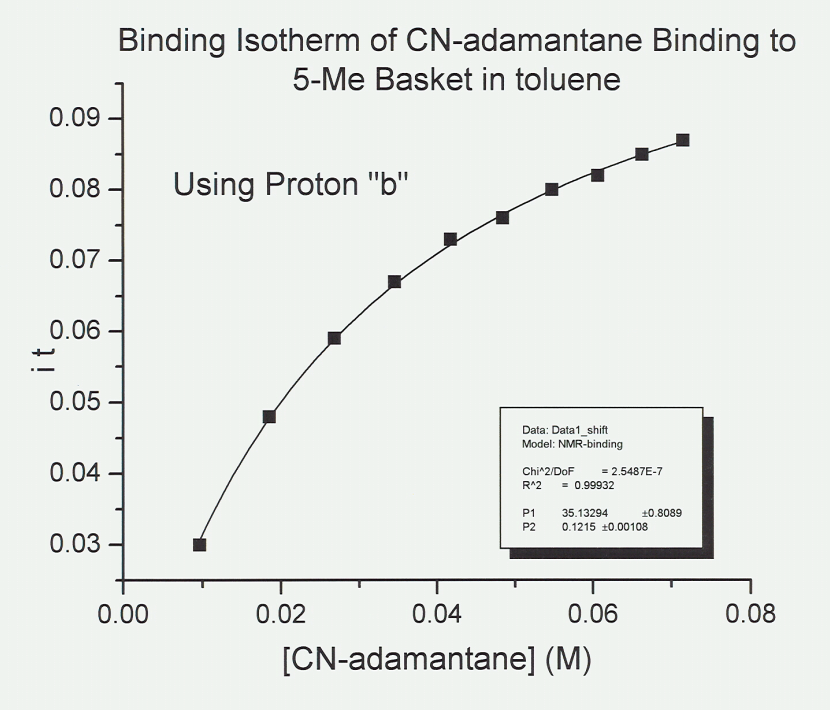

Figure 6.2 Binding isotherm for the complexation of host **70** and cyanoadamantane in toluene-d_8

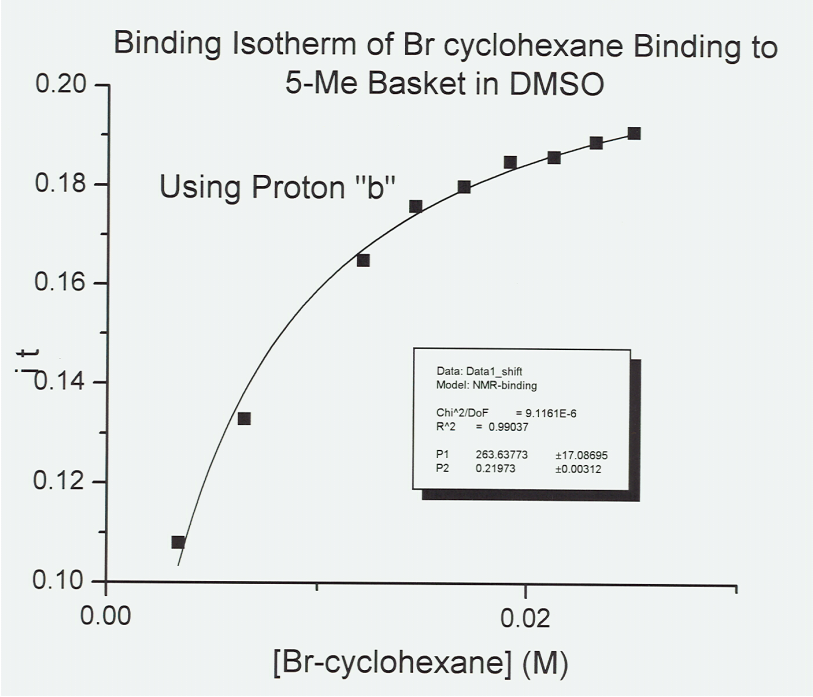

Figure 6.3 Binding isotherm for the complexation of host **70** and bromocyclohexane in DMSO-d_6

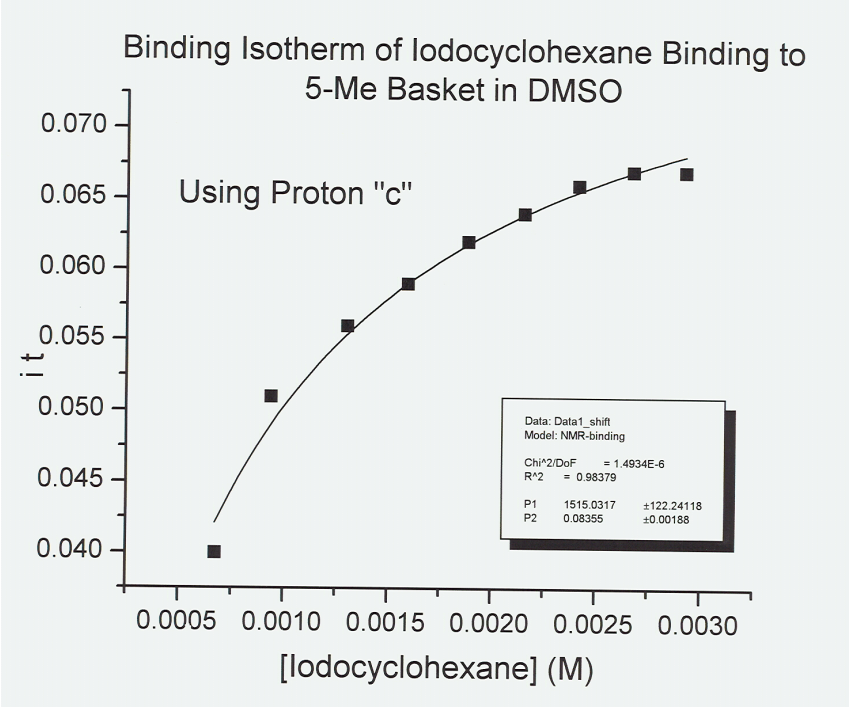

Figure 6.4 Binding isotherm for the complexation of host **70** and iodocyclohexane in DMSO-d_6

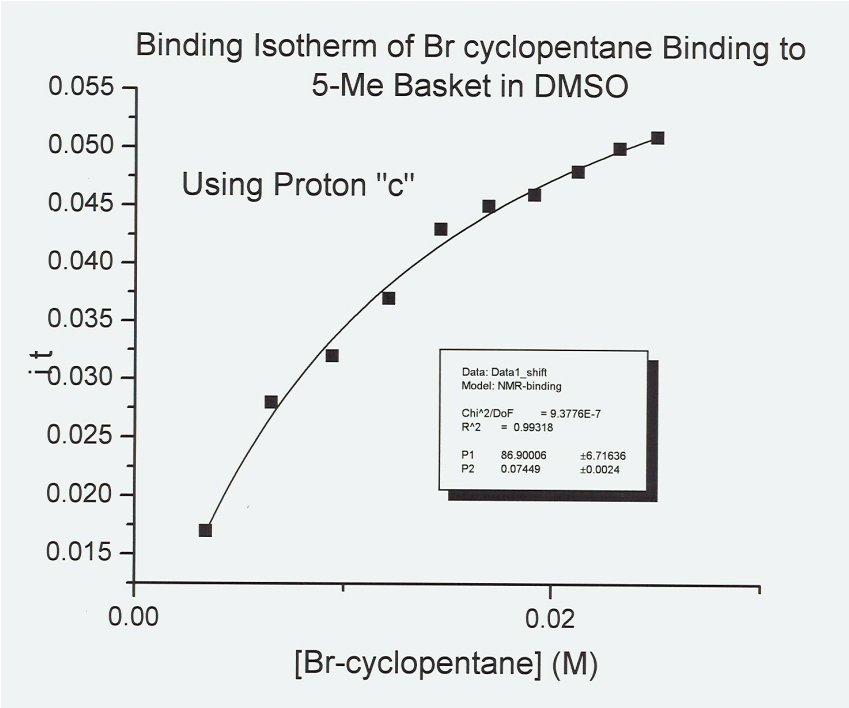

Figure 6.5 Binding isotherm for the complexation of host **70** and bromocyclopentane in DMSO-d_6

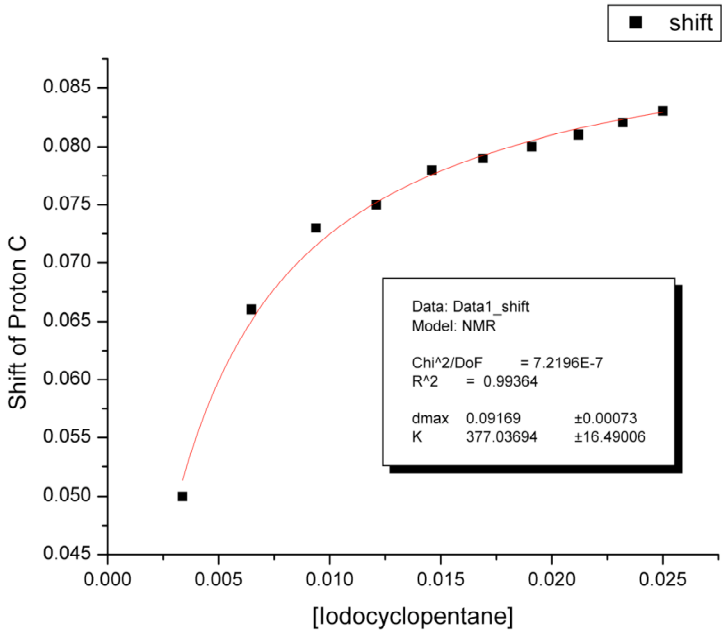

Figure 6.6 Binding isotherm for the complexation of host **70** and iodocyclopentane in DMSO-d_6

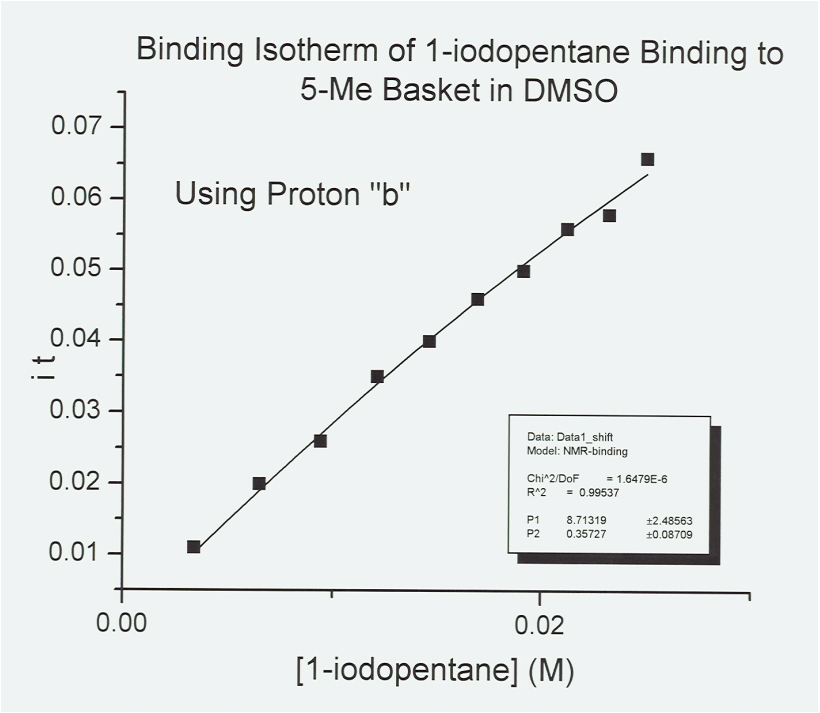

Figure 6.7 Binding isotherm for the complexation of host **70** and 1-iodopentane in DMSO-d_6

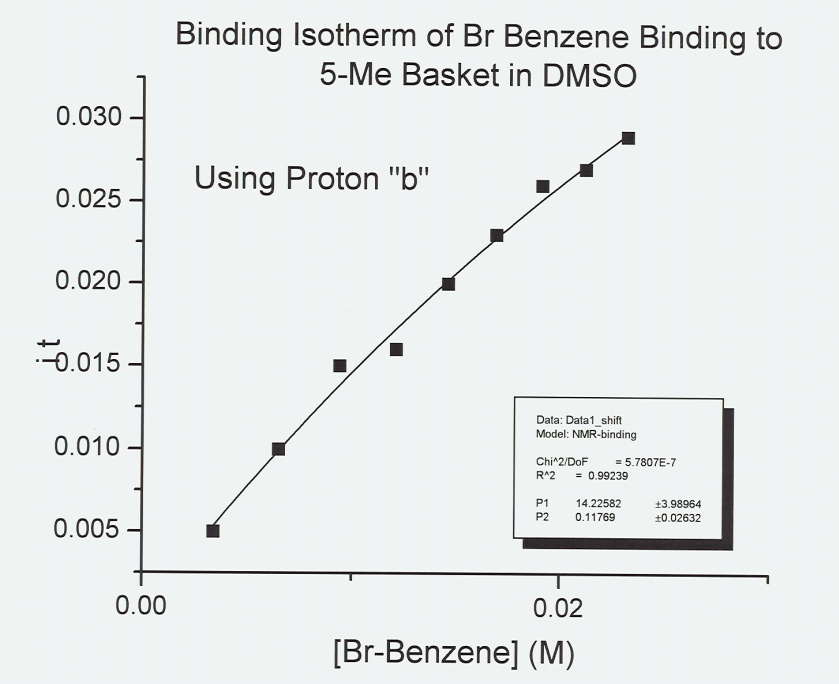

Figure 6.8 Binding isotherm for the complexation of host **70** and bromobenzene in DMSO-d_6

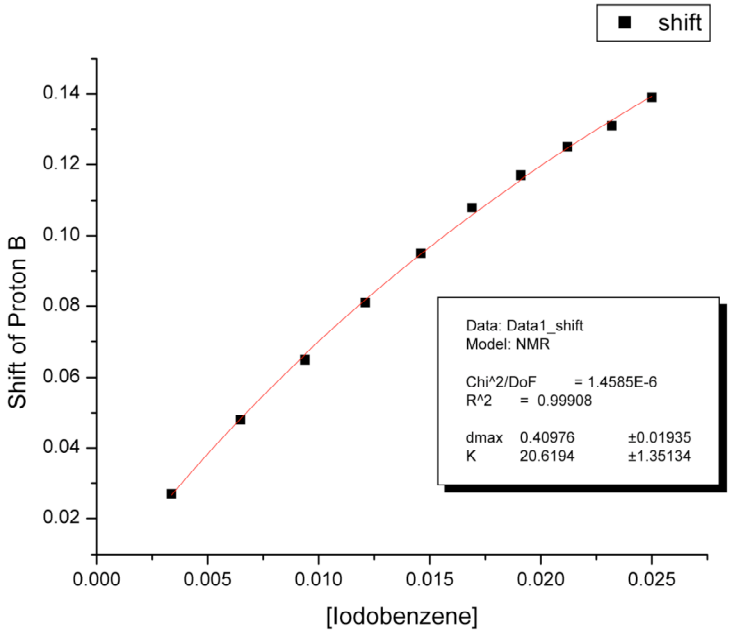

Figure 6.9 Binding isotherm for the complexation of host **70** and iodobenzene in DMSO-d_6

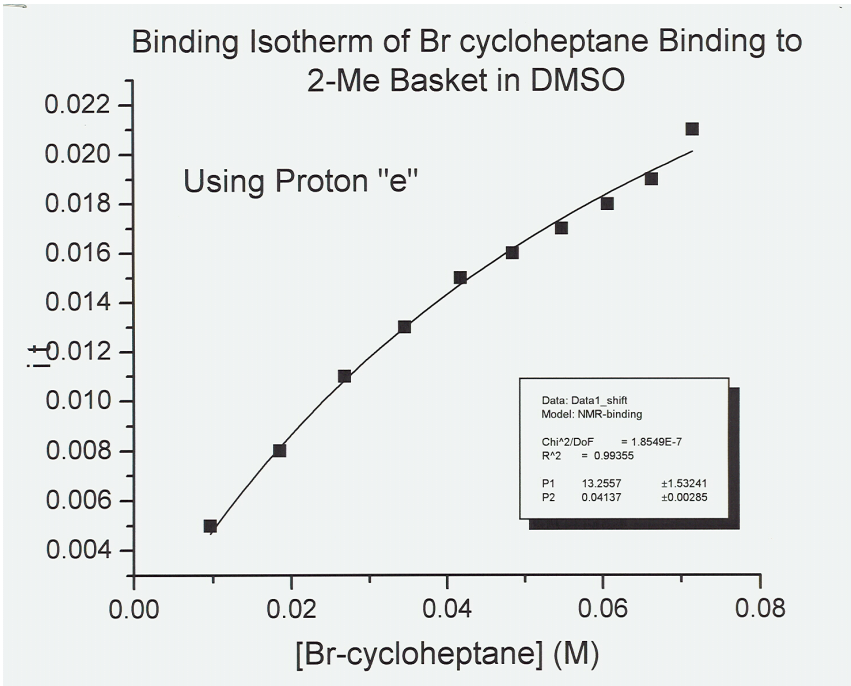

Figure 6.10 Binding isotherm for the complexation of host **71** and bromocycloheptane in DMSO-d_6

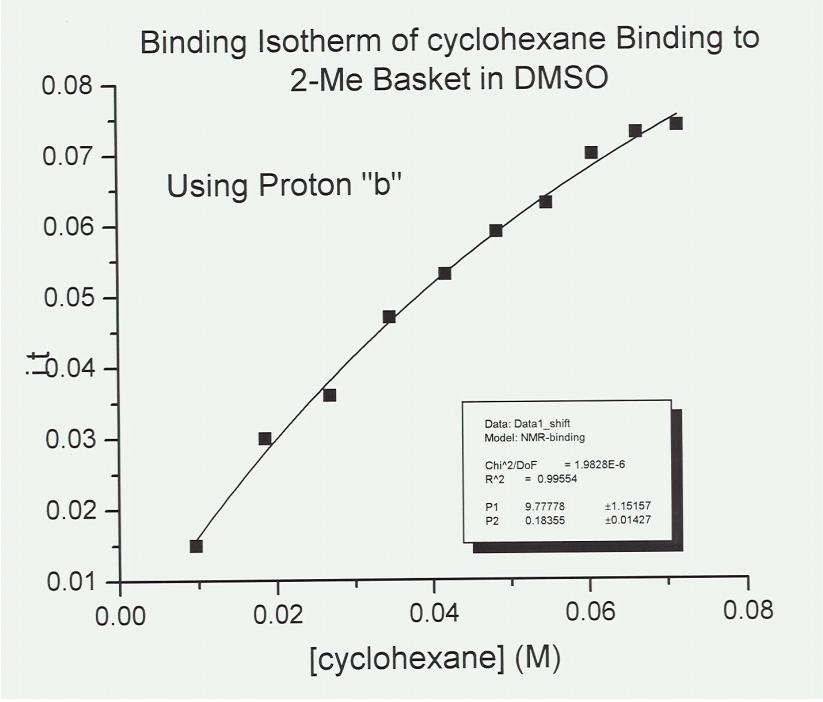

Figure 6.11 Binding isotherm for the complexation of host **71** and cyclohexane in DMSO-d_6

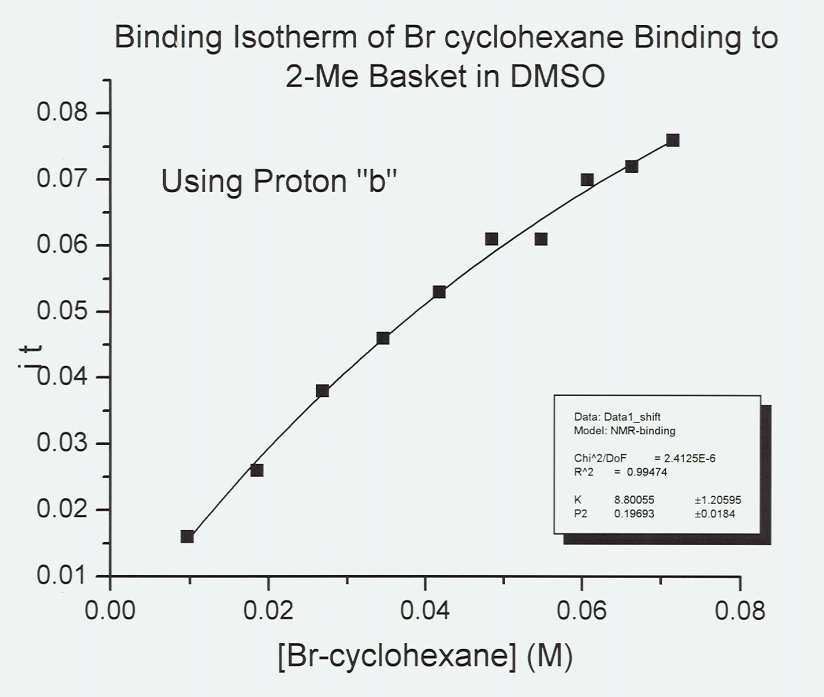

Figure 6.12 Binding isotherm for the complexation of host **71** and bromocyclohexane in DMSO-d_6

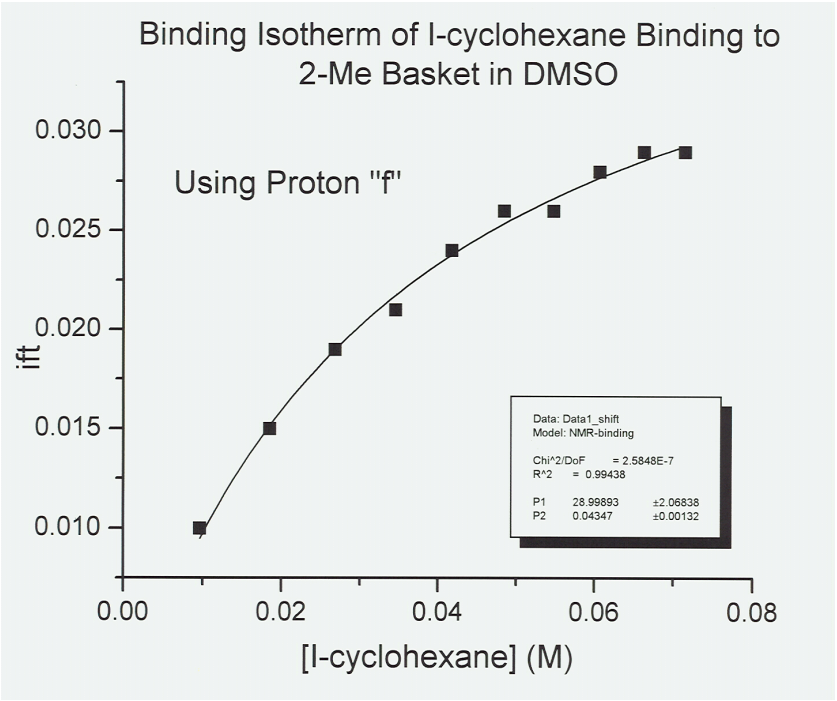

Figure 6.13 Binding isotherm for the complexation of host **71** and iodocyclohexane in DMSO-d_6

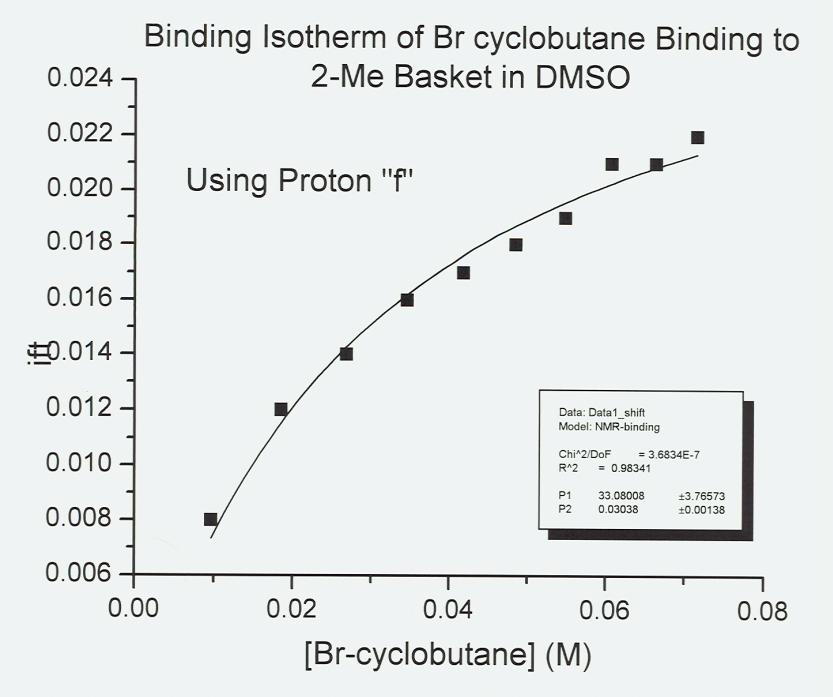

Figure 6.14 Binding isotherm for the complexation of host **71** and bromocyclobutane in DMSO-d_6

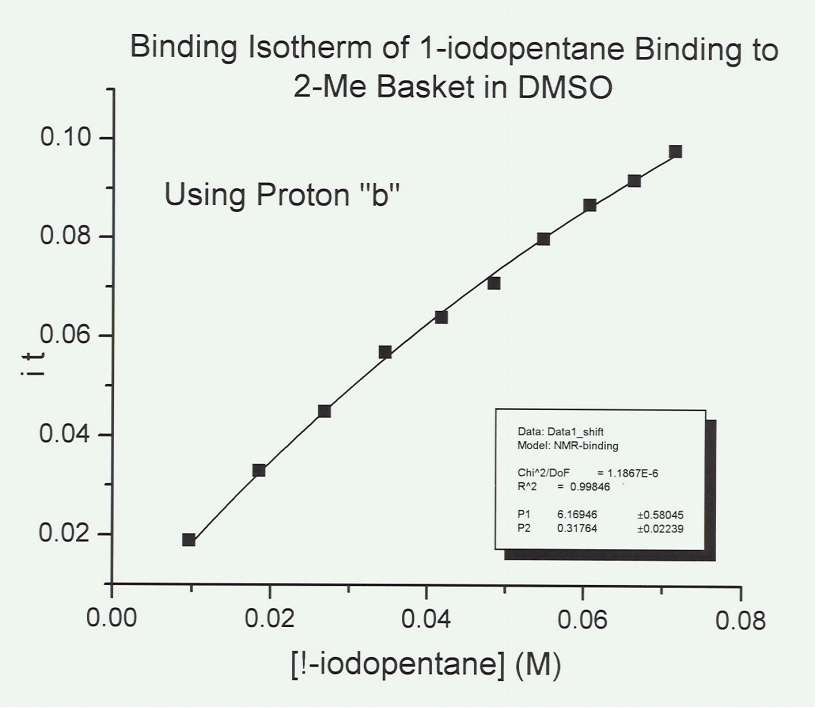

Figure 6.15 Binding isotherm for the complexation of host **71** and iodopentane in DMSO-d_6

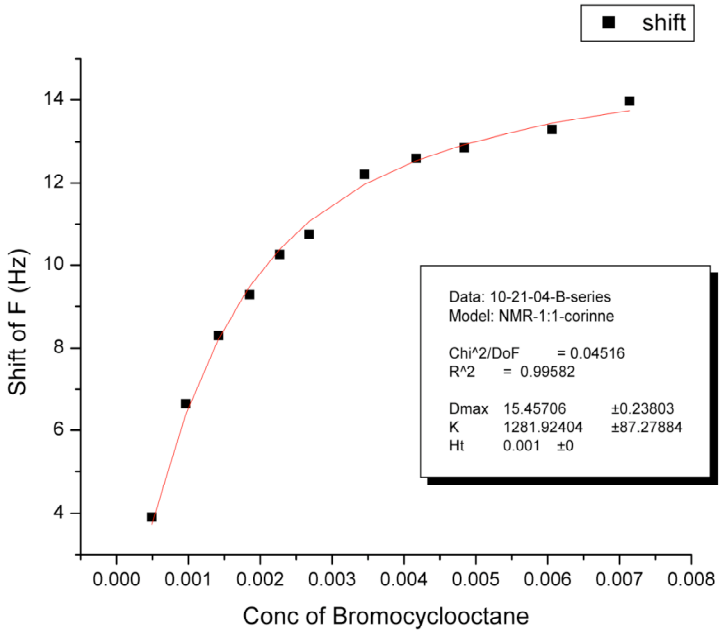

Figure 6.16 Binding isotherm for the complexation of host **99** and bromocyclooctane in DMSO-d_6

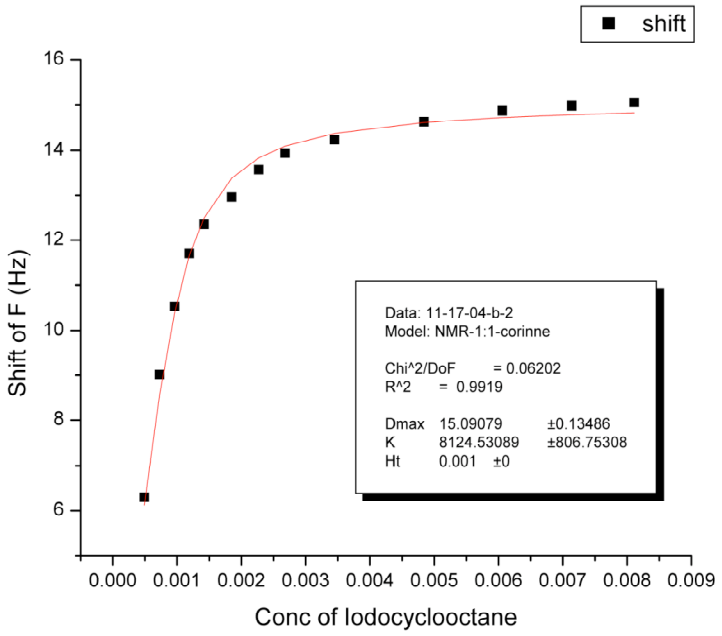

Figure 6.17 Binding isotherm for the complexation of host **99** and iodocyclooctane in DMSO-d_6

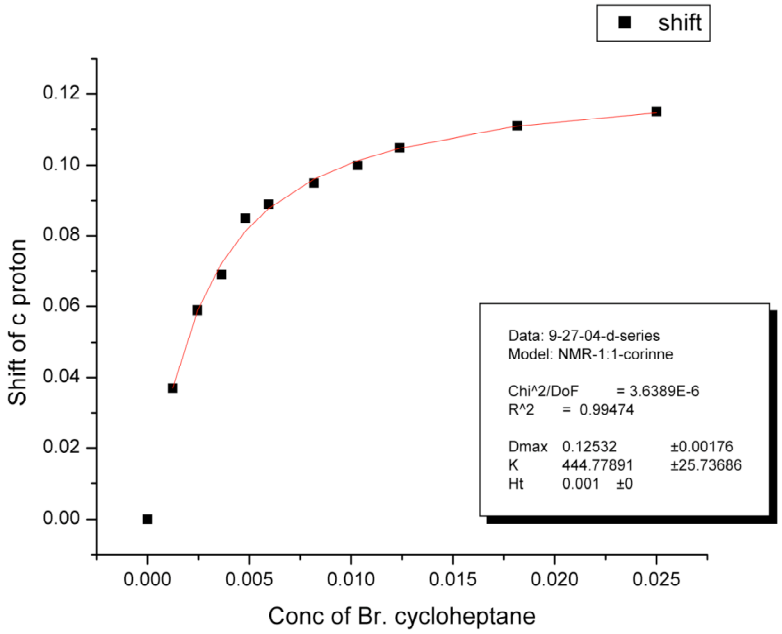

Figure 6.18 Binding isotherm for the complexation of host **99** and bromocycloheptane in DMSO-d_6

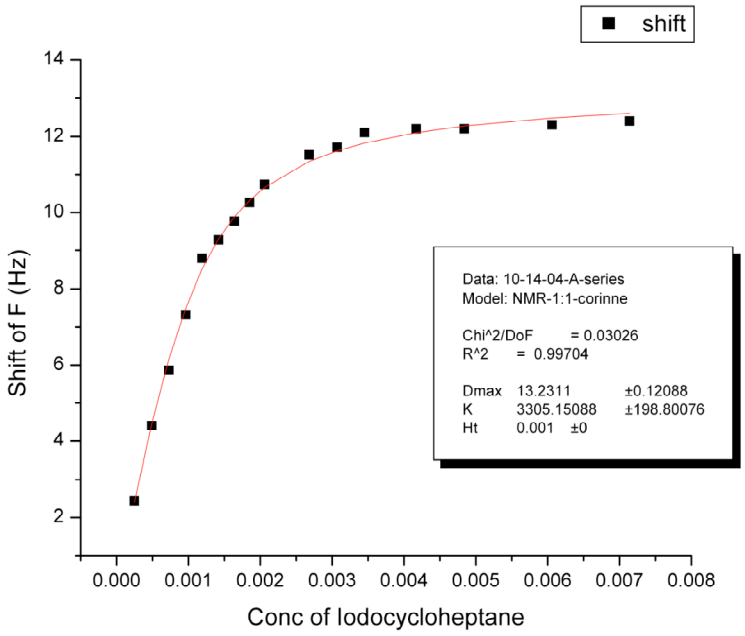

Figure 6.19 Binding isotherm for the complexation of host **99** and iodocycloheptane in DMSO-d_6

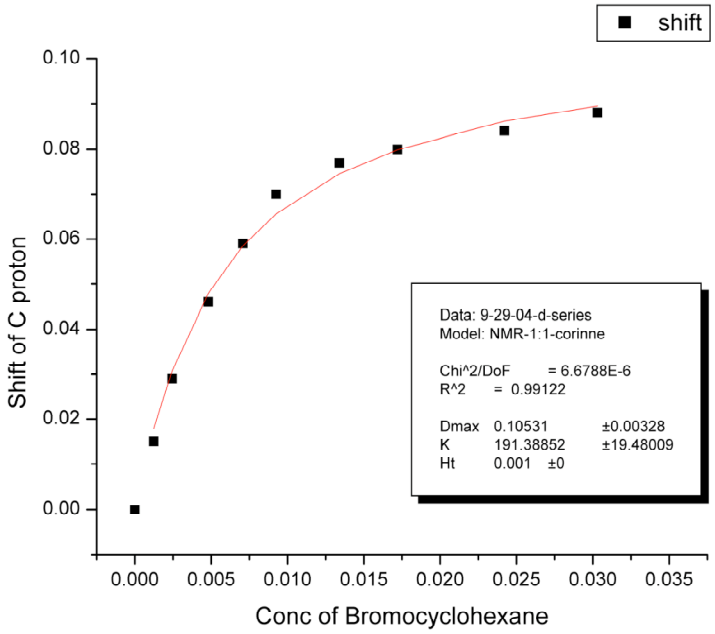

Figure 6.20 Binding isotherm for the complexation of host **99** and bromocyclohexane in DMSO-d_6

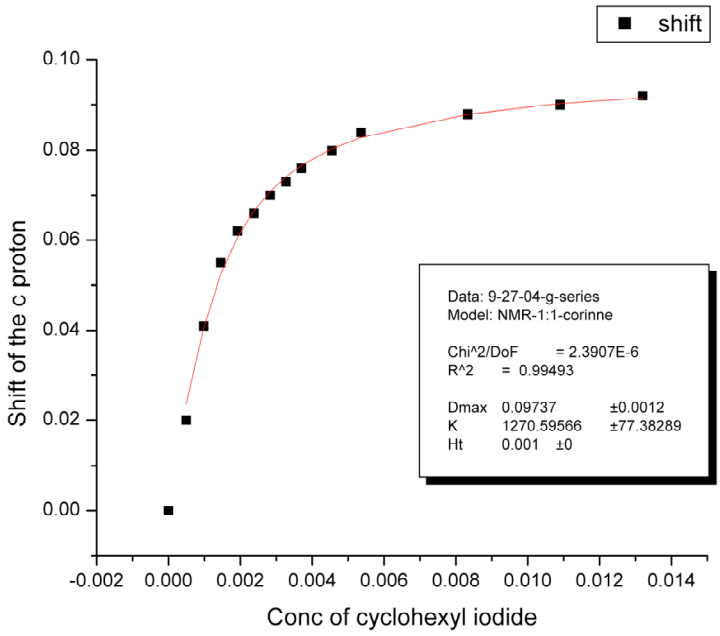

Figure 6.21 Binding isotherm for the complexation of host **99** and iodocyclohexane in DMSO-d_6

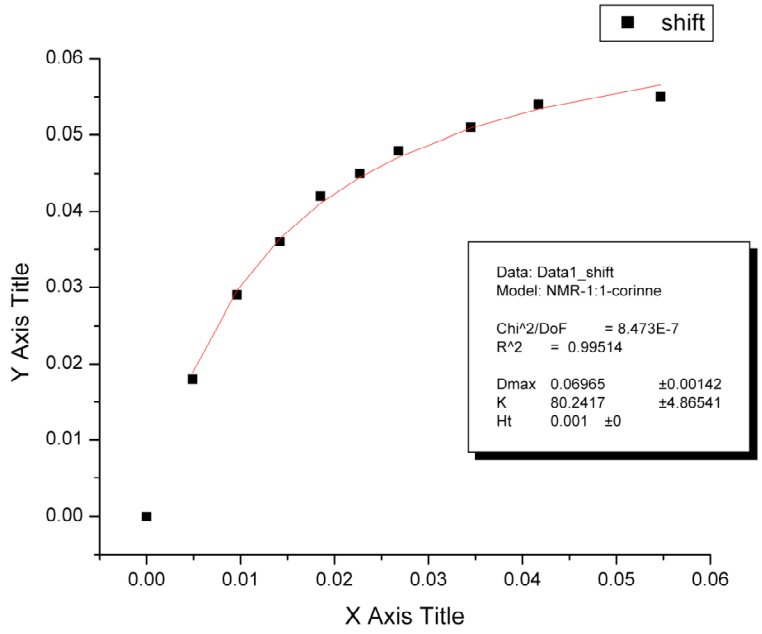

Figure 6.22 Binding isotherm for the complexation of host **99** and bromocyclopentane in DMSO-d_6

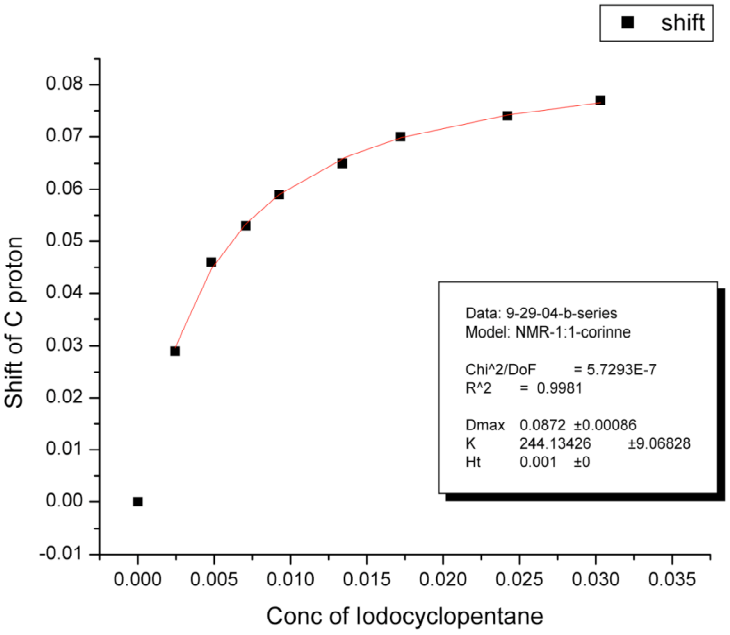

Figure 6.23 Binding isotherm for the complexation of host **99** and iodocyclopentane in DMSO-d_6

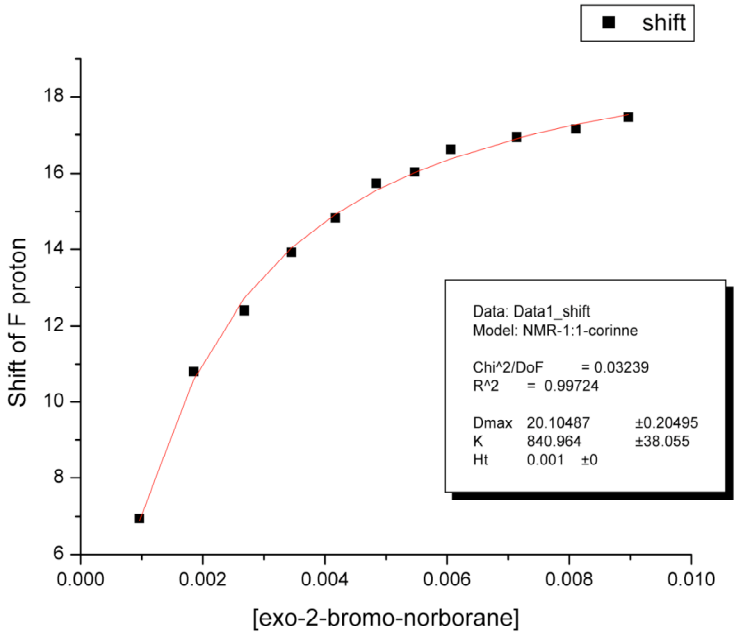

Figure 6.24 Binding isotherm for the complexation of host **99** and *exo*-2-bromo-norborane in DMSO-d_6

6.4 1D- and 2D-NMRs of aldehyde *m*-baskets

^{1}H-NMR and 2D- NOESY/ROESY NMRs for products (+/-)-**105**, **107**, and (+/-)-**109** are shown below. All 2D-NMRs run on the Varian Inova 500 MHz NMR at 298 K.

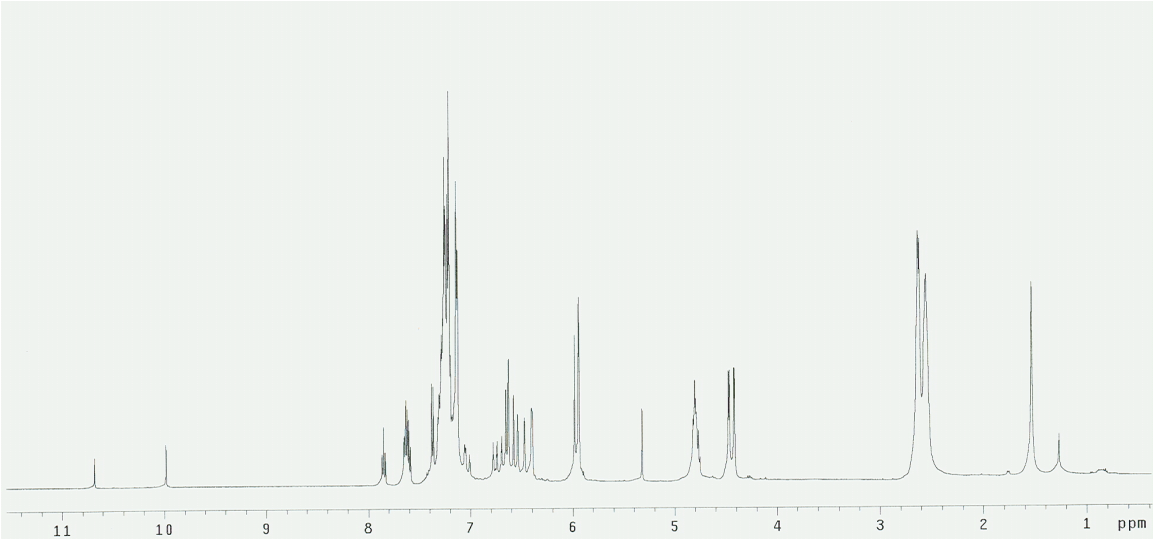

Figure 6.25 ^{1}H-NMR of (+/-)-**105** in $CDCl_3$

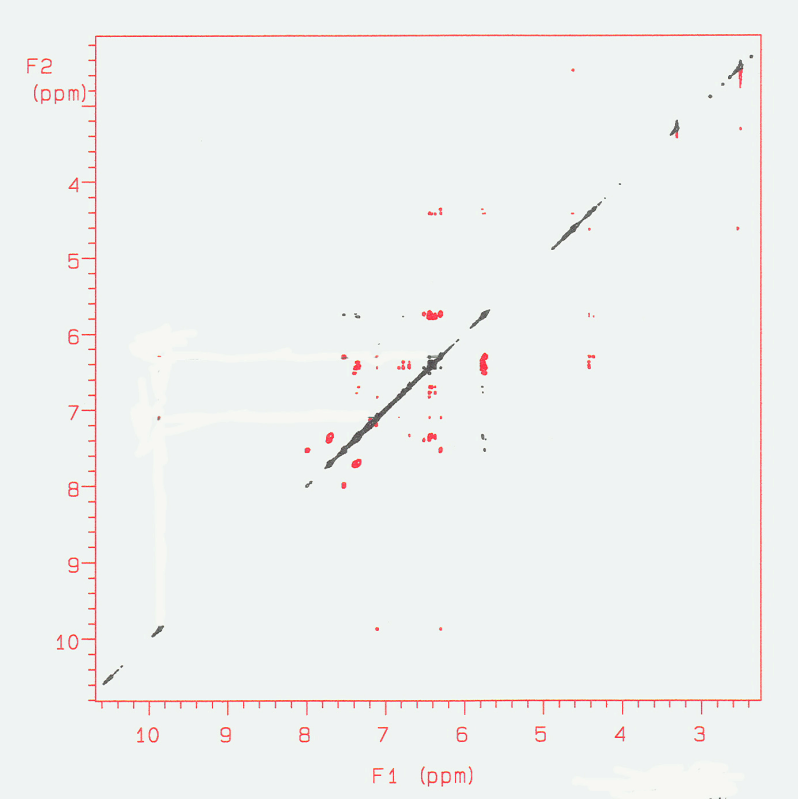

Figure 6.26 2D-ROESY NMR of (+/-)-**105** in DMSO-d_6

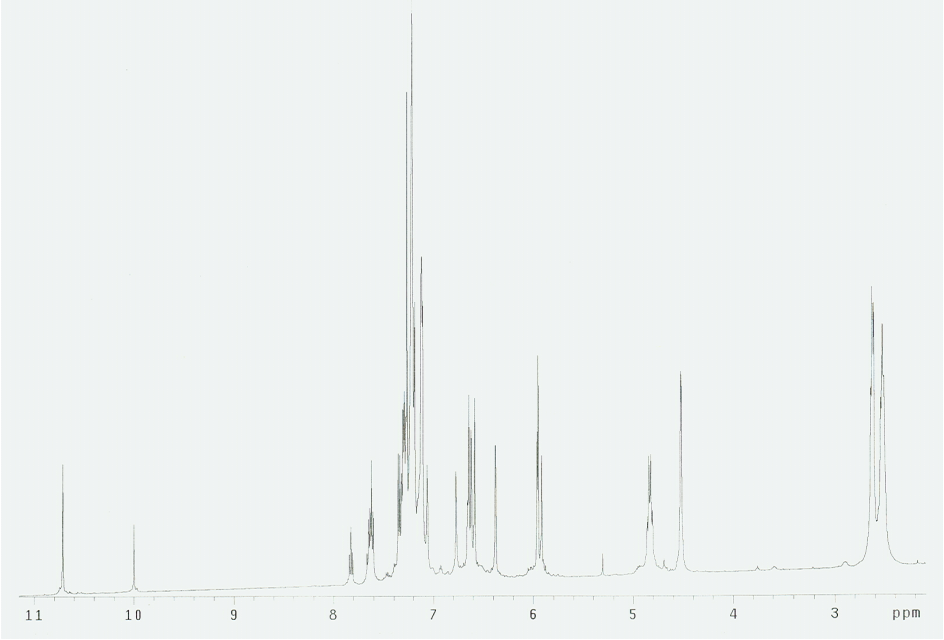

Figure 6.27 ^{1}H-NMR of **107** in $CDCl_3$

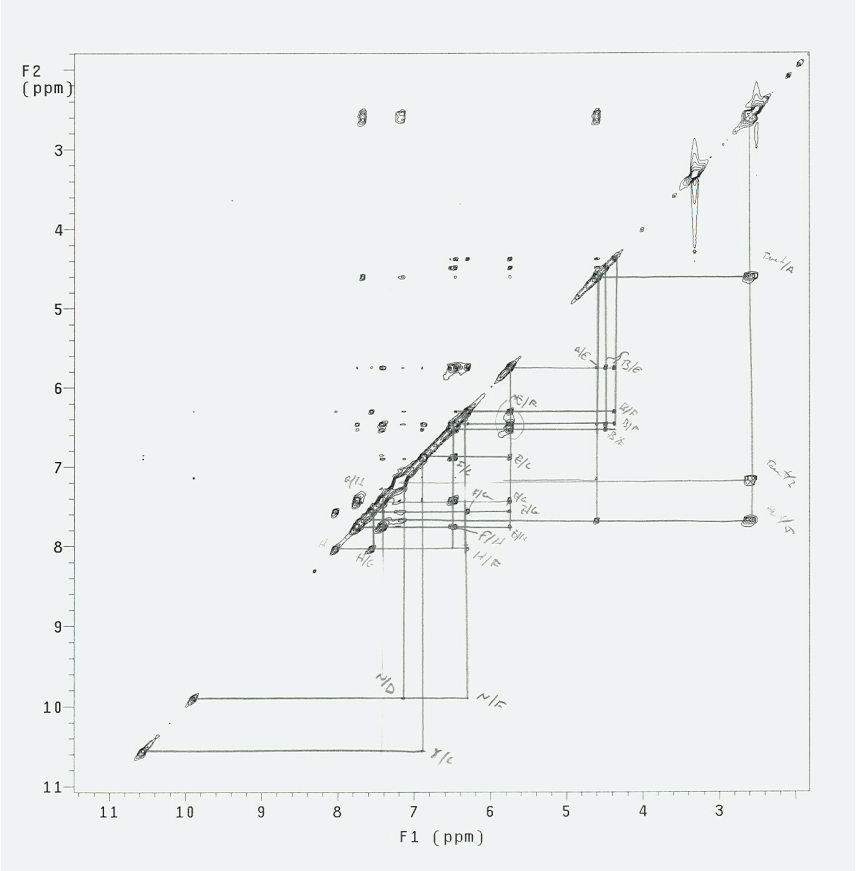

Figure 6.28 2D-NOESY NMR of **107** in DMSO-d_6

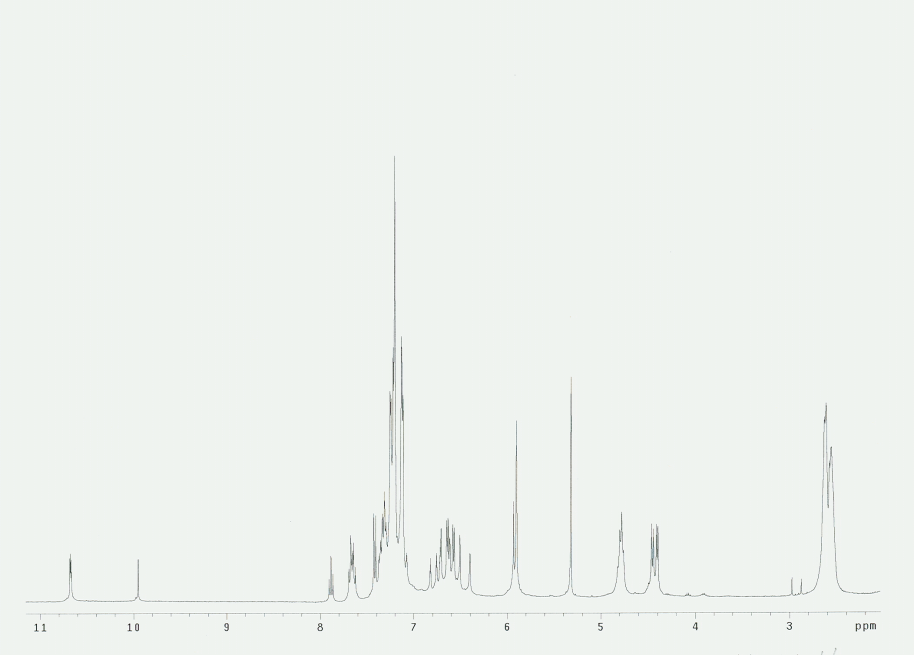

Figure 6.29 ^{1}H-NMR of (+/-)-**109** in CD_2Cl_2

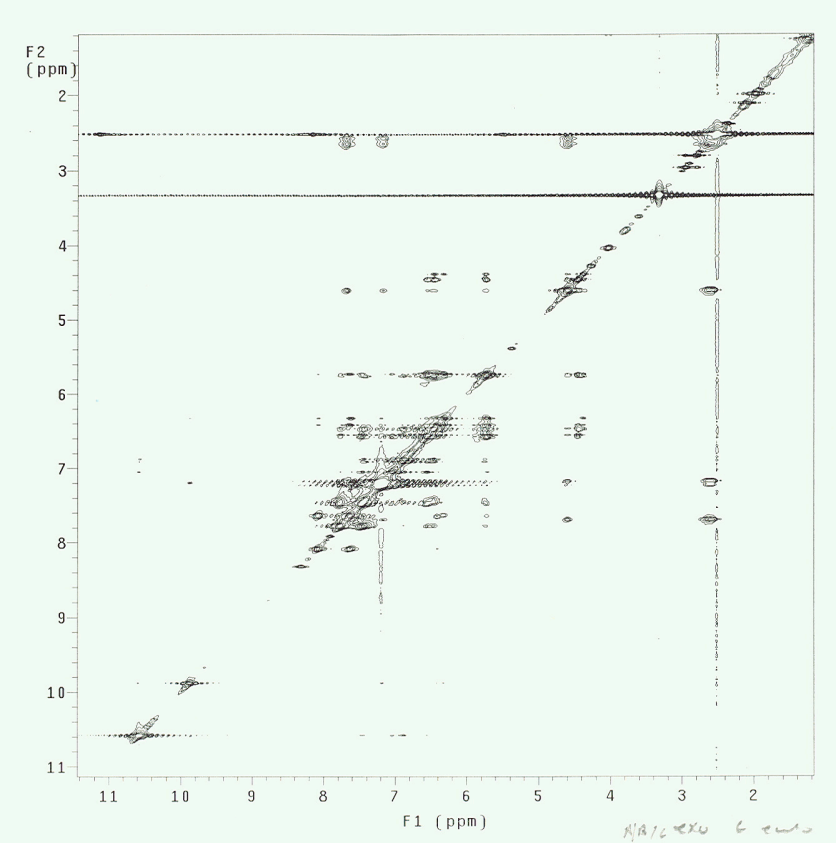

Figure 6.30 2D-ROESY NMR of (+/-)-**109** in DMSO-d_6

6.5 NMR and UV-Vis Zinc binding studies of 156

NMR – A stock solution of 2 mM of **156** in CD_2Cl_2 was prepared. A zinc perchlorate hexahydrate solution (50 mM) was prepared in acetone-d_6. 0.5 mL of the **156** solution was placed in a NMR tube. A NMR spectra was obtained. Then six 5 uL aliquots of the zinc solution were measured into the tube and the spectra recorded after each addition. After the fourth aliquot (1:1 ligand:zinc) no further change in the NMR was noted. The NMR sample was allowed to sit over 24 hours at r.t. and an additional spectra was recorded with no change in the NMR spectra.

UV-Vis – A stock solution of 0.1 mM solution of **156** in CH_2Cl_2 was prepared. 0.5 mL of this solution was placed in a series of 10 mL volumetric flasks. Then various amounts of a 0.5 mM zinc perchlorate hexahydrate solution were placed in the volumetric flasks beginning with 0 eq to 1.4 eq of zinc (0 – 140 uL). CH_2Cl_2 was added to the volumetric flasks to bring the volume to 10 mL. Therefore the concentration of **156** was 0.005 mM in each volumetric flask and the concentration of the zinc was varied. Samples of each of the volumetric flasks were recorded on the UV-Vis spectrometer and the change in absorbance was plotted as a function of the concentration of zinc. An iterative curve-fitting method using Origin 6.1 was used to generate the association constants using the equation:

$$\Delta A = \frac{S_t K_A \Delta\varepsilon_{11}[L]b}{1 + K_A[L]}$$

where ΔA was the change in absorbance; S_t is the host concentration (constant); K_A is the association constant; $\Delta\varepsilon_{11}$ is the maximum change of the molar absorbtivity when the host is fully bound; [L] is the zinc concentration and b is the path length.

6.6 **Crystal structure of 145**

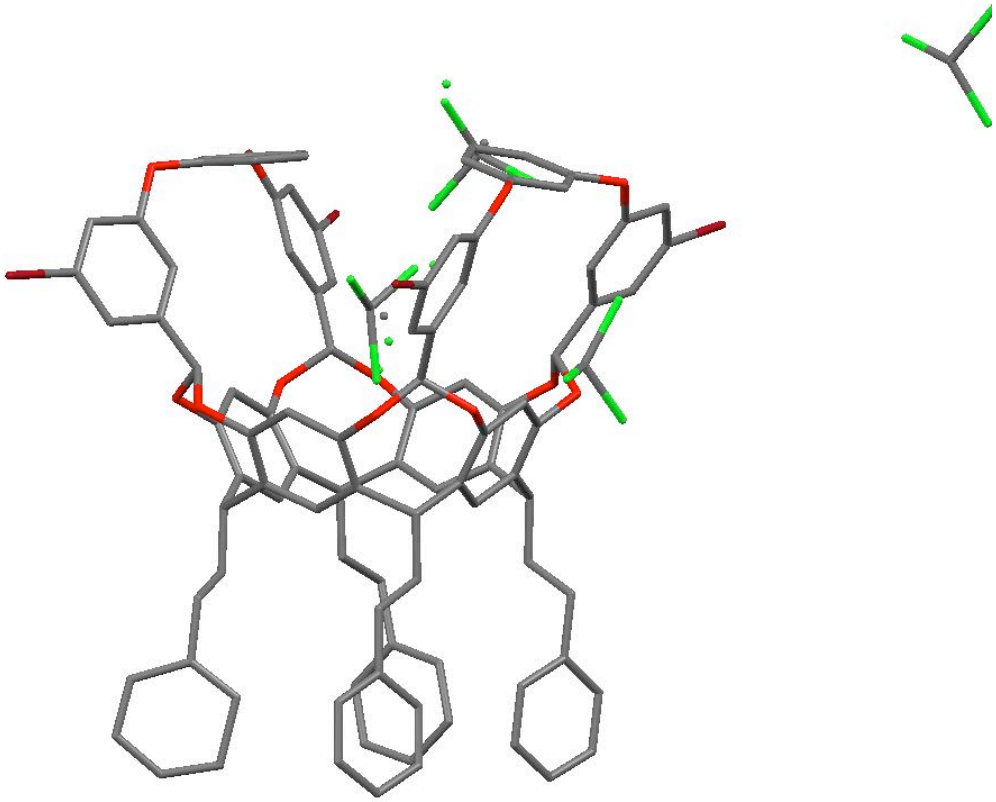

Figure 6.31 X-ray crystal structure of **145** (hydrogens removed for clarity). Image generated by Mercury.[204]

The crystal was grown by dissolving **145** in $CHCl_3$ and hexanes. The crystal structure of **145** was determined by x-ray diffraction by Dr. Edwin Stevens and Zakhia Moore at the University of New Orleans. Data was collected at 113 K on Bruker SMART 1K CCD and a graphite monochronator utilizing MoK_α radiation ($\lambda = 0.71073$ Å). Cell parameters were refined using up to 8773 reflection. The structure was solved by the direct methods in SHELXTL and refined using full-matrix least squares.

Table 6.1 Crystal data and structure refinement for **145**

Empirical formula	$C_{105}H_{77}Br_4Cl_{15}O_{12}$
Formula weight	2382.06
Temperature	150(2)K
Wavelength	0.71073Å
Crystal system, space group	Monoclinic, C2/c
Unit cell dimensions	a = 36.579(3)Å alpha = 90 deg. b = 17.7624(16)Å beta = 95.899(2) deg. c = 31.060(3)Å gamma = 90 deg.
Volume	20074(3) $Å^3$
Z, Calculated density	8, 1.576 Mg/m^3
Absorption coefficient	2.065 mm^-1
F(000)	9584
Crystal size	0.6 x 0.5 x 0.1 mm
Theta range for data collection	3.72 to 23.30 deg.
Limiting indices	$-40 \le h \le 40$, $-17 \le k \le 19$, $-34 \le l \le 33$
Reflections collected / unique	65983 / 14280 [R(int) = 0.0612]
Completeness to theta = 23.30	98.5 %
Absorption correction	Empirical
Max. and min. transmission	1.000000 and 0.594313
Refinement method	Full-matrix least-squares on F^2
Data / restraints / parameters	14280 / 1698 / 1299
Goodness-of-fit on F^2	1.070
Final R indices [I>2sigma(I)]	R1 = 0.0797, wR2 = 0.2043
R indices (all data)	R1 = 0.0994, wR2 = 0.2195
Largest diff. peak and hole	1.307 and -1.231 e. $Å^{-3}$

Table 6.2 Atomic coordinates (x10^4) and equivalent isotropic displacement parameters (Å^2 x10^3) for **145**
.

	x	y	z	U(eq)
Cl(1)	359(1)	6770(2)	633(1)	88(1)
C(1)	-1609(2)	-1257(4)	3177(2)	17(2)
Cl(2)	1052(1)	6710(2)	1155(1)	67(1)
C(2)	-1582(2)	-1149(4)	2739(2)	18(2)
Cl(3)	682(1)	8134(1)	992(1)	51(1)
C(3)	-1234(2)	-1324(4)	2525(2)	20(2)
Cl(4)	1900(2)	7350(3)	3711(2)	150(2)
Cl(4A)	-1624(6)	1918(7)	1150(9)	94(7)
C(4)	-1022(2)	-596(4)	2483(2)	19(2)
Cl(5)	2526(1)	8322(3)	3862(2)	126(2)
C(5)	-747(2)	-380(4)	2802(2)	17(2)
Cl(6)	1964(2)	8253(3)	4431(2)	147(2)
Cl(6A)	-1985(3)	3311(7)	1003(10)	94(5)
C(6)	-549(2)	290(4)	2793(2)	18(2)
Cl(7)	-1643(1)	1987(2)	2434(1)	61(1)
C(7)	-268(2)	501(4)	3163(2)	18(2)
Cl(8)	-1514(1)	897(2)	3122(1)	48(1)
C(8)	-468(2)	959(4)	3483(2)	18(2)
Cl(9)	-2035(1)	2092(2)	3200(1)	59(1)
C(9)	-616(2)	629(4)	3836(2)	17(2)
Cl(10)	-1590(12)	2460(30)	2754(17)	100(13)
Cl(11)	-1520(20)	890(20)	2947(18)	88(12)
Cl(12)	-1650(20)	1930(30)	3614(14)	129(15)
C(10)	-808(2)	1043(4)	4119(2)	21(2)
C(11)	-972(2)	688(4)	4505(2)	22(2)
C(12)	-1374(2)	495(4)	4364(2)	18(2)
C(13)	-1482(2)	-208(4)	4196(2)	18(2)
Cl(15)	-1193(3)	3120(10)	1532(6)	119(6)
Cl(5A)	-1244(4)	3299(8)	1397(6)	65(4)
C(14)	-1842(2)	-381(4)	4056(2)	20(2)
Cl(14)	-1638(3)	1871(4)	1277(4)	54(2)
C(15)	-1953(2)	-1149(4)	3854(2)	20(2)
Cl(16)	-1960(2)	3331(3)	1299(4)	62(3)
C(16)	-1925(2)	-1067(4)	3374(2)	17(2)
Cl(17)	-653(2)	4737(3)	4359(2)	173(3)
C(17)	-1889(2)	-858(4)	2492(2)	18(2)
Cl(18)	-225(1)	3483(3)	4655(2)	119(2)
C(18)	-2198(2)	-654(4)	2673(2)	17(2)
Cl(19)	-736(2)	4091(4)	5179(2)	186(3)
O(20)	-2546(1)	-589(3)	3277(2)	19(1)
C(20)	-2215(2)	-759(4)	3110(2)	18(2)
C(21)	-2560(2)	124(4)	3485(2)	22(2)
O(22)	-2475(1)	56(3)	3939(2)	22(1)

C(23)	-2106(2)	189(4)	4079(2)	21(2)
C(24)	-2006(2)	888(4)	4249(2)	23(2)
C(25)	-1643(2)	1035(4)	4386(2)	19(2)
O(26)	-1558(1)	1741(3)	4555(2)	23(1)
C(27)	-1415(2)	2250(4)	4270(2)	23(2)
O(28)	-1025(1)	2270(3)	4323(2)	26(1)
C(29)	-849(2)	1806(4)	4042(2)	22(2)
C(30)	-708(2)	2148(4)	3698(2)	22(2)
C(31)	-525(2)	1721(4)	3417(2)	18(2)
O(32)	-381(1)	2085(3)	3076(2)	20(1)
C(33)	-589(2)	2045(4)	2664(2)	19(2)
O(34)	-465(1)	1462(3)	2409(2)	19(1)
C(35)	-644(2)	772(4)	2443(2)	18(2)
C(36)	-912(2)	577(4)	2119(2)	17(2)
C(37)	-1099(2)	-93(4)	2142(2)	17(2)
O(38)	-1371(1)	-248(3)	1804(1)	21(1)
C(39)	-1732(2)	-113(4)	1907(2)	19(2)
O(40)	-1894(1)	-780(3)	2046(2)	21(1)
C(41)	-2941(2)	428(4)	3382(2)	24(2)
C(42)	-3221(2)	264(5)	3637(3)	33(2)
C(43)	-3573(2)	554(5)	3506(3)	38(2)
Br(44)	-3959(1)	349(1)	3844(1)	77(1)
C(45)	-3641(2)	978(5)	3145(3)	39(2)
C(46)	-3358(2)	1123(5)	2894(3)	38(2)
O(47)	-3442(2)	1556(4)	2522(2)	56(2)
C(48)	-3155(2)	1773(5)	2296(3)	38(2)
C(49)	-3130(3)	1423(5)	1911(3)	47(2)
C(50)	-2841(3)	1622(5)	1675(3)	46(2)
O(51)	-2820(2)	1281(4)	1277(2)	54(2)
C(52)	-2503(3)	850(5)	1233(3)	44(2)
C(53)	-2423(3)	712(6)	819(3)	50(2)
C(54)	-2112(3)	306(6)	763(3)	43(2)
Br(55)	-2004(1)	120(1)	187(1)	81(1)
C(56)	-1877(2)	42(5)	1100(2)	33(2)
C(57)	-1964(2)	171(4)	1512(2)	25(2)
C(58)	-2278(2)	570(5)	1584(3)	32(2)
C(59)	-2584(3)	2151(5)	1829(3)	46(2)
C(60)	-2624(3)	2486(5)	2222(3)	46(2)
C(61)	-2905(3)	2300(5)	2461(3)	43(2)
C(62)	-3009(2)	843(4)	3015(3)	31(2)
6(3)	-552(2)	2802(4)	2451(2)	21(2)
C(64)	-352(2)	2917(4)	2104(2)	22(2)
C(65)	-317(2)	3642(4)	1951(2)	24(2)
Br(66)	-41(1)	3839(1)	1481(1)	37(1)
C(67)	-484(2)	4261(4)	2126(2)	26(2)
C(68)	-691(2)	4118(4)	2465(3)	30(2)

O(69)	-856(2)	4752(3)	2646(2)	45(2)
C(70)	-1185(2)	4615(4)	2791(3)	34(2)
C(71)	-1223(3)	4781(5)	3215(3)	40(2)
C(72)	-1563(3)	4650(5)	3369(3)	44(2)
O(73)	-1597(2)	4875(3)	3794(2)	59(2)
C(74)	-1625(3)	4307(5)	4094(3)	44(2)
C(75)	-1769(3)	4504(6)	4469(3)	51(3)
C(76)	-1799(3)	3959(5)	4778(3)	43(2)
Br(77)	-2018(1)	4227(1)	5285(1)	76(1)
C(78)	-1695(2)	3236(5)	4725(3)	34(2)
C(79)	-1547(2)	3044(5)	4351(2)	29(2)
C(80)	-1515(2)	3580(5)	4036(3)	36(2)
C(81)	-1852(3)	4356(5)	3118(3)	45(2)
C(82)	-1807(2)	4188(5)	2690(3)	44(2)
C(83)	-1477(2)	4299(5)	2527(3)	35(2)
C(84)	-723(2)	3409(4)	2633(3)	25(2)
C(85)	633(2)	7169(3)	1058(3)	53(3)
C(86)	2076(3)	8171(6)	3917(3)	106(5)
C(87)	-1575(3)	2819(6)	1211(6)	43(5)
C(87A)	-1570(3)	2856(8)	1054(8)	25(6)
C(88)	-636(3)	3932(5)	4664(3)	83(4)
C(89)	-1789(4)	1567(7)	2874(3)	104(5)
C(90)	-1707(13)	1740(30)	3074(14)	88(11)
C(91)	-1005(2)	-1959(4)	2754(2)	23(2)
C(92)	-680(2)	-2216(4)	2513(3)	28(2)
C(93)	-417(2)	-2708(4)	2794(3)	30(2)
C(94)	-468(2)	-3482(5)	2815(3)	40(2)
C(95)	-233(3)	-3936(6)	3075(3)	52(3)
C(96)	59(3)	-3611(6)	3317(3)	53(3)
C(97)	112(2)	-2845(6)	3309(3)	48(2)
C(98)	-126(2)	-2397(5)	3041(3)	36(2)
C(99)	-58(2)	-182(4)	3359(2)	21(2)
C(100)	252(2)	14(4)	3704(2)	25(2)
C(101)	426(2)	-673(5)	3922(2)	28(2)
C(102)	751(2)	-971(6)	3810(3)	49(2)
C(103)	908(3)	-1591(7)	4025(4)	67(3)
C(104)	739(3)	-1933(6)	4345(4)	61(3)
C(105)	417(3)	-1656(6)	4452(3)	51(2)
C(10G)	260(2)	-1034(5)	4248(3)	38(2)
C(107)	-747(2)	30(4)	4707(2)	24(2)
C(108)	-892(2)	-243(5)	5121(2)	30(2)
C(109)	-682(2)	-868(5)	5356(3)	32(2)
C(110)	-832(3)	-1211(6)	5698(3)	49(2)
C(111)	-644(3)	-1764(6)	5941(4)	61(3)
C(112)	-304(3)	-1990(6)	5842(4)	59(3)
C(113)	-146(3)	-1642(5)	5504(3)	47(2)

C(114)	-337(2)	-1096(5)	5265(3)	37(2)
C(115)	-1750(2)	-1806(5)	4076(3)	30(2)
C(116)	-1838(3)	-1885(6)	4546(3)	53(3)
C(117)	-1669(4)	-2538(6)	4787(3)	66(3)
C(118)	-1944(5)	-3065(8)	4918(4)	96(4)
C(119)	-1840(5)	-3703(8)	5139(5)	97(4)
C(120)	-1462(5)	-3842(8)	5187(5)	89(4)
C(121)	-1172(6)	-3365(10)	5131(4)	104(4)
C(122)	-1306(4)	-2575(8)	4902(3)	85

Table 6.3 Bond lengths [Å] and angles [deg] for **145**

Cl(1)-C(85)	1.727(6)
C(1)-C(2)	1.387(10)
C(1)-C(16)	1.406(10)
Cl(2)-C(85)	1.734(6)
C(2)-C(17)	1.395(10)
C(2)-C(3)	1.527(10)
Cl(3)-C(85)	1.739(6)
C(3)-C(4)	1.519(10)
C(3)-C(91)	1.536(10)
Cl(4)-C(86)	1.695(7)
Cl(4A)-C(87A)	1.708(8)
C(4)-C(5)	1.390(10)
C(4)-C(37)	1.392(10)
Cl(5)-C(86)	1.692(7)
C(5)-C(6)	1.395(10)
Cl(6)-C(86)	1.694(7)
Cl(6A)-C(87A)	1.714(7)
C(6)-C(35)	1.397(10)
C(6)-C(7)	1.512(10)
Cl(7)-C(89)	1.693(7)
C(7)-C(8)	1.527(10)
C(7)-C(99)	1.528(10)
Cl(8)-C(89)	1.693(7)
C(8)-C(31)	1.381(10)
C(8)-C(9)	1.402(10)
Cl(9)-C(89)	1.699(7)
C(9)-C(10)	1.390(10)
Cl(10)-C(90)	1.705(8)
Cl(11)-C(90)	1.707(8)
Cl(12)-C(90)	1.707(8)
C(10)-C(29)	1.383(11)
C(10)-C(11)	1.530(10)
C(11)-C(107)	1.526(11)
C(11)-C(12)	1.532(10)
C(12)-C(25)	1.380(10)
C(12)-C(13)	1.394(10)
C(13)-C(14)	1.378(10)
Cl(15)-C(87)	1.716(7)
Cl(5A)-C(87A)	1.707(8)
C(14)-C(23)	1.407(11)
C(14)-C(15)	1.538(10)
Cl(14)-C(87)	1.716(7)
C(15)-C(115)	1.511(11)
C(15)-C(16)	1.513(10)
Cl(16)-C(87)	1.721(7)

C(16)-C(20)	1.383(10)
Cl(17)-C(88)	1.712(7)
C(17)-C(18)	1.361(10)
C(17)-O(40)	1.390(8)
Cl(18)-C(88)	1.706(7)
C(18)-C(20)	1.379(10)
Cl(19)-C(88)	1.700(7)
O(20)-C(20)	1.396(8)
O(20)-C(21)	1.424(9)
C(21)-O(22)	1.420(9)
C(21)-C(41)	1.497(10)
O(22)-C(23)	1.395(8)
C(23)-C(24)	1.385(11)
C(24)-C(25)	1.377(10)
C(25)-O(26)	1.383(9)
O(26)-C(27)	1.402(9)
C(27)-O(28)	1.421(9)
C(27)-C(79)	1.521(11)
O(28)-C(29)	1.402(9)
C(29)-C(30)	1.376(10)
C(30)-C(31)	1.379(10)
C(31)-O(32)	1.390(8)
O(32)-C(33)	1.420(8)
C(33)-O(34)	1.409(8)
C(33)-6(3)	1.511(10)
O(34)-C(35)	1.399(9)
C(35)-C(36)	1.377(10)
C(36)-C(37)	1.377(10)
C(37)-O(38)	1.401(8)
O(38)-C(39)	1.409(8)
C(39)-O(40)	1.411(9)
C(39)-C(57)	1.506(10)
C(41)-C(62)	1.359(11)
C(41)-C(42)	1.388(11)
C(42)-C(43)	1.407(11)
C(43)-C(45)	1.353(13)
C(43)-Br(44)	1.881(9)
C(45)-C(46)	1.384(13)
C(46)-C(62)	1.384(11)
C(46)-O(47)	1.396(11)
O(47)-C(48)	1.377(11)
C(48)-C(49)	1.358(14)
C(48)-C(61)	1.369(13)
C(49)-C(50)	1.395(14)
C(50)-C(59)	1.379(14)
C(50)-O(51)	1.387(11)

O(51)-C(52)	1.406(11)
C(52)-C(53)	1.369(13)
C(52)-C(58)	1.390(11)
C(53)-C(54)	1.372(14)
C(54)-C(56)	1.365(12)
C(54)-Br(55)	1.900(8)
C(56)-C(57)	1.372(11)
C(57)-C(58)	1.385(11)
C(59)-C(60)	1.379(14)
C(60)-C(61)	1.369(14)
6(3)-C(64)	1.377(11)
6(3)-C(84)	1.395(10)
C(64)-C(65)	1.384(11)
C(65)-C(67)	1.396(11)
C(65)-Br(66)	1.888(7)
C(67)-C(68)	1.380(11)
C(68)-C(84)	1.374(11)
C(68)-O(69)	1.421(10)
O(69)-C(70)	1.351(10)
C(70)-C(71)	1.371(13)
C(70)-C(83)	1.395(13)
C(71)-C(72)	1.398(13)
C(72)-C(81)	1.352(14)
C(72)-O(73)	1.399(12)
O(73)-C(74)	1.384(11)
C(74)-C(80)	1.370(12)
C(74)-C(75)	1.372(13)
C(75)-C(76)	1.374(14)
C(76)-C(78)	1.354(13)
C(76)-Br(77)	1.900(8)
C(78)-C(79)	1.375(11)
C(79)-C(80)	1.378(12)
C(81)-C(82)	1.391(14)
C(82)-C(83)	1.370(12)
C(91)-C(92)	1.536(11)
C(92)-C(93)	1.510(11)
C(93)-C(98)	1.364(12)
C(93)-C(94)	1.389(12)
C(94)-C(95)	1.378(13)
C(95)-C(96)	1.370(15)
C(96)-C(97)	1.375(15)
C(97)-C(98)	1.391(13)
C(99)-C(100)	1.518(10)
C(100)-C(101)	1.505(11)
C(101)-C(102)	1.377(12)
C(101)-C(10G)	1.391(11)

C(102)-C(103)	1.382(14)
C(103)-C(104)	1.367(16)
C(104)-C(105)	1.350(15)
C(105)-C(10G)	1.369(14)
C(107)-C(108)	1.521(11)
C(108)-C(109)	1.497(12)
C(109)-C(114)	1.383(12)
C(109)-C(110)	1.386(12)
C(110)-C(111)	1.381(14)
C(111)-C(112)	1.371(16)
C(112)-C(113)	1.393(15)
C(113)-C(114)	1.368(13)
C(115)-C(116)	1.534(13)
C(116)-C(117)	1.478(15)
C(117)-C(122)	1.343(19)
C(117)-C(118)	1.463(19)
C(118)-C(119)	1.358(19)
C(119)-C(120)	1.40(2)
C(120)-C(121)	1.38(2)
C(121)-C(122)	1.63(2)

C(2)-C(1)-C(16)	122.5(6)
C(1)-C(2)-C(17)	117.1(6)
C(1)-C(2)-C(3)	123.1(6)
C(17)-C(2)-C(3)	119.8(6)
C(4)-C(3)-C(2)	108.6(6)
C(4)-C(3)-C(91)	114.0(6)
C(2)-C(3)-C(91)	112.7(6)
C(5)-C(4)-C(37)	116.0(7)
C(5)-C(4)-C(3)	120.8(6)
C(37)-C(4)-C(3)	123.1(6)
C(4)-C(5)-C(6)	124.1(7)
C(5)-C(6)-C(35)	116.8(6)
C(5)-C(6)-C(7)	120.7(6)
C(35)-C(6)-C(7)	122.3(6)
C(6)-C(7)-C(8)	107.0(5)
C(6)-C(7)-C(99)	112.4(6)
C(8)-C(7)-C(99)	114.8(6)
C(31)-C(8)-C(9)	117.5(6)
C(31)-C(8)-C(7)	120.1(6)
C(9)-C(8)-C(7)	122.3(6)
C(10)-C(9)-C(8)	122.3(7)
C(29)-C(10)-C(9)	117.6(7)
C(29)-C(10)-C(11)	119.7(6)
C(9)-C(10)-C(11)	122.8(7)
C(107)-C(11)-C(10)	113.6(6)

C(107)-C(11)-C(12)	114.1(6)
C(10)-C(11)-C(12)	108.1(5)
C(25)-C(12)-C(13)	117.7(6)
C(25)-C(12)-C(11)	120.0(6)
C(13)-C(12)-C(11)	122.2(6)
C(14)-C(13)-C(12)	122.8(7)
C(13)-C(14)-C(23)	117.6(7)
C(13)-C(14)-C(15)	122.1(7)
C(23)-C(14)-C(15)	120.2(6)
C(115)-C(15)-C(16)	116.4(6)
C(115)-C(15)-C(14)	113.7(6)
C(16)-C(15)-C(14)	106.0(5)
C(20)-C(16)-C(1)	117.0(6)
C(20)-C(16)-C(15)	119.8(6)
C(1)-C(16)-C(15)	123.2(6)
C(18)-C(17)-O(40)	117.3(6)
C(18)-C(17)-C(2)	121.9(6)
O(40)-C(17)-C(2)	120.7(6)
C(17)-C(18)-C(20)	119.6(6)
C(20)-O(20)-C(21)	115.8(5)
C(18)-C(20)-C(16)	121.8(6)
C(18)-C(20)-O(20)	117.7(6)
C(16)-C(20)-O(20)	120.4(6)
O(22)-C(21)-O(20)	111.1(6)
O(22)-C(21)-C(41)	110.3(6)
O(20)-C(21)-C(41)	107.5(5)
C(23)-O(22)-C(21)	113.6(5)
C(24)-C(23)-O(22)	118.6(6)
C(24)-C(23)-C(14)	120.6(6)
O(22)-C(23)-C(14)	120.8(6)
C(25)-C(24)-C(23)	119.7(7)
C(24)-C(25)-C(12)	121.5(7)
C(24)-C(25)-O(26)	117.5(6)
C(12)-C(25)-O(26)	121.0(6)
C(25)-O(26)-C(27)	115.4(5)
O(26)-C(27)-O(28)	112.3(6)
O(26)-C(27)-C(79)	110.4(6)
O(28)-C(27)-C(79)	106.8(6)
C(29)-O(28)-C(27)	115.7(5)
C(30)-C(29)-C(10)	121.6(7)
C(30)-C(29)-O(28)	117.2(7)
C(10)-C(29)-O(28)	121.2(6)
C(29)-C(30)-C(31)	119.6(7)
C(30)-C(31)-C(8)	121.4(7)
C(30)-C(31)-O(32)	118.2(6)
C(8)-C(31)-O(32)	120.3(6)

C(31)-O(32)-C(33)	117.1(5)
O(34)-C(33)-O(32)	111.6(5)
O(34)-C(33)-6(3)	111.0(6)
O(32)-C(33)-6(3)	106.7(5)
C(35)-O(34)-C(33)	114.8(5)
C(36)-C(35)-C(6)	121.1(6)
C(36)-C(35)-O(34)	118.0(6)
C(6)-C(35)-O(34)	121.0(6)
C(35)-C(36)-C(37)	119.8(6)
C(36)-C(37)-C(4)	122.3(6)
C(36)-C(37)-O(38)	116.7(6)
C(4)-C(37)-O(38)	121.1(6)
C(37)-O(38)-C(39)	114.0(5)
O(38)-C(39)-O(40)	111.0(5)
O(38)-C(39)-C(57)	109.5(6)
O(40)-C(39)-C(57)	108.1(6)
C(17)-O(40)-C(39)	115.2(5)
C(62)-C(41)-C(42)	120.6(7)
C(62)-C(41)-C(21)	117.4(7)
C(42)-C(41)-C(21)	121.8(7)
C(41)-C(42)-C(43)	117.6(8)
C(45)-C(43)-C(42)	122.0(8)
C(45)-C(43)-Br(44)	119.0(6)
C(42)-C(43)-Br(44)	118.9(7)
C(43)-C(45)-C(46)	119.0(8)
C(62)-C(46)-C(45)	120.1(8)
C(62)-C(46)-O(47)	122.9(8)
C(45)-C(46)-O(47)	117.0(7)
C(48)-O(47)-C(46)	117.4(6)
C(49)-C(48)-C(61)	122.7(9)
C(49)-C(48)-O(47)	116.3(9)
C(61)-C(48)-O(47)	121.0(9)
C(48)-C(49)-C(50)	118.0(9)
C(59)-C(50)-O(51)	120.7(10)
C(59)-C(50)-C(49)	121.1(9)
O(51)-C(50)-C(49)	118.2(9)
C(50)-O(51)-C(52)	116.5(6)
C(53)-C(52)-C(58)	120.3(9)
C(53)-C(52)-O(51)	116.6(8)
C(58)-C(52)-O(51)	123.1(8)
C(52)-C(53)-C(54)	118.2(8)
C(56)-C(54)-C(53)	123.3(8)
C(56)-C(54)-Br(55)	119.0(7)
C(53)-C(54)-Br(55)	117.7(6)
C(54)-C(56)-C(57)	117.9(8)
C(56)-C(57)-C(58)	120.7(7)

C(56)-C(57)-C(39)	122.6(7)
C(58)-C(57)-C(39)	116.6(7)
C(57)-C(58)-C(52)	119.5(8)
C(60)-C(59)-C(50)	118.1(10)
C(61)-C(60)-C(59)	121.9(9)
C(48)-C(61)-C(60)	118.2(10)
C(41)-C(62)-C(46)	120.5(8)
C(64)-6(3)-C(84)	119.9(7)
C(64)-6(3)-C(33)	123.7(6)
C(84)-6(3)-C(33)	116.4(6)
6(3)-C(64)-C(65)	118.9(7)
C(64)-C(65)-C(67)	122.6(7)
C(64)-C(65)-Br(66)	120.9(6)
C(67)-C(65)-Br(66)	116.5(5)
C(68)-C(67)-C(65)	116.7(7)
C(84)-C(68)-C(67)	122.2(7)
C(84)-C(68)-O(69)	121.3(7)
C(67)-C(68)-O(69)	116.4(7)
C(70)-O(69)-C(68)	114.7(6)
O(69)-C(70)-C(71)	117.4(8)
O(69)-C(70)-C(83)	122.2(8)
C(71)-C(70)-C(83)	120.3(8)
C(70)-C(71)-C(72)	118.2(9)
C(81)-C(72)-C(71)	122.7(9)
C(81)-C(72)-O(73)	120.8(9)
C(71)-C(72)-O(73)	116.4(9)
C(74)-O(73)-C(72)	116.6(7)
C(80)-C(74)-C(75)	119.7(9)
C(80)-C(74)-O(73)	123.8(8)
C(75)-C(74)-O(73)	116.5(8)
C(74)-C(75)-C(76)	118.5(9)
C(78)-C(76)-C(75)	122.7(8)
C(78)-C(76)-Br(77)	119.0(7)
C(75)-C(76)-Br(77)	118.2(7)
C(76)-C(78)-C(79)	118.5(8)
C(78)-C(79)-C(80)	119.9(8)
C(78)-C(79)-C(27)	121.9(7)
C(80)-C(79)-C(27)	118.2(7)
C(74)-C(80)-C(79)	120.7(8)
C(72)-C(81)-C(82)	118.1(9)
C(83)-C(82)-C(81)	121.2(9)
C(82)-C(83)-C(70)	119.4(8)
C(68)-C(84)-6(3)	119.7(7)
Cl(1)-C(85)-Cl(2)	111.9(4)
Cl(1)-C(85)-Cl(3)	111.9(4)
Cl(2)-C(85)-Cl(3)	112.6(4)

Cl(5)-C(86)-Cl(6)	114.5(6)
Cl(5)-C(86)-Cl(4)	115.7(6)
Cl(6)-C(86)-Cl(4)	108.1(5)
Cl(15)-C(87)-Cl(14)	110.4(7)
Cl(15)-C(87)-Cl(16)	112.0(7)
Cl(14)-C(87)-Cl(16)	112.2(6)
Cl(5A)-C(87A)-Cl(4A)	115.3(9)
Cl(5A)-C(87A)-Cl(6A)	113.3(8)
Cl(4A)-C(87A)-Cl(6A)	111.0(9)
Cl(19)-C(88)-Cl(18)	111.6(5)
Cl(19)-C(88)-Cl(17)	112.4(6)
Cl(18)-C(88)-Cl(17)	111.3(5)
Cl(7)-C(89)-Cl(8)	117.0(5)
Cl(7)-C(89)-Cl(9)	118.0(5)
Cl(8)-C(89)-Cl(9)	116.3(5)
Cl(10)-C(90)-Cl(11)	113.7(11)
Cl(10)-C(90)-Cl(12)	113.7(11)
Cl(11)-C(90)-Cl(12)	113.4(11)
C(3)-C(91)-C(92)	113.8(6)
C(93)-C(92)-C(91)	111.7(6)
C(98)-C(93)-C(94)	118.4(8)
C(98)-C(93)-C(92)	120.3(7)
C(94)-C(93)-C(92)	121.3(7)
C(95)-C(94)-C(93)	121.8(9)
C(96)-C(95)-C(94)	118.7(9)
C(95)-C(96)-C(97)	120.7(9)
C(96)-C(97)-C(98)	119.7(9)
C(93)-C(98)-C(97)	120.7(9)
C(100)-C(99)-C(7)	114.0(6)
C(101)-C(100)-C(99)	112.5(6)
C(102)-C(101)-C(10G)	117.3(8)
C(102)-C(101)-C(100)	122.3(7)
C(10G)-C(101)-C(100)	120.4(7)
C(101)-C(102)-C(103)	120.9(9)
C(104)-C(103)-C(102)	120.5(10)
C(105)-C(104)-C(103)	119.2(10)
C(104)-C(105)-C(10G)	121.2(9)
C(105)-C(10G)-C(101)	121.0(9)
C(108)-C(107)-C(11)	111.8(6)
C(109)-C(108)-C(107)	116.2(7)
C(114)-C(109)-C(110)	118.1(8)
C(114)-C(109)-C(108)	123.6(7)
C(110)-C(109)-C(108)	118.3(8)
C(111)-C(110)-C(109)	121.1(10)
C(112)-C(111)-C(110)	119.9(10)
C(111)-C(112)-C(113)	119.6(9)

C(114)-C(113)-C(112)	119.9(10)
C(113)-C(114)-C(109)	121.4(9)
C(15)-C(115)-C(116)	111.5(7)
C(117)-C(116)-C(115)	115.9(10)
C(122)-C(117)-C(118)	125.8(12)
C(122)-C(117)-C(116)	121.5(11)
C(118)-C(117)-C(116)	112.4(12)
C(119)-C(118)-C(117)	120.6(16)
C(118)-C(119)-C(120)	115.1(16)
C(121)-C(120)-C(119)	130.0(14)
C(120)-C(121)-C(122)	112.6(15)
C(117)-C(122)-C(121)	113.8(15)

Table 6.4 Anisotropic displacement parameters ($Å^2$ x10^3) for **145**. The anisotropic displacement factor exponent takes the form:

$$-2pi^2[h^2a^{*2}U11 + ... + 2hka^*b^*U12]$$

	U11	U22	U33	U23	U13	U12
Cl(1)	88(2)	83(2)	85(2)	-37(2)	-30(2)	-4(2)
C(1)	19(3)	8(3)	21(4)	0(3)	-8(3)	-2(3)
Cl(2)	52(2)	61(2)	87(2)	30(2)	1(1)	13(1)
C(2)	20(3)	11(3)	22(4)	-5(3)	-3(3)	0(3)
Cl(3)	47(1)	47(1)	57(2)	3(1)	-5(1)	7(1)
C(3)	21(4)	17(4)	22(4)	-6(3)	-3(3)	1(3)
Cl(4)	221(6)	77(3)	154(4)	-34(3)	22(4)	-67(3)
Cl(4A)	109(9)	55(7)	134(15)	-3(7)	83(9)	-10(6)
C(4)	19(3)	20(4)	18(3)	-5(3)	3(3)	6(3)
Cl(5)	63(2)	177(5)	141(4)	6(4)	21(2)	-1(3)
C(5)	14(3)	18(4)	17(3)	0(3)	1(3)	6(3)
Cl(6)	251(7)	103(3)	94(3)	-13(3)	52(4)	-23(4)
Cl(6A)	56(5)	79(7)	146(16)	-2(8)	6(7)	17(4)
C(6)	17(3)	19(4)	18(3)	-3(3)	4(3)	5(3)
Cl(7)	49(2)	76(2)	57(2)	25(2)	7(1)	14(2)
C(7)	17(3)	22(4)	17(3)	-4(3)	3(3)	3(3)
Cl(8)	58(2)	43(2)	43(2)	2(1)	3(2)	8(1)
C(8)	16(3)	23(4)	15(3)	-2(3)	-1(3)	0(3)
Cl(9)	57(2)	74(2)	46(2)	-4(1)	3(1)	20(2)
C(9)	10(3)	21(4)	19(4)	-5(3)	-2(3)	-1(3)
Cl(10)	60(20)	90(20)	150(30)	0(20)	-10(20)	16(19)
Cl(11)	100(20)	100(20)	70(20)	-1(19)	30(20)	1(18)
Cl(12)	130(30)	130(30)	120(30)	-10(30)	10(30)	0(30)
C(10)	17(3)	27(4)	17(3)	-1(3)	0(3)	-8(3)
C(11)	22(4)	29(4)	13(3)	-3(3)	-1(3)	-10(3)
C(12)	17(3)	25(4)	12(3)	3(3)	0(3)	-2(3)
C(13)	20(4)	24(4)	12(3)	2(3)	3(3)	-6(3)
Cl(15)	51(4)	195(13)	105(10)	-92(9)	-21(5)	19(6)
Cl(5A)	65(7)	56(6)	70(8)	-38(5)	-15(5)	-5(5)
C(14)	26(4)	21(4)	10(3)	5(3)	-2(3)	-4(3)
Cl(14)	56(4)	40(3)	72(5)	20(3)	32(3)	14(3)
C(15)	20(3)	19(4)	21(4)	4(3)	-3(3)	-4(3)
Cl(16)	42(3)	43(3)	105(7)	6(3)	28(3)	14(2)
C(16)	21(4)	9(3)	20(4)	-1(3)	-3(3)	-2(3)
Cl(17)	129(4)	143(5)	237(7)	107(5)	-37(4)	-20(4)
C(17)	21(4)	15(4)	17(3)	2(3)	-3(3)	-2(3)
Cl(18)	106(3)	127(4)	123(3)	-18(3)	7(3)	34(3)
C(18)	15(3)	13(4)	21(4)	0(3)	-8(3)	-2(3)
Cl(19)	256(8)	170(6)	151(5)	-45(4)	113(5)	-18(6)
O(20)	15(2)	20(3)	23(3)	-2(2)	-1(2)	1(2)
C(20)	14(3)	14(4)	25(4)	0(3)	-2(3)	-1(3)

C(21)	26(4)	15(4)	21(4)	-2(3)	-4(3)	-2(3)
O(22)	14(2)	30(3)	22(3)	-2(2)	-2(2)	-6(2)
C(23)	22(4)	27(4)	13(3)	5(3)	2(3)	-5(3)
C(24)	21(4)	29(4)	18(4)	2(3)	4(3)	1(3)
C(25)	26(4)	24(4)	8(3)	-2(3)	5(3)	-7(3)
O(26)	25(3)	25(3)	18(3)	-9(2)	5(2)	-6(2)
C(27)	26(4)	23(4)	21(4)	-11(3)	11(3)	-6(3)
O(28)	29(3)	26(3)	25(3)	-9(2)	11(2)	-6(2)
C(29)	20(4)	27(4)	17(4)	-9(3)	3(3)	-6(3)
C(30)	26(4)	18(4)	24(4)	-5(3)	4(3)	-7(3)
C(31)	18(3)	15(4)	19(3)	-2(3)	3(3)	-6(3)
O(32)	20(2)	21(3)	21(3)	-1(2)	5(2)	-4(2)
C(33)	15(3)	18(4)	24(4)	-2(3)	2(3)	1(3)
O(34)	21(2)	20(3)	19(2)	-3(2)	6(2)	-1(2)
C(35)	18(3)	17(4)	18(3)	-7(3)	5(3)	1(3)
C(36)	25(4)	12(4)	15(3)	2(3)	7(3)	8(3)
C(37)	22(4)	15(4)	14(3)	-7(3)	3(3)	5(3)
O(38)	26(3)	24(3)	12(2)	-4(2)	0(2)	1(2)
C(39)	22(4)	18(4)	17(3)	-4(3)	-2(3)	4(3)
O(40)	26(3)	19(3)	16(2)	0(2)	-4(2)	-1(2)
C(41)	25(4)	19(4)	27(4)	-7(3)	-2(3)	5(3)
C(42)	30(4)	37(5)	30(4)	-8(4)	0(3)	9(4)
C(43)	30(4)	48(5)	36(5)	-5(4)	4(4)	16(4)
Br(44)	36(1)	129(1)	68(1)	22(1)	20(1)	35(1)
C(45)	29(4)	37(5)	49(5)	-9(4)	-4(4)	12(4)
C(46)	35(4)	27(4)	48(5)	5(4)	-9(4)	13(4)
O(47)	35(3)	53(4)	76(5)	30(4)	-8(3)	17(3)
C(48)	33(4)	30(5)	49(5)	16(4)	-8(4)	22(4)
C(49)	42(5)	30(5)	64(6)	12(5)	-19(5)	13(4)
C(50)	51(5)	34(5)	47(5)	5(4)	-18(4)	31(4)
O(51)	54(4)	58(4)	45(4)	-6(3)	-24(3)	31(3)
C(52)	48(5)	41(5)	37(5)	0(4)	-17(4)	15(4)
C(53)	68(6)	51(6)	27(5)	6(4)	-14(4)	13(5)
C(54)	63(6)	51(6)	14(4)	0(4)	-3(4)	3(5)
Br(55)	108(1)	118(1)	15(1)	-3(1)	-3(1)	17(1)
C(56)	42(5)	35(5)	21(4)	-2(3)	-3(3)	2(4)
C(57)	34(4)	20(4)	21(4)	0(3)	-6(3)	1(3)
C(58)	39(4)	31(4)	23(4)	2(3)	-8(3)	10(4)
C(59)	44(5)	34(5)	56(6)	11(4)	-11(4)	16(4)
C(60)	48(5)	25(5)	62(6)	5(4)	-13(5)	6(4)
C(61)	46(5)	27(5)	54(5)	10(4)	-7(4)	12(4)
C(62)	30(4)	18(4)	43(5)	2(4)	-2(4)	8(3)
6(3)	16(3)	18(4)	29(4)	-4(3)	0(3)	3(3)
C(64)	18(4)	19(4)	27(4)	-1(3)	0(3)	3(3)
C(65)	24(4)	23(4)	25(4)	8(3)	2(3)	2(3)
Br(66)	52(1)	27(1)	35(1)	8(1)	17(1)	1(1)

C(67)	27(4)	15(4)	34(4)	2(3)	3(3)	-1(3)
C(68)	32(4)	14(4)	45(5)	-11(3)	7(4)	0(3)
O(69)	38(3)	13(3)	87(5)	3(3)	18(3)	0(2)
C(70)	46(5)	11(4)	47(5)	1(3)	18(4)	18(3)
C(71)	51(5)	17(4)	55(5)	-1(4)	14(4)	8(4)
C(72)	62(6)	16(4)	56(5)	-3(4)	20(5)	14(4)
O(73)	96(5)	23(3)	66(4)	-9(3)	40(4)	13(3)
C(74)	64(6)	26(5)	48(5)	-7(4)	29(4)	-3(4)
C(75)	62(6)	36(5)	60(6)	-29(5)	30(5)	-7(5)
C(76)	55(5)	35(5)	44(5)	-27(4)	28(4)	-18(4)
Br(77)	111(1)	57(1)	70(1)	-38(1)	63(1)	-21(1)
C(78)	45(5)	30(5)	30(4)	-14(4)	12(4)	-14(4)
C(79)	31(4)	32(4)	27(4)	-12(3)	10(3)	-12(3)
C(80)	49(5)	27(5)	35(5)	-8(4)	18(4)	3(4)
C(81)	42(5)	24(5)	71(6)	3(4)	16(5)	15(4)
C(82)	32(5)	35(5)	64(6)	7(4)	1(4)	7(4)
C(83)	36(5)	27(5)	43(5)	0(4)	9(4)	10(4)
C(84)	24(4)	20(4)	33(4)	1(3)	5(3)	-1(3)
C(85)	45(6)	58(7)	53(6)	-1(5)	-10(5)	-2(5)
C(86)	113(10)	73(8)	138(11)	-20(8)	48(9)	-27(8)
C(87)	53(8)	48(9)	29(11)	3(7)	12(7)	8(7)
C(87A)	30(10)	29(10)	18(15)	-7(9)	14(8)	7(8)
C(88)	79(9)	66(8)	102(10)	-18(8)	-2(8)	-5(7)
C(89)	122(10)	121(10)	72(8)	11(8)	22(8)	52(9)
C(90)	103(19)	105(19)	55(19)	1(18)	1(18)	50(18)
C(91)	22(4)	18(4)	28(4)	0(3)	-3(3)	3(3)
C(92)	29(4)	23(4)	31(4)	-3(3)	-1(3)	10(3)
C(93)	28(4)	23(4)	37(4)	-5(3)	-1(3)	10(3)
C(94)	40(5)	29(5)	49(5)	-8(4)	-11(4)	14(4)
C(95)	59(6)	34(5)	61(6)	2(5)	-9(5)	19(5)
C(96)	49(5)	58(6)	51(6)	5(5)	-4(5)	30(5)
C(97)	33(5)	68(7)	41(5)	-5(5)	-2(4)	6(5)
C(98)	32(4)	33(5)	42(5)	-4(4)	4(4)	3(4)
C(99)	18(4)	20(4)	24(4)	-3(3)	-1(3)	2(3)
C(100)	16(4)	32(4)	27(4)	1(3)	-2(3)	-4(3)
C(101)	24(4)	36(5)	24(4)	3(3)	-2(3)	-1(3)
C(102)	33(5)	63(6)	52(5)	29(5)	11(4)	16(4)
C(103)	40(5)	84(8)	79(7)	20(6)	11(5)	30(5)
C(104)	56(6)	58(6)	65(6)	24(5)	-16(5)	11(5)
C(105)	54(6)	57(6)	41(5)	19(5)	-6(4)	-15(5)
C(10G)	36(5)	43(5)	36(5)	7(4)	5(4)	-8(4)
C(107)	23(4)	30(4)	19(4)	-1(3)	-1(3)	-4(3)
C(108)	27(4)	42(5)	19(4)	6(3)	-3(3)	-4(4)
C(109)	34(4)	31(4)	28(4)	9(3)	-6(3)	-15(4)
C(110)	38(5)	50(6)	57(6)	22(5)	-2(4)	-12(4)
C(111)	57(6)	50(6)	71(7)	35(5)	-13(5)	-14(5)

C(112)	62(6)	34(5)	77(7)	27(5)	-16(5)	-1(5)
C(113)	44(5)	37(5)	57(6)	3(5)	-11(4)	-1(4)
C(114)	43(5)	35(5)	33(4)	1(4)	-1(4)	-6(4)
C(115)	33(4)	23(4)	32(4)	7(3)	-7(3)	-9(3)
C(116)	50(5)	63(6)	44(5)	27(5)	-6(4)	-13(5)
C(117)	126(8)	40(5)	26(5)	12(4)	-28(5)	-22(6)
C(118)	164(11)	66(8)	51(7)	18(6)	-25(7)	-32(8)
C(119)	156(11)	66(8)	67(8)	4(7)	-3(8)	-13(8)
C(120)	110(10)	48(7)	99(9)	-4(7)	-32(8)	22(7)
C(121)	147(11)	113(10)	52(7)	-15(7)	7(8)	1(9)
C(122)	131(10)	86(8)	34(5)	12(6)	-9(6)	59(7)

Table 6.5 Hydrogen coordinates ($x10^4$) and isotropic displacement parameters ($Å^2 x10^3$) for **145**

	x	y	z	U(eq)
H(1)	-1405	-1468	3351	20
H(3)	-1314	-1502	2224	24
H(5)	-690	-709	3040	20
H(7)	-85	842	3045	22
H(9)	-584	104	3884	21
H(11)	-972	1086	4732	26
H(13)	-1299	-584	4178	22
H(15)	-2219	-1221	3890	25
H(18)	-2401	-441	2499	20
H(21)	-2381	474	3367	26
H(24)	-2187	1266	4271	27
H(27)	-1500	2101	3966	27
H(30)	-736	2675	3653	27
H(33)	-853	1957	2705	22
H(36)	-969	904	1879	20
H(39)	-1726	273	2142	23
H(42)	-3177	-34	3891	39
H(45)	-3880	1174	3065	47
H(49)	-3305	1054	1806	56
H(53)	-2578	893	577	60
H(56)	-1660	-223	1049	39
H(58)	-2338	653	1870	38
H(59)	-2385	2281	1669	55
H(60)	-2451	2856	2331	55
H(61)	-2927	2531	2733	51
H(62)	-2816	941	2840	37
H(64)	-240	2506	1973	26
H(67)	-457	4756	2018	31
H(71)	-1023	4980	3399	48
H(75)	-1846	5006	4515	61
H(78)	-1724	2870	4942	41
H(80)	-1416	3443	3776	43
H(81)	-2080	4268	3232	54
H(82)	-2009	3992	2506	53
H(83)	-1447	4161	2237	42
H(84)	-862	3331	2872	31
H(85)	502	7097	1322	64
H(86)	1938	8579	3748	127
H(87)	-1528	2902	903	51
H(87A)	-1479	2886	762	30
H(88)	-830	3586	4526	100
H(89)	-1990	1243	2731	125
H(90)	-1978	1674	3003	106

H(91A)	-1167	-2396	2789	28
H(91B)	-909	-1785	3047	28
H(92A)	-775	-2498	2251	34
H(92B)	-547	-1768	2421	34
H(94)	-671	-3704	2646	49
H(95)	-273	-4464	3086	63
H(96)	227	-3918	3492	64
H(97)	311	-2623	3485	57
H(98)	-86	-1870	3031	43
H(99A)	-233	-519	3487	25
H(99B)	45	-463	3124	25
H(10A)	442	303	3570	30
H(10B)	155	340	3925	30
H(10C)	868	-747	3583	59
H(10D)	1135	-1782	3948	81
H(10E)	847	-2361	4491	73
H(10F)	297	-1896	4672	61
H(10H)	34	-847	4331	45
H(10I)	-753	-390	4497	29
H(10J)	-488	189	4772	29
H(10K)	-898	190	5321	36
H(10L)	-1149	-413	5049	36
H(10M)	-1069	-1063	5765	58
H(10N)	-750	-1989	6177	73
H(10O)	-177	-2382	6003	71
H(10P)	93	-1783	5441	57
H(10Q)	-229	-869	5031	45
H(10R)	-1482	-1733	4071	36
H(10S)	-1821	-2274	3916	36
H(10T)	-1756	-1421	4704	63
H(10U)	-2108	-1920	4547	63
H(10U)	-2198	-2961	4849	116
H(10W)	-2011	-4031	5253	117
H(10X)	-1394	-4341	5271	106
H(10Y)	-922	-3486	5216	125
H(10Z)	-1142	-2176	4855	102

Table 6.6 Torsion angles [deg] for **145**

C(16)-C(1)-C(2)-C(17)	-1.7(10)
C(16)-C(1)-C(2)-C(3)	177.4(6)
C(1)-C(2)-C(3)-C(4)	-98.3(8)
C(17)-C(2)-C(3)-C(4)	80.8(8)
C(1)-C(2)-C(3)-C(91)	28.9(9)
C(17)-C(2)-C(3)-C(91)	-152.0(6)
C(2)-C(3)-C(4)-C(5)	93.2(7)
C(91)-C(3)-C(4)-C(5)	-33.3(9)
C(2)-C(3)-C(4)-C(37)	-84.0(8)
C(91)-C(3)-C(4)-C(37)	149.6(7)
C(37)-C(4)-C(5)-C(6)	-0.6(10)
C(3)-C(4)-C(5)-C(6)	-178.0(6)
C(4)-C(5)-C(6)-C(35)	1.5(10)
C(4)-C(5)-C(6)-C(7)	176.8(6)
C(5)-C(6)-C(7)-C(8)	-90.5(7)
C(35)-C(6)-C(7)-C(8)	84.5(8)
C(5)-C(6)-C(7)-C(99)	36.4(9)
C(35)-C(6)-C(7)-C(99)	-148.5(6)
C(6)-C(7)-C(8)-C(31)	-83.4(8)
C(99)-C(7)-C(8)-C(31)	151.1(6)
C(6)-C(7)-C(8)-C(9)	93.5(7)
C(99)-C(7)-C(8)-C(9)	-31.9(9)
C(31)-C(8)-C(9)-C(10)	-1.1(10)
C(21)-O(20)-C(20)-C(18)	-99.5(7)
C(21)-O(20)-C(20)-C(16)	84.4(8)
C(20)-O(20)-C(21)-O(22)	-95.7(7)
C(20)-O(20)-C(21)-C(41)	143.5(6)
O(20)-C(21)-O(22)-C(23)	94.4(7)
C(41)-C(21)-O(22)-C(23)	-146.4(6)
C(21)-O(22)-C(23)-C(24)	99.6(7)
C(21)-O(22)-C(23)-C(14)	-81.8(8)
C(13)-C(14)-C(23)-C(24)	-2.0(10)
C(15)-C(14)-C(23)-C(24)	-178.1(6)
C(13)-C(14)-C(23)-O(22)	179.5(6)
C(15)-C(14)-C(23)-O(22)	3.3(10)
O(22)-C(23)-C(24)-C(25)	-179.6(6)
C(14)-C(23)-C(24)-C(25)	1.8(10)
C(23)-C(24)-C(25)-C(12)	-0.9(10)
C(23)-C(24)-C(25)-O(26)	-179.7(6)
C(13)-C(12)-C(25)-C(24)	0.1(10)
C(11)-C(12)-C(25)-C(24)	177.9(6)
C(13)-C(12)-C(25)-O(26)	178.9(6)
C(11)-C(12)-C(25)-O(26)	-3.3(10)
C(24)-C(25)-O(26)-C(27)	-100.0(7)
C(12)-C(25)-O(26)-C(27)	81.2(8)

C(25)-O(26)-C(27)-O(28)	-96.1(7)
C(25)-O(26)-C(27)-C(79)	144.8(6)
O(26)-C(27)-O(28)-C(29)	95.1(7)
C(79)-C(27)-O(28)-C(29)	-143.8(6)
C(9)-C(10)-C(29)-C(30)	0.2(10)
C(11)-C(10)-C(29)-C(30)	-179.7(6)
C(9)-C(10)-C(29)-O(28)	-177.2(6)
C(11)-C(10)-C(29)-O(28)	2.9(10)
C(27)-O(28)-C(29)-C(30)	102.8(7)
C(27)-O(28)-C(29)-C(10)	-79.6(8)
C(10)-C(29)-C(30)-C(31)	1.0(11)
O(28)-C(29)-C(30)-C(31)	178.5(6)
C(29)-C(30)-C(31)-C(8)	-2.3(10)
C(29)-C(30)-C(31)-O(32)	-179.3(6)
C(9)-C(8)-C(31)-C(30)	2.3(10)
C(7)-C(8)-C(31)-C(30)	179.4(6)
C(9)-C(8)-C(31)-O(32)	179.2(6)
C(7)-C(8)-C(31)-O(32)	-3.7(10)
C(30)-C(31)-O(32)-C(33)	-99.5(7)
C(8)-C(31)-O(32)-C(33)	83.4(8)
C(31)-O(32)-C(33)-O(34)	-96.2(6)
C(31)-O(32)-C(33)-6(3)	142.4(6)
O(32)-C(33)-O(34)-C(35)	92.2(6)
6(3)-C(33)-O(34)-C(35)	-149.0(6)
C(5)-C(6)-C(35)-C(36)	-2.1(10)
C(7)-C(6)-C(35)-C(36)	-177.4(6)
C(5)-C(6)-C(35)-O(34)	179.2(6)
C(7)-C(6)-C(35)-O(34)	3.9(10)
C(33)-O(34)-C(35)-C(36)	101.1(7)
C(33)-O(34)-C(35)-C(6)	-80.2(7)
C(6)-C(35)-C(36)-C(37)	1.9(10)
O(34)-C(35)-C(36)-C(37)	-179.3(6)
C(35)-C(36)-C(37)-C(4)	-1.0(10)
C(35)-C(36)-C(37)-O(38)	179.0(6)
C(5)-C(4)-C(37)-C(36)	0.3(10)
C(3)-C(4)-C(37)-C(36)	177.6(6)
C(5)-C(4)-C(37)-O(38)	-179.7(6)
C(3)-C(4)-C(37)-O(38)	-2.4(10)
C(36)-C(37)-O(38)-C(39)	-101.4(7)
C(4)-C(37)-O(38)-C(39)	78.6(8)
C(37)-O(38)-C(39)-O(40)	-95.3(6)
C(37)-O(38)-C(39)-C(57)	145.3(6)
C(18)-C(17)-O(40)-C(39)	97.1(7)
C(2)-C(17)-O(40)-C(39)	-84.3(8)
O(38)-C(39)-O(40)-C(17)	99.7(6)
C(57)-C(39)-O(40)-C(17)	-140.2(6)

O(22)-C(21)-C(41)-C(62)	150.3(7)
O(20)-C(21)-C(41)-C(62)	-88.3(8)
O(22)-C(21)-C(41)-C(42)	-32.9(9)
O(20)-C(21)-C(41)-C(42)	88.5(8)
C(62)-C(41)-C(42)-C(43)	-1.2(12)
C(21)-C(41)-C(42)-C(43)	-177.9(7)
C(41)-C(42)-C(43)-C(45)	0.1(13)
C(41)-C(42)-C(43)-Br(44)	-179.7(6)
C(42)-C(43)-C(45)-C(46)	0.9(14)
Br(44)-C(43)-C(45)-C(46)	-179.3(7)
C(43)-C(45)-C(46)-C(62)	-0.8(13)
C(43)-C(45)-C(46)-O(47)	179.4(8)
C(62)-C(46)-O(47)-C(48)	-6.8(13)
C(45)-C(46)-O(47)-C(48)	173.0(8)
C(46)-O(47)-C(48)-C(49)	107.6(9)
C(46)-O(47)-C(48)-C(61)	-70.8(10)
C(61)-C(48)-C(49)-C(50)	-1.0(12)
O(47)-C(48)-C(49)-C(50)	-179.3(7)
C(48)-C(49)-C(50)-C(59)	0.8(12)
C(48)-C(49)-C(50)-O(51)	-178.3(7)
C(59)-C(50)-O(51)-C(52)	62.0(11)
C(49)-C(50)-O(51)-C(52)	-118.8(9)
C(50)-O(51)-C(52)-C(53)	-160.0(9)
C(50)-O(51)-C(52)-C(58)	19.9(14)
C(58)-C(52)-C(53)-C(54)	-1.1(15)
O(51)-C(52)-C(53)-C(54)	178.8(9)
C(52)-C(53)-C(54)-C(56)	-1.0(16)
C(52)-C(53)-C(54)-Br(55)	-179.9(8)
C(53)-C(54)-C(56)-C(57)	2.2(15)
Br(55)-C(54)-C(56)-C(57)	-178.9(6)
C(54)-C(56)-C(57)-C(58)	-1.3(13)
C(54)-C(56)-C(57)-C(39)	178.1(8)
O(38)-C(39)-C(57)-C(56)	22.3(10)
O(40)-C(39)-C(57)-C(56)	-98.8(8)
O(38)-C(39)-C(57)-C(58)	-158.3(7)
O(40)-C(39)-C(57)-C(58)	80.6(8)
C(56)-C(57)-C(58)-C(52)	-0.8(13)
C(39)-C(57)-C(58)-C(52)	179.8(8)
C(53)-C(52)-C(58)-C(57)	2.0(14)
O(51)-C(52)-C(58)-C(57)	-177.9(8)
O(51)-C(50)-C(59)-C(60)	178.4(7)
C(49)-C(50)-C(59)-C(60)	-0.7(12)
C(50)-C(59)-C(60)-C(61)	0.7(13)
C(49)-C(48)-C(61)-C(60)	1.0(12)
O(47)-C(48)-C(61)-C(60)	179.3(7)
C(59)-C(60)-C(61)-C(48)	-0.9(13)

C(42)-C(41)-C(62)-C(46)	1.3(12)
C(21)-C(41)-C(62)-C(46)	178.1(7)
C(45)-C(46)-C(62)-C(41)	-0.3(13)
O(47)-C(46)-C(62)-C(41)	179.5(8)
O(34)-C(33)-6(3)-C(64)	-12.8(9)
O(32)-C(33)-6(3)-C(64)	109.0(7)
O(34)-C(33)-6(3)-C(84)	169.3(6)
O(32)-C(33)-6(3)-C(84)	-68.9(8)
C(84)-6(3)-C(64)-C(65)	1.8(10)
C(33)-6(3)-C(64)-C(65)	-176.0(6)
6(3)-C(64)-C(65)-C(67)	-1.6(11)
6(3)-C(64)-C(65)-Br(66)	179.1(5)
C(64)-C(65)-C(67)-C(68)	-0.3(11)
Br(66)-C(65)-C(67)-C(68)	179.0(6)
C(65)-C(67)-C(68)-C(84)	2.1(12)
C(65)-C(67)-C(68)-O(69)	179.1(7)
C(84)-C(68)-O(69)-C(70)	-36.6(11)
C(67)-C(68)-O(69)-C(70)	146.4(8)
C(68)-O(69)-C(70)-C(71)	123.7(8)
C(68)-O(69)-C(70)-C(83)	-54.6(10)
O(69)-C(70)-C(71)-C(72)	179.4(7)
C(83)-C(70)-C(71)-C(72)	-2.2(12)
C(70)-C(71)-C(72)-C(81)	1.1(13)
C(70)-C(71)-C(72)-O(73)	-175.7(7)
C(81)-C(72)-O(73)-C(74)	72.6(11)
C(71)-C(72)-O(73)-C(74)	-110.6(10)
C(72)-O(73)-C(74)-C(80)	19.9(14)
C(72)-O(73)-C(74)-C(75)	-160.6(9)
C(80)-C(74)-C(75)-C(76)	-0.1(15)
O(73)-C(74)-C(75)-C(76)	-179.6(9)
C(74)-C(75)-C(76)-C(78)	-0.4(16)
C(74)-C(75)-C(76)-Br(77)	-177.3(8)
C(75)-C(76)-C(78)-C(79)	1.3(14)
Br(77)-C(76)-C(78)-C(79)	178.2(6)
C(76)-C(78)-C(79)-C(80)	-1.6(13)
C(76)-C(78)-C(79)-C(27)	178.7(8)
O(26)-C(27)-C(79)-C(78)	16.3(10)
O(28)-C(27)-C(79)-C(78)	-106.0(8)
O(26)-C(27)-C(79)-C(80)	-163.4(7)
O(28)-C(27)-C(79)-C(80)	74.3(9)
C(75)-C(74)-C(80)-C(79)	-0.2(15)
O(73)-C(74)-C(80)-C(79)	179.2(9)
C(78)-C(79)-C(80)-C(74)	1.1(13)
C(27)-C(79)-C(80)-C(74)	-179.1(8)
C(71)-C(72)-C(81)-C(82)	-0.7(13)
O(73)-C(72)-C(81)-C(82)	176.0(8)

C(72)-C(81)-C(82)-C(83)	1.5(13)
C(81)-C(82)-C(83)-C(70)	-2.7(13)
O(69)-C(70)-C(83)-C(82)	-178.6(7)
C(71)-C(70)-C(83)-C(82)	3.0(12)
C(67)-C(68)-C(84)-6(3)	-1.9(12)
O(69)-C(68)-C(84)-6(3)	-178.8(7)
C(64)-6(3)-C(84)-C(68)	-0.1(11)
C(33)-6(3)-C(84)-C(68)	177.9(7)
C(4)-C(3)-C(91)-C(92)	-63.1(8)
C(2)-C(3)-C(91)-C(92)	172.6(6)
C(3)-C(91)-C(92)-C(93)	167.3(6)
C(91)-C(92)-C(93)-C(98)	-91.1(9)
C(91)-C(92)-C(93)-C(94)	87.3(9)
C(98)-C(93)-C(94)-C(95)	-0.6(14)
C(92)-C(93)-C(94)-C(95)	-179.0(9)
C(93)-C(94)-C(95)-C(96)	-0.1(15)
C(94)-C(95)-C(96)-C(97)	1.5(16)
C(95)-C(96)-C(97)-C(98)	-2.1(15)
C(94)-C(93)-C(98)-C(97)	-0.1(13)
C(92)-C(93)-C(98)-C(97)	178.4(8)
C(96)-C(97)-C(98)-C(93)	1.4(14)
C(6)-C(7)-C(99)-C(100)	174.5(6)
C(8)-C(7)-C(99)-C(100)	-62.9(8)
C(7)-C(99)-C(100)-C(101)	173.9(6)
C(99)-C(100)-C(101)-C(102)	99.7(9)
C(99)-C(100)-C(101)-C(10G)	-80.2(9)
C(10G)-C(101)-C(102)-C(103)	-1.8(15)
C(100)-C(101)-C(102)-C(103)	178.4(10)
C(101)-C(102)-C(103)-C(104)	1.6(18)
C(102)-C(103)-C(104)-C(105)	-0.3(19)
C(103)-C(104)-C(105)-C(10G)	-0.8(17)
C(104)-C(105)-C(10G)-C(101)	0.6(15)
C(102)-C(101)-C(10G)-C(105)	0.7(13)
C(100)-C(101)-C(10G)-C(105)	-179.4(8)
C(10)-C(11)-C(107)-C(108)	173.0(6)
C(12)-C(11)-C(107)-C(108)	-62.5(8)
C(11)-C(107)-C(108)-C(109)	-177.6(6)
C(107)-C(108)-C(109)-C(114)	12.7(12)
C(107)-C(108)-C(109)-C(110)	-170.7(8)
C(114)-C(109)-C(110)-C(111)	0.1(14)
C(108)-C(109)-C(110)-C(111)	-176.8(9)
C(109)-C(110)-C(111)-C(112)	-0.9(16)
C(110)-C(111)-C(112)-C(113)	2.0(17)
C(111)-C(112)-C(113)-C(114)	-2.2(16)
C(112)-C(113)-C(114)-C(109)	1.4(14)
C(110)-C(109)-C(114)-C(113)	-0.3(13)

C(108)-C(109)-C(114)-C(113)	176.4(8)
C(16)-C(15)-C(115)-C(116)	-173.0(7)
C(14)-C(15)-C(115)-C(116)	63.4(9)
C(15)-C(115)-C(116)-C(117)	176.8(8)
C(115)-C(116)-C(117)-C(122)	69.6(13)
C(115)-C(116)-C(117)-C(118)	-116.8(11)
C(122)-C(117)-C(118)-C(119)	-7(2)
C(116)-C(117)-C(118)-C(119)	179.3(12)
C(117)-C(118)-C(119)-C(120)	-6(2)
C(118)-C(119)-C(120)-C(121)	16(2)
C(119)-C(120)-C(121)-C(122)	-11(2)
C(118)-C(117)-C(122)-C(121)	11.8(18)
C(116)-C(117)-C(122)-C(121)	-175.5(10)
C(120)-C(121)-C(122)-C(117)	-3.4(16)

6.7 Crystal structure of 149

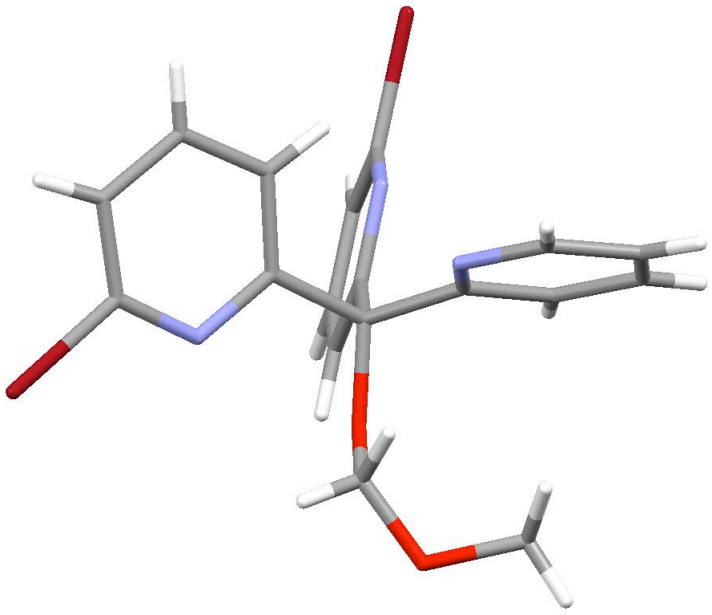

Figure 6.32 Crystal structure of **149**. Image generated by Mercury.[204]

The crystal was grown by dissolving **149** in acetone. The crystal structure of **149** was determined by x-ray diffraction by Dr. Edwin Stevens at the University of New Orleans. Data was collected at 113 K on Bruker SMART 1K CCD and a graphite monochronator utilizing MoK_{α} radiation (λ = 0.71073 Å). Cell parameters were refined using up to 8773 reflection. The structure was solved by the direct methods in SHELXTL and refined using full-matrix least squares.

Table 6.7. Crystal data and structure refinement for **149**.

Empirical formula	$C_{18}H_{15}Br_2N_3O_2$
Formula weight	465.15
Temperature	150(2)K
Wavelength	0.71073Å
Crystal system, space group	Triclinic, P-1
Unit cell dimensions	a = 9.3194(5)Å alpha = 69.432(1) deg. b = 13.9682(8)Å beta = 72.337(1) deg. c = 15.1140(8)Å gamma = 87.366(1) deg.
Volume	1751.16(17) $Å^3$
Z, Calculated density	4, 1.764 Mg/m^3
Absorption coefficient	4.646 mm^{-1}
F(000)	920
Crystal size	0.3 x 0.4 x 0.5 mm
Theta range for data collection	1.56 to 27.50 deg.
Limiting indices	$-12 \le h \le 12$, $-18 \le k \le 18$, $-19 \le l \le 19$
Reflections collected / unique	38022 / 8034 [R(int) = 0.0477]
Completeness to theta = 27.50	100.0 %
Absorption correction	Empirical
Max. and min. transmission	0.862545 and 0.650141
Refinement method	Full-matrix least-squares on F^2
Data / restraints / parameters	8034 / 428 / 571
Goodness-of-fit on F^2	1.015
Final R indices [I>2sigma(I)]	R1 = 0.0330, wR2 = 0.0799
R indices (all data)	R1 = 0.0446, wR2 = 0.0830
Largest diff. peak and hole	0.573 and -0.718 $e.Å^{-3}$

Table 6.8 Atomic coordinates ($x10^4$) and equivalent isotropic displacement parameters ($Å^2$ $x10^3$) for **149**. U(eq) is defined as one third of the trace of the orthogonalized Fuji tensor.

	x	y	z	U(eq)
Br(1)	7499(1)	4281(1)	3358(1)	24(1)
C(1)	2869(3)	5360(2)	2147(2)	15(1)
O(2)	2550(2)	5941(1)	1257(1)	17(1)
C(3)	1057(3)	6245(2)	1351(2)	21(1)
O(4)	910(2)	7240(2)	1340(1)	25(1)
C(5)	1687(4)	7987(2)	408(3)	34(1)
C(6)	4568(3)	5238(2)	1825(2)	14(1)
N(7)	5184(2)	4886(2)	2562(2)	16(1)
C(8)	6636(3)	4761(2)	2306(2)	17(1)
C(9)	7573(3)	4953(2)	1349(2)	19(1)
C(10)	6912(3)	5309(2)	602(2)	21(1)
C(11)	5383(3)	5459(2)	846(2)	18(1)
C(12)	2071(3)	4282(2)	2593(2)	14(1)
N(13)	1439(2)	4018(2)	2023(2)	16(1)
Br(14)	-80(1)	2731(1)	1540(1)	31(1)
C(14)	800(3)	3084(2)	2376(2)	18(1)
C(15)	716(3)	2350(2)	3286(2)	23(1)
C(16)	1391(3)	2627(2)	3861(2)	23(1)
C(17)	2082(3)	3599(2)	3514(2)	19(1)
C(18)	2514(3)	5954(2)	2862(2)	16(1)
N(19)	1521(3)	5548(2)	3749(2)	21(1)
C(20)	1260(3)	6091(2)	4356(2)	24(1)
C(21)	1943(3)	7033(2)	4099(2)	24(1)
C(22)	2951(3)	7461(2)	3158(2)	26(1)
C(23)	3240(3)	6921(2)	2528(2)	22(1)
C(51)	-1982(3)	9503(2)	2522(2)	14(1)
O(52)	-2031(2)	9538(1)	1580(1)	16(1)
C(53)	-3455(3)	9309(2)	1517(2)	19(1)
O(54)	-3295(2)	8692(2)	953(2)	29(1)
C(55)	-2834(4)	7695(3)	1395(3)	38(1)
C(56)	-328(3)	9775(2)	2365(2)	15(1)
N(57)	19(2)	9629(2)	3197(2)	16(1)
Br(58)	1904(1)	9646(1)	4276(1)	27(1)
C(58)	1422(3)	9868(2)	3091(2)	18(1)
C(59)	2560(3)	10257(2)	2205(2)	24(1)
C(60)	2183(3)	10406(2)	1359(2)	26(1)
C(61)	711(3)	10170(2)	1431(2)	21(1)
C(62)	-2934(3)	10318(2)	2855(2)	15(1)
N(63)	-3481(2)	10999(2)	2186(2)	16(1)
Br(64)	-5054(1)	12652(1)	1496(1)	30(1)
C(64)	-4248(3)	11717(2)	2450(2)	18(1)

C(65)	-4533(3)	11837(2)	3353(2)	23(1)
C(66)	-3970(3)	11125(2)	4040(2)	24(1)
C(67)	-3155(3)	10351(2)	3792(2)	21(1)
C(68)	-2478(3)	8425(2)	3281(2)	15(1)
N(69)	-3901(2)	8269(2)	3870(2)	20(1)
C(70)	-4392(3)	7309(2)	4464(2)	25(1)
C(71)	-3548(4)	6477(2)	4494(2)	27(1)
C(72)	-2065(3)	6652(2)	3881(2)	27(1)
C(73)	-1518(3)	7641(2)	3264(2)	20(1)

Table 6.9 Bond lengths [Å] and angles [deg] for **149**.

Br(1)-C(8)	1.898(3)
C(1)-O(2)	1.418(3)
C(1)-C(6)	1.529(3)
C(1)-C(18)	1.535(3)
C(1)-C(12)	1.536(3)
O(2)-C(3)	1.416(3)
C(3)-O(4)	1.385(3)
O(4)-C(5)	1.420(4)
C(6)-N(7)	1.338(3)
C(6)-C(11)	1.371(3)
N(7)-C(8)	1.312(3)
C(8)-C(9)	1.382(4)
C(9)-C(10)	1.378(4)
C(10)-C(11)	1.385(4)
C(12)-N(13)	1.333(3)
C(12)-C(17)	1.385(4)
N(13)-C(14)	1.316(3)
Br(14)-C(14)	1.901(3)
C(14)-C(15)	1.379(4)
C(15)-C(16)	1.376(4)
C(16)-C(17)	1.381(4)
C(18)-N(19)	1.318(3)
C(18)-C(23)	1.392(4)
N(19)-C(20)	1.346(4)
C(20)-C(21)	1.363(4)
C(21)-C(22)	1.381(4)
C(22)-C(23)	1.369(4)
C(51)-O(52)	1.422(3)
C(51)-C(68)	1.525(3)
C(51)-C(56)	1.532(3)
C(51)-C(62)	1.541(3)
O(52)-C(53)	1.417(3)
C(53)-O(54)	1.386(3)
O(54)-C(55)	1.427(4)
C(56)-N(57)	1.336(3)
C(56)-C(61)	1.381(4)
N(57)-C(58)	1.313(3)
Br(58)-C(58)	1.896(3)
C(58)-C(59)	1.375(4)
C(59)-C(60)	1.371(4)
C(60)-C(61)	1.389(4)
C(62)-N(63)	1.333(3)
C(62)-C(67)	1.386(4)

N(63)-C(64)	1.312(3)
Br(64)-C(64)	1.896(3)
C(64)-C(65)	1.378(4)
C(65)-C(66)	1.377(4)
C(66)-C(67)	1.386(4)
C(68)-N(69)	1.331(3)
C(68)-C(73)	1.385(4)
N(69)-C(70)	1.333(4)
C(70)-C(71)	1.368(4)
C(71)-C(72)	1.386(4)
C(72)-C(73)	1.381(4)

O(2)-C(1)-C(6)	104.80(19)
O(2)-C(1)-C(18)	110.17(19)
C(6)-C(1)-C(18)	109.1(2)
O(2)-C(1)-C(12)	110.7(2)
C(6)-C(1)-C(12)	107.40(19)
C(18)-C(1)-C(12)	114.2(2)
C(3)-O(2)-C(1)	116.83(19)
O(4)-C(3)-O(2)	112.6(2)
C(3)-O(4)-C(5)	113.2(2)
N(7)-C(6)-C(11)	122.9(2)
N(7)-C(6)-C(1)	115.4(2)
C(11)-C(6)-C(1)	121.6(2)
C(8)-N(7)-C(6)	116.6(2)
N(7)-C(8)-C(9)	125.8(2)
N(7)-C(8)-Br(1)	116.07(19)
C(9)-C(8)-Br(1)	118.14(19)
C(10)-C(9)-C(8)	116.6(2)
C(9)-C(10)-C(11)	119.1(2)
C(6)-C(11)-C(10)	119.0(2)
N(13)-C(12)-C(17)	121.7(2)
N(13)-C(12)-C(1)	116.3(2)
C(17)-C(12)-C(1)	121.9(2)
C(14)-N(13)-C(12)	117.3(2)
N(13)-C(14)-C(15)	126.0(3)
N(13)-C(14)-Br(14)	116.13(19)
C(15)-C(14)-Br(14)	117.8(2)
C(14)-C(15)-C(16)	116.1(2)
C(15)-C(16)-C(17)	119.6(3)
C(12)-C(17)-C(16)	119.3(3)
N(19)-C(18)-C(23)	122.7(2)
N(19)-C(18)-C(1)	119.5(2)
C(23)-C(18)-C(1)	117.8(2)
C(18)-N(19)-C(20)	117.5(2)
N(19)-C(20)-C(21)	123.8(3)

C(20)-C(21)-C(22)	118.1(3)
C(23)-C(22)-C(21)	119.2(3)
C(22)-C(23)-C(18)	118.8(3)
O(52)-C(51)-C(68)	109.56(19)
O(52)-C(51)-C(56)	105.13(19)
C(68)-C(51)-C(56)	110.65(19)
O(52)-C(51)-C(62)	111.66(19)
C(68)-C(51)-C(62)	111.9(2)
C(56)-C(51)-C(62)	107.70(19)
C(53)-O(52)-C(51)	116.87(19)
O(54)-C(53)-O(52)	110.0(2)
C(53)-O(54)-C(55)	114.0(2)
N(57)-C(56)-C(61)	122.8(2)
N(57)-C(56)-C(51)	114.9(2)
C(61)-C(56)-C(51)	122.2(2)
C(58)-N(57)-C(56)	116.7(2)
N(57)-C(58)-C(59)	126.0(2)
N(57)-C(58)-Br(58)	116.27(19)
C(59)-C(58)-Br(58)	117.7(2)
C(60)-C(59)-C(58)	116.5(3)
C(59)-C(60)-C(61)	119.7(3)
C(56)-C(61)-C(60)	118.3(3)
N(63)-C(62)-C(67)	122.5(2)
N(63)-C(62)-C(51)	116.6(2)
C(67)-C(62)-C(51)	120.9(2)
C(64)-N(63)-C(62)	117.0(2)
N(63)-C(64)-C(65)	126.0(2)
N(63)-C(64)-Br(64)	116.03(19)
C(65)-C(64)-Br(64)	118.0(2)
C(66)-C(65)-C(64)	116.4(2)
C(65)-C(66)-C(67)	119.5(3)
C(62)-C(67)-C(66)	118.6(3)
N(69)-C(68)-C(73)	122.9(2)
N(69)-C(68)-C(51)	116.8(2)
C(73)-C(68)-C(51)	120.0(2)
C(68)-N(69)-C(70)	117.3(2)
N(69)-C(70)-C(71)	124.6(3)
C(70)-C(71)-C(72)	117.5(3)
C(73)-C(72)-C(71)	119.2(3)
C(72)-C(73)-C(68)	118.5(3)

Table 6.10 Anisotropic displacement parameters ($Å^2$ x10^3) for **149**. The anisotropic displacement factor exponent takes the form: $-2pi^2[h^2 a^{*2} U11 + ... + 2hka^*b^*U12]$

	U11	U22	U33	U23	U13	U12
Br(1)	17(1)	31(1)	22(1)	-5(1)	-8(1)	1(1)
C(1)	13(1)	13(1)	14(1)	-3(1)	-2(1)	1(1)
O(2)	15(1)	17(1)	15(1)	-2(1)	-5(1)	2(1)
C(3)	17(1)	20(1)	22(1)	-2(1)	-7(1)	0(1)
O(4)	25(1)	25(1)	24(1)	-8(1)	-7(1)	10(1)
C(5)	41(2)	20(2)	33(2)	-5(1)	-7(2)	5(1)
C(6)	14(1)	11(1)	16(1)	-5(1)	-4(1)	0(1)
N(7)	16(1)	17(1)	14(1)	-5(1)	-2(1)	1(1)
C(8)	19(1)	14(1)	18(1)	-4(1)	-6(1)	-1(1)
C(9)	13(1)	18(1)	24(1)	-8(1)	0(1)	2(1)
C(10)	21(1)	23(1)	15(1)	-7(1)	3(1)	-1(1)
C(11)	20(1)	17(1)	14(1)	-4(1)	-6(1)	2(1)
C(12)	12(1)	13(1)	15(1)	-6(1)	-1(1)	2(1)
N(13)	16(1)	15(1)	16(1)	-6(1)	-4(1)	2(1)
Br(14)	37(1)	25(1)	42(1)	-17(1)	-20(1)	-1(1)
C(14)	16(1)	17(1)	24(1)	-10(1)	-5(1)	3(1)
C(15)	22(1)	13(1)	29(1)	-6(1)	-1(1)	-1(1)
C(16)	29(1)	16(1)	16(1)	-1(1)	-2(1)	5(1)
C(17)	21(1)	18(1)	17(1)	-6(1)	-4(1)	4(1)
C(18)	13(1)	18(1)	19(1)	-8(1)	-5(1)	4(1)
N(19)	24(1)	21(1)	17(1)	-9(1)	-2(1)	1(1)
C(20)	25(1)	27(1)	17(1)	-10(1)	-1(1)	2(1)
C(21)	23(1)	26(1)	29(1)	-17(1)	-8(1)	6(1)
C(22)	24(1)	19(1)	36(2)	-13(1)	-7(1)	-1(1)
C(23)	18(1)	22(1)	23(1)	-10(1)	-2(1)	0(1)
C(51)	16(1)	18(1)	11(1)	-7(1)	-6(1)	3(1)
O(52)	17(1)	22(1)	11(1)	-7(1)	-5(1)	2(1)
C(53)	21(1)	22(1)	18(1)	-9(1)	-10(1)	5(1)
O(54)	35(1)	33(1)	28(1)	-18(1)	-18(1)	8(1)
C(55)	38(2)	34(2)	65(3)	-30(2)	-33(2)	12(1)
C(56)	17(1)	13(1)	18(1)	-8(1)	-6(1)	3(1)
N(57)	17(1)	16(1)	17(1)	-9(1)	-6(1)	2(1)
Br(58)	28(1)	32(1)	29(1)	-15(1)	-17(1)	5(1)
C(58)	20(1)	17(1)	23(1)	-11(1)	-9(1)	5(1)
C(59)	14(1)	25(1)	32(2)	-13(1)	-6(1)	0(1)
C(60)	20(1)	29(2)	23(1)	-9(1)	3(1)	-3(1)
C(61)	22(1)	21(1)	18(1)	-7(1)	-5(1)	2(1)
C(62)	15(1)	16(1)	18(1)	-8(1)	-6(1)	2(1)
N(63)	15(1)	14(1)	17(1)	-4(1)	-3(1)	0(1)
Br(64)	39(1)	21(1)	27(1)	-3(1)	-13(1)	13(1)
C(64)	19(1)	14(1)	21(1)	-3(1)	-7(1)	1(1)

C(65)	23(1)	23(1)	30(1)	-16(1)	-9(1)	8(1)
C(66)	26(1)	33(2)	23(1)	-19(1)	-11(1)	11(1)
C(67)	19(1)	30(1)	19(1)	-14(1)	-8(1)	9(1)
C(68)	16(1)	17(1)	13(1)	-5(1)	-6(1)	1(1)
N(69)	18(1)	23(1)	17(1)	-7(1)	-3(1)	0(1)
C(70)	20(1)	31(2)	21(1)	-7(1)	-3(1)	-6(1)
C(71)	36(2)	19(1)	23(1)	1(1)	-12(1)	-7(1)
C(72)	32(2)	19(1)	33(2)	-9(1)	-17(1)	8(1)
C(73)	19(1)	19(1)	22(1)	-7(1)	-7(1)	3(1)

Table 6.11 Hydrogen coordinates ($x10^4$) and isotropic displacement parameters ($Å^2$ $x10^3$) for **149**.

	x	y	z	U(eq)
H(3A)	900(30)	6210(20)	740(20)	20(7)
H(3B)	420(30)	5850(20)	2000(20)	22(8)
H(5A)	2810(40)	7920(30)	320(30)	39(10)
H(5B)	1400(50)	8660(30)	460(30)	59(12)
H(5C)	1610(50)	7880(30)	-110(40)	63(14)
H(9)	8600(30)	4820(20)	1256(19)	9(6)
H(10)	7410(30)	5400(20)	-50(20)	25(8)
H(11)	4980(40)	5750(20)	390(20)	26(8)
H(15)	250(30)	1700(20)	3510(20)	17(7)
H(16)	1400(30)	2170(20)	4480(20)	25(8)
H(17)	2560(30)	3770(20)	3930(20)	23(8)
H(20)	590(40)	5790(30)	4980(30)	31(9)
H(21)	1700(30)	7370(20)	4590(20)	25(8)
H(22)	3380(40)	8090(30)	2990(30)	37(10)
H(23)	3960(30)	7220(20)	1870(20)	17(7)
H(53A)	4080(30)	8950(20)	2180(20)	17(7)
H(53B)	-3730(30)	9860(20)	1198(19)	3(6)
H(55C)	1970(40)	7710(30)	1470(30)	33(9)
H(55A)	-3610(40)	7410(30)	2120(30)	42(10)
H(55B)	2850(40)	7290(30)	1010(30)	30(9)
H(9)	3500(40)	10400(20)	2190(20)	21(8)
H(72)	2900(40)	10660(20)	730(20)	23(8)
H(61)	420(30)	10260(20)	890(20)	15(7)
H(65)	-5050(30)	12410(20)	3430(20)	24(8)
H(66)	-4120(40)	11160(30)	4640(30)	32(9)
H(67)	-2790(40)	9840(30)	4260(30)	34(9)
H(70)	-5390(40)	7180(30)	4890(30)	31(9)
H(71)	-4000(30)	5810(20)	4910(20)	20(7)
H(72)	-1460(40)	6150(30)	3870(20)	27(8)
H(73)	-600(30)	7810(20)	2860(20)	15(7)

Table 6.12 Torsion angles [deg] for **149**.

C(6)-C(1)-O(2)-C(3)	-174.76(19)
C(18)-C(1)-O(2)-C(3)	-57.6(3)
C(12)-C(1)-O(2)-C(3)	69.7(3)
C(1)-O(2)-C(3)-O(4)	97.9(3)
O(2)-C(3)-O(4)-C(5)	67.5(3)
O(2)-C(1)-C(6)-N(7)	167.5(2)
C(18)-C(1)-C(6)-N(7)	49.5(3)
C(12)-C(1)-C(6)-N(7)	-74.7(3)
O(2)-C(1)-C(6)-C(11)	-13.7(3)
C(18)-C(1)-C(6)-C(11)	-131.7(2)
C(12)-C(1)-C(6)-C(11)	104.1(3)
C(11)-C(6)-N(7)-C(8)	0.2(4)
C(1)-C(6)-N(7)-C(8)	179.0(2)
C(6)-N(7)-C(8)-C(9)	-0.4(4)
C(6)-N(7)-C(8)-Br(1)	179.05(17)
N(7)-C(8)-C(9)-C(10)	0.1(4)
Br(1)-C(8)-C(9)-C(10)	-179.42(19)
C(8)-C(9)-C(10)-C(11)	0.5(4)
N(7)-C(6)-C(11)-C(10)	0.3(4)
C(1)-C(6)-C(11)-C(10)	-178.4(2)
C(9)-C(10)-C(11)-C(6)	-0.7(4)
O(2)-C(1)-C(12)-N(13)	10.1(3)
C(6)-C(1)-C(12)-N(13)	-103.8(2)
C(18)-C(1)-C(12)-N(13)	135.2(2)
O(2)-C(1)-C(12)-C(17)	-173.5(2)
C(6)-C(1)-C(12)-C(17)	72.6(3)
C(18)-C(1)-C(12)-C(17)	-48.5(3)
C(17)-C(12)-N(13)-C(14)	1.1(3)
C(1)-C(12)-N(13)-C(14)	177.5(2)
C(12)-N(13)-C(14)-C(15)	0.3(4)
C(12)-N(13)-C(14)-Br(14)	-179.69(17)
N(13)-C(14)-C(15)-C(16)	-1.2(4)
Br(14)-C(14)-C(15)-C(16)	178.79(19)
C(14)-C(15)-C(16)-C(17)	0.7(4)
N(13)-C(12)-C(17)-C(16)	-1.5(4)
C(1)-C(12)-C(17)-C(16)	-177.7(2)
C(15)-C(16)-C(17)-C(12)	0.5(4)
O(2)-C(1)-C(18)-N(19)	121.2(2)
C(6)-C(1)-C(18)-N(19)	-124.3(2)
C(12)-C(1)-C(18)-N(19)	-4.2(3)
O(2)-C(1)-C(18)-C(23)	-57.2(3)
C(6)-C(1)-C(18)-C(23)	57.3(3)

C(12)-C(1)-C(18)-C(23)	177.4(2)
C(23)-C(18)-N(19)-C(20)	-2.5(4)
C(1)-C(18)-N(19)-C(20)	179.1(2)
C(18)-N(19)-C(20)-C(21)	1.1(4)
N(19)-C(20)-C(21)-C(22)	0.6(5)
C(20)-C(21)-C(22)-C(23)	-0.8(4)
C(21)-C(22)-C(23)-C(18)	-0.5(4)
N(19)-C(18)-C(23)-C(22)	2.3(4)
C(1)-C(18)-C(23)-C(22)	-179.4(2)
C(68)-C(51)-O(52)-C(53)	60.8(3)
C(56)-C(51)-O(52)-C(53)	179.78(19)
C(62)-C(51)-O(52)-C(53)	-63.7(3)
C(51)-O(52)-C(53)-O(54)	-137.9(2)
O(52)-C(53)-O(54)-C(55)	66.2(3)
O(52)-C(51)-C(56)-N(57)	-169.79(19)
C(68)-C(51)-C(56)-N(57)	-51.6(3)
C(62)-C(51)-C(56)-N(57)	71.0(3)
O(52)-C(51)-C(56)-C(61)	12.0(3)
C(68)-C(51)-C(56)-C(61)	130.2(2)
C(62)-C(51)-C(56)-C(61)	-107.2(3)
C(61)-C(56)-N(57)-C(58)	-0.7(4)
C(51)-C(56)-N(57)-C(58)	-179.0(2)
C(56)-N(57)-C(58)-C(59)	0.2(4)
C(56)-N(57)-C(58)-Br(58)	-179.49(17)
N(57)-C(58)-C(59)-C(60)	0.0(4)
Br(58)-C(58)-C(59)-C(60)	179.7(2)
C(58)-C(59)-C(60)-C(61)	0.3(4)
N(57)-C(56)-C(61)-C(60)	1.1(4)
C(51)-C(56)-C(61)-C(60)	179.2(2)
C(59)-C(60)-C(61)-C(56)	-0.9(4)
O(52)-C(51)-C(62)-N(63)	-8.2(3)
C(68)-C(51)-C(62)-N(63)	-131.5(2)
C(56)-C(51)-C(62)-N(63)	106.7(2)
O(52)-C(51)-C(62)-C(67)	173.8(2)
C(68)-C(51)-C(62)-C(67)	50.6(3)
C(56)-C(51)-C(62)-C(67)	-71.2(3)
C(67)-C(62)-N(63)-C(64)	0.2(4)
C(51)-C(62)-N(63)-C(64)	-177.7(2)
C(62)-N(63)-C(64)-C(65)	0.3(4)
C(62)-N(63)-C(64)-Br(64)	-178.48(18)
N(63)-C(64)-C(65)-C(66)	-0.7(4)
Br(64)-C(64)-C(65)-C(66)	178.0(2)
C(64)-C(65)-C(66)-C(67)	0.6(4)
N(63)-C(62)-C(67)-C(66)	-0.4(4)
C(51)-C(62)-C(67)-C(66)	177.4(2)
C(65)-C(66)-C(67)-C(62)	-0.1(4)

O(52)-C(51)-C(68)-N(69)	-99.0(2)
C(56)-C(51)-C(68)-N(69)	145.5(2)
C(62)-C(51)-C(68)-N(69)	25.4(3)
O(52)-C(51)-C(68)-C(73)	74.3(3)
C(56)-C(51)-C(68)-C(73)	-41.2(3)
C(62)-C(51)-C(68)-C(73)	-161.3(2)
C(73)-C(68)-N(69)-C(70)	0.2(4)
C(51)-C(68)-N(69)-C(70)	173.2(2)
C(68)-N(69)-C(70)-C(71)	-1.4(4)
N(69)-C(70)-C(71)-C(72)	1.8(5)
C(70)-C(71)-C(72)-C(73)	-1.0(4)
C(71)-C(72)-C(73)-C(68)	-0.1(4)
N(69)-C(68)-C(73)-C(72)	0.5(4)
C(51)-C(68)-C(73)-C(72)	-172.4(2)

VII. References

[1] J. W. Steed, J. L. Atwood, *Supramolecular Chemistry*, John Wiley and Sons, New York, **2000**.

[2] G. F. Swiegers, T. J. Malefetse, *Chem. Rev.* **2000**, *100*, 3483.

[3] M. Fujita, M. Tominaga, A. Hori, B. Therrien, *Acc. Chem. Res.* **2005**, *38*, 369.

[4] H. Umeyama, K. Morokuma, *J. Am. Chem. Soc.* **1977**, *99*, 1316.

[5] G. A. Jeffrey, *An Introduction to Hydrogen Bonds*, Oxford University Press, New York, **1997**.

[6] G. R. Desiraju, T. Steiner, *The Weak Hydrogen Bond*, Oxford University Press, Oxford, **1999**.

[7] T. Steiner, *Chem. Commun.* **1997**, 727.

[8] J. D. Watson, F. H. C. Crick, *Nature* **1953**, *171*, 737.

[9] P. Ballester, A. Shivanyuk, A. R. Far, J. J. Rebek, *J. Am. Chem. Soc.* **2002**, *124*, 14014.

[10] A. Gissot, J. J. Rebek, *J. Am. Chem. Soc.* **2004**, *126*, 7424.

[11] F. Cuevas, S. Di Stefano, J. O. Magrans, P. Prados, J. de Mendoza, *Chem. Eur. J.* **2000**, *6*, 3228.

[12] J. O. Magrans, A. R. Ortiz, M. A. Molins, P. H. P. Lebouille, J. Sánchez-Quesada, P. Prados, M. Pons, F. Gago, J. de Mendoza, *Angew. Chem. Int. Ed.* **1996**, *35*, 1712.

[13] J. C. Ma, D. A. Dougherty, *Chem. Rev.* **1997**, *97*, 1303.

[14] L. K. Tsou, C. D. Tatko, M. L. Waters, *J. Am. Chem. Soc.* **2002**, *124*, 14917.

[15] R. M. Hughes, M. L. Waters, *J. Am. Chem. Soc.* **2005**.

[16] C. A. Hunter, K. R. Lawson, J. Perkins, C. J. Urch, *J. Chem. Soc. Perkin Trans. 2* **2001**, 651.

[17] Y. Kikuchi, Y. Aoyama, *Bull. Chem. Soc. Jpn.* **1996**, *69*, 217.

[18] M. L. Waters, *Curr. Opin. Chem. Bio.* **2002**, *6*, 736.

[19] M. L. Waters, *Biopolymers* **2004**, *76*, 435.

[20] D. B. Smithrud, E. M. Sanford, I. Chao, S. B. Ferguson, D. R. Carcanague, J. D. Evanseck, K. N. Houk, F. Diederich, *Pure Appl. Chem.* **1990**, *62*, 2227.

[21] A. Casnati, F. Sansone, R. Ungaro, *Acc. Chem. Res.* **2003**, *36*, 246.

[22] A. Fersht, *Enzyme Structure and Mechanism*, 2nd ed., W. H. Freeman and Company, New York, **1985**.

[23] T. E. Creighton, *Proteins: Structures and Molecular Properties*, 2nd ed., W. H. Freeman and Company, New York, **1993**.

[24] R. Cacciapaglia, S. Di Stefano, L. Mandolini, *Acc. Chem. Res.* **2004**, *37*, 113.

[25] T. Shen, K. Tai, R. H. Henchman, J. A. McCammon, *Acc. Chem. Res.* **2002**, *35*, 332.

[26] J. J. Rebek, *Angew. Chem. Int. Ed.* **2005**, *44*, 2068.

[27] F. M. Raymo, J. F. Stoddart, *Chem. Rev.* **1999**, *99*, 1643.

[28] A. Jasat, J. C. Sherman, *Chem. Rev.* **1999**, *99*, 931.

[29] J. Szejtli, *Chem. Rev.* **1998**, *98*, 1743.

[30] K. A. Connors, *Chem. Rev.* **1997**, *97*, 1325.

[31] M. V. Rekharsky, Y. Inoue, *Chem. Rev.* **1998**, *98*, 1875.

[32] A. Bom, M. Bradley, K. Cameron, J. K. Clark, J. van Egmond, H. Feilden, E. J. MacLean, A. W. Muir, R. Palin, D. C. Rees, M.-Q. Zhang, *Angew. Chem. Int. Ed.* **2002**, *41*, 266.

[33] V. T. D'Souza, *Supramolecular Chemistry* **2003**, *15*, 221.

[34] V. Böhmer, *Angew. Chem. Int. Ed.* **1995**, *34*, 713.

[35] C. D. Gutsche, in *Calixarenes 2001* (Eds.: Z. Asfari, V. Böhmer, J. Harrowfield, J. Vicens), Kluwer Academic Publishers, Dordrecht, **2001**, pp. 1.

[36] A. Arduini, A. Pochini, A. Secchi, F. Ugozzoli, in *Calixarenes 2001* (Eds.: Z. Asfari, V. Böhmer, J. Harrowfield, J. Vicens), Kluwer Academic Publishers, Dordrecht, **2001**, pp. 457.

[37] A. Arduini, W. M. McGregor, A. Pochini, A. Secchi, F. Ugozzoli, R. Ungaro, *J. Org. Chem.* **1996**, *61*, 6881.

[38] A. Arduini, W. M. McGregor, D. Paganuzzi, A. Pochini, A. Secchi, F. Ugozzoli, R. Ungaro, *J. Chem. Soc. Perkin Trans 2* **1996**, 839.

[39] F. Sansone, L. Baldini, A. Casnati, M. Lazzarotto, F. Ugozzoli, R. Ungaro, *Proc. Nat. Acad. Sci. USA* **2002**, *99*, 4842.

[40] Z.-L. Zhong, A. Ikeda, S. Shinkai, in *Calixarenes 2001* (Eds.: Z. Asfari, V. Böhmer, J. Harrowfield, J. Vicens), Kluwer Academic Publishers, Dordrecht, **2001**, pp. 467.

[41] U. Lüning, F. Löffler, J. Eggert, in *Calixarenes 2001* (Eds.: Z. Asfari, V. Böhmer, J. Harrowfield, J. Vicens), Kluwer Academic Publishers, Dordrecht, **2001**, pp. 71.

[42] Y. Chen, S. Gong, *J. Inclusion Phenom. Mol. Recognit. Chem.* **2003**, *45*, 165.

[43] S. Kanamathareddy, C. D. Gutsche, *J. Am. Chem. Soc.* **1993**, *115*, 6572.

[44] H. Otsuka, K. Araki, H. Matsumoto, T. Harada, S. Shinkai, *J. Org. Chem.* **1995**, *60*, 4862.

[45] U. Lüning, H. Ross, I. Thondorf, *J. Chem. Soc. Perkin Trans 2* **1998**, 1313.

[46] H. Otsuka, Y. Suzuki, A. Ikeda, K. Araki, S. Shinkai, *Tetrahedron* **1998**, *54*, 423.

[47] K. C. Nam, Y. J. Choi, D. S. Kim, J. M. Kim, C. C. Chun, *J. Am. Chem. Soc.* **1997**, *62*, 6441.

[48] K. C. Nam, S. W. Ko, S. O. Kang, S. H. Lee, D. S. Kim, *J. Inclusion Phenom. Mol. Recognit. Chem.* **2001**, *40*, 285.

[49] E. M. Choi, H. Oh, S. W. Ko, Y.-K. Choi, K. C. Nam, S. Jeon, *Bull. Korean Chem. Soc.* **2001**, *22*, 1345.

[50] U. Darbost, M. Giorgi, O. Reinaud, I. Jabin, *J. Org. Chem.* **2004**, *69*, 4879.

[51] I. Jabin, O. Reinaud, *J. Org. Chem.* **2003**, *68*, 3416.

[52] X. Zeng, N. Hucher, O. Reinaud, I. Jabin, *J. Org. Chem.* **2004**, *69*, 6886.

[53] K. Araki, K. Akao, A. Ikeda, T. Suzuki, S. Shinkai, *Tetrahedron Lett.* **1996**, *37*, 73.

[54] M. Takeshita, S. Nishio, S. Shinkai, *J. Org. Chem.* **1994**, *59*, 4032.

[55] D. J. Cram, *Science* **1983**, *219*, 1177.

[56] P. Timmerman, W. Verboom, D. N. Reinhoudt, *Tetrahedron* **1996**, *52*, 2663.

[57] C. Naumann, E. Román, C. Peinador, T. Ren, B. O. Patrick, A. E. Kaifer, J. C. Sherman, *Chem. Eur. J.* **2001**, *7*, 1637.

[58] H. Konishi, T. Nakamura, K. Ohata, K. Kobayashi, O. Morikawa, *Tetrahedron Lett.* **1996**, *37*, 7383.

[59] H. Konishi, K. Ohata, O. Morikawa, K. Kobayashi, *Chem. Commun.* **1995**, 309.

[60] Y. Aoyama, Y. Tanaka, H. Toi, H. Ogoshi, *J. Am. Chem. Soc.* **1988**, *110*, 634.

[61] Y. Aoyama, Y. Tanaka, S. Sugahara, *J. Am. Chem. Soc.* **1989**, *111*, 5397.

[62] Y. Kikuchi, Y. Kato, Y. Tanaka, H. Toi, Y. Aoyama, *J. Am. Chem. Soc.* **1991**, *113*, 1349.

[63] K. Kobayashi, Y. Asakawa, Y. Kato, Y. Aoyama, *J. Am. Chem. Soc.* **1992**, *114*, 10307.

[64] K. Kobayashi, M. Tominaga, Y. Asakawa, Y. Aoyama, *Tetrahedron Lett.* **1993**, *34*, 5121.

[65] R. Yanagihara, M. Tominaga, Y. Aoyama, *J. Org. Chem.* **1994**, *59*, 6865.

[66] J. R. Moran, S. Karbach, D. J. Cram, **1982**.

[67] J. A. Tucker, C. B. Knobler, K. N. Trueblood, D. J. Cram, *J. Am. Chem. Soc.* **1989**, *111*, 3688.

[68] D. J. Cram, S. Karbach, H.-E. Kim, C. B. Knobler, E. F. Maverick, J. L. Ericson, R. C. Helgeson, *J. Am. Chem. Soc.* **1988**, *110*, 2229.

[69] D. J. Cram, K. D. Stewart, I. Goldberg, K. N. Trueblood, *J. Am. Chem. Soc.* **1985**, *107*, 2574.

[70] L. Sebo, F. Diederich, V. Gramlich, *HeIv. Chim. Acta* **2000**, *83*, 93.

[71] D. Falábu, A. Shivanyuk, M. Nissinen, K. Rissanen, *Org. Lett.* **2002**, *4*, 3019.

[72] J. L. Atwood, A. Szumna, *J. Am. Chem. Soc.* **2002**, *124*, 10646.

[73] E. Dalcanale, P. Soncini, G. Bacchilega, F. Ugozzoli, *Chem. Commun.* **1989**, 500.

[74] P. Soncini, S. Bonsignore, E. Dalcanale, F. Ugozzoli, *J. Org. Chem.* **1992**, *57*, 4608.

[75] J. R. Moran, J. L. Ericson, E. Dalcanale, J. A. Bryant, C. B. Knobler, D. J. Cram, *J. Am. Chem. Soc.* **1991**, *113*, 5707.

[76] D. J. Cram, H.-J. Choi, J. A. Bryant, C. B. Knobler, *J. Am. Chem. Soc.* **1992**, *114*, 7748.

[77] D. M. Rudkevich, G. Hilmersson, J. J. Rebek, *J. Am. Chem. Soc.* **1997**, *119*, 9911.

[78] D. M. Rudkevich, G. Hilmersson, J. Rebek, Jr., *J. Am. Chem. Soc.* **1998**, *120*, 12216.

[79] S. Saito, C. Nuckolls, J. J. Rebek, *J. Am. Chem. Soc.* **2000**, *122*, 9628.

[80] F. C. Tucci, D. M. Rudkevich, J. J. Rebek, *J. Org. Chem.* **1999**, *64*, 4555.

[81] J. O. Green, J.-H. Baird, B. C. Gibb, *Org. Lett.* **2000**, *2*, 3845.

[82] H. Xi, C. L. D. Gibb, E. D. Stevens, B. C. Gibb, *Chem. Commun.* **1998**, 1743.

[83] H. Xi, C. L. D. Gibb, B. C. Gibb, *J. Org. Chem.* **1999**, *64*, 9286.

[84] C. L. D. Gibb, E. D. Stevens, B. C. Gibb, *J. Am. Chem. Soc.* **2001**, *123*, 5849.

[85] C. L. D. Gibb, H. Xi, P. A. Politzer, M. Concha, B. C. Gibb, *Tetrahedron* **2002**, *58*, 673.

[86] T. Spaniel, H. Görls, J. Scholz, *Angew. Chem. Int. Ed.* **1998**, *37*, 1862.

[87] R. Taylor, O. Kennard, *J. Am. Chem. Soc.* **1982**, *104*, 5063.

[88] O. Navon, J. Bernstein, V. Khodorkovsky, *Angew. Chem. Int. Ed.* **1997**, *36*, 601.

[89] K. Kobayashi, K. Ishii, S. Sakamoto, T. Shirasaka, K. Yamaguchi, *J. Am. Chem. Soc.* **2003**, *125*, 10615.

[90] T. Ratajczyk, I. Czerski, K. Kamienska-Trela, S. Szymanski, J. Wojcik, *Angew. Chem. Int. Ed.* **2005**, *44*, 1230.

[91] A. Collet, J.-P. Dutasta, B. Lozach, J. Canceill, *Top. Curr. Chem.* **1993**, *165*, 103.

[92] A. Collet, *Tetrahedron* **1987**, *43*, 5725.

[93] A. Collet, in *Comprehensive Supramolecular Chemistry, Vol. 6* (Eds.: J. L. Atwood, J. E. D. Davies, D. D. McNicol, F. Vögtle), Pergamon, Oxford, **1996**, pp. 281.

[94] J. W. Steed, H. Zhang, J. L. Atwood, *Supramolecular Chemistry* **1996**, *7*, 37.

[95] M. J. Hardie, P. D. Godfrey, C. L. Raston, *Chem. Eur. J.* **1999**, *5*, 1828.

[96] R. Ahmad, A. Franken, J. D. Kennedy, M. J. Hardie, *Chem. Eur. J.* **2004**, 2190.

[97] M. R. Caira, A. Jacobs, L. R. Nassimbeni, *Supramolecular Chemistry* **2004**, *16*, 337.

[98] M. J. Hardie, C. L. Raston, *Chem. Commun.* **2001**, 905.

[99] F. M. Menger, M. Takeshita, J. F. Chow, *J. Am. Chem. Soc.* **1981**, *103*, 5938.

[100] D. J. Cram, J. Weiss, R. C. Helgeson, C. B. Knobler, A. E. Dorigo, K. N. Houk, *Chem. Commun.* **1988**, 407.

[101] J. A. Wytko, J. Weiss, *Tetrahedron Lett.* **1991**, *32*, 7261.

[102] J. A. Wytko, J. Weiss, *J. Inclusion Phenom. Mol. Recognit. Chem.* **1994**, *19*, 207.

[103] D. S. Bohle, D. J. Stasko, *Inorg. Chem.* **2000**, *39*, 5768.

[104] D. S. Bohle, D. Stasko, *Chem. Commun.* **1998**, 567.

[105] A. Arduini, F. Calzavacca, D. Demuru, A. Pochini, A. Secchi, *J. Org. Chem.* **2004**, *69*, 1386.

[106] E. T. Rump, D. T. S. Rijkers, H. W. Wilbers, P. G. de Groot, R. M. J. Liskamp, *Chem. Eur. J.* **2002**, *8*, 4613.

[107] J. van Ameijde, R. M. J. Liskamp, *Org. Biomol. Chem.* **2003**, 2661.

[108] A. M. A. van Wageningen, R. M. J. Liskamp, *Tetrahedron Lett.* **1999**, *40*, 9347.

[109] C. Chamorro, R. M. J. Liskamp, *J. Comb. Chem.* **2003**, *5*, 794.

[110] C. Chamorro, R. M. J. Liskamp, *Tetrahedron* **2004**, *60*, 11145.

[111] W. L. Mock, in *Comprehensive Supramolecular Chemistry, Vol. 2* (Eds.: J. L. Atwood, J. E. D. Davies, D. D. McNicol, F. Vögtle), Pergamon, Oxford, **1996**, pp. 477.

[112] K. Kim, N. Selvapalam, D. H. Oh, *J. Inclusion Phenom. Mol. Recognit. Chem.* **2004**, *50*, 31.

[113] J. W. Lee, S. Samal, N. Selvapalam, H.-J. Kim, K. Kim, *Acc. Chem. Res.* **2003**, *36*, 621.

[114] O. A. Gerasko, D. G. Samsonenko, V. P. Fedin, *Russian Chemical Reviews* **2002**, *71*, 741.

[115] W. A. Freeman, W. L. Mock, N.-Y. Shih, *J. Am. Chem. Soc.* **1981**, *103*, 7367.

[116] W. L. Mock, *Top. Curr. Chem.* **1995**, *175*, 1.

[117] C. Marquez, W. M. Nau, *Angew. Chem. Int. Ed.* **2001**, *40*, 3155.

[118] K. Kim, *Chem. Soc. Rev.* **2002**, *31*, 96.

[119] W. L. Mock, in *Topics in Current Chemistry, Vol. 175* (Eds.: J. D. Dunitz, D. K. Hafner, S. Ito, J.-M. Lehn, K. N. Raymond, C. W. Rees, J. Thiem, F. Vögtle), Springer, New York, **1995**, pp. 1.

[120] J. Kim, I.-S. Jung, S.-Y. Kim, E. Lee, J.-K. Kang, S. Sakamoto, K. Yamaguchi, K. Kim, *J. Am. Chem. Soc.* **2000**, *122*, 540.

[121] W. Ong, A. E. Kaifer, *Angew. Chem. Int. Ed.* **2003**, *42*, 2164.

[122] H.-J. Kim, J. Heo, W. S. Jeon, E. Lee, J. Kim, S. Sakamoto, K. Yamaguchi, K. Kim, *Angew. Chem. Int. Ed.* **2001**, *40*, 1526.

[123] A. I. Day, R. J. Blanch, A. P. Arnold, S. Lorenzo, G. R. Lewis, D. I., *Angew. Chem. Int. Ed.* **2002**, *41*, 275.

[124] Y. Miyahara, K. Abe, T. Inazu, *Angew. Chem. Int. Ed.* **2002**, *41*, 3020.

[125] J. Zhao, H.-J. Kim, J. Oh, S.-Y. Kim, J. W. Lee, S. Sakamoto, K. Yamaguchi, K. Kim, *Angew. Chem. Int. Ed.* **2001**, *40*, 4233.

[126] S. Y. Jon, N. Selvapalam, D. H. Oh, J.-K. Kang, S.-Y. Kim, Y. J. Jeon, J. W. Lee, K. Kim, *J. Am. Chem. Soc.* **2003**, *125*, 10186.

[127] R. Breslow, S. D. Dong, *Chem. Rev.* **1998**, *98*, 1997.

[128] E. Engeldinger, D. Armspach, D. Matt, *Chem. Rev.* **2003**, *103*, 4147.

[129] O. S. Tee, J. J. Hoeven, *J. Am. Chem. Soc.* **1989**, *111*, 8318.

[130] O. S. Tee, *Adv. Phys. Org. Chem.* **1994**, *29*, 1.

[131] R. Breslow, J. W. Canary, M. Varney, S. T. Waddell, D. Yang, *J. Am. Chem. Soc.* **1990**, *112*, 5212.

[132] C. Rousseau, N. Nielsen, M. Bols, *Tetrahedron Lett.* **2004**, 8709.

[133] F. Ortega-Caballero, C. Rousseau, B. Christensen, T. E. Petersen, M. Bols, *J. Am. Chem. Soc.* **2005**, *127*, 3238.

[134] G. Ozturk, E. U. Akkaya, *Org. Lett.* **2004**, *6*, 241.

[135] H. Y. Cho, J. Y. Kim, S.-K. Chang, *Chem. Lett.* **1999**, 493.

[136] J. Y. Kim, Y. H. Kim, J.-I. Choe, S.-K. Chang, *Bull. Korean Chem. Soc.* **2001**, *22*, 635.

[137] P. Molenveld, S. Kapsabelis, J. F. J. Engbersen, D. N. Reinhoudt, *J. Am. Chem. Soc.* **1997**, *119*, 2948.

[138] P. Molenveld, J. F. L. Engbersen, H. Kooijman, A. L. Spek, D. N. Reinhoudt, *J. Am. Chem. Soc.* **1998**, *120*, 6726.

[139] P. Molenveld, W. M. G. Stikvoort, H. Kooijman, A. L. Spek, J. F. L. Engbersen, D. N. Reinhoudt, *J. Org. Chem.* **1999**, *64*, 3896.

[140] P. Molenveld, J. F. L. Engbersen, D. N. Reinhoudt, *Angew. Chem. Int. Ed.* **1999**, *38*, 3189.

[141] P. Molenveld, J. F. L. Engbersen, D. N. Reinhoudt, *Chem. Soc. Rev.* **2000**, *29*, 75.

[142] R. Cacciapaglia, A. Casnati, L. Mandolini, D. N. Reinhoudt, R. Salvio, A. Sartori, R. Ungaro, *J. Org. Chem.* **2005**.

[143] R. Cacciapaglia, A. Casnati, S. Di Stefano, L. Mandolini, D. Paolemili, D. N. Reinhoudt, A. Sartori, R. Ungaro, *Chem. Eur. J.* **2004**, 4436.

[144] R. Cacciapaglia, A. Casnati, L. Mandolini, D. N. Reinhoudt, R. Salvio, A. Sartori, R. Ungaro, *J. Org. Chem.* **2005**, *70*, 5398.

[145] H. Ross, U. Lüning, *Tetrahedron Lett.* **1997**, *38*, 4539.

[146] F. Löffler, M. Hagen, U. Lüning, *Synlett* **1999**, 1826.

[147] S. Blanchard, L. Le Clainche, M.-N. Rager, B. Chansou, J.-P. Tuchagues, A. F. Duprat, Y. Le Mest, O. Reinaud, *Angew. Chem. Int. Ed.* **1998**, *37*, 2732.

[148] S. Blanchard, M.-N. Rager, A. F. Duprat, O. Reinaud, *New J. Chem.* **1998**, 1143.

[149] O. Sêneque, O. Reinaud, *Tetrahedron* **2003**, *59*, 5563.

[150] O. Sénéque, Y. Rondelez, L. Le Clainche, C. Inisan, M.-N. Rager, M. Giorgi, O. Reinaud, *Eur. J. Inorg. Chem.* **2001**, 2597.

[151] O. Sénéque, M.-N. Rager, M. Giorgi, O. Reinaud, *J. Am. Chem. Soc.* **2001**, *123*, 8442.

[152] O. Sénéque, M. Giorgi, O. Reinaud, *Chem. Commun.* **2001**, 984.

[153] O. Sénéque, M. Giorgi, O. Reinaud, *Supramolecular Chemistry* **2003**, *15*, 573.

[154] L. Le Clainche, M. Giorgi, O. Reinaud, *Inorg. Chem.* **2000**, *39*, 3436.

[155] Y. Rondelez, O. Sénéque, M.-N. Rager, A. F. Duprat, O. Reinaud, *Chem. Eur. J.* **2000**, *6*, 4218.

[156] Y. Rondelez, G. Bertho, O. Reinaud, *Angew. Chem. Int. Ed.* **2002**, *41*, 1044.

[157] Y. Rondelez, M.-N. Rager, A. Duprat, O. Reinaud, *J. Am. Chem. Soc.* **2002**, *124*, 1334.

[158] O. Sénéque, M. Campion, M. Giorgi, Y. Le Mest, O. Reinaud, *Eur. J. Inorg. Chem.* **2004**, 1817.

[159] A. R. Renslo, J. J. Rebek, *Angew. Chem. Int. Ed.* **2000**, *39*, 3281.

[160] P. L. Wash, A. R. Renslo, J. J. Rebek, *Angew. Chem. Int. Ed.* **2001**, *40*, 1221.

[161] B. W. Purse, P. Ballester, J. J. Rebek, *J. Am. Chem. Soc.* **2003**, *125*, 14682.

[162] J. J. Rebek, C. Gibson, *Org. Lett.* **2002**, *4*, 1887.

[163] S. Richeter, J. J. Rebek, *J. Am. Chem. Soc.* **2004**, *126*, 16280.

[164] *Calixarenes 2001*, Kluwer Academic Publishers, Dordrecht, **2001**.

[165] J. Chen, S. Korner, S. L. Craig, D. M. Rudkevich, J. J. Rebek, *Nature* **2002**, *415*, 385.

[166] D. M. Rudkevich, J. J. Rebek, *Eur. J. Org. Chem.* **1999**, 1991.

[167] Z. R. Laughrey, C. L. D. Gibb, T. Senechal, B. C. Gibb, *Chem. Eur. J.* **2003**, *9*, 130.

[168] PC Spartan Pro, v. 1.1; Wavefunction, Inc.; 1999.

[169] K. A. Connors, *Binding Constants: The Measurement of Molecular Complex Stability*, John Wiley and Sons, New York, **1987**.

[170] Z. Zhong, E. V. Anslyn, *J. Am. Chem. Soc.* **2002**, *124*, 9014.

[171] Origin, v. 6.0; Microcal Software Inc.; **2000**.

[172] *CRC Handbook of Chemistry and Physics*, 81st ed., CRC Press, Boca Raton, **2000**.

[173] J. J. Rebek, S. Mecozzi, *Chem. Eur. J.* **1998**, *4*, 1016.

[174] R. L. Hilderbrandt, Q. Shen, *J. Phys. Chem.* **1982**, 587.

[175] X. Zheng, C. W. Lee, D. L. Philips, *J. Chem. Phys.* **1999**, 11034.

[176] M. Turowski, N. Yamakawa, J. Meller, K. Kimata, T. Ikegami, K. Hosoya, N. Tanaka, E. R. Thornton, *J. Am. Chem. Soc.* **2003**, *125*, 13836.

[177] Y.-L. Zhao, K. N. Houk, D. Rechavi, A. Scarso, J. Rebek, Jr., *J. Am. Chem. Soc.* **2004**, *126*, 11428.

[178] D. Wade, *Chem.-Biol. Interact.* **1999**, *117*, 191.

[179] S. Scheiner, M. Cuma, *J. Am. Chem. Soc.* **1996**, *118*, 1511.

[180] M. V. Rekharsky, Y. Inoue, *J. Am. Chem. Soc.* **2002**, *124*, 12361.

[181] D. Rechavi, A. Scarso, J. Rebek, Jr., *J. Am. Chem. Soc.* **2004**, *126*, 7738.

[182] H. Friebolin, *Basic One- and Two-Dimensional NMR Spectroscopy*, 3rd Revised ed., Wiley-VCH, Weinheim, **1998**.

[183] J. March, *Advanced Organic Chemistry: Reactions, Mechanisms, and Structure*, 4th ed., John Wiley and Sons Inc., New York, **1992**.

[184] G. A. Olah, S. C. Narang, B. G. B. Gupta, R. Malhotra, *J. Org. Chem.* **1979**, *44*, 1247.

[185] R. Montoro, T. Wirth, *Org. Lett.* **2003**, *5*, 4729.

[186] J. Barluenga, F. González-Bobes, J. M. González, *Angew. Chem. Int. Ed.* **2002**, *41*, 2556.

[187] N. Le Poul, M. Campion, G. Izzet, B. Douziech, O. Reinaud, Y. Le Mest, *J. Am. Chem. Soc.* **2005**, *127*, 5280.

[188] N. S. Narasimhan, R. S. Mali, *Top. Curr. Chem.* **1987**, *138*, 63.

[189] V. Snieckus, *Chem. Rev.* **1990**, *90*, 879.

[190] M. C. Whisler, S. MacNeil, V. Snieckus, P. Beak, *Angew. Chem. Int. Ed.* **2004**, *43*, 2206.

[191] W. Bauer, P. von Ragué Schleyer, *J. Am. Chem. Soc.* **1989**, *111*, 7191.

[192] C. L. D. Gibb, B. C. Gibb, *J. Am. Chem. Soc.* **2004**, *126*, 11408.

[193] T. W. Greene, P. G. M. Wuts, *Protective Groups in Organic Synthesis*, 3rd ed., John Wiley and Sons, New York, **1999**.

[194] H.-H. Wu, F. Yang, P. Cui, J. Tang, M.-Y. He, *Tetrahedron Lett.* **2004**, *45*, 4963.

[195] F. A. J. Meskens, *Synthesis* **1981**, *7*, 501.

[196] E. L. Eliel, S. H. Wilen, M. P. Doyle, *Basic Organic Stereochemistry*, Wiley Interscience, New York, **2001**.

[197] G. Parkin, *Chem. Commun.* **2000**, *20*, 1971.

[198] G. Parkin, *Chem. Rev.* **2004**, *104*, 699.

[199] D. W. Christianson, C. A. Fierke, *Acc. Chem. Res.* **1996**, *29*, 331.

[200] E. Kimura, *Acc. Chem. Res.* **2001**, *34*, 171.

[201] A. Looney, B. Han, K. Mcueil, G. Parkin, *J. Am. Chem. Soc.* **1993**, *115*, 4690.

[202] X. Li, C. L. D. Gibb, M. E. Kuebel, B. C. Gibb, *Tetrahedron* **2001**, *57*, 1175.

[203] J. Gong, B. C. Gibb, *Org. Lett.* **2004**, *6*, 1353.

[204] Mercury, CCDC Software; **2005**.

[205] N. Miyaura, A. Suzuki, *Chem. Rev.* **1995**, *95*, 2457.

[206] J. Hassan, M. Sevignon, C. Gozzi, E. Schulz, M. Lemaire, *Chem. Rev.* **2002**, *102*, 1359.

[207] C. L. D. Gibb, B. C. Gibb, *Proc. Nat. Acad. Sci. USA* **2002**, *99*, 4857.

[208] J. F. Bunnett, *Acc. Chem. Res.* **1972**, *5*, 139.

VITA

The author was born in Denver, Colorado. In 1998, he began his undergraduate study in chemistry at the University of New Orleans, where he received a B.A. degree in 2000. He continued his graduate study in Organic and Supramolecular chemistry at the University of New Orleans under the guidance of Professor Bruce Gibb.